

A Comparison of Future IDF Curves for Southern Ontario

Addendum – IDF Statistics, Curves and Equations

Prepared by:

Dr. Paulin Coulibaly^{1*}, P.Eng., Dr. Donald H. Burn², P.Eng., Harris Switzman^{3§},
John Henderson⁴, and Edmundo Fausto³

¹ McMaster University
Department of Civil Engineering and
School of Geography and Earth Sciences
1280 Main Street West
Hamilton, Ontario, Canada L8S 4L7
Tel: (905) 525-9140; Fax (905) 529-9688
Email: couliba@mcmaster.ca
*Corresponding Author

² University of Waterloo
Department of Civil and Environmental Engineering
200 University Avenue West
Waterloo, Ontario, Canada N2L 3G1
Email: dhburn@uwaterloo.ca

³ Ontario Climate Consortium (OCC) and Toronto and Region Conservation Authority (TRCA)
70 Canuck Avenue, Toronto, Ontario, Canada M3K 2C5
Email: efausto@trca.on.ca

⁴ Essex Region Conservation Authority (ERCA)
360 Fairview Avenue West, Suite 311
Essex, Ontario, Canada N8M 1Y6
Email: JHenderson@erca.org

§ Currently a consulting hydrologist in Calgary, AB

February 2016

ACKNOWLEDGEMENTS

This report is being jointly led by Toronto and Region Conservation Authority (TRCA) and Essex Region Conservation Authority (ERCA). The TRCA and ERCA are grateful for the funding support of the County of Essex, the Towns of Amherstburg, Essex, Kingsville, LaSalle, Tecumseh, the Cities of Windsor, Toronto and the Regional Municipalities of Peel and York.

The authors acknowledge the contribution of Serge Traore, Marc D'Alessandro, and Tara Razavi in carrying out the analysis and preparing the draft report.

The authors are grateful to Ryan Ness and Fabio Tonto (TRCA) for their contribution in sites selection, data collection, and their inputs, comments and review of the draft report. We also thank Heather Auld and Neil Comer from Risk Sciences International for their independent review of the main project report.

DISCLAIMER

This Report is being provided for information purposes only and is not intended, nor should it be construed as providing legal advice or recommendations in any circumstances from the Owner as represented by TRCA and ERCA.

TRCA, ERCA and the Authors make no representation or warranty of any kind whatsoever with respect to the completeness or accuracy of the information contained in the Report.

TRCA, ERCA and the Authors are not liable of any use or speculative interpretation of the contents of this Report. In no event shall the Authors, TRCA, ERCA be liable for any damage whatsoever arising out the use of the information provided in this Report. Readers are advised to obtain competent advice prior to relying on or using any information contained in the Report with respect to its suitability for general or specific application/use.

1. PURPOSE OF THIS ADDENDUM

This summary report is an Addendum to a larger technical report entitled “Comparison of Emerging Techniques for Updating Intensity-Duration-Frequency (IDF) Curves in Southern Ontario”.

The aim of this Addendum is to provide the Toronto and Region Conservation Authority and Essex Region Conservation Authority and their partners with IDF statistics, curve plots and equations in a form similar to Environment and Climate Change Canada’s official plots familiar to municipal staff and engineering consultants. Accompanying this summary is a PDF document of the selected plots and a text file summarizing the data.

2. STUDY BACKGROUND & OBJECTIVES

2.1. IDF Statistics in Water Management

Rainfall intensity-duration-frequency (IDF) statistics are used in many water management applications, including drainage design, stormwater and watershed planning, flooding and erosion risk management, and infrastructure operations. In Ontario for example, regulatory agencies, such as the Ministry of Transportation, Ministry of Environment and Climate Change, municipalities, and Conservation Authorities mandate the use IDF statistics as one of the major criteria in the design of stormwater management systems¹. Currently, many of these regulatory frameworks require the use of IDF statistics based on historical rainfall records, which are officially produced and updated by Environment Canada and available online².

2.2. IDF Statistics and Climate Change

Because IDF statistics have been deemed to be useful in expressing likelihoods of occurrence for a range of storm-event types in a given area, they have become a staple in water management. However, IDF statistics used in Ontario are based on historical time series data. Therefore, their ability to capture potential characteristics of future rainfall regimes associated with scenarios of climate change has been questioned. This is a key issue, as many studies have projected increases in the intensity and frequency of the extreme rainfall events that are of greatest concern to water managers under scenarios of climate change³. As a result of this, there is a need to understand how such changes might affect future IDF statistics. This is particularly relevant to the

design and planning of built and natural water management infrastructure, as it is designed for 50- to 100-year lifespans during which substantial change in rainfall regimes are projected³.

2.3. Uncertainty in Future IDF Statistics

There is a rapidly emerging body of knowledge and guidance on the development and use future IDF statistics⁴ that aims to account for the expected change in climate; however, there is also a lack of consensus on the most appropriate methods. This is due in large part to the wide array of distribution functions, future climate model datasets, downscaling methods, and future scenarios that could be used in creating future IDF statistics. With the large range of potential approaches available, there is the potential for significant variability among future IDF statistics for a given area. This variability and the current lack of consensus on the most adequate methods ultimately translates into uncertainty associated with the development of IDF statistics and on how climate change is projected to affect local rainfall regimes.

2.4. Study Objectives and Research Questions

Given the potential variability among IDF statistics at the local or regional scale, the aim of this study was to understand the limitations and applicability of different techniques for updating IDF statistics in light of climate change for two local study sites in southern Ontario (Fig. 1): (1) Windsor-Essex Region (WER) and (2) the Greater Toronto Area (GTA). More specifically, we sought to answer the following research questions:

- What is the variability among IDF statistics when using a set of the most robust downscaled climate change datasets in each study area?
- What trends can be ascertained about future extreme rainfall based on the downscaled IDF statistics?
- Given the datasets used and the results of comparing them, what are the implications for water management practice?

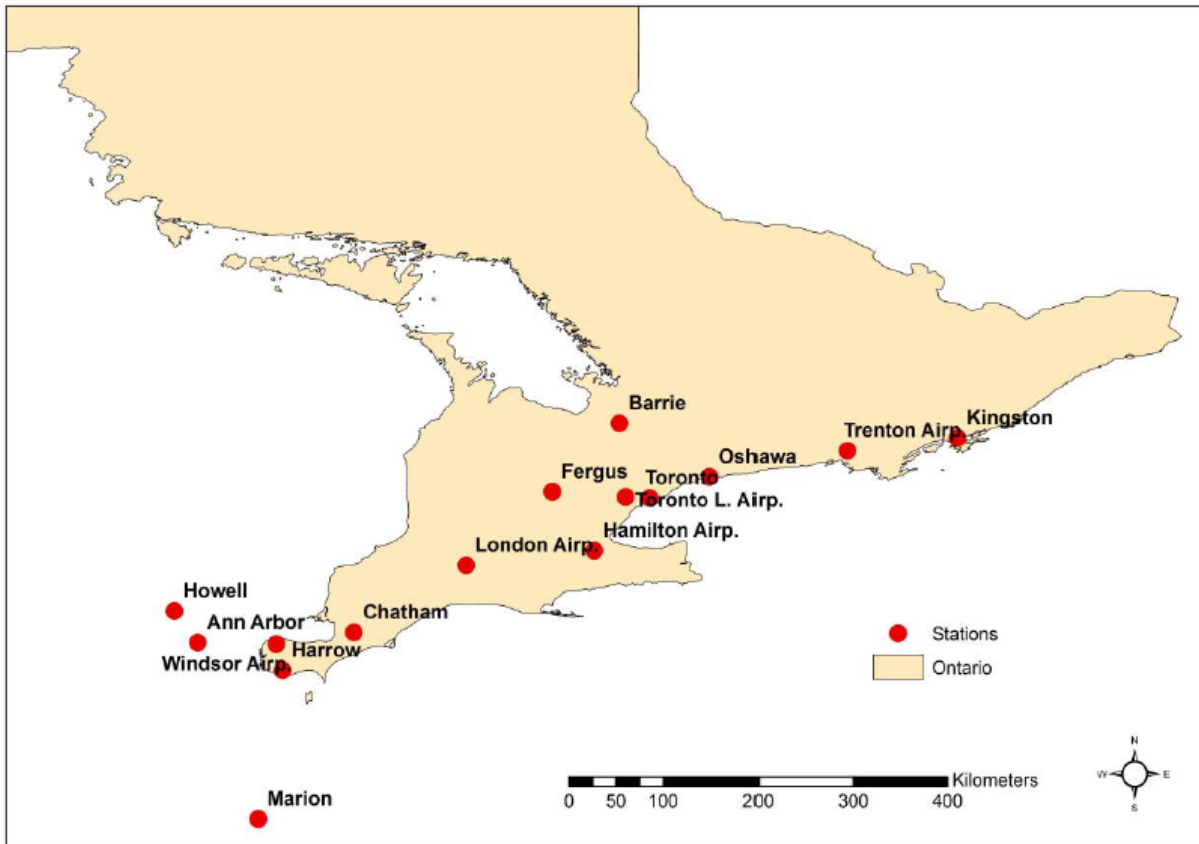


Figure 1: Location map of selected stations in Southern Ontario

3. METHODOLOGY & DATASETS

The following steps were undertaken to address the research questions in this study (Fig. 2):

1. Identify and review emerging techniques from the last 10 years to determine the most robust approaches for developing future IDF statistics for the selected sites (including climate model datasets, downscaling and bias-correction methods, IDF statistic and curve derivation).
2. Adapt and apply a set of the most robust approaches to multiple stations in the Toronto and Essex region (see Fig. 2 for details of datasets and methods used); and
3. Use statistical and graphical methods to compare the datasets produced from the various approaches to elucidate trends and characterize uncertainty.

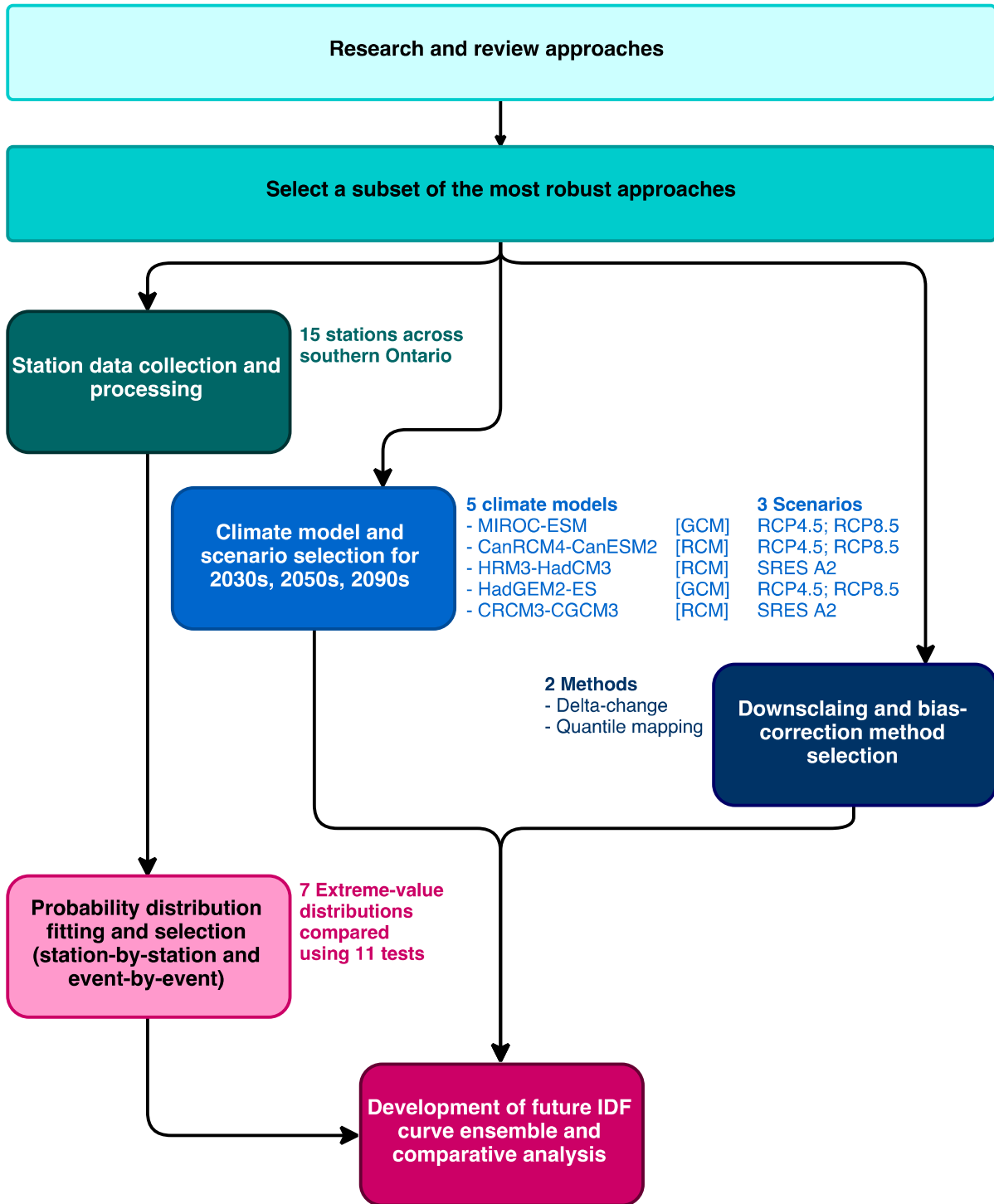


Fig. 2: Summary of overall study methodology

4. STUDY FINDINGS & INTERPRETATION

The following represent the most relevant findings for water managers, based on the comparative analysis among the ensemble of future IDF statistics generated:

- There is significant variability among future IDF statistics, which is manifested in a large range of intensity values for each storm durations and return period.
- In some cases, particularly in the GTA, the future IDF statistics show increases and decreases in rainfall intensity values. For instance, the relative change in intensity for the 30-minute, 100-year return-period event for the 2090s at Pearson Airport station ranged from +127% to -25% compared to the baseline period. The range in relative change for 2-hour event for 10- and 100-year return period events is shown in Fig. 3 and illustrates a similar pattern of large intensity ranges for the 2090s, especially at Pearson Airport.
- In general, variability among projections is greater for more extreme storms (e.g., 100-year vs. 10-year). This pattern can be seen in Figure 3, with the exception of the 10-year return period event for Windsor Airport station for the 2030s and 2050s. In Figure 3, a relative change of 0% would represent no change from the historical baseline storm intensity modeled with the Gumbel distribution.
- Based on the comparison of distribution functions, the GEV function was the most robust. While the Gumbel function may have been appropriate in the past, results of this study suggest the need to continually re-evaluate the suitability of existing methods, such as the distribution function, in IDF statistics updating. The fit of different probability distribution functions to extreme rainfall data is station-specific and is influenced by data quality.
- Variability among future IDF statistics due to climate model projections is generally greater than that associated with geographic variability among stations. More of the variability is due to the climate model projections than geographic differences within each study area.
- There is no definitive trend with respect to variability among projections with regard to storm duration (i.e., projections related to shorter storms are not necessarily more uncertain than longer-duration storms).

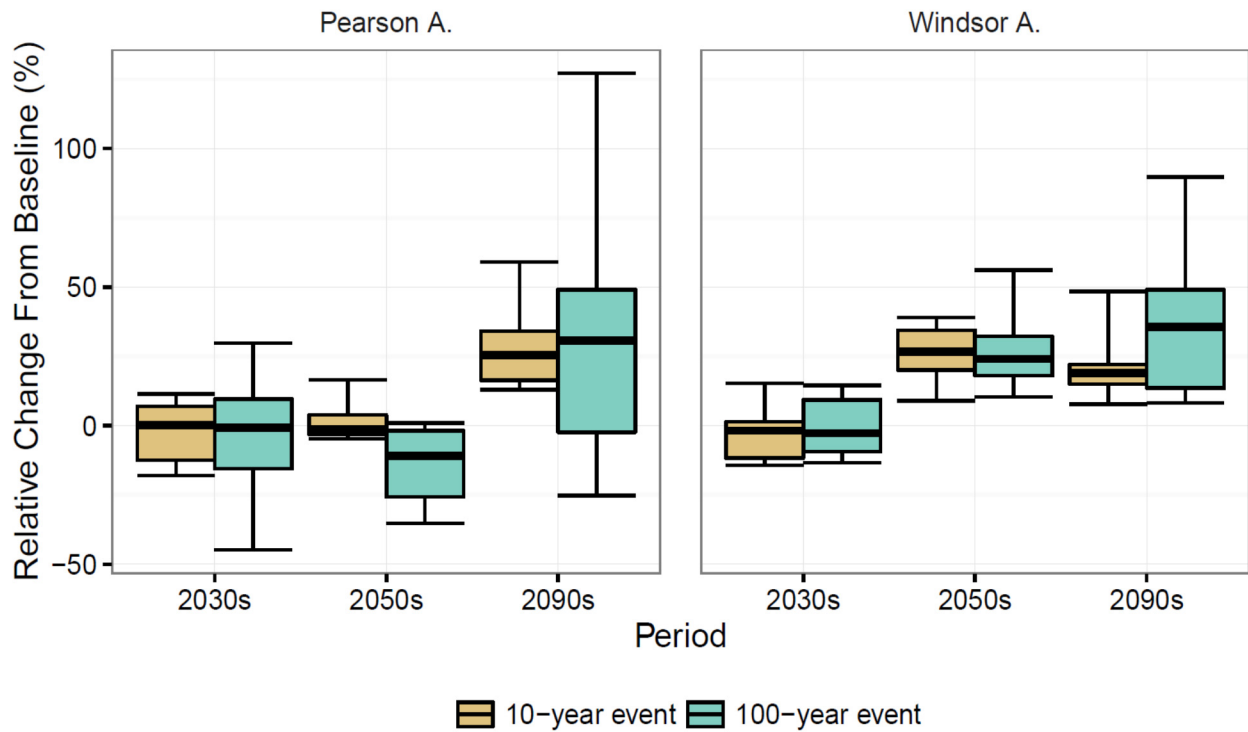


Fig. 3: Comparison of the range in relative change in rainfall intensity from baseline for the 2-hour event for 10- and 100-year return periods (0% on y-axis is no-change from historical baseline). Shaded boxes represent the inter-quartile range (25th to 75th percentile), the horizontal bar represents the median, and whiskers represent the minimum-maximum range for the ensemble.

4.1. Implications for Water Managers

Based on the findings of this study, it appears that no single method within the permutations analyzed can be deemed the “best” approach for developing future IDF statistics. Despite developing an ensemble using a robust subset of downscaled datasets, there is still significant variability among future IDF statistics. In some cases, datasets diverge in the direction of change projected, which results in significant uncertainty for practitioners.

These findings do not, however, mean that projected changes of increased storm intensity and frequency are incorrect, but rather points to the well-documented scientific limitations associated with future extreme rainfall analysis. Among these limitations are (1) the accuracy of climate models in representing the atmospheric dynamics that produce extreme rainfall at the local scale, particularly for short-duration events; (2) the quality of historical data used as inputs into statistical

models, and (3) the assumptions within future emission scenarios, downscaling and bias-correction techniques.

The methods for deriving IDF statistics, both for historical and future periods, are based on the assumption of stationarity (i.e., extreme rainfall time series have a constant mean over time). Climate change however, challenges this assumption. This is not to suggest that future IDF statistics are not useful, but rather that practitioners should use them as one of many tools within resilient water management, and not as the only source of design information about extreme rainfall. Risk-based management approaches that inherently address uncertainty can be a viable way forward and include approaches such as scenario-testing, sensitivity analysis, and re-evaluating the levels of extreme rainfall hazard tolerance acceptable to decision-makers.

Additionally, the high levels of uncertainty point to a need to continually refine the extreme rainfall information used in decision making by augmenting observational data quality and coverage, regularly updating IDF statistics based on ongoing monitoring, and continually assessing the most robust climate change models, and downscaling techniques.

5. ABOUT IDF STATISTICS PLOTS AND DATASETS

The results of this study have been prepared as “overlays” of the IDF curve ensemble on top of historical IDF curves (Fig. 4). All plots are provided in Appendix A to this summary. There is also an output text file summarizing the numerical values and the IDF curve equations for each plot (Appendix B).

Each graph represents a unique combination of a given station, return-period and future period. Within each graph the ensemble is represented as a series of curves. Each curve reflects a specific percentile from the distribution. Since each storm-type and future period has a number of different projections, the presentation of these as percentiles from the ensemble allows for the full distribution to be represented. The following list summarizes the IDF plots:

Figure A-18: IDF Curve Comparison for Pearson Airport, 2090s 100-year Return Period Event (10th-90th Percentile)

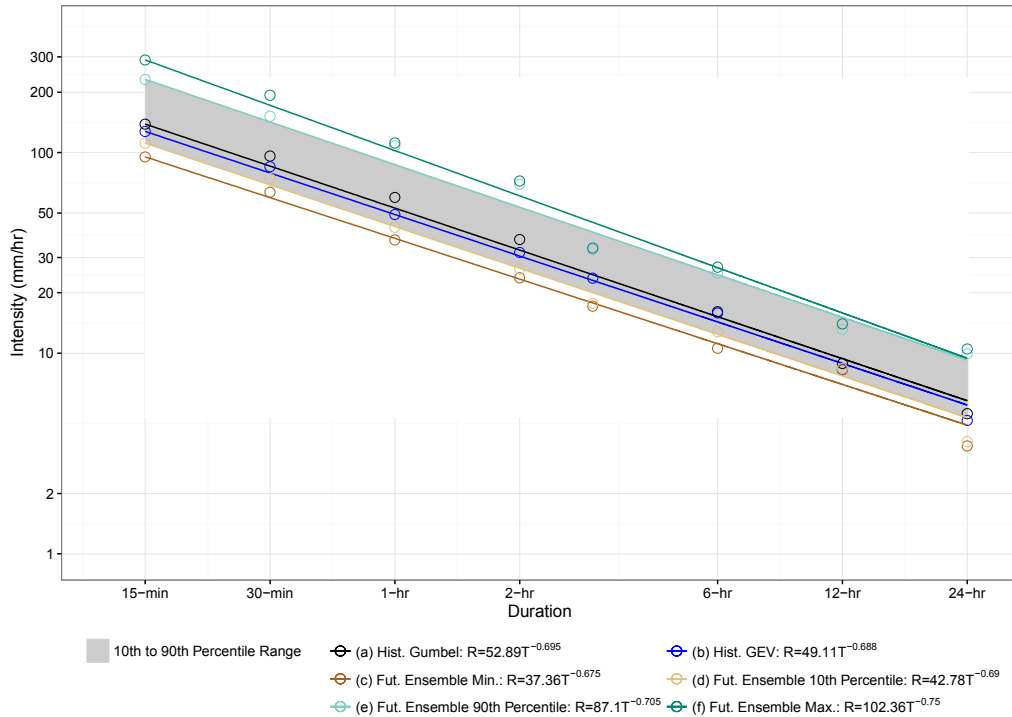


Fig. 4: Example of IDF curve overlay graph

- **Future Periods:** Plots are available for three different periods (2030s, 2050s, 2090s).
- **Storm Types:** Plots are available for 6 different return-periods (2-, 5-, 10-, 25-, 50-, 100-year return period events) and cover 8 storm durations (15-minute, 30-minute, 1-hour, 2-hour, 3-hour, 6-hour, 12-hour, and 24-hour events).
- **Ensemble Representation:** For all periods, the ensemble statistics represented are the minimum, maximum, 10th percentile and 90th percentile values. For the 2090s, there are additional plots containing the 50th and 75th percentiles.
- **Historical IDF Curves:** On all plots, this historical data are represented as two separate curves using the Gumbel and GEV distributions.
- **IDF Curve Equations:** Each curve is represented by an equation listed in the legend. The curve is based on the following equation that is also implemented in Environment and Climate Change Canada's IDF curves:

$$R = aT^b$$

Where R is the rainfall intensity (mm hr^{-1}), T is the storm duration (hr), and a and b are coefficients estimated using a least squares method implemented using a weighted version of the nonlinear least squares “nls” function in the computer program R.

5.1. Notable Limitations

The following represent the main limitations within the IDF statistics that should be considered by all users:

- **Limited ensemble:** The ensemble represented on each graph is a limited subset of the potential climate change scenarios for each study area. There are conceivably a very large number of potential climate future projections that could be derived, considering the number of climate models, downscaling methods and scenarios available. In this study, only five different climate models, two statistical bias-correction methods, and three emission scenarios are considered for future periods. While the models selected are deemed robust for the southern Ontario region, they are still only a subset of all models available. As such, the full variability and uncertainty are likely not captured within this dataset.
- **Different models for different periods:** Not all climate models had output for all future periods, and as such the size of the ensemble and models represented varies as is summarized in Table 1 below. Additionally, there is slight difference in the definition of the 2050s future period, however, this does not affect the results in any significant manner.
- **Curve fit:** It is evident in some plots that the IDF curves do not perfectly fit the point data. This is because there are some outliers within the dataset that make curve fitting a challenge. The accompanying text file contains information on the curve-fitting error in the form of the “standard error”. The standard error for the entire dataset ranges between 1% and 5% and averages 2% which is an acceptable error term in this context.

Table 1: Future Period Ensemble Composition

Future Period	No. Ensemble Members	Models and Scenarios
2030s	12	MIROC-ESM (RCP4.5, RCP8.5), HadGEM2-ES (RCP4.5, RCP8.5), CanRCM4-CanESM2 (RCP4.5, RCP8.5)
2050s	8	HRM3-HadCM3 (SRES A2), CRCM3-CGCM3 (SRES A2), CanRCM4-CanESM2 (RCP4.5, RCP8.5)
2090s	12	MIROC-ESM (RCP4.5, RCP8.5), HadGEM2-ES (RCP4.5, RCP8.5), CanRCM4-CanESM2 (RCP4.5, RCP8.5),

NOTES:

¹ See the following: MOE, “Stormwater Management Planning and Design Manual” (Toronto, ON, 2003); MTO, “Drainage Management Manual,” 1997; TRCA, “Stormwater Management Criteria” (Toronto, ON, 2012); City of Mississauga, “Subdivision Requirements Section 2 Design Requirements” (Mississauga, ON, 2009).

² Environment Canada’s IDF curves are available online at the following URL and are updated periodically: ftp://ftp.tor.ec.gc.ca/Pub/Engineering_Climate_Dataset/IDF/. At the time of this report, the curves were updated to 2013 rainfall data.

³ For example, see: J. Zhu, “Impact of Climate Change on Extreme Rainfall across the United States,” *Journal of Hydrologic Engineering* 18, no. 10 (2013): 1301–9; O. Seidou, A. Ramsay and I. Nistor, “Climate Change Impacts on Extreme Floods I: Combining Imperfect Deterministic Simulations and Non-Stationary Frequency Analysis,” *Natural Hazards* 61, no. 2 (2012): 647–59; S. Westra et al., “Future Changes to the Intensity and Frequency of Short-Duration Extreme Rainfall,” *Reviews of Geophysics*, September (2014), doi:10.1002/2014RG000464; C. Cheng et al., “A Synoptic Weather-Typing Approach to Project Future Daily Rainfall and Extremes at Local Scale in Ontario, Canada,” *Journal of Climate* 24, no. 14 (2011): 3667–85.

⁴ Technical report for this project contains a full review of approaches

A Comparison of Future IDF Curves for Southern Ontario

Technical Report

Prepared by:

Dr. Paulin Coulibaly^{1*}, P.Eng., Dr. Donald H. Burn², P.Eng., Harris Switzman³,
John Henderson⁴, and Edmundo Fausto³

¹McMaster University
Department of Civil Engineering and
School of Geography and Earth Sciences
1280 Main Street West
Hamilton, Ontario, Canada L8S 4L7
Tel: (905) 525-9140; Fax (905) 529-9688
Email: couliba@mcmaster.ca
*Corresponding Author

²University of Waterloo
Department of Civil and Environmental Engineering
200 University Avenue West
Waterloo, Ontario, Canada N2L 3G1
Email: dhburn@uwaterloo.ca

³Ontario Climate Consortium (OCC) and Toronto and Region Conservation Authority (TRCA)
70 Canuck Avenue, Toronto, Ontario, Canada M3K 2C5
Email: efausto@trca.on.ca

⁴Essex Region Conservation Authority (ERCA)
360 Fairview Avenue West, Suite 311
Essex, Ontario, Canada N8M 1Y6
Email: JHenderson@erca.org

July 2015

ACKNOWLEDGEMENTS

This report is being jointly led by Toronto and Region Conservation Authority (TRCA) and Essex Region Conservation Authority (ERCA). The TRCA and ERCA are grateful for the funding support of the County of Essex, the Towns of Amherstburg, Essex, Kingsville, LaSalle, Tecumseh, the Cities of Windsor, Toronto and the Regional Municipalities of Peel and York.

The authors acknowledge the contribution of Serge Traore, Marc D'Alessandro, and Tara Razavi in carrying out the analysis and preparing the draft report.

The authors are grateful to Ryan Ness and Fabio Tonto (TRCA) for their contribution in sites selection, data collection, and their inputs, comments and review of the draft report. We also thank Heather Auld and Neil Comer from Risk Sciences International for their independent review of the report.

DISCLAIMER

This Report is being provided for information purposes only and is not intended, nor should it be construed as providing legal advice or recommendations in any circumstances from the Owner as represented by TRCA and ERCA.

TRCA, ERCA and the Authors make no representation or warranty of any kind whatsoever with respect to the completeness or accuracy of the information contained in the Report.

TRCA, ERCA and the Authors are not liable of any use or speculative interpretation of the contents of this Report. In no event shall the Authors, TRCA, ERCA be liable for any damage whatsoever arising out the use of the information provided in this Report. Readers are advised to obtain competent advice prior to relying on or using any information contained in the Report with respect to its suitability for general or specific application/use.

EXECUTIVE SUMMARY

Background and Need

In Ontario, similar to other jurisdictions worldwide, extreme rainfall statistics in the form of intensity-duration-frequency (IDF) curves are used extensively in the design of water management infrastructure and policies. Common applications include the design and operation of drainage, stormwater conveyance and storage infrastructure (MOE 2003) and the delineation of floodplains and characterization of flood risk (MNR 2002). Typically, these applications rely on historical records of precipitation to determine critical thresholds or levels of risk that are reflected in system design. Recently observed and projected trends in North America's climate suggest however, that historical assumptions about the magnitude and frequency of extreme events may not hold true into the future. As such, there is significant work taking place among water managers and researchers to develop IDF curves to represent the impact of climate change on extreme precipitation. There are however, a number of different methods and datasets that can, and have, been used across Ontario, Canada and beyond to produce future IDF statistics based on climate model output.

When examining results of multiple studies for selected communities in southern Ontario in an attempt to generate future IDF curves for those locales, the Toronto and Region Conservation Authority, and Essex Region Conservation Authority discovered that results from different studies can be divergent or inconsistent. Additionally, there is no uniformly accepted method and approach for developing IDF information in light of climate change. This makes it difficult for water management stakeholders, including engineers, planning and other practitioners to interpret future IDF curves and understand the level of uncertainty associated with such information.

Study Objectives and Methods

This report presents results from a study conducted over the period (2014 to mid-2015) and aimed at understanding the limitations and applicability of different techniques for updating IDF statistics in light of climate change. This report has attempted to address this issue by conducting a comparison and analysis of the outcome of using different methods that are available for the development of future IDF curves. Within the study, five different climate model outputs are compared, including two global climate models and three regional climate models. Depending on the model and data availability at the time of the study, two different emission scenarios were also compared. Each model's output was downscaled to 15 Environment Canada precipitation

monitoring stations concentrated in the Essex-Windsor and Greater Toronto Areas (GTA) using two different methods: (1) quantile-base bias correction and (2) the delta-change method. Alternative distribution functions were also investigated to determine the influence of that assumption on IDF curves.

Results

Results demonstrate that there is significant variability among the subset of future climate projections, with the greatest uncertainty associated with short-duration and high-intensity events (15 minute to 1-hour event above the 25-year return period). Variability was also greater in the Windsor area compared to the GTA. A comparison of the different models to historical observations revealed significant discrepancies between the modeled and observed extreme precipitation records, suggesting that further downscaling was needed to correct inherent climate model biases. Another critical finding was that, although the Gumbel distribution is used by many who develop IDF curves, it was actually the poorest fit of all distributions identified for comparison. Ultimately, the Generalized Extreme Value (GEV) distribution was determined to be a more robust model for representing extreme precipitation in the study areas examined.

Implications for Water Management and Practitioners

Given the significant uncertainty associated with future and historical IDF curves, as presented and discussed in this study, it is reasonable for water managers to reevaluate the current levels of risk within existing assets and policies, in addition to those contained in guidelines on the design of infrastructure and policies. The findings have also led to the conclusion that some of the fundamental theoretical and practical assumptions made during the development and use of future IDF information, are not robust for the areas examined in this study, which are influenced by short-duration, high-intensity storm events that are not well represented in climate models. A key implication of the findings in this study is that precise design thresholds embedded within water management policy and infrastructure design do not capture the full profile to extreme precipitation risk for the study areas considered. Given the uncertainty in future IDF curves (or statistics), it is recommended that weight-of-evidence approaches be used when responding to potential extreme precipitation risks at the local scale.

While future IDF curves, such as those generated in this study may form part of the evidence base for adaptation to extreme precipitation risk, it is also critical that approaches incorporate historical extremes, and information on the thresholds and vulnerabilities of systems exposed to

the extreme precipitation regime in question. The corollary for policy and infrastructure decision making is that resiliency-based strategies, including characterizing hydrologic responses and vulnerabilities to a range of extreme precipitation regimes using a combination of empirical evidence of impacts and dynamical stress testing, or modeling, offer the most promising response to changes in extreme precipitation associated with global climate warming.

Overall, based on this study results, it is recommended that further study is needed in the selected study areas to better understand and refine the uncertainties involve in the future IDF statistics. This appears necessary before major change in infrastructure design standards in the study areas. Further study should involve the analysis of non-stationarity in the extreme rainfall series, the development of regional IDF statistics using non-stationary methods such as Bayesian inference; and a comprehensive statistical uncertainty analysis. Such study is part of the FloodNet Research Program and will require active contribution from FloodNet partners in selected study areas.

CONTENTS

Acknowledgements.....	ii
Disclaimer	ii
Executive Summary	iii
Background and Need.....	iii
Study Objectives and Methods	iii
Results	iv
Implications for Water Management and Practitioners.....	iv
Contents	vi
Figures.....	vii
Tables.....	viii
1. Introduction	1
1.1. Partnership	1
1.2. Background.....	1
1.3. Objectives.....	3
2. Study Areas	4
3. Methods and Datasets	7
3.1. Overall approach	7
3.2. Short, medium and long duration rainfall records	12
3.3. Comparison of distribution density functions	16
3.4. Future climate datasets and downscaling methods	17
3.4.1. Future Datasets	17
3.4.2. Downscaling Methods.....	20
4. Results.....	23
4.1. Identified distributions	23
4.2. Current period estimates.....	29
4.3. Future Projections.....	35
5. Discussion and Conclusions	42
6. Recommendations.....	44

References	46
7. Appendix 1: Summary of literature review	51
8. Appendix 2: Trend Analysis Results.....	88
9. Appendix 3: Distributions and selection criteria	96

FIGURES

Figure 1: Location map of selected stations in Southern Ontario.....	6
Figure 2: Flowchart of the different steps in the development of the projected IDF curves.	11
Figure 3: Plots of maximum annual precipitation for short durations at Hamilton, Toronto, and Windsor Airports.	15
Figure 4: QQ-plot of hourly annual maximum precipitation at Toronto and Windsor Airports. Note: Gumbel distribution is EV1 (extreme value).....	24
Figure 5: Histogram plot of 15-min annual maximum precipitation at Toronto and Windsor Airports.	25
Figure 6: Variability of historical storm event intensities for all the stations in each study area. Each curve is based on the GEV distribution.	28
Figure 7: Scatterplots of the observed versus modeled and bias-corrected storm intensities for all stations in the Windsor and Toronto study areas. Solid points represent the bias-corrected dataset (CBC) and the crosses represent the raw current climate model data (CC).	31
Figure 8: Residual plots of climate model results for current period for the Windsor region. The closest residuals to the zero line indicate the best climate model.	33
Figure 9: Residual plots of climate model results for current period for the Toronto region. The closest residuals to the zero line indicate the best climate model.	34
Figure 10: Overlay of historical IDF curves for all stations in the Toronto study area compared with box plots of the downscaled future IDF curves. Boxes represent the 25 th to 75 th percentiles of projections for each period from the downscaled datasets and whiskers represent the minimum and maximum values within the ensemble.....	38

Figure 11: Overlay of historical IDF curves for all stations in the Windsor study area compared with box plots of the downscaled future IDF curves. Boxes represent the 10th to 90th percentiles of projections for each period from the downscaled datasets and whiskers represent the minimum and maximum values within the ensemble.....39

Figure 12: Summary of all future projections for the 10 and 25 year return period storms for the 2050s (2038-2070) for the high-forcing A2 and RCP8.5 scenarios summarized for all stations in each case study area. Box plots represent the three future climate datasets of data raw climate model output, and downscaled datasets using DC (or AI: adjusted intensity) method and bias-correction method. Black dots represent historical values.40

Figure 13: Summary of all future projections for the 50 and 100 year return period storms for the 2050s (2038-2070) for the high-forcing A2 and RCP8.5 scenarios summarized for all stations in each case study area. Box plots represent the three future climate datasets of data raw climate model output, and downscaled datasets using DC (or AI: adjusted intensity) method and bias-correction method. Black dots represent historical values.41

TABLES

Table 1: Selected stations and their statistical parameters for 1 hour duration maximum annual rainfall. Unless otherwise specified, all stations are Environment Canada precipitation stations. 5

Table 2: Climate models and experiments selected 18

Table 3: Time periods used for the projected IDF along with the model and scenarios 19

Table 4: Selected “best” and “second best” fit distributions to the observed data26

1. INTRODUCTION

1.1. Partnership

This research project is a partnership coordinated through the Ontario Climate Consortium (OCC) and led by the Toronto and Region Conservation Authority (TRCA) and Essex Region Conservation Authority (ERCA). Research and analysis was conducted by OCC-member researchers at McMaster and the University of Waterloo. Funding support was provided to this project from the County of Essex, the Towns of Amherstburg, Essex, Kingsville, LaSalle, Tecumseh, the Cities of Windsor, Toronto and the Regional Municipalities of Peel and York. The OCC is a collective of scientists, researchers and practitioners from academia, the public and private sectors across Ontario with a focus on addressing climate change issues pertinent to Ontario and beyond.

The particular need to generate intensity-duration-frequency (IDF) curves for representing scenarios of climate change has been identified in several key policy and guidance documents in Ontario, including the province's 2011-2014 climate change strategy, *Climate Ready*, and the Canadian Standard Association's 2012 technical guide entitled *Development, interpretation, and use of rainfall intensity-duration-frequency information: Guideline for Canadian water resources practitioners*. As members of the OCC network began independently exploring methods and climate change datasets for generating future IDF curves for use in water management applications, it became apparent that many different approaches exist and it was unclear the extent to which they differ or converge in their results. A research partnership was formed between Conservation Authorities in the Toronto and Essex Regions and researchers at McMaster and Waterloo with shared interests in understanding the outcomes of using different calculation methods and climate datasets in the development of future IDF curves.

1.2. Background

In Ontario, similar to other jurisdictions worldwide, extreme rainfall statistics in the form of intensity-duration-frequency (IDF) curves are used extensively in policy and in design methodologies for water management infrastructure. Common applications include the design and operation of drainage, stormwater conveyance and storage infrastructure (MOE 2003) and the delineation of floodplains and characterization of flood risk (MNR 2002). Typically, these applications rely on historical records of precipitation to determine critical thresholds or levels of

risk that are reflected in system design. Recently observed and projected trends in North America's climate suggest however, that historical assumptions about the magnitude and frequency of extreme events may not hold true into the future. Such trends are well documented in scientific studies (Sillman et al. 2013; King et al. 2012; Peck et al. 2012; Cheng et al. 2011, 2010) and climate model outputs (Wang et al. 2014; Wang and Huang 2014; Senes 2011), which suggest that the intensity and frequency of extreme precipitation events are increasing and will continue to increase in southern Ontario (Lemmen et al. 2008). Given the anticipated impacts of climate change on extreme rainfall, there is a great deal of interest by municipalities, Conservation Authorities, provincial agencies, infrastructure proponents, and risk managers in developing rainfall IDF statistics that reflect anticipated future climate conditions, so that these can be reflected in design and operation of water management systems.

The initial intent of this study was to develop future IDF curves for two study areas in consideration – the Greater Toronto Area and Windsor-Essex. Upon beginning preliminary research to identify a methodology and climate projection datasets to use in generating future IDF curves, it became evident that there are a number of challenges involved in the derivation of future extreme rainfall statistics. Chief among these is the lack of a “universal” or “well established” methodology for updating IDF curves based on projected climate change scenarios. In Canada alone there have been 5-10 different methodologies applied in various studies (e.g. Coulibaly and Shi 2005; Mailhot et al. 2007; Nguyen et al. 2008; Solaiman and Simonovic 2011; Srivastav et al. 2014; Wang and Huang 2014; and others see Appendix 1). There is also an extensive number of potential future climate projections from various climate modelling experiments that one could select to represent the future local climate and no clear picture regarding the effect of this range on overall result uncertainty. Additionally, given the highly localized nature of many of the atmospheric processes driving extreme precipitation regimes in southern Ontario, it is necessary to use locally downscaled datasets for a given study area. This is necessary because the spatial and temporal resolution of global climate model (GCM) output, which is the basis for climate change projections, is too coarse to represent the physical processes of convection and the land-atmosphere interactions that produce the majority of extreme rainfall events of concern. Downscaling can be accomplished using GCM output in either a statistical model that relates large-scale variables to local ones (*statistical* downscaling), or as boundary conditions in a regional-scale climate model (RCM) that runs at finer spatial and temporal resolutions (*dynamical* downscaling). However, there are a variety of statistical and dynamical downscaling methods and models that can be used to this end. A recent inventory of existing downscaled climate projections available for southern

Ontario by the OCC, revealed 20 unique possible datasets with many having multiple subsets combining different GCMs, RCMs and downscaling methods. Therefore, there is a very large number of potential combinations of climate model experiments, downscaling methods and methodologies for calculating future IDF statistics, suggesting that there may be major uncertainty associated with the estimation of future extreme rainfall characteristics.

Given these aforementioned challenges and possible sources of uncertainty, this study is designed to fill gaps in current knowledge and enhance understanding of the possible range of variability of IDF curves in Southern Ontario based on the use of different downscaled datasets.

1.3. Objectives

The main objective of this study is to compare the most robust emerging techniques for updating IDF curves using several different global and regional climate model projections along with different techniques for downscaling and derivation of future IDF statistics. This approach aims to examine the range of variability in calculated IDF curves and statistics due to variability inherent to the climate model predictions and the downscaling techniques. The study is conducted for two study areas in southern Ontario: (1) the Greater Toronto Area and (2) Windsor-Essex region. The specific objectives are to

- Briefly review emerging techniques over the last ten years (2003-2013) for the derivation of future IDF curves and statistics;
- Identify the most robust emerging techniques;
- Adapt and apply selected techniques for updating IDF curves or statistics in Toronto and Essex region respectively using a number of different climate projection datasets as input; and
- Compare the results of selected techniques, document strengths, limitations, and sources of uncertainty, and discuss the implications for water management practice
- Report findings and recommendations to ERCA and TRCA in the form of technical report.

So far, to the best of the authors' knowledge, no such comparative study has been carried out in Ontario. Such a comparison is essential to further understanding the possible range of variability of future IDF statistics (commonly referred to as IDF curves) due to uncertainty associated with climate projections, multiple methodologies and methodological limitations in a context of non-stationary environment.

2. STUDY AREAS

This case study has been commissioned by Toronto and Region Conservation Authority (TRCA) and the Essex Region Conservation Authority (ERCA), and is therefore focused on those two regions. Several short duration rainfall recording stations have been screened for data quality and length requirements, and 15 were ultimately selected to generate the IDF curves with a focus on the two study areas in question. The regional zones of extreme precipitation representing each study area described in Paixao et al., (2011) were initially used to screen all Environment Canada extreme precipitation stations in each study area. This included identifying the homogeneous zone each station belongs to which better guides the station selection. The criteria established to screen stations were a minimum of 20-years of data with the most recent year available being after 2000, stations with the least gaps in the precipitation record, and an adequate geographic coverage across of each study area. Additional stations were selected from outside the immediate study areas to understand broader geographic trends. The list of the selected stations is presented in Table 1 along with some statistical properties of the hourly maximum annual rainfalls. The selected stations' locations are presented in Figure 1 and additional information on the datasets is presented in Section 3 of this report. Except Hamilton Airport, most stations in Toronto area have lower altitude compared to those in Windsor area which may be related to orographic effect caused by the escarpment. The statistical parameters (mean, variance and skewness) calculated did not exhibit any specific geographic pattern. In both areas, most of the stations have low and positive skewness coefficients. Apart from very few stations, the mean values are in the same range, but there are more disparities in the variances. Very similar results are obtained when other storm durations are considered which is not surprising because extreme rainfall is usually assumed a random variable. Given that each station data are used independently from the others, the information presented in Table 1 is descriptive and do not affect the development of the station-based IDF statistics. In a regional IDF development, features such as orography and station variances at the regional scale can have an impact.

Table 1: Selected stations and their statistical parameters for 1 hour duration maximum annual rainfall. Unless otherwise specified, all stations are Environment Canada precipitation stations.

No.	Selected Stations		Latitude	Longitude	Earliest Year	Most Recent Year	Elevation (m)	Mean (mm)	Variance	Skewness
1	Barrie	Other	44.38	-79.69	1968	2007	221	23.41	71.43	0.77
2	Fergus S. D.	Other	43.73	-80.33	1960	2007	417.6	27.1	230	2.1
3	Hamilton A	Tor.	43.17	-79.93	1970	2006	237.7	25.8	142.3	2.26
4	Kingston P. station	Other	44.24	-76.48	1960	2007	76.5	20.9	52	0.37
5	London Airport	Other	43.03	-81.15	1960	2002	278	24.4	78.6	0.6
6	Oshawa WPCP	Tor.	43.87	-78.83	1969	2007	83.8	20	71.2	0.50
7	Toronto	Tor.	43.67	-79.4	1937	2002	112.5	24.6	117.6	0.76
8	Toronto P. Airport	Tor.	43.68	-79.63	1960	2013	173.4	24.5	77	0.50
9	Trenton Airport	Other	44.12	-77.53	1964	2013	86.3	20.1	82.8	1.9
10	Windsor Airport	Wind.	42.28	-82.96	1960	2007	189.6	28.9	112.5	0.86
11	Chatham WPCP	Wind.	42.39	-82.22	1983	2007	180	27.9	65.3	0.44
12	Harrow CDA	Wind.	42.03	-82.9	1966	2001	190.5	28.8	136.5	0.98
13	Ann Arbor (NOAA)	Wind.	42.29	-83.71	variable	variable	274.3	26.36	143.24.	0.9
14	Howell (NOAA)	Wind.	42.59	-83.93	variable	variable	279.5	25.26	85.69	1.5
15	Marion (NOAA)	Wind.	40.62	-83.13	1949	2000	294	26.56	97.79	2.1

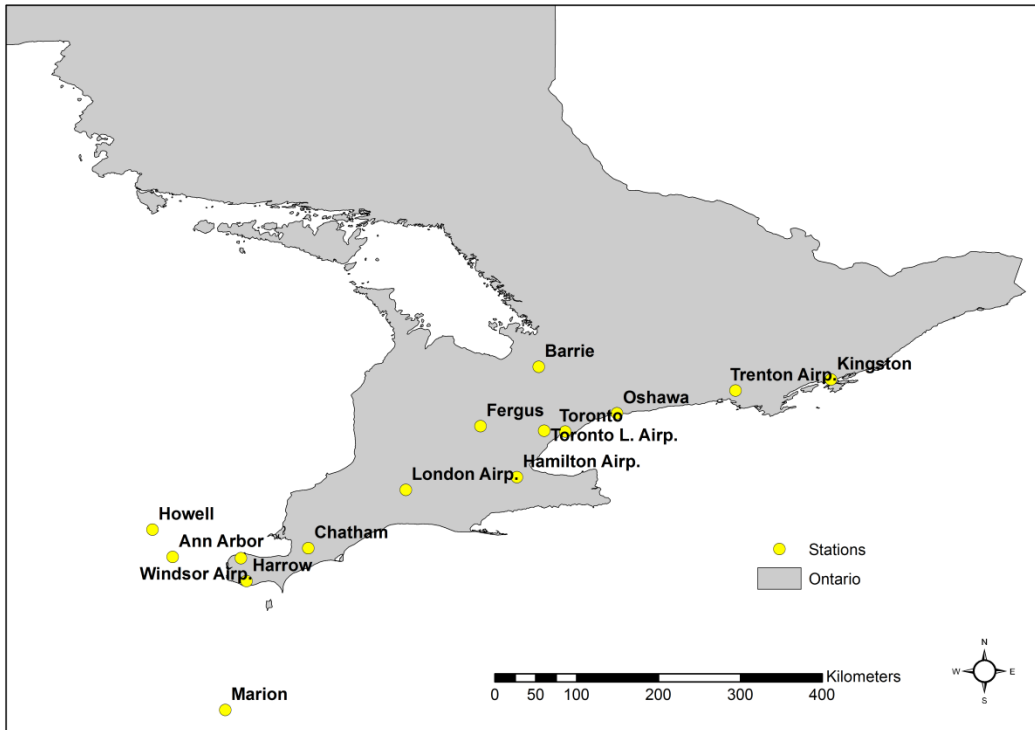


Figure 1: Location map of selected stations in Southern Ontario.

3. METHODS AND DATASETS

3.1. Overall approach

The development and comparative analysis of the IDF statistics presented in this report involved several different steps as described in Figure 2 and can be summarized as follows.

- 1. Literature review of techniques for updating IDF curves:** First, emerging techniques for updating IDF curves based on projected climate change scenarios were reviewed. From this literature review (see **Appendix 1** for a summary of literature review), the “delta change” (DC) approach and “bias correction” (BC) methods for model output bias correction and local downscaling have been selected for model output bias adjustment and local downscaling. Both the delta change and bias correction methods were selected based on their performance in previous studies (e.g. Ines and Hansen 2006; Olsson et al. 2012; Samuel et al. 2012; Chen et al. 2013, and others see Appendix 1).

It should be noted that two other approaches (Srivastav et al. 2014; Wang and Huang, 2014) recently proposed for generating future IDFs are not included in the literature review because they were not available when this work was initially completed. Given that the work in both Srivastav et al. (2014) and Wang and Huang (2014) has resulted in the development of online data tools for practitioners to use in order to access future IDF curves, a description of these is included as follows. This discussion is provided to assist the reader in understanding how these recent developments compare with the analysis conducted in this study and other existing datasets.

These methods include a variant of quantile matching (or mapping) methods employed in the IDF_CC Tool (Srivastav et al. 2014) and a dynamical downscaling approach used in the Ontario Climate Change Data Portal (Ontario CCDP) (Wang and Huang, 2014). Both methods use the Gumbel distribution for deriving the IDF curves. In the IDF_CC Tool, in addition to the Gumbel-based quantile mapping, a linear relationship is assumed and used to generate future IDFs (see Srivastav et al. 2014 for more details). In the Ontario CCDP, a dynamical downscaling model, called the PRECIS model from UK Met Office Hadley Centre, is used at 25x25 km spatial resolution to generate hourly rainfall data directly used to develop the future IDF curves (see Wang and Huang, 2014 for more details). These datasets represent important new developments in the derivation of future

IDF curves, however from the perspective of understanding the range of variability in IDF curves due to uncertainties in future climate projections, these simply add new data to the overall spread of existing information. Although there are significant uncertainties in the historical IDF values, there are greater uncertainties and limitations associated with the new climate change datasets that can be summarized as follows:

- With respect to the dynamical downscaling procedure used Wang and Huang (2014), it has been shown that at a spatial resolution of 25x25km, additional downscaling may be required to capture local scale atmospheric and physical processes (e.g. convective cells, orographic effects) that drive extreme precipitation. It may not be possible to project the shortest duration events due to the limitations in models to capture patterns and trends in fine convective activity over time. Fine scale regional climate models are better suited and likely to be successful in resolving orographic influences, provided that sufficient baseline (ground truth) data is available to calibrate these orographic effects. The baseline data on convective influences will always be limited unless input data densities are relatively high. (Barsugli et al. 2013; see <http://www.gfdl.noaa.gov/climate-model-downscaling>). “Over time, high-resolution GCMs and advances in model formulation will reduce these impediments, but the myriad of climate impacts questions makes it unlikely that even these improved models will be able to effectively address all scales and applications of interest” (Barsugli et al. 2013; <http://www.gfdl.noaa.gov/climate-model-downscaling>).
- A source of uncertainty associated with quantile mapping approach as used in the IDF_CC tool is in that method’s inability to deal with future extremes that may be outside the range of observed data (Chen et al. 2013). The use of a constant extrapolation based only on the single highest quantile for extremes may not effectively capture the extreme tail of the precipitation distribution (Maraun et al., 2010). Furthermore, assuming a linear relationship between daily and sub-daily precipitation for temporal downscaling as proposed in the IDF_CC tool (Srivastac et al. 2014) is a significant source of uncertainty, given the nonstationary nature of future extreme precipitation. For example, stochastic or nonlinear methods for

temporal disaggregation as used in Nguyen et al. (2007) or Hailegoergis et al. (2013) present alternative approaches.

- 2. Historical precipitation data collection and analysis:** Rainfall data are then collected at different stations across the selected study areas. Those observed data have been pre-processed and analyzed for trend detection using Mann-Kendall (MK) trend test (Mann 1945, Kendall 1975). The purpose of the Mann-Kendall test is to statistically assess if there is a consistently upward or downward trend of the variable of interest over time. This is simply part of common exploratory data analysis although there is no objective way to discriminate trends among natural climatic trends, anthropogenic driven changes, and sampling variability. This is described further in Section 3.2

- 3. Evaluation of distribution functions:** Many studies pertaining to IDF curves in Ontario (see **Appendix 1**), including Srivastav et al. (2014), Paixao et al (2011) and Wang and Huang (2014) have used the Gumbel distribution as compared to other possible distribution functions to develop their IDF curves. The use of the Gumbel distribution is attributed to the fact that it has been used by Environment Canada across Canada. That being said, to the best of our best knowledge, the performance of other possible distribution functions over Ontario has not been fully tested. The most extensive analysis so far was done by Paixao et al. 2011. They examined five distribution functions, the generalized logistic (GLO), the generalized extreme value (GEV); the normal (NO); the Pearson Type III (PE3), and the generalized Pareto (GPD) using one goodness-of-fit (Z statistic) test. It was found that the GEV and GLO were the best fit to the data based on the Z statistic condition for 53 of the 81 cases.

It is now well documented that the performance of a statistical distribution function can vary from one region to another and even from one rainfall duration to another (Hailegeorgis et al. 2013, Paixao et al, 2011). In a recent study on the estimates of changes in design rainfall values for Canada (Burn and Taleghani, 2013), it was shown that the Gumbel distribution performed the least robustly compared to all others examined. A similar comparison was done for southern Ontario in Paixao et al, 2011 with similar conclusions, although Gumbel did work reasonably well for some small regions in southern Ontario. Given these findings, a thorough comparison of these

distributions was undertaken to identify the most appropriate distribution function for the areas in question in this study. This evaluation was completed by fitting different distributions to each station observed data and then determining how they rank based on several different goodness of fit criteria. Ultimately the best fit distribution function was then selected for generating future IDF curves. Additional details on this analysis are provided in Section 3.3 of this report.

- 4. Future precipitation dataset identification and processing:** Given the range of potential future precipitation datasets available for southern Ontario, a critical step was selecting a subset of datasets from climate change model outputs to compare through this study. For the future climate projections, different time periods and different scenarios are considered depending on the outputs available for each climate model. The criteria and process of future scenario selection is described in more detail in Section 3.4. In general, the performance of the climate models, the temporal resolution of the data; and the data availability were among the main criteria used in the future scenario selection.
- 5. Development of historical and future IDF curves:** Finally, the selected distribution is then used to establish the projected IDF curves for different storm durations and return periods using both bias correction (BC) technique and a delta change (DC) method.

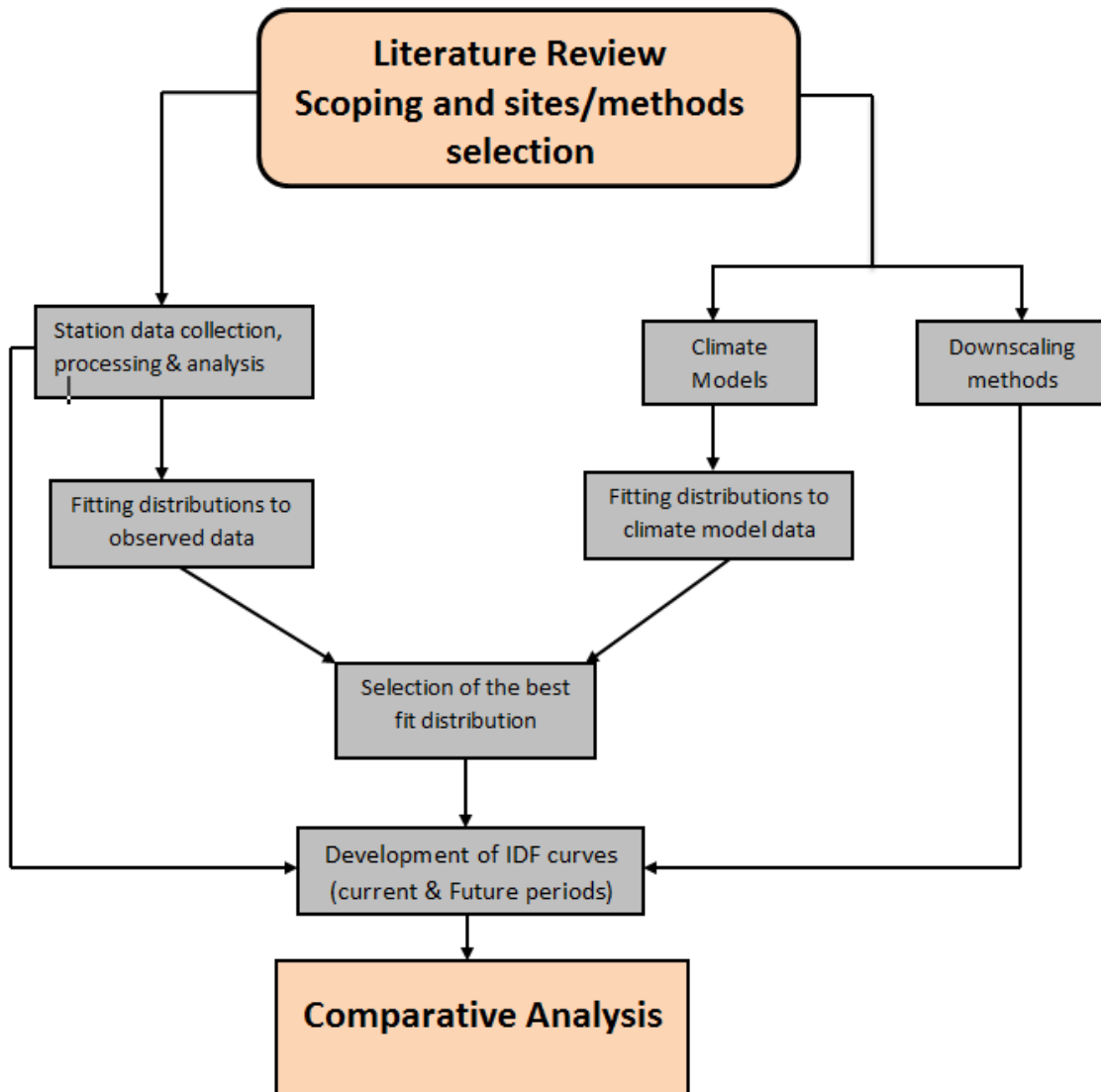


Figure 2: Flowchart of the different steps in the development of the projected IDF curves.

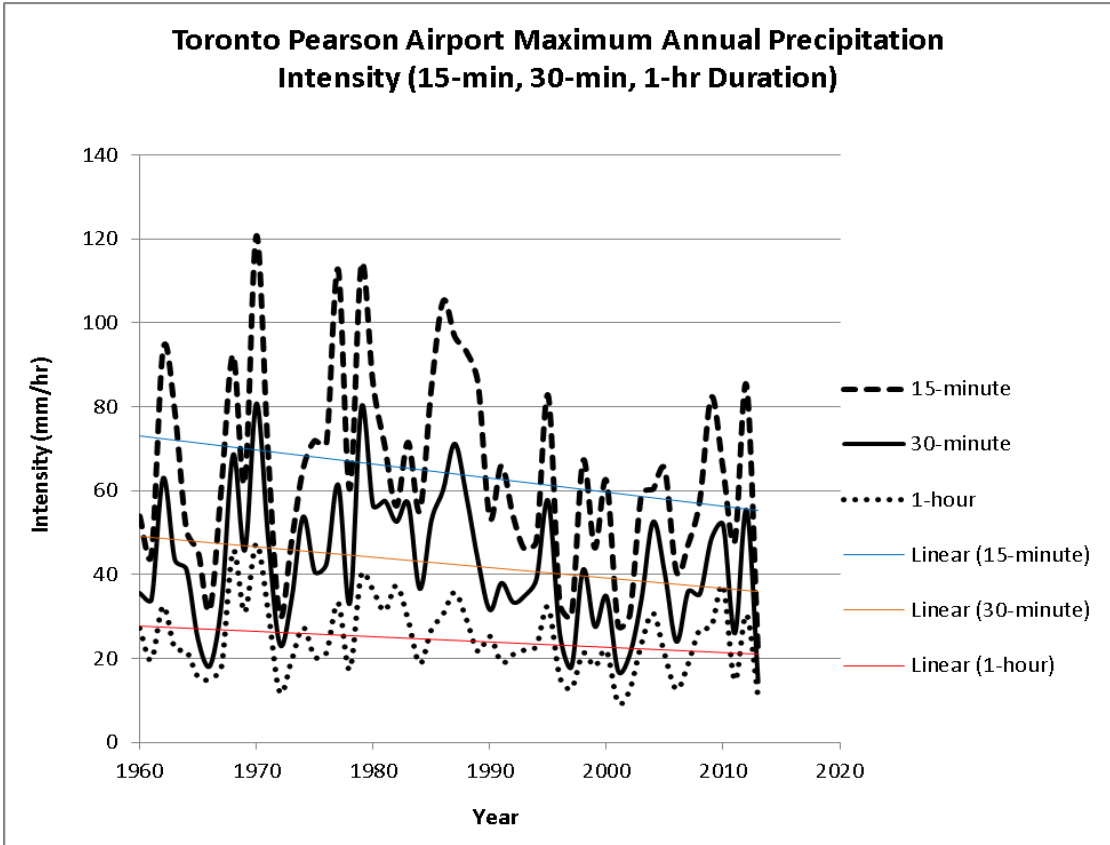
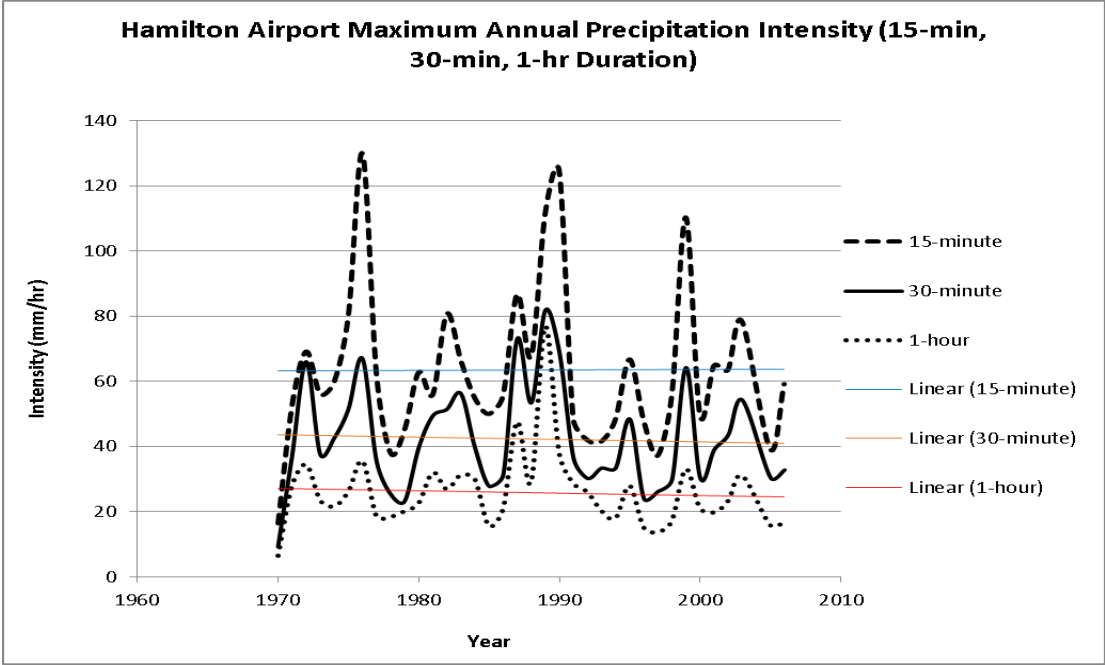
3.2. Short, medium and long duration rainfall records

For the maximum rainfall data collection, different storm durations have been considered. This includes the typical time of concentration for small urban watersheds (durations of 15 and 30 minutes) and the typical time of concentration for larger rural watersheds (durations of 1, 2, 3, 6, 12, and 24 hours) (Bougadis and Adamowski 2006). The 15 stations used for the IDF curves development are selected based on the quality and record length of the data and also by taking into account the spatial distribution of the stations. Apart from three stations (Ann Arbor, Howell, Marion) all the maximum annual rate of rainfall data for the different storm durations have been provided by Environment Canada through its historical climate data archive. The datasets used were created from the DLY02 and DLY04 precipitation records. These data have been previously quality controlled by Environment Canada and erroneous records flagged. Observed data at the other three stations were downloaded from NOAA website at: http://hdsc.nws.noaa.gov/hdsc/pfds/pfds_series.html. This dataset has also been quality controlled by NOAA.

As an example, Figure 3 presents the annual maximum precipitation for 15-minute, 30-minute and 1-hour duration events for Hamilton Airport, Toronto Airport, and Windsor Airport. The temporal variability of these time series does not show a clear linear trend for Hamilton, but for both Toronto and Windsor, there is slight apparent linear decreasing trend. To further assess trends in the extreme rainfall data, the Mann-Kendall trend test is applied to all station data and for all durations. The test results are presented in Appendix 2 although they don't have a direct implication in the IDF development, they are part of the common exploratory analysis which is used to assess whether there are some inconsistencies in the datasets. For example a decreasing trend followed by an increasing trend in a same time series will indicate an inconsistency that would require further investigation. The trend analysis results indicate that there is no inconsistency in the datasets. In general both increasing and decreasing trends are found statistically "non-significant" at 95% confidence level. These trend test results should however, be taken with caution because (a) there is no objective way to discriminate trends among natural climatic trends, anthropogenic caused changes, and sampling variability; (b) a minimum of 25 years of records is required for a reliable trend analysis given the strong temporal variability of sub-daily extreme precipitation time series (Bengtsson and Milotti 2010); (c) Mann-Kendall test assumes independence of time series from year to year and therefore cannot be properly applied in the presence of persistence induced by low-frequency oscillations (e.g. annual, decadal and

multi-decadal climate oscillations) (Coulibaly 2006, Willems and Yiu 2010; Willems et al. 2012). That being said, previous studies have provided evidence of increases in the longer duration synoptic processes associated with extreme precipitation in southern Ontario (Cheng et al. 2011, 2010).

A dilemma for many water practitioners is the decision on how to proceed when short duration extreme rainfall trends are downwards while indications under climate change are for increases in intense rainfall events, including decisions on whether to adopt the more recently updated but decreased IDF values in light of projected increases for future periods. Many influences can lead to downward trends when updating historical IDF values, including: changes in rainfall quality control procedures that screen out anomalously high extreme values, instrument and data recording/logging practices, changes in extreme value statistical analyses techniques, use of different distribution density functions, analyses procedures for missing data, atmosphere-ocean 'oscillation' influences on the climatology, relative changes in the contribution of fine scale convection rainfall events, etc. Some guidance in such situation would be to avoid change to the updated lower IDF value for now (Paixao et al. 2011) which may not be appropriate in the absence of a systematic uncertainty analysis. Based on the findings herein (to be discussed in section 4.3), major change to design standards is not recommended until further study including regional IDF and statistical uncertainty analysis are completed on the area of interest.



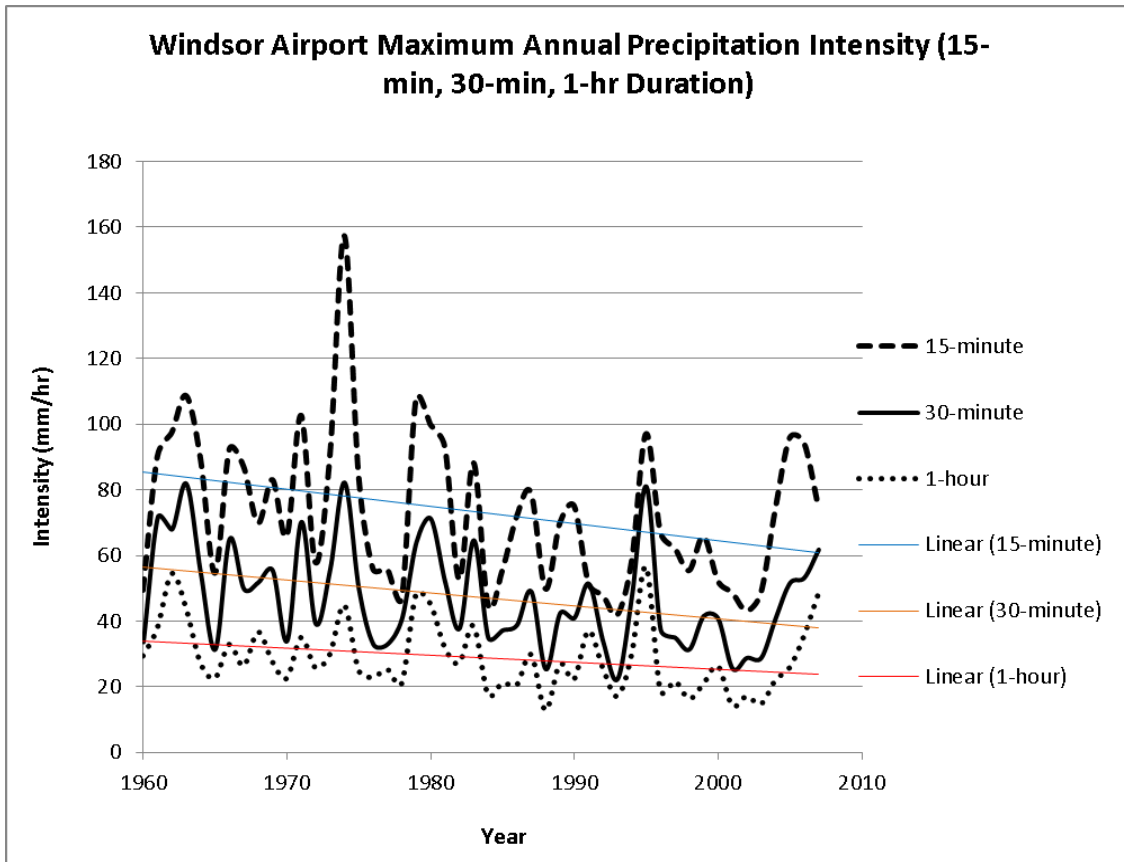


Figure 3: Plots of maximum annual precipitation for short durations at Hamilton, Toronto, and Windsor Airports.

3.3. Comparison of distribution density functions

The establishment of IDF statistics requires the use of a cumulative distribution function to estimate the rainfall intensity for the different return periods. Since the use of different distribution functions can provide very different results, the selection of an appropriate theoretical distribution is an important step in this process. From the comprehensive literature review completed (see Appendix 1), the most commonly used distribution functions were selected for further investigation in the study area. Specifically, the following distributions functions were fitted to the maximum annual rainfall using the maximum-likelihood and L-moment method for the parameter estimation:

- Weibull;
- Gamma;
- Normal or Gaussian;
- Lognormal;
- Gumbel (EV1);
- Generalized extreme value (GEV); and
- Log-Pearson type 3 (LP3)

For all stations, different storm durations are considered. The fitting quality is evaluated using eleven different goodness of fit criteria, including the Akaike Information Criterion (AIC), the Kolmogorov-Smirnov and the Chi square goodness of fit criteria, as well as the quantile-quantile plot and the L-moment diagram. The complete list and detailed description of all the eleven goodness of fit criteria used are presented in **Appendix 3**. The AIC is among the most widely used criteria in model selection (Kuipper and Hoijtink, 2011) and represents a relative estimate of information lost when a given model is used to represent a process that generates the data, and therefore allows to rank multiple competing models used to approximate the unknown truth (Symonds and Moussalli, 2010). The L-moment diagram (Anctil et al., 2005, Meylan et al. 2012) and the quantile-quantile plot (Opere et al. 2006) are simple and practical goodness of fit criteria that can be used to compare and select suitable statistical distribution. The best distribution is selected after all candidates are evaluated and ranked based on those different criteria. No previous study has conducted such a thorough evaluation of distribution functions on extreme rainfall for short, medium and long durations in Southern Ontario.

3.4. Future climate datasets and downscaling methods

3.4.1. Future Datasets

Three regional climate models (RCMs) and two global climate models (GCM) outputs have been considered in this study. The specific datasets analysed are the fourth generation of the Canadian regional climate model (CanRCM4) driven by the second generation of Canadian earth system model (CanESM2), the third generation of Canadian regional climate model (CRCM3) driven by the Canadian Global Climate Model 3 (CGCM3), and the third generation of the Hadley Center regional climate model (HRM3) driven by the HadCM2. In addition, based on the results of the Fifth Coupled Model Intercomparison Project (CMIP5), the GCMs HadGEM2-ES and the MIROC-ESM are selected. The MIROC-ESM was selected based on the fact that it was among the best performing models for eastern North America (Sheffield et al. 2013; Kharin et al. 2013) and the HadGEM2-ES model was selected because its performance and the fact that it is commonly used in Ontario for climate change impact studies (e.g. Peck et al. 2012; Samuel et al. 2012; Das et al. 2013; Wang and Huang 2014). Additionally, the HadGEM2-ES model data was selected because of the availability of their outputs for the required short-duration (e.g. hourly) temporal resolution (see Table 2 below).

The data outputs of each of those models are downloaded for the current and future time periods and at the highest temporal resolution available. For the climate model using the Representative Concentration Pathways (RCPs), the scenario RCP4.5 and RCP8.5 have been selected to assess both the medium and high greenhouse gas emission scenarios. In addition, for the CRCM3 and HRM3, the often referred to as “business as usual” or A2 scenario of the Special Report on Emissions Scenarios (SRES) (IPCC 2001, Nakicenovic et al., 2000) was selected because of data availability and for comparison purpose. The SRES A2 scenario has been the most widely used by different climate modeling groups (Maurer 2007) including the CMIP3 (Covey et al. 2003) which allows inter-comparison of different climate model results.

The RCP8.5 is characterized by increasing greenhouse gas emissions over time while the RCP4.5 is a stabilization scenario (Detlef et al., 2011). The list of those different climate models along with the experiments and time periods available is presented in Table 2.

Table 2: Climate models and experiments selected

Climate Model	Model Spatial Resolution	Scenario	Temporal Resolution	Simulation Period
CanRCM4-CanESM2	40 km	Historical	1 hour	1950-2005
		RCP4.5	1 hour	2006-2100
		RCP8.5	1 hour	2006-2100
CRCM3-CGCM3	50 km	Historical	3 hours	1968-2000
		SRES A2	3 hours	2038-2070
HRM3-HadCM3	50 km	Historical	3 hours	1968-2000
		SRES A2	3 hours	2038-2070
HadGEM2-ES	1.25 × 1.875 degrees (approx. 120 x 139 km)	Historical	3 hours	1960-2005
		RCP4.5	3 hours	2026-2045 and 2081-2099
		RCP8.5	3 hours	2026-2045 and 2081-2099
MIROC-ESM	1.4 x 1.4 degrees (approx. 150 km)	Historical	3 hours	1960-2005
		RCP4.5	3 hours	2026-2045 and 2081-2100
		RCP8.5	3 hours	2026-2045 and 2081-2100

Note: All RCMs are run to conform with standard NCEP boundaries as part of NARCAAP and CORDEX experiments (see Cordex website: <http://www.cordex.org/>), and GCM grids are established using standards from the WCRP. CORDEX is a WCRP project.

Data from regional climate models are downloaded at the three closest grid points of each station and the inverse distance weighted average is calculated. For the GCMs, because of their coarse spatial resolution, data are downloaded at the closest grid point. Apart from the CanRCM4 which has 1-hourly data, all the other models have 3-hourly data and in order to get data for different storm durations to match the observed data, we first applied aggregation method to the continuous precipitation to get lower resolution data and then derived the higher resolution data from the 24-hourly data using the ratio formula first introduced by Hershfield (1961), and adapted by Huff and Angel (1989) and Coulibaly and Shi (2005). This method has been largely used in the literature (e.g. Rahmani et al. 2014; Gensini et al., 2011; Coulibaly and Shi 2005, and others) and was preferred because it appears appropriate where sub-daily (hourly) data are not available.

Given that the selected climate models don't always have the same projected time periods, three time slices have been selected to allow a consistent inter-comparison and analysis of the

projected IDF. Those future time periods for the selected climate models are presented in the Table 3 along with the different climate models and scenario. Each climate model scenario is downscaled using both Delta change (DC) and Bias correction (BC) techniques (as described in section 3.4.2, below). Therefore, for each station an ensemble of IDF projections are generated. In this study, each ensemble represents 32 possible IDF curves.

Table 3: Time periods used for the projected IDF along with the model and scenarios

Projection (time periods)	Climate Model	Scenario	Downscaling
The 2030s (2026-2045) (12 IDF projections per station)	HadGEM2-ES	RCP4.5	BC & DC
		RCP8.5	BC & DC
	MIROC-ESM	RCP4.5	BC & DC
		RCP8.5	BC & DC
	CanRCM4-CanESM2	RCP4.5	BC & DC
		RCP8.5	BC & DC
The 2050s (2038-2070) (8 IDF projections per station)	CRCM3-CGCM3	SRES A2	BC & DC
	HRM3-HadCM3	SRES A2	BC & DC
	CanRCM4-CanESM2	RCP4.5	BC & DC
		RCP8.5	BC & DC
The 2080s (2081-2100) (12 IDF projections per station)	HadGEM2-ES	RCP4.5	BC & DC
		RCP8.5	BC & DC
	MIROC-ESM	RCP4.5	BC & DC
		RCP8.5	BC & DC
	CanRCM4-CanESM2	RCP4.5	BC & DC
		RCP8.5	BC & DC
Note: For each station an ensemble of 32 IDF projections are generated.			

3.4.2. Downscaling Methods

While regional climate model output represents dynamic downscaling of global climate model output, for many applications such as the derivation of IDF statistics, additional spatial and temporal downscaling may be required (Sharma et al. 2011; Lafon et al. 2012; Barsugli et al. 2013; Chen et al. 2013). As indicated in Section 3.1, the downscaling approaches selected in this study are the Delta change (DC) and the bias correction (BC) methods. The Delta change approach used herein is an enhanced version of the DC method first introduced by Olsson (2009). It is a simple but robust method for developing climate change information, and has been selected and implemented with the EU-project SUDPLAN (*Sustainable Urban Development Planner for Climate Change Adaptation*) (SUDPLAN, 2012).

In this DC approach, there is no need to match climate simulations to observations. The climate projections are used directly to estimate the change in design storm, and this change is applied to the historical intensities (Olsson et al., 2012). For a given combination of duration and frequency, the projected design storm I_p can then be expressed as:

$$I_p = I_o \frac{I_f}{I_c} \quad \text{Eq. (1)}$$

Where I_f and I_c are design storms (or intensity of a rainfall event for a given duration and return period) estimated using climate model simulations for current and future time period respectively and I_o is the design storm based on observed rainfall data. The key advantages of this method are that the main features (temporal and spatial variability) of the original time series are preserved and the bias inherent in climate model simulation is reduced (Olsson et al., 2012). In the particular case of IDF curve development where the main variable is sub-daily (even sub-hourly) data, this method is usually preferred to the other methods that are based on statistical relationships between variables or different durations. The rationale is that the performances of downscaling approaches based on statistical relationship become very limited when using sub-daily data due to the fact that the statistical properties of recorded station rainfall strongly diverge from the properties of grid-scale rainfall from climate model output when the time scale decreases, leading to a decrease in the strength of relationship between those two different scale variables (SUDPLAN, 2012). Because of its multiple advantages, this Delta change approach was recently

retained as the most appropriate rainfall downscaling method in the EU-project SUDPLAN (<http://sudplan.eu>).

In the bias correction (BC) method, a cumulative probability distribution function of simulated rainfall is adjusted to measured rainfall at meteorological stations, by assuming that both observed and simulated probability distribution functions are well approximated by a theoretical probability distribution function (Andrej and Kajfez-Bogataj, 2012). The first step in this method is therefore the selection of the appropriate theoretical probability distribution function that best approximates both observed and model-simulated rainfall. The BC method improves climate model simulations by correcting bias in model output data (Piani et al. 2010; Ines and Hansen 2006; Samuel et al. 2012) and became popular because of its performance and straightforward application. Inter-comparison studies have shown that distribution-based bias correction methods significantly outperform other bias correction techniques such as the moments-based (i.e. based on mean or standard deviation) and the regression-based techniques (Themebel et al. 2010; Teutschbein and Seibert 2012; Lafon et al. 2012; Chen et al. 2013). Samuel et al. 2012 have shown that Gamma distribution based bias correction is effective in correcting errors in GCM daily precipitation in Northern Ontario.

In this study, the BC method used is adopted from Samuel et al. 2012 to this context where only the precipitation intensities are corrected using the cumulative density function (CDF) of the GEV distribution, which was the most robust method according to the eleven tests described in Section 3.3. In fact, in this context of the IDF curves development, we are dealing typically with maximum annual rainfall for different storm durations and there is no need to correct precipitation frequency. For the bias correction implementation, the GEV distribution with three parameters is first fitted to observed and current model maximum annual rainfall intensities. Then the CDF of the GEV distribution (Eq.2) fitted to the current model data is mapped to the CDF of the observed data as shown in Eq. (3):

$$F_{(x; \mu, \sigma, k)} = \exp \left\{ - \left[1 + k \frac{(x - \mu)}{\sigma} \right]^{\frac{-1}{k}} \right\} \quad \text{Eq. (2)}$$

$$F_{(x; \mu, \sigma, k)} = \int_{\bar{x}}^x f(t) dt \quad \text{Eq. (3)}$$

where k , μ and σ are the shape, location, and scale parameters of GEV distribution, respectively. The parameters are determined using the Maximum Likelihood Estimation function (available in MATLAB Statistical Toolbox 2014). The bias corrected maximum annual rainfall intensity for the year k_2 was calculated by substituting the fitted GEV CDFs into Eq. (4) as follows:

$$I_{f_bc(k_2)} = F_{I_o}^{-1}(F_{I_f(k_2)}) \quad \text{Eq. (4)}$$

Where $F_{I_f(k_2)}$ is the CDF of future maximum annual rainfall intensity and F_{I_o} is the CDF of the observed annual maximum rainfall intensity.

4. RESULTS

4.1. Identified distributions

By considering all the eleven goodness of fit criteria presented in Appendix 3, the “best” and “second best” distributions for each station are identified. For the observed data, the GEV distribution is by far the best fit distribution followed by the lognormal distribution. Both distributions present a good fitting quality. Some of the other distributions (e.g. Gam, N) also present acceptable fitting quality for some stations, except the Gumbel distribution (EV1) and to a lesser extent the Weibull distribution. Similar findings on Gumbel distribution were reported by Burn and Taleghani (2012). The two best distributions for each station and for the different storm durations are presented in the Table 4. It is noteworthy that these results (Table 4) are not immune to uncertainties in the extreme rainfall data due to missing and/or erroneous rainfall extremes or quality control procedures.

The Gumbel distribution appears to be the least robust distribution amongst the set of candidates used, particularly when maximum-likelihood (ML) method is used for the parameter estimation. Most of the time, this distribution completely mismatches the lower tail of the data (see e.g. Figure 4, 5). When the distributions are fitted to the climate model data, the fitting quality is not as good as in the case of the observed data, but acceptable and GEV distribution still leads the group followed closely by the lognormal distribution. Detailed results of all the test results can be found in the Appendix to this report. For consistency and also to allow adequate comparison, the same distribution function should be used for all the design storms. Given its globally outstanding fitting quality for both observed and climate model data, the GEV distribution is then retained for all the design storm estimation.

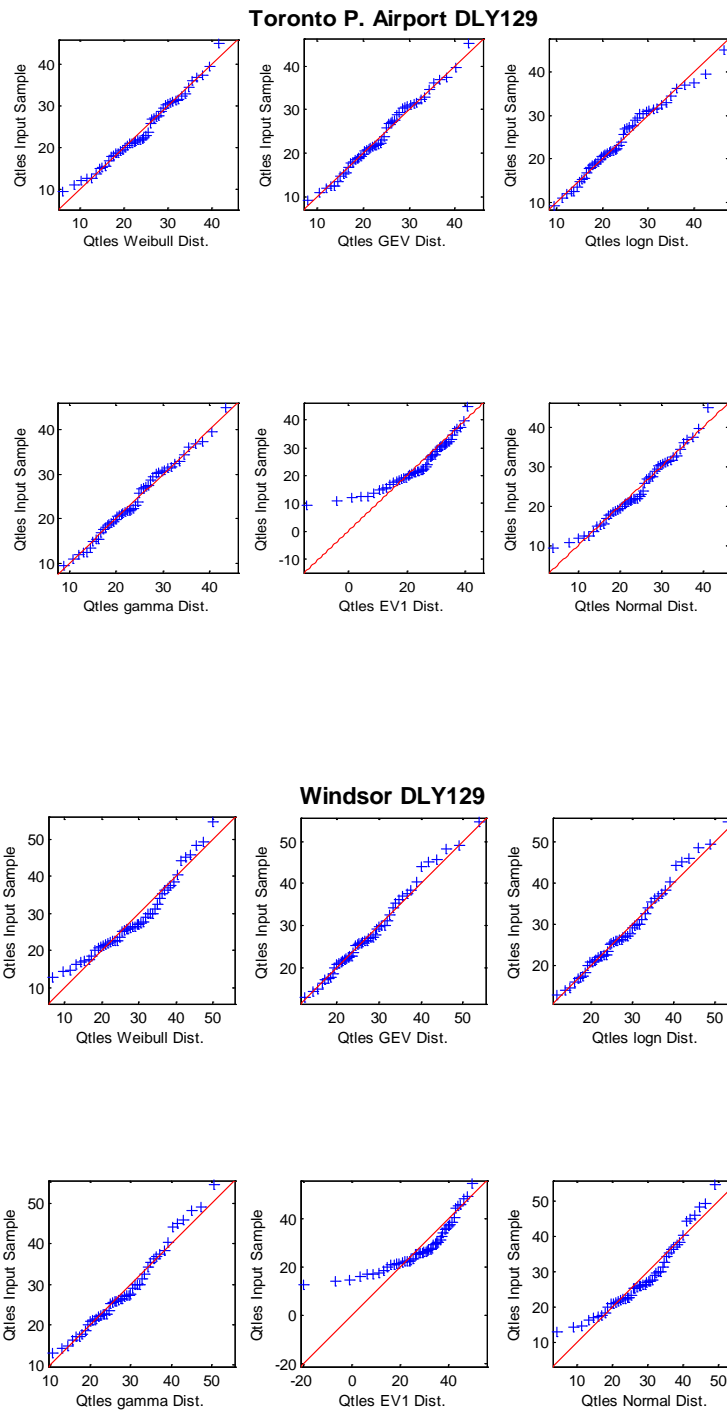
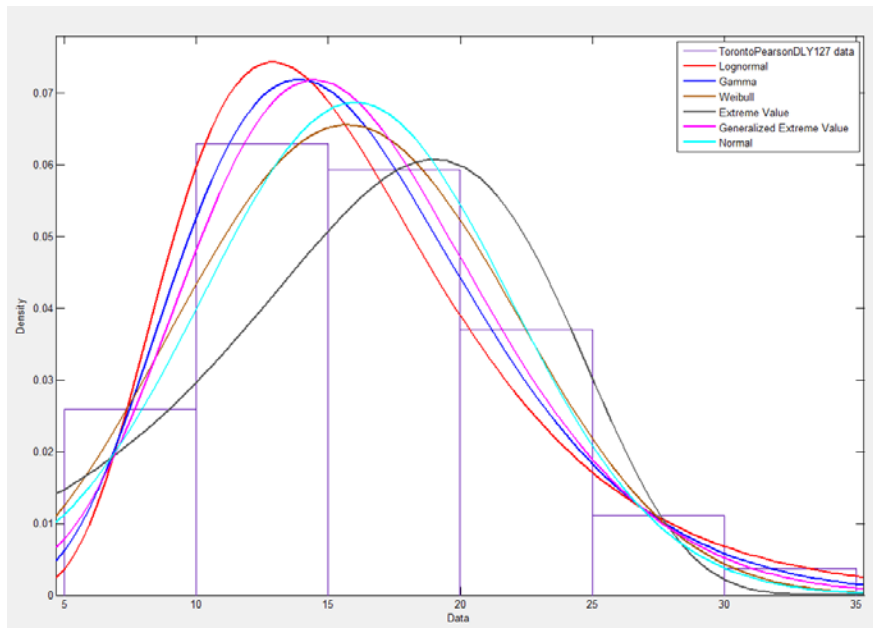


Figure 4: QQ-plot of hourly annual maximum precipitation at Toronto and Windsor Airports. Note: Gumbel distribution is EV1 (extreme value).

(a) Toronto P. Airport



(b) Windsor Airport

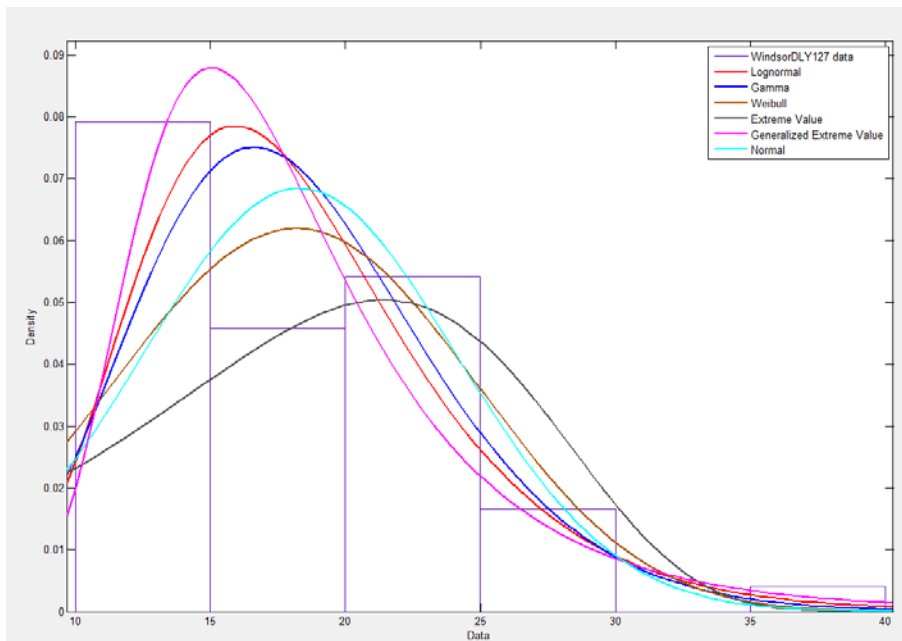


Figure 5: Histogram plot of 15-min annual maximum precipitation at (a) Toronto Airport and (b) Windsor Airport.

Table 4: Selected “best” and “second best” fit distributions to the observed data

DURATION	15-min		30-min		1-hr		2-hr		6-hr		12-hr		24-hr	
STATION	Best	2 nd best	Best	2 nd best	Best	2 nd best	Best	2 nd best	Best	2 nd best	Best	2 nd best	Best	2 nd best
Barrie	GEV	Gam	GEV	Gam	GEV	Gam	GEV	LN	GEV	LN	GEV	LN	GEV	LN
Fergus S. D	GEV	LN	GEV	LN	GEV	LN	GEV	LN	GEV	LN	LN	GEV	GEV	LN
Hamilton A.	GEV	LN	GEV	LN	GEV	LN	GEV	LN	GEV	LN	GEV	LN	LN	GEV
Kingston PS.	LN	N, GEV	GEV	N	GEV	N	GEV	LN	GEV	LN	GEV	LN	GEV	LN
London A.	GEV	LN	GEV	LN	GEV	LN	GEV	LN, Gam	GEV	LN	GEV	LN	LN	GEV
Oshawa WPCP	GEV	N	GEV	N	GEV	Gam, N	GEV	LN, Gam	GEV	LN	GEV	LN	GEV	LN
Toronto	GEV	LN	GEV	LN	GEV	LN, N	GEV	LN	GEV	LN, N	GEV	N	GEV	LN
Toronto A.	GEV	LN, N	GEV	Gam	GEV	Gam	GEV	LN	GEV	LN	GEV	LN	GEV	LN
Trenton A.	GEV	LN	GEV	LN	GEV	LN	GEV	LN	GEV	LN	GEV	LN	GEV	LN
Windsor A.	GEV	LN	GEV	LN	GEV	LN	GEV	LN, Gam	GEV	LN	GEV	LN	GEV	LN
Chatham WPCP	GEV	LN	GEV	LN, Gam	GEV	Gam	GEV	Gam	GEV	Gam	GEV	Gam	LN	GEV
Harrow CDA	GEV	N, Wbl	GEV	Gam	GEV	LN	GEV	LN	GEV	LN	GEV	LN	GEV	LN
ANN_Arbor	GEV	LN	GEV	LN	LN	GEV	LN	GEV, Gam	GEV	LN	GEV	LN	GEV	LN
Howell	Gam	GEV	GEV	LN,Gam	GEV	LN	GEV	LN	GEV	LN	GEV	LN	GEV	LN
Marion	LN	GEV, Gam	LN	GEV, Gam	GEV	LN	GEV	LN	GEV	LN, Gam	LN	GEV, Gam	LN	GEV, Gam

The Generalized extreme value (GEV) is a three parameter distribution and its cumulative distribution function can be written as:

$$F_{(x)} = \exp \left\{ - \left[1 + k \frac{(x-\mu)}{\sigma} \right]^{\frac{-1}{k}} \right\} \quad \text{For } k \neq 0 \quad \text{Eq. (5)}$$

Where k , μ and σ are the shape, location, and scale parameters. This distribution is widely used in hydrology because of its flexibility. In fact, it is a combination of three different distributions (specific cases for $k=0$, $k>0$ or $k<0$), and allows an application without any a priori assumption/constraint about the value of the parameter k .

Using the GEV distribution, the current IDF curves obtained from historical storm events for the Windsor and Toronto regions for three storm durations namely short (15 min), medium (3 hour) and long (12 hour) are presented in Figure 6. First, it can be seen that in general, Windsor stations reveal higher storm event intensities compared to Toronto area stations. Second, storms of short duration (15 min) have higher intensities, and conversely storms of longer duration (12-hr) exhibit lower intensities. In the Windsor region, station Harrow shows a consistently different pattern compared to other stations within the area. This may be due to the specific location of the station or the occurrence of a large storm in 1989 that was not recorded in any of the other Windsor area stations. However further analysis is needed to substantiate the hypothesis.

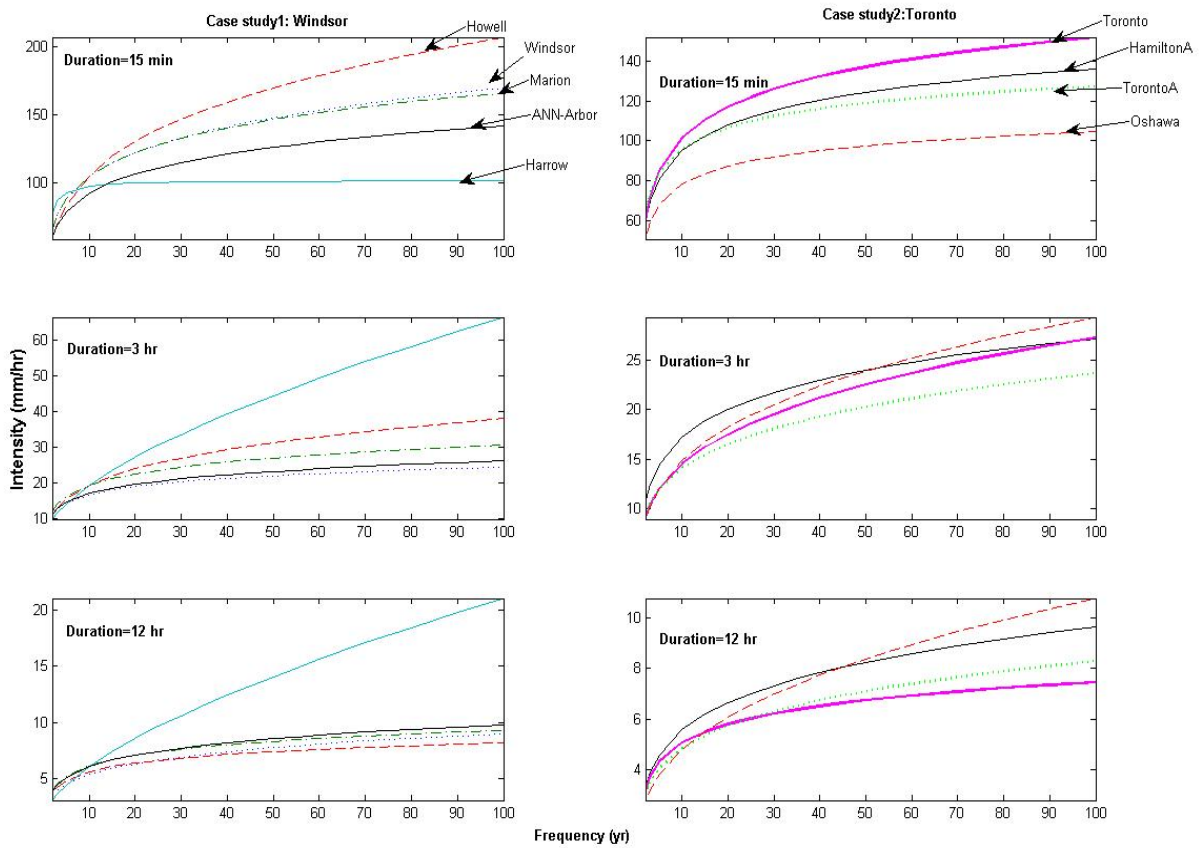


Figure 6: Variability of historical storm event intensities for all the stations in each study area. Each curve is based on the GEV distribution.

4.2. Current period estimates

Although the projected future IDF statistics are established using downscaling methods, the ability of the climate models to reproduce the historically observed IDF data should be investigated. It is known that one of the biggest challenges in climate change impact studies remains the limitations of climate models themselves. Downscaling does not remove all the bias in modeled data and therefore the model that best reproduces the historical IDF records is generally regarded as being the most robust for producing future projection or as being the best able to capture the atmospheric physics associated with past extreme rainfall events (Barsugli et al. 2013). Conversely, models with a less robust ability to reproduce historical IDF values are regarded as being less reliable in the development of future IDF estimates. That being said, the IPCC (2014) and recent work by Charon (2014) on the use and interpretation of climate projections suggest that no single climate model can be regarded as “the best”, or most accurate in term of future climate projections, and that all projections should be regarded as plausible. Additionally, in the development of guidance for the application of climate model scenarios for water budget modeling under Ontario’s Source Water Protection program, the province also advised that no single projection should be used, but rather an ensemble of projections (AquaResource, 2011). Similar approaches have been presented for the analysis of flood risk in Wilby et al. (2014). The purpose of the model assessment presented in this section is not to suggest that one model should be used over another, but rather to demonstrate the variability in climate model skill in producing IDF information.

To analyze and compare the ability of the selected climate models in reproducing the current (or historic) IDF in Toronto and Windsor areas, scatterplots are presented in Figure 7. Those graphs show that for both Toronto and Windsor areas, the CanRCM4, and to some extent the HadGEM2-ES and HRM3 outputs capture better the current extreme rainfall events. The MIROC and the CRCM3 mostly underestimate the current extreme rainfall events compared to other models while the HRM3 estimates are predominately higher than the historic ones. These differences are net result of variations in the assumptions and parameterization of the different GCMs and RCMs, however additional study is needed to elucidate the specific level of contribution of each factor. When comparing both regions, it can be noticed that the climate model current estimates are better in the Toronto area than in the Windsor area, particularly for higher-intensity, or more infrequent, storms. Those disparities in the models’ performances can be explained mostly by the difference in the climate models (e.g. different physical parameterizations, numerical schemes, thermodynamic processes, resolutions, etc.) and in part by the varying complexity and frequency of storm events/types. It is typically assumed that the climate models with better performance for

the current period will provide better results after downscaling as well. Figure 7 also demonstrated that, as expected, when these biases are corrected, the overall skill improves significantly.

However, it should be mentioned that some studies suggest that the practice of picking best models may have some pitfalls and use of a larger ensemble is best (e.g. Weigel et al. 2010). Some other literature supports the use of best performing models but more literature likely suggests rejection of poorly performing models (e.g. Barsugli et al. 2013; Thober and Samaniego 2014).

As indicated in Section 3.4, here the best performing climate models in Eastern North America (Sheffield et al. 2013; Kharin et al. 2013) were selected. The downscaled results confirm that best performing climate models do yield better downscaled results. This is particularly important in the context of extreme rainfall events that are usually poorly captured by climate models including RCMs (Barsugli et al. 2013). Results shown in Figure 7 also confirm that bias correction is needed even for RCM data.

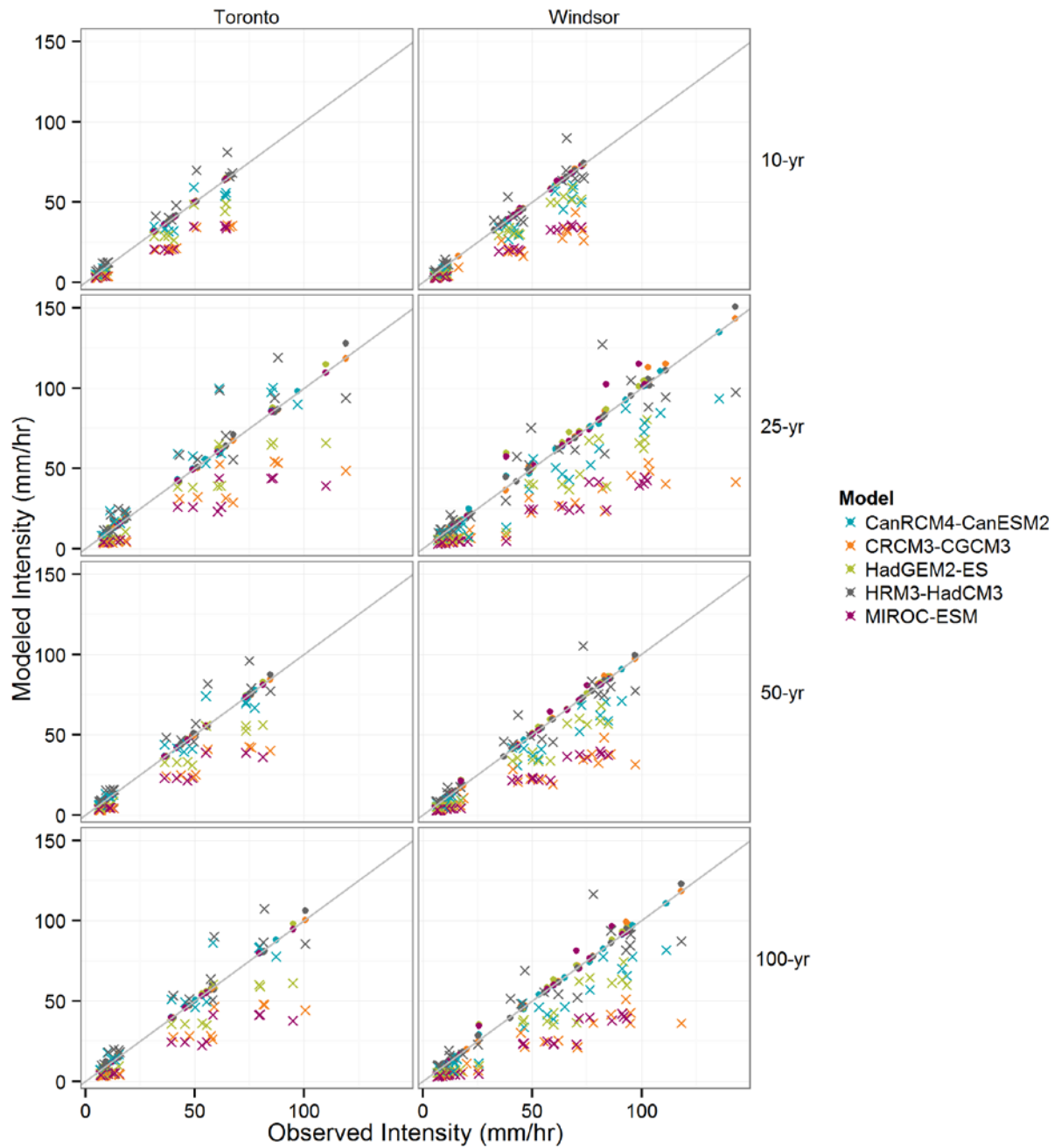


Figure 7: Scatterplots of the observed versus modeled and bias-corrected storm intensities for all stations in the Windsor and Toronto study areas. Solid points represent the bias-corrected dataset (CBC) and the crosses represent the raw current climate model data (CC).

We can also notice that the bias between observed and modeled intensities tend to increase with decreasing storm duration and increasing return period (Figures 8 and 9). This is not surprising since the highest storm intensities are those with the shorter durations and longer return periods or convectively driven rainfall processes. From the residual plots in Figures 8 and 9, the most robust model outputs are considered to be those with smaller residuals (i.e. residuals are closer to zero line), while the least robust models exhibit larger residuals. Negative residuals indicate that the model under-estimates the observations whereas positive residuals indicate over-estimation. It can be observed that in general that, based on these criteria, for both the Toronto and Windsor regions, HADGEM and CANRCM4 are the “best performing” climate models, while MIROC, CRCM3, HRM3 are the lesser performing (MIROC, CRCM3 the worst). It is also notable that in general, the models tend to under-estimate historical precipitation more in the Windsor stations compared to the stations in Toronto. For the 15-minute and 3-hour storms, almost all residuals in Windsor are negative, whereas those in Toronto tend to show positive residuals for some models.

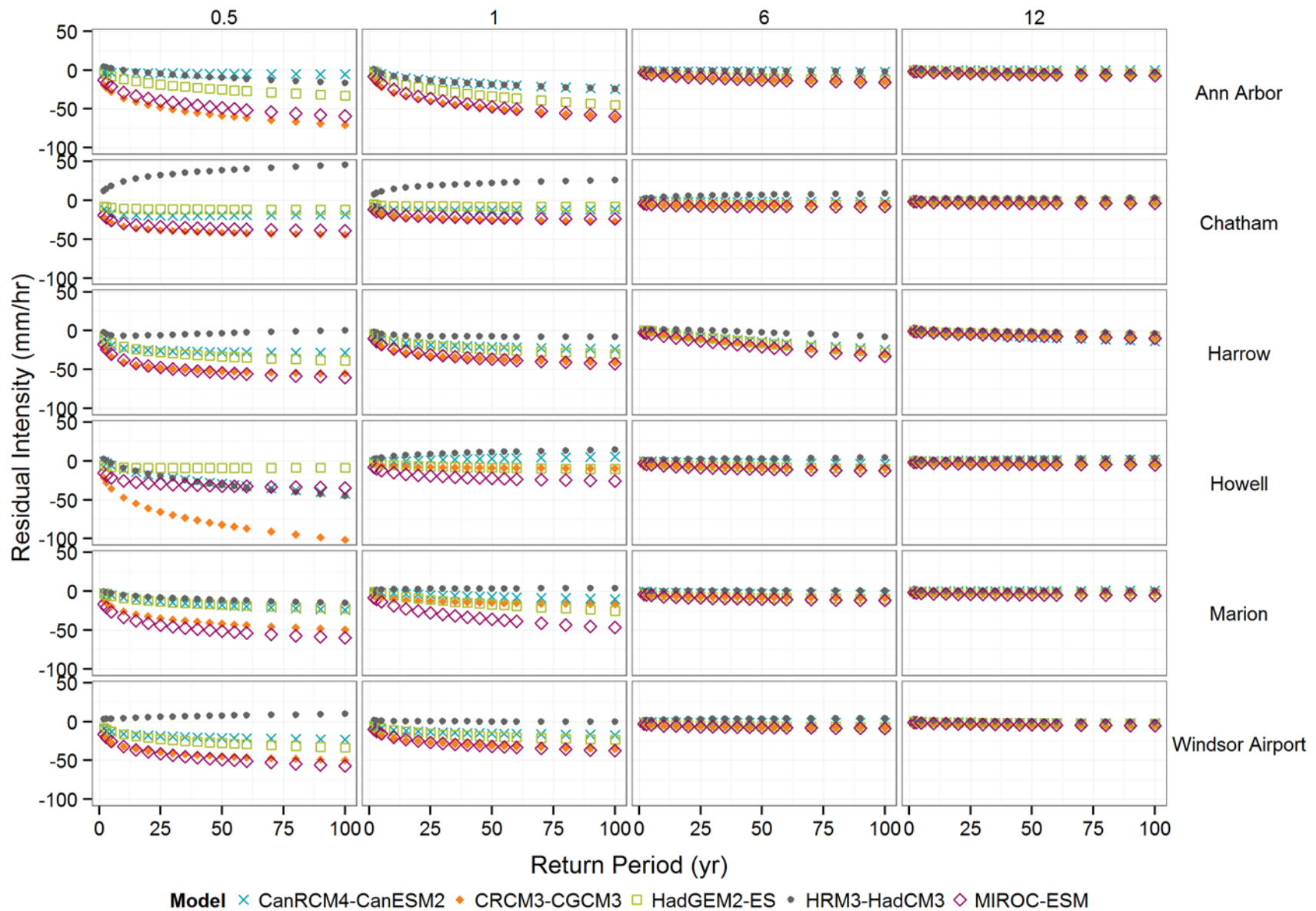


Figure 8: Residual plots of climate model results for current period for the Windsor region. The closest residuals to the zero line indicate the most robust climate model.

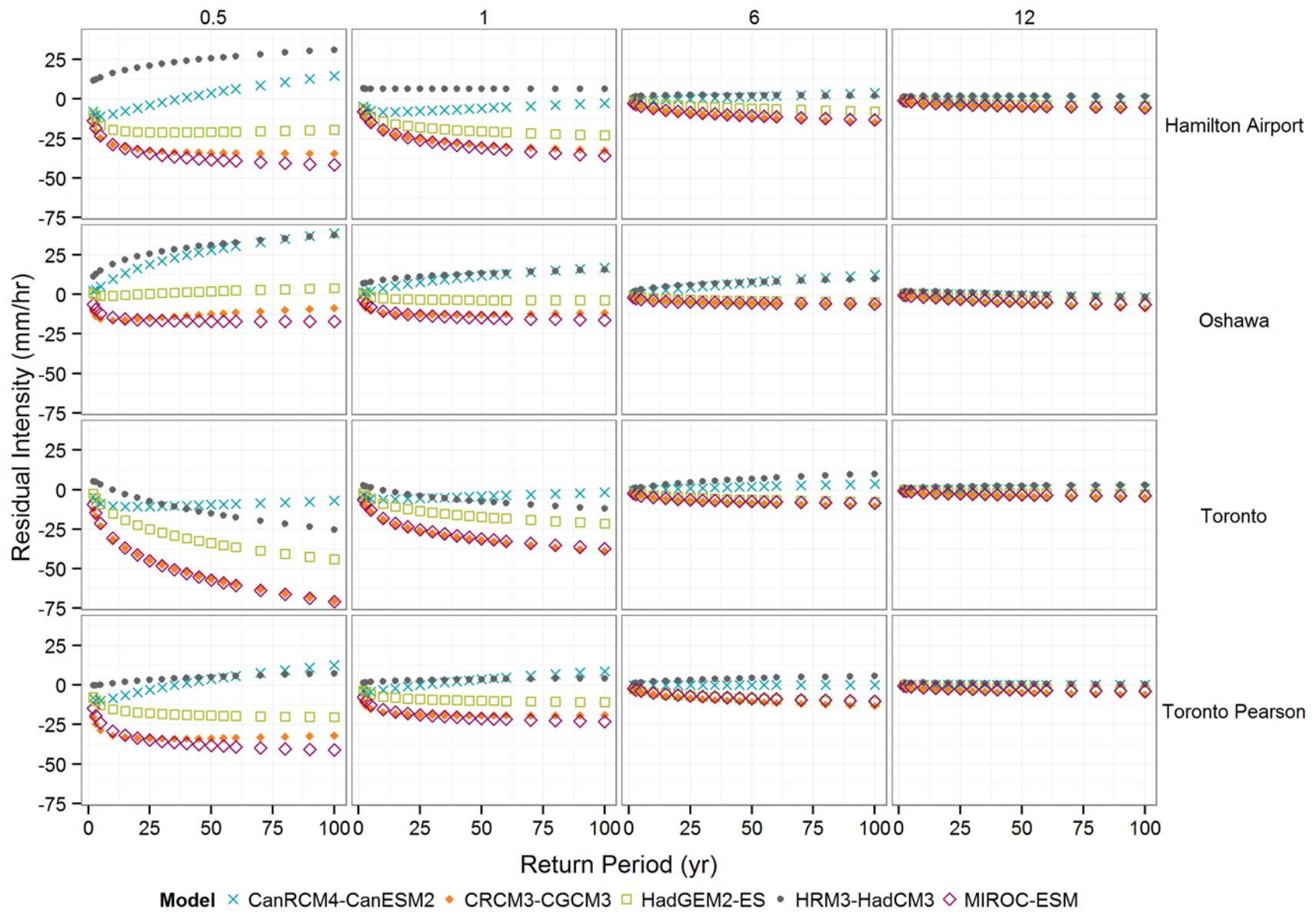


Figure 9: Residual plots of climate model results for current period for the Toronto region. The closest residuals to the zero line indicate the most robust climate model.

4.3. Future Projections

As described previously, future projections of IDF curves are affected by a number sources of variability and uncertainty. Within the context of this study, the major sources of variability and uncertainty are introduced by: a) selection of climate model, both regional and global, b) selection of emission scenario, and d) selection of downscaling techniques. To capture the variability of IDF projections, an ensemble of IDF curves are generated using different climate models with different forcing emission scenarios and downscaling techniques. This includes three RCMs (CRCM3 and HRM3 with A2 SRES scenario, CanRCM4 with RCP4.5, RCP8.5 scenario) and two GCMs (HadGEM2-ES and MIROC-ESM with RCP4.5, RCP8.5 each) downscaled using BC and DC techniques for three future periods (2050s, 2070s,2100s) and three types of storms (short, medium and long duration). As a result, an ensemble of 32 IDF projections are generated for each station.

In some very few cases outliers were introduced into the ensemble due to extreme values present in the climate model projection time series and thus preserved through the downscaling (specifically the BC) process. For example some extremely high rainfall intensity values of about 2 times larger than historical observed values were present in the future IDF results after downscaling. It should be noted that the DC method corrects automatically such outliers, thus the outliers were only present in the future bias corrected dataset (FBC). A correction was therefore applied to remove these outliers prior to the comparison. This correction procedure involved first identifying all the outliers (or large values) in the IDF tables, which was done by ordering all the values in the database and flagging all extreme values above a threshold of 300 mm/hr which is the maximum historical rainfall intensity plus standard deviation. Each value was then manually checked by comparing it with the other records for the stations of similar storm types (frequency and intensity). Following this, a correction was applied to all projected outliers that were 2 times larger than the historic observed value. This correction involved transferring the change ratio derived from the current bias corrected data (CBC) to the climate model raw future (CF) predictions to obtain the corrected future bias corrected data (FBC). Precisely, when a large FBC value is found, it is replaced by (Eq. 6):

$$\text{corrected FBC} = \frac{\text{CBC}}{\text{CC}} \text{CF} \quad \text{Eq. (6)}$$

Where CC is climate model current value. Despite implementing this correction routine, it is still possible that outliers exist within the ensemble due to extreme values in the climate model time series for a particular storm type.

Figures 10 and 11 present boxplots of ensemble IDF curves obtained from all climate models, downscaling techniques and emission scenarios for all stations in the study areas of Toronto and Windsor respectively overlain with the historically observed data from each station. These plots are broken down by future time period. The aim of this analysis is to examine the variability associated with the combination of the set of climate model projections and downscaling approaches analyzed in this study. The 25th and 75th percentiles of ensemble storm event intensities (box plots upper and lower quartiles) show the range of uncertainty after removing outliers, as described by the procedure above. Overall, it can be seen (Figures 10 and 11) that higher variability in future IDF curves is predicted in Windsor region compared to Toronto area, however in both study areas there is a common trend of uncertainty decreasing as storm durations increase and return periods decrease. Additionally, despite removing outliers, it appears that the Windsor dataset still contains some more extreme values as compared to Toronto, especially for the 3-hour storm duration. There also appears to be an outlier value for the 24-hour 100-year event in the Toronto study area (Figure 10).

Overall, it is apparent from Figure 10 and 11 that the variability among climate model projections is in general greater than that associated with geographic variability among stations. The 25th to 75th percentile ranges in Windsor area are also greater than that for Toronto region. For shorter return period events (25 years or less), the overall variability range is however about the same for both Windsor and Toronto regions. Interestingly, it appears that for 5, 10 and 20 year return periods, the future IDF curve variability as shown in Figures 10 and 11 is quite small and might be even smaller if worst performing models were rejected or alternatively, only best performing climate models (HADGEM and CANRCM4) results were plotted. That being said, the subset of projection datasets presented in this study only represents a very small proportion of all possible future climate datasets, and as such it is important to look at the overall range of minimum to maximum projections presented in Figures 10 and 11. Such an examination reveals that even for relatively low-to-moderate-risk storm frequencies that are often considered in roadway drainage design (MOE 2003), such as the 10-year 1-hour storm, variability among the climate models examined in this study exceeds that associated with inter-station variability in each study area. This variability is significant for the more extreme storm events, such as the 15 or 30 minute duration storms.

Figures 12 and 13 present a comparison of the IDF curve values for a single period (2050s) only for the higher forcing scenario of A2 or RCP8.5, depending on the model for the 10 and 25 year, and 50 and 100 year return period storms, respectively. This comparison demonstrates that the uncertainty is reduced when one considers only one scenario, as compared to Figures 10 and 11, which incorporated the A2, RCP4.5 and RCP8.5 scenarios. For both study areas and all storm return periods presented in Figures 10 and 11, variability among projections remains the highest for shorter-duration events. Interestingly, this analysis shows that almost all future projections for the Toronto area are within the bounds of the historical observed data for that study area. That being said, if one were only to examine a single station, there would be great variability. The same pattern is not visible for the Windsor stations. Figures 12 and 13 demonstrate significant variability, above the historical range of all stations in Windsor area for all storm durations of 3-hours and below, except for the outlier at the 3-hour duration which is from the Harrow station representing a 1989 event recorded only at that location.

The results in Figure 12 and 13 also demonstrate that the bias correction and delta change downscaling methods resulted in almost identical effects in correcting the raw climate change model outputs for the Toronto Airport station for the 10 and 25 year events (Figure 12). That being said, the bias correction method resulted in lower overall variability at the Toronto study area for the 50 and 100 year events. The delta change method reduced the variability more in the Windsor study area across almost all storm events. It is also relevant to note that both downscaling methods had a much larger effect in Windsor compared to Toronto.

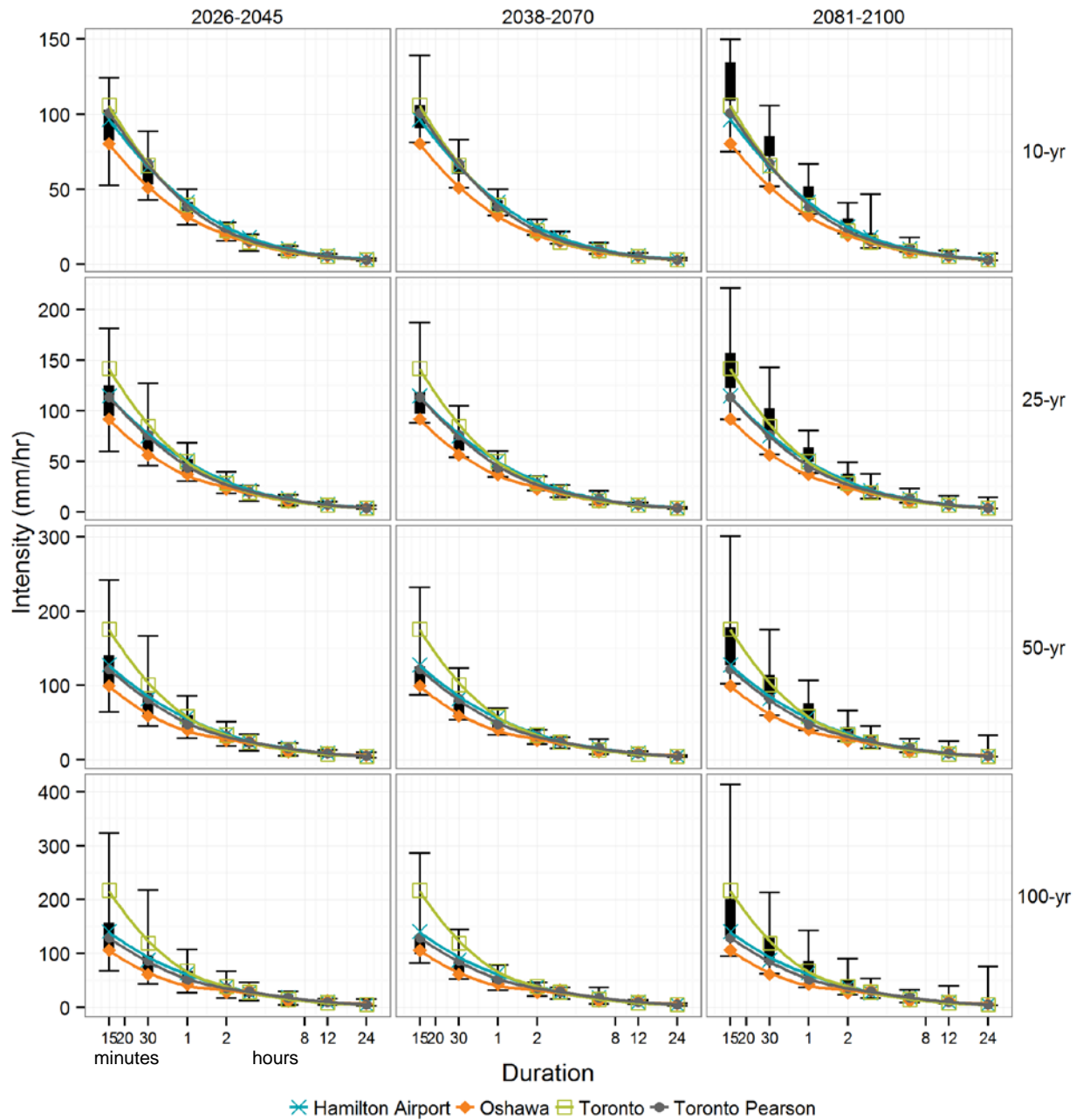


Figure 10: Overlay of historical IDF curves for all stations in the Toronto study area compared with box plots of the downscaled future IDF curves. Boxes represent the 25th to 75th percentiles of projections for each period from the downscaled datasets and whiskers represent the minimum and maximum values within the ensemble.

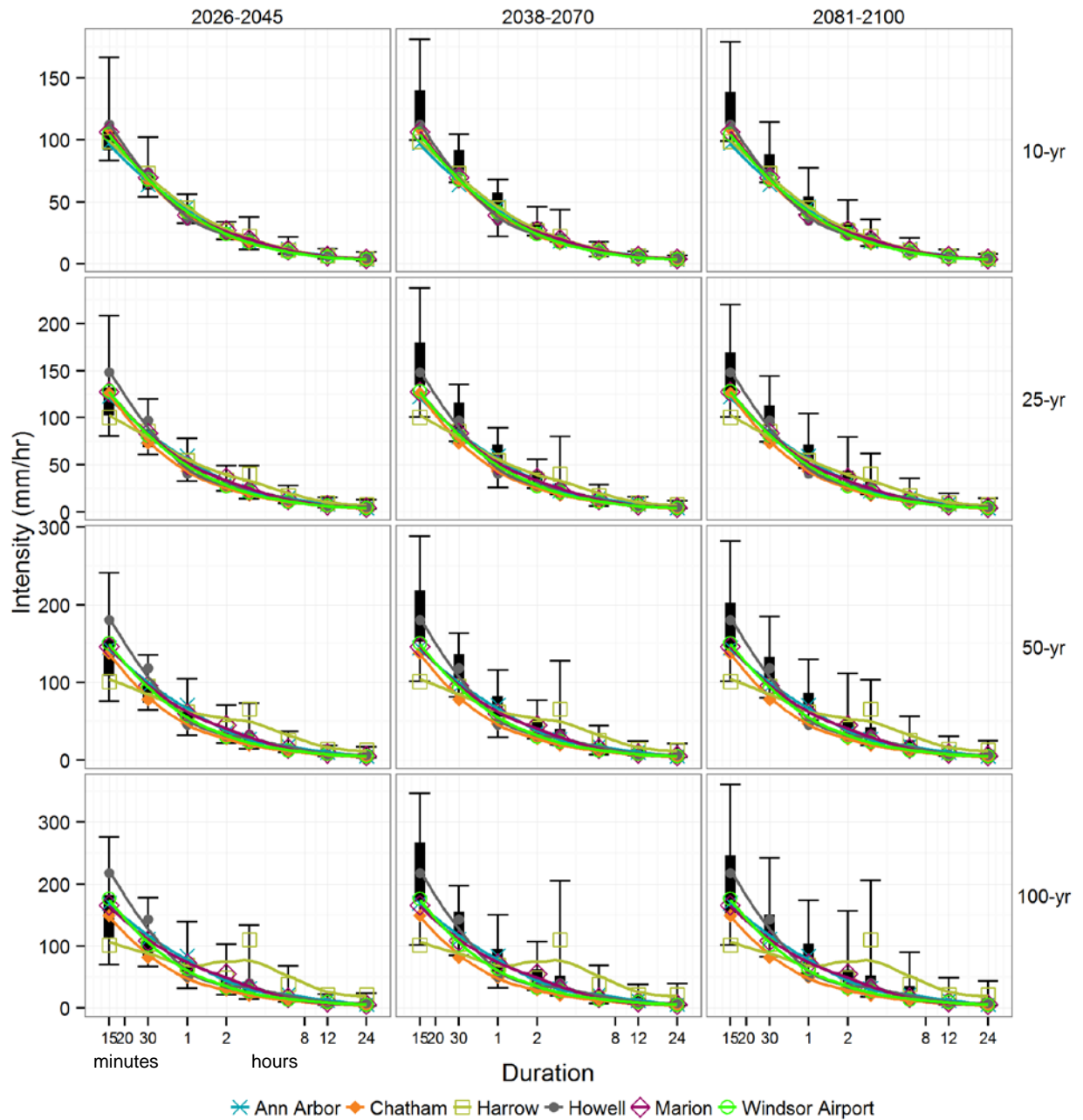


Figure 11: Overlay of historical IDF curves for all stations in the Windsor study area compared with box plots of the downscaled future IDF curves. Boxes represent the 10th to 90th percentiles of projections for each period from the downscaled datasets and whiskers represent the minimum and maximum values within the ensemble.

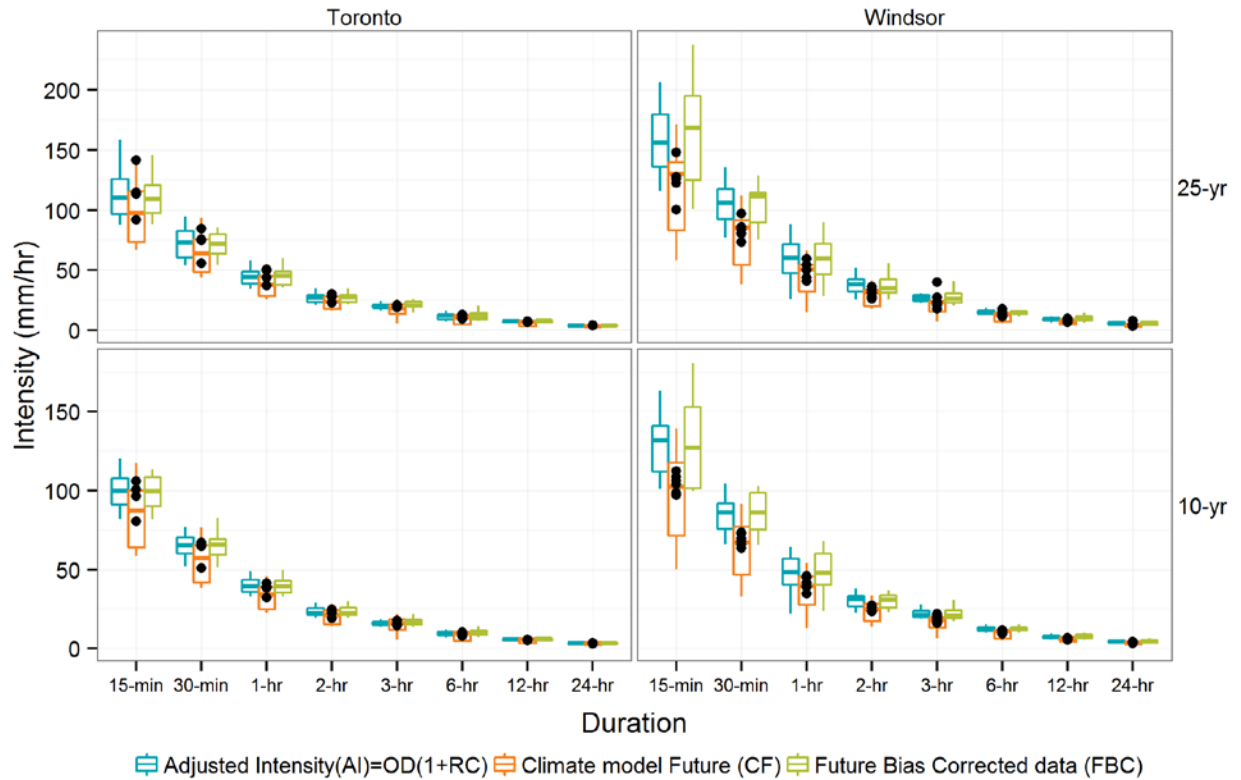


Figure 12: Summary of all future projections for the 10 and 25 year return period storms for the high-forcing A2 and RCP8.5 scenarios summarized for all stations in each case study area. Box plots represent the three future climate datasets of data raw climate model output, and downscaled datasets using DC (or AI: adjusted intensity) method and bias-correction method. Black dots represent historical values.

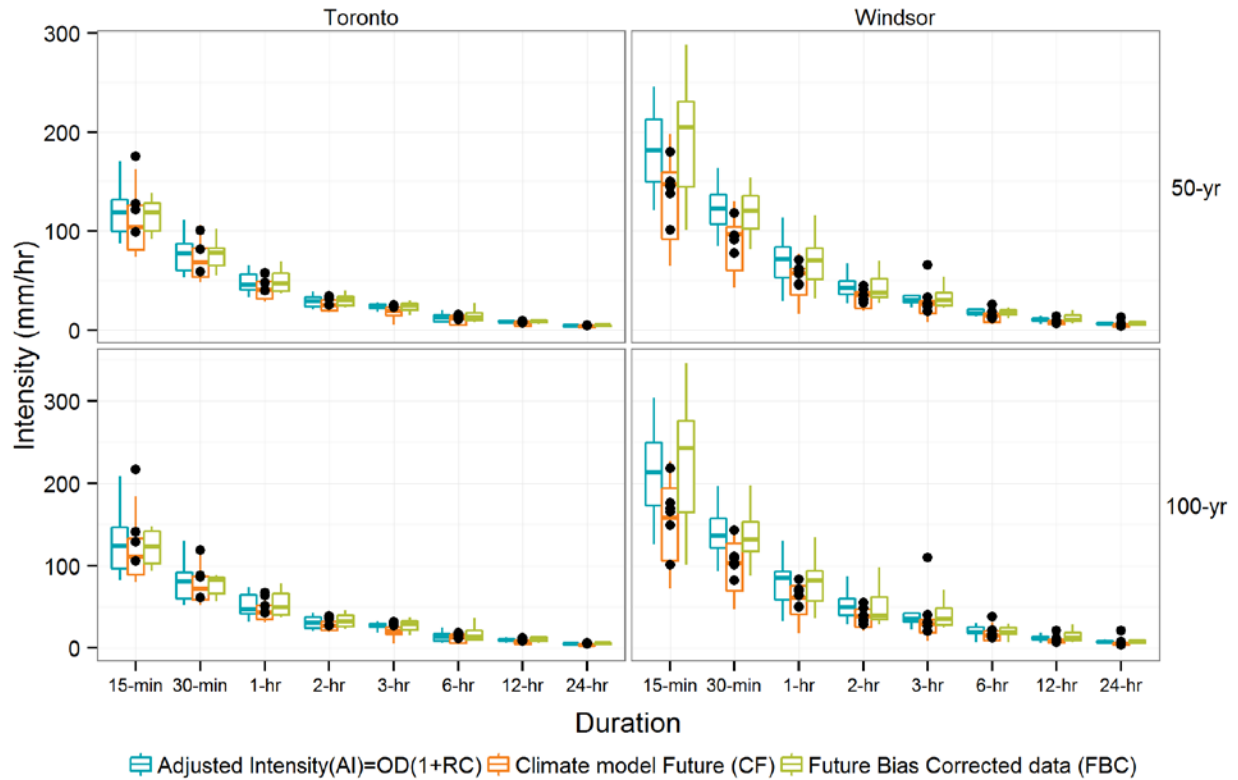


Figure 13: Summary of all future projections for the 50 and 100 year return period storms for the 2050s (2038-2070) for the high-forcing A2 and RCP8.5 scenarios summarized for all stations in each case study area. Box plots represent the three future climate datasets of data raw climate model output, and downscaled datasets using DC (or AI: adjusted intensity) method and bias-correction method. Black dots represent historical values.

5. DISCUSSION AND CONCLUSIONS

The results of this study highlight the extent of variability associated with using an array of climate projections to develop future IDF curves. This variability is due to a wide range of choices in distribution functions, climate models, emission scenarios, and downscaling techniques. Results of the distribution function evaluation demonstrate clearly that current IDF curves generated with a Gumbel distribution may not be the most robust for a given study area. In fact, for both the Windsor and Toronto study areas, the GEV distribution produced stronger results which is consistent with previous findings based on the evaluation completed using a multi-criteria framework of model performance tests (Paixao et al., 2011). This raises an important general conclusion, which is that baseline IDF curves based on historic observed data are generated using a range of assumptions, which require re-examination in light of the nonstationarity and alterations in local precipitation regimes associated with climate change and new data processes such as more use of automated data quality control procedures. This should include the re-examination of distribution functions as well as the commonly used methods assume stationarity of rainfall time series.

Based on the ensemble of results developed through this study, the variability among future projections should be regarded as significant, resulting in a high level of uncertainty with respect to the future IDF curves. This high level of variability is associated with levels of uncertainty, which is greatest for short-duration and moderate-to-high return period events, for example the 15-minute to 1-hour 25- to 100-year storms, making it difficult to interpret a single design threshold for water management applications. Shorter return-period and longer-duration events, (i.e., 5-20 year return-period and 3-24 hour events), were substantially lower in their uncertainty, suggesting a useful range of design storm values for practitioners to choose from, albeit with caution. Overall, the analysis in this study showed larger variability in future IDFs for Windsor region compared to Toronto area, suggesting that it would not be appropriate to transfer results from one location to another. Analysis also suggested that there is significant baseline variability among IDF curves for a given study area, further reinforcing the conclusions that (1) it is difficult to apply IDF statistics from one station to even a nearby one and (2) that relying on a single IDF curve for water management applications may not capture the full range of extreme precipitation risk in a given area. Ultimately, when one considers the compounding effect of uncertainties in baseline IDF curves due to analytical assumptions (i.e., distribution selection, statistical uncertainty, data quality control, missing data), natural geographic variability for given study area, and the variability in future climate projections, it is reasonable to call for a re-questioning of the levels of risk accepted

in stormwater design. In particular, given the assumptions of stationarity inherently implied in IDF analysis, it is also reasonable to question the applicability of the current approach for managing short-duration and high-intensity events in southern Ontario. These conclusions become even more salient considering that the results presented in this study are for a small subset of future climate projections that represent the most current best-performing models for the study area as per Sheffield et al. (2013).

Depending on the specific storm event under consideration, the projected changes in the IDF curves are quite small for the short term (2030s) and increase after that period when the impact of GHGs on the climate becomes more significant. At this stage of the knowledge, for Toronto and Windsor regions, it can be suggested that for the future climate datasets evaluated in this study, the IDF changes from the GEV distribution and downscaled using either the DC and/or BC methods on the HadGEM2-EM and CanCRM4 predictions appear the most robust. The rationale is that for longer return periods (> 50 years) and for commonly used rainfall durations (30min, 1hr, 2hr, 3hr), there is no significant difference between DC and BC in term for future IDF projections based on HadGEM2-EM and CanCRM4 data. The choice of the distribution function, the climate model and emission scenario appears the most critical in that case.

Given however, that individual models show large spread in the projected design storms, the use of multi-model approach based on best performing climate models (or rejection of the poorest performing climate models) based on climatological expertise with climate model performance should be recommended in order to extract more robust climate change signals. In addition, probabilistic analysis should be performed to quantify the uncertainty related to each step of the IDF development process. However, it is essential to first assess the most appropriate and efficient climate models and statistical distribution functions for the region of interest. The use of multiple emission scenarios is also essential since it is currently unclear which scenario will prevail in the future.

Finally, it is also recommended that future study should investigate the development of regional IDF curves using copula techniques to address the issue of nonstationarity in some of the rainfall series. A space-time variability analysis of annual maximum precipitation should be first carried out to document nonstationarity in the time series, and guidance should be provided for cases where recent historical extreme rainfall IDF trends are downwards. This appears essential for areas with complex rainfall patterns such as Windsor and Hamilton regions. Given the uncertainty in future IDF curves, it is recommended that weight-of-evidence approaches be used when

responding to potential extreme precipitation risks at the local scale. Such an approach would rely on professional judgement, multiple lines of evidence, and a variety of analytical tools, as is typically implemented in risk assessment, to identify and characterize the hazards and vulnerabilities associated with extreme precipitation (CSA, 2012). This notion is well captured in the concept of resilience, which is often used as a management objective and framework to responding to climate risks. Resiliency is typically defined as the ability of a system to withstand a range of conditions and maintain its adaptive capacity despite exposure to hazardous conditions (adapted from Tyler and Moench 2012; CSA PLUS 2012) and can be achieved through changes to infrastructure, policy and through a systems-based analysis of risk. While future IDF curves, such as those generated in this study may form part of the evidence base for adaptation to extreme precipitation risk, it is also critical that approaches incorporate historical extremes (including interpretation and guidance when historical extremes are decreasing), and information on the thresholds and vulnerabilities of systems exposed to the extreme precipitation regime in question. The corollary for policy and infrastructure decision making is that resiliency-based strategies, including characterizing hydrologic responses and vulnerabilities to a range of extreme precipitation regimes using a combination of empirical evidence of impacts and dynamical modeling, offer the most promising response to climate change, as it effects extreme precipitation.

6. RECOMMENDATIONS

This study highlighted the complexity of the development of future IDF projections and the various sources of uncertainty involved. An important step was completed in the search for adequate IDF information for water resources manager in the study areas. This study results bring us among the most advanced groups in Canada in term of future IDF development and provide the baseline information needed to move forwards, and lead to the following recommendations.

- Based on this study results, it is recommended that further study is needed in the selected study areas to better understand and refine the uncertainties involve in the future IDF statistics. This appears necessary before major change in infrastructure design standards in the study areas.
- Further study should first involve the analysis of non-stationarity in the extreme rainfall series in the study areas. It has been recently shown that the assumption of stationarity currently used in future IDF development methods may lead to underestimation of extreme precipitation by as much as 60% (Cheng and Aghakouchak 2014) which could significantly affect infrastructure design.

Second, further study should include the investigation of regional IDF development methods which have been recently shown to outperform the single station-based methods (Burn 2014, Cannon 2015). The regional IDF methods should incorporate non-stationary approaches such as Bayesian inference that allows for estimating IDF with their uncertainties. Such study is part of the FloodNet Research Program¹ and will require active contribution from FloodNet partners in selected study areas.

The development of future IDF statistics adequate for municipal engineers and decision makers, is at the frontier of science and engineering, and requires active collaboration between end users and experts because the outcome may involve a learning to use a range of values instead of the old single number approach.

¹<http://www.nsercfloodnet.ca>

REFERENCES

- Anctil F., J. Rousselle, N. Lauzon, 2005. Hydrologie: Cheminements de l'eau. Editions Presse Internationale Polytechnique, 2005. 317 p.
- Barsugli, J., Guentchev, G., Horton, R.M, Wood, A., Mearns, L.D. (2013). The Practitioner's Dilemma: How to Assess the Credibility of Downscaled Climate Projections. EOS 94(46): 424-425.
- Bengtsson L, Milotti S. 2010. Intensive storms in Malmö. *Hydrological Processes* 24: 3462–3475
- Bougadis, J., Adamowski, K. (2006). Scaling model of a rainfall intensity-duration-frequency relationship, *Hydrol. Process.* 20, 3747–3757.
- Burn and Taleghani (2012). Estimates of changes in design rainfall values for Canada
- Burn, D.H. 2014. A framework for regional estimation of intensity–duration– frequency (IDF) curves. *Hydrol. Processes*, 28: 4209-4218.
- Cannon, A.J. 2015. An intercomparison of regional and at-site rainfall extreme value analyses in southern British Columbia, Canada. *Can. J. Civ. Eng.* **42**: 107–119. [dx.doi.org/10.1139/cjce-2014-0361](https://doi.org/10.1139/cjce-2014-0361)
- Cheng, C. S., Li, G., Li, Q. and Auld, H. 2011. A Synoptic Weather-Typing Approach to Project Future Daily Rainfall and Extremes at Local Scale in Ontario, Canada. *J. Clim.* 24, 3667–3685.
- Cheng, L. & AghaKouchak, A. 2014. Nonstationary Precipitation Intensity-Duration-Frequency Curves for Infrastructure Design in a Changing Climate. Scientific Report 4, 7093; DOI:10.1038/srep07093
- Coulibaly, P. 2006. Spatial and temporal variability of Canadian seasonal precipitation (1900-2000). *Advances in Water Resources*, 29: 1846-1865.
- Covey C, Rao KM, Cubasch U, Jones P, Lambert SJ, Mann ME, Phillips TJ, Taylor KE (2003) An overview of results from the Coupled Model Intercomparison Project (CMIP). *Glob Planet Change* 37:103–133
- Cheng, C. S., Li, G., Li, Q. & Auld, H. 2010. A Synoptic Weather Typing Approach to Simulate Daily Rainfall and Extremes in Ontario, Canada: Potential for Climate Change Projections. *J. Appl. Meteorol. Climatol.* 49, 845–866.

Ceglar Andrej and Lucka Kajfez-Bogataj 2012. Simulation of maize yield in current and changed climatic conditions: Addressing modelling uncertainties and the importance of bias correction in climate model simulations. *Europ. J. Agronomy* 37 (2012) 83– 95.

Chen, J., Brissette, F., Chaumont, D. and Braun, M. 2013. Finding appropriate bias correction methods in downscaling precipitation for hydrologic impact studies over North America. *Water Resources Research*, 49: 4187-4205, doi:10.1002/wrcr.20331

CSA PLUS 4013 (2nd ed.) 2012 - Technical Guide: Development, interpretation and use of rainfall intensity-duration-frequency (IDF) information: Guideline for Canadian water resources practitioners

Detlef, P., Van Vuuren, Jae Edmonds , Mikiko Kainuma , Keywan Riahi , Allison Thomson , Kathy Hibbard , George C. Hurtt , Tom Kram, Volker Krey, Jean-Francois Lamarque , Toshihiko Masui, Malte Meinshausen, Nebojsa Nakicenovic , Steven J. Smith and Steven K. Rose, 2011: The representative concentration pathways: an overview. *Climatic Change* (2011) 109:5–31. DOI 10.1007/s10584-011-0148-z
Gensini, V., Black, A., Changnon, D, Changnon, S. 2011. September 2008 Heavy Rains in Northeast Illinois: Meteorological Analysis and Impacts. *Transactions of the Illinois State Academy of Science*, Volume 104 (1&2): 17-33.

Ines, A.V.M., Hansen, J.W., 2006. Bias correction of daily GCM rainfall for crop simulation studies. *Agric. For. Meteorol.* 138, 44–53.

IPCC, 2001: *Climate Change 2001: the scientific basis*. Contribution of Working Group I to the third assessment report of the Intergovernmental Panel on Climate Change. In: Houghton JT, Ding Y, Griggs DJ, Noguer M, van der Linden PJ, Dai X, Maskell K, Johnson CA (eds) Cambridge University Press, p 881

Khari, V., Zwiers, F. W., Zhang, X., Wehner, M. 2013. Change in temperature and precipitation extremes in the CMIP5 ensemble. *Climate change* 119: 345-357.

King, Leanna MM, et al. "The effects of climate change on extreme precipitation events in the Upper Thames River Basin: a comparison of downscaling approaches. *Canadian Water Resources Journal* 37.3 (2012): 253-274.

Kuiper R. M., H. Hoijtink, and M. J. Silvapulle, 2011. An Akaike-type information criterion for model selection under inequality constraints. *Biometrika* (2011), 98, 2, pp. 495–501. doi: 10.1093/biomet/asr002

Lafon, T., S. Dadson, G. Buys, and C. Prudhomme, 2012. Bias correction of daily precipitation simulated by a regional climate model: A comparison of methods, *Int. J. Climatol.*, 33, 1367–1381, doi:10.1002/joc.3518.

Lemmen, D.S., Warren, F.J., Lacroix, J., and Bush, E. (2008). *From Impacts to Adaptation: Canada in a Changing Climate 2007*; Government of Canada, Ottawa, ON, 448p.

Maraun, D., et al. 2010. Precipitation downscaling under climate change: Recent developments to bridge the gap between dynamical models and the end user, *Rev. Geophys.*, 48, RG3003, doi:10.1029/2009RG000314

Maurer, E. P. 2007. Uncertainty in hydrologic impacts of climate change in the Sierra Nevada, California, under two emissions scenarios. *Climatic Change* (2007) 82:309–325

Meylan P., A. Favre and A. Musy, 2011: *Predictive Hydrology: A Frequency Analysis Approach*. Published by Science Publishers, CRC Press Taylor & Francis Group. ISBN: 13: 978-1-4398-8341-9 219 pages.

Nakicenovic et al., 2000. *Special Report on Emissions Scenarios. A Special Report of Working Group III of the Intergovernmental Panel on Climate Change*. Cambridge University Press: Cambridge. 599 pp.

Nguyen, V.-T.-V., Nguyen, T.-D., Cung, A., 2007. A statistical approach to downscaling of sub-daily extreme rainfall processes for climate-related impacts studies in urban areas. *Water Science and Technology: Water Supply* 7 (2), 183–192.

Olsson, J.; Berggren, K.; Olofsson, M.; Viklander, M., 2009: Applying climate model precipitation scenarios for urban hydrological assessment: A case study in Kalmar City, Sweden. *Atmos. Res.* 92, 364–375.

Olsson J., Gidhagen L., Gamerith V.2, Gruber G., Hoppe H. and Kutschera P. (2012): Downscaling of Short-Term Precipitation from Regional Climate Models for Sustainable Urban Planning. *Sustainability* 2012, 4, 866-887; doi:10.3390/su4050866.

Ontario Ministry of the Environment (MOE). 2003. *Stormwater Management Planning and Design Manual*. PIBS 4329e. Queen’s Printer for Ontario: Toronto, ON. pp. 379

Ontario Ministry of the Natural Resources (MOE). 2002. *Technical Guide - River and Stream Systems: Flooding Hazard Limit*. Queen's Printer for Ontario: Peterborough, ON. pp. 118

Opere A. O., S. Mkhanda, P. Willems, 2006. At site flood frequency analysis for the Nile Equatorial basins. *Physics and Chemistry of the Earth* 31 (2006) 919–927.

Paixao, E., Auld, H., Mirza, M. M. Q., Klaassen, J. & Shephard, M. W. Regionalization of heavy rainfall to improve climatic design values for infrastructure: case study in Southern Ontario, Canada. *Hydrol. Sci. J.* **56**, 1067–1089 (2011).

Peck, Angela, Predrag Prodanovic, and Slobodan P. Simonovic, 2012. "Rainfall intensity duration frequency curves under climate change: city of London, Ontario, Canada. *Canadian Water Resources Journal* 37.3 : 177-189.

Piani C., G.P. Weedon , M. Best , S.M. Gomes , P. Viterbo , S. Hagemann , J.O. Haerter (2010): Statistical bias correction of global simulated daily precipitation and temperature for the application of hydrological models. *Journal of Hydrology* 395 (2010) 199–215.

Rahmani, V., Hutchinson; S.L., Hutchinson, J.M and Anandh, A. (2014). Extreme Daily Rainfall Event Distribution Patterns in Kansas. *ASCE Journal of Hydrologic Engineering*, 19(4): 707-716.

Samuel J; P. Coulibaly, and R. A. Metcalfe (2012): Evaluation of future flow variability in ungauged basins: Validation of combined methods. *Advances in Water Resources* 35: 121-140.

SENES Consultants Limited. (2011). "Toronto's Future Weather and Climate Driver Study: Volume 1 - Overview." Toronto, Canada.

Sharma, M., Coulibaly, P., Dibike, Y. B. (2011). Assessing the need for downscaling RCM data for hydrologic impact study. *ASCE Journal of Hydrologic Engineering* 16(6): 534-539

Sheffield, J., et al. (2013). North American Climate in CMIP5 Experiments. Part I: Evaluation of Historical Simulations of Continental and Regional Climatology. *Journal of Climate* 26: 9209-9245

SUDPLAN 2012: Sustainable Urban Development Planner for Climate Change Adaptation.

Project 247708, Final Report Available online at:

http://sudplan.eu/polopoly_fs/1.30418!/SUDPLAN_final.pdf

Srivastav, R.K, Schardong, A., Simonovic, SP (2014). Equidistance Quantile Matching Method for Updating IDF Curves under Climate Change. *Water Resour Manage*. DOI 10.1007/s11269-014-0626

Symonds M. R. E. & A. Moussalli, 2010. A brief guide to model selection, multimodel inference and model averaging in behavioural ecology using Akaike's information criterion. *Behav Ecol Sociobiol* (2011) 65:13–21. DOI 10.1007/s00265-010-1037-6.

Teutschbein, C., and J. Seibert, 2012. Bias correction of regional climate model simulations for hydrological climate-change impact studies: Review and evaluation of different methods, *J. Hydrol.*, 456–457, 12–29, doi:10.1016/j.jhydrol.2012.05.052.

Themebl, M. J., A. Gobiet, and A. Leuprecht, 2010. Empirical statistical downscaling and error correction of daily precipitation from regional climate models, *Int. J. Climatol.*, 31, 1530–1544, doi:10.1002/joc.2168.

Thober, S., and L. Samaniego, 2014, Robust ensemble selection by multivariate evaluation of extreme precipitation and temperature characteristics, *J. Geophys. Res. Atmos.*, 119, 594–613, doi:10.1002/2013JD020505.

Wang, X and G.Huang. 2014. *Technical Report: Developing Future Projected IDF Curves and a Public Climate Change Data Portal for the Province of Ontario*. IEESC, University of Regina, Canada. Available online: http://www.ontarioccdp.ca/final_tech_report.pdf

Wang, X., G. Huang, and J. Liu. 2014. Projected increases in intensity and frequency of rainfall extremes through a regional climate modeling approach. *J. Geophys. Res. Atmos.*, 119, 13,271–13,286, doi:10.1002/2014JD022564.

Weigel, A., R. Knutti, M.A. Liniger, and C. Appenzeller, 2010: Risks of Model Weighting in Multimodel Climate Projections. *J. Climate*, 23, 4175–4191.

7. APPENDIX 1: SUMMARY OF LITERATURE REVIEW

Table A1: List of Acronyms

AD	<i>Anderson-Darling</i>	HadCM	<i>Hadley Centre Coupled Model</i>
AF	<i>Adjustment factor</i>	HRM3	<i>Hadley Regional Model 3</i>
AMP	<i>Annual Maximum Precipitation</i>	K-S	<i>Kolmogorov–Smirnov (test)</i>
ANN	<i>Artificial Neural Network</i>	LN2	<i>Log Normal distribution with 2 parameters</i>
AOGCM	<i>Atmospheric-Oceanic Global Climate Model</i>	LP3	<i>Log-Pearson type 3 distribution with 3 parameters</i>
ARF	<i>Areal Reduction Factor</i>	MM5	<i>Fifth-Generation Penn State/NCAR Mesoscale Model</i>
CGCM	<i>Canadian Global Climate Model</i>	NARCAP	<i>North American Regional Climate Change Assessment Program</i>

CNCM	<i>Community Climate System Model</i>	NCEP	<i>National Centers for Environmental Prediction reanalysis</i>
DAI	<i>Data Access Integration portal</i>	NMSE	<i>Normalized Mean Square Error</i>
EC	<i>Environment Canada</i>	NOAA	<i>National Oceanic and Atmospheric Administration</i>
EGMAM	<i>ECHO-G middle atmosphere model</i>	NSRP	<i>Neyman-Scott Rectangular Pulses model</i>
ERA	<i>European Reanalysis of Global Climate Observations</i>	POT	<i>Peaks Over Threshold</i>
EV1	<i>Gumbel Extreme value type 1</i>	PPCC	<i>Probability Plot Correlation Coefficient</i>
GCM	<i>Global Climate Model</i>	PSO	<i>Particle Swarm Optimization</i>
GEV	<i>generalized extreme value (distribution)</i>	RCM	<i>Regional Climate Model</i>
GFDL	<i>Geophysical Fluid Dynamics Laboratory</i>	RMSE	<i>Root Mean Square Error</i>
GLO	<i>Generalized LOGistic probability distribution</i>	SDSM	<i>Statistical Downscaling Model</i>

GPA	<i>Generalized PAreto probability density function</i>	SRES	<i>Special Report on Emissions Scenarios</i>
GPD	<i>Generalized Pareto Distribution</i>	WG	<i>Weather Generator</i>
GP	<i>Genetic Programming</i>		

Table A2: Summary table of literature reviewed

Reference	Study area	Data	Methods	Major findings
<p>Lee and Maeng (2003)</p> <p>Frequency analysis of extreme rainfall using L-moment</p>	<p>South Korea</p>	<p>–Recorded daily rainfall at 38 stations</p>	<p>–Wald–Wolfowitz, Mann–Whitney and Grubbs–Beck tests used to test respectively independence, homogeneity and outlier in data.</p> <p>–Fitted GEV, GPA, and GLO distributions to data.</p> <p>–L-moment ratio diagram and K-S test used to appreciate goodness of fit.</p> <p>–L-moment method used to estimate distribution parameters</p> <p>–Used Monte Carlo method to simulate annual maximum rainfall and design rainfall estimated based on both observed and simulated data.</p>	<p>–GEV and GLO distributions were the most appropriate distribution for all the station</p> <p>–Design rainfall derived from GEV distribution found to be more reliable than those based on GLO distribution</p>

<p>Coulibaly and Shi (2005)</p> <p>Identification of the Effect of Climate Change on Future Design Standards of Drainage Infrastructure in Ontario</p>	<p>Grand-River, Kenora & Rainy River regions (Ontario)</p>	<ul style="list-style-type: none"> -CGCM2 under SRES-B2 -Predictors from NCEP -Recorded precipitation at 8 stations 	<ul style="list-style-type: none"> -Used Mann-Kendall trend test -SDSM used to downscale CGCM2 outputs -Ratio approach (transformation factor) of obtaining shorter-duration rainfall. -Gumbel distribution used for frequency analysis. 	<ul style="list-style-type: none"> -Increasing trends in the annual maximum daily precipitation data for most stations. -Significant changes in the precipitation intensity between the current and the future time periods. -Most of the highway infrastructures can be significantly affected by the heavy and more frequent rainfall intensity predicted. -There is a need of recommendations for revising the existing design standards to account for the changing climate conditions.
<p>Bougadis and Adamowski (2006)</p> <p>Scaling model of a rainfall intensity-duration-frequency relationship</p>	<p>Eastern Ontario, Canada</p>	<p>Recorded data at 5 stations</p>	<ul style="list-style-type: none"> -GEV & Gumbel distributions used -L-moments method for parameter estimation -GEV used as parent distribution for the scaling procedure -Statistical non-central moments over different durations used to 	<ul style="list-style-type: none"> -Rainfall does follow a simple scaling process. -Estimates found from the scaling procedure are comparable to estimates obtained from traditional techniques. -Scaled approach was more efficient and gives more accurate estimates.

			<p>examine the scaling properties of rainfall data</p>	<ul style="list-style-type: none"> –Scaling approach reduces the amount of parameters required to compute the quantiles. –Scaling estimates are most accurate for durations less than 1 h and return periods less than 10 years. –Scaling approach allows statistical rainfall inferences from a higher aggregation model to a finer resolution model
<p>Svensson et al.(2007)</p> <p>An experimental comparison of methods for estimating rainfall intensity-duration frequency relations from fragmentary records</p>	<p>Eskdalemuir, Scotland</p>	<p>- Recorded hourly data</p>	<ul style="list-style-type: none"> –Created modified records containing gaps of varying degrees from reliable record –Applied different blocks and POT methods to develop IDF relationship with each artificially fragmented series based on monthly and annual maximum values and compared them with the ones obtained from the full record regarding bias and dispersion. 	<ul style="list-style-type: none"> –When missing data is present, the use of monthly maximum data gives better frequency analysis estimates than annual maximum data. –Dispersions are much smaller when using monthly maximum series. –Dispersions tend to increase with increasing return period. –The use of monthly maximum is recommended when calculating quantiles, allowing up to 20% missing data in each month.

			<ul style="list-style-type: none"> –Generalized Pareto and EV1 distributions used with maximum likelihood parameter estimate. 	
<p>Mailhot et al. (2007)</p> <p>Assessment of future change in intensity duration–frequency (IDF) curves for Southern Quebec using the Canadian Regional Climate Model (CRCM)</p>	<p>Southern Quebec, Canada</p>	<ul style="list-style-type: none"> –Annual May to October maximum rainfall depth (MOAM). –CRCM3 simulation driven by CGCM2 under SRES-A2. –Recorded data from 51 stations 	<ul style="list-style-type: none"> –Preliminary analysis of data for independency, homogeneity and stationarity using Wald-Wolfwitz, Wilcoxon and Mann-Kendall tests –Fitted data to GEV and GLO distributions –Used L-moment method to estimate distributions parameters. –Used Chi-square test and parametric bootstrap technique to test the adequacy of the distributions. –Used areal reduction factor (ARF) to assess the performance of CRCM. –Used regional frequency analysis: Regional average estimates at the grid box scale used to generate IDF curves in control and future climate 	<ul style="list-style-type: none"> –No clear indication of non-stationarity in all series. –Increasing ARF values as a function of return period –CRCM simulations revealed increase in regional MOAM –Uncertainties about change increase as return periods or durations increase. –For a given duration, spatial correlation of simulated annual maximum series decreases in the future climate. –Spatial correlation in future climate is very similar for all durations. –Reduction of return periods in future climate (~halved for 2 and 6 h events). –For 12- and 24-h events, reduction of return periods in future climate decreases as return periods increase.

			<ul style="list-style-type: none"> -Control period (1961-1990) and future projection (2041-2070) -Duration considered: 2- 6- 12- and 24-h 	
<p>Nguyen et al. (2008)</p> <p>Estimation of Design Storms in Consideration of Climate Variability and Change</p>	<p>Quebec, Canada</p>	<ul style="list-style-type: none"> -HadCM3A2 and CGCM2A2 simulations under SRES-A2 -Recorded precipitation at 15 stations (1961-1990) 	<ul style="list-style-type: none"> -SDSM used for spatial downscaling -Scaling General Extreme Value (GEV) distribution based on scale-invariance concept used to generate sub daily AM precipitation (temporal downscaling) -Scaling GEV distribution used to derive the IDF relationships for AM precipitations for different durations -Non-central moment (NCMs) used to estimate GEV distribution parameters -Future periods considered are 2020s, 2050s and 2080s with (1961-1990) as baseline. 	<ul style="list-style-type: none"> -Scaling GEV distribution has been shown to be able to provide accurate estimates of sub-daily AM precipitations from GCM-downscaled daily AM amounts. -Resulting design storm rainfall intensities from HadCM3A2 displayed a small decreasing change in the future, while those from the CGCM2A2 indicated a large increasing trend for future periods

<p>Palynchuk and Guo (2008)</p> <p>Threshold analysis of rainstorm depth and duration statistics at Toronto, Canada</p>	<p>Toronto, Canada</p>	<p>–Recorded hourly rainfall data at Toronto Pearson Airport (1960-2001)</p>	<ul style="list-style-type: none"> –Developed a storm-event based probabilistic models to characterize storm depth and duration and compared with the conventional rainfall depth–duration–frequency (DDF) analysis –Applied a Generalized Pareto distributions (GPD), through threshold-excess measures of rainstorm depth are used to characterize storm-event –Used maximum likelihood method to estimates GPD parameters –Goodness-of-fit was evaluated by means of the Anderson-Darling Statistic –Compared the storm-event analysis (SEA) procedure with the conventional depth–duration–frequency DDF analysis procedure. 	<ul style="list-style-type: none"> –Generalized Pareto distribution Type I is an acceptable model of rainstorm depth for long-return period events –Comparisons between conventional and storm-event analysis (SEA) models highlights the improvements and benefits of using storm-event-based probability distributions –The application of threshold-excess extreme value analysis techniques to storm-event statistics provides a simple, statistically efficient means of characterizing frequency of extreme storm-event depths and durations and may be used for the development of more representative design storms that reflect the frequency of occurrence of short duration convective storms more accurately
---	------------------------	--	---	---

<p>Madsen et al. (2009)</p> <p>Update of regional intensity–duration frequency curves in Denmark: Tendency towards increased storm intensities</p>	<p>Denmark</p>	<p>–Recorded rainfall data at 66 stations</p>	<ul style="list-style-type: none"> –Updated regional extreme value model with new data from 25 new stations. –Used generalised least squares regression (GLS) to evaluate regional homogeneity and to describe the variability from physiographic & climatic characteristics. –Used L-moment analysis to determine a regional distribution. –Model was based on partial duration series (PDS) method. –Calculated goodness of fit statistics for different regional distributions (generalised Pareto (GP), log-normal, gamma, Weibull and exponential distributions). –Compared results with previous analysis. 	<ul style="list-style-type: none"> –GP distribution is the best fit. –Regional variability of extreme precipitation confirmed. –The new L-CV is in general larger compared to the previous analysis. –General increase in quantiles is observed. –The increase is more pronounced for small and medium durations (<3h) and for large return periods. –For intensities with durations larger than 12h, a decrease of about 2-5% is observed. –Changes were not statistically significant compared to regional model uncertainties.
<p>Ben-Zvi A. (2009)</p>	<p>Israel</p>	<p>–Recorded data at 4 stations</p>	<p>–Derived larger than usual PDS from event maxima series.</p>	<p>–The use of large PDS with respect to the AMS and to the commonly practiced PDS, would lessen the effect of</p>

<p>Rainfall intensity–duration–frequency relationships derived from large partial duration series (PDS)</p>			<ul style="list-style-type: none"> –Fitted generalized Pareto distribution (GP) to PDS and used Anderson-Darling (AD) test for goodness of fit evaluation –Compared results with that of other distributions (GEV, EV1, LN) fitted to PDS and to annual maxima series (AMS). 	<ul style="list-style-type: none"> sampling variations, improve accuracy of prediction and enable better predictions of frequent intensities. –Different good fit distributions based on AD test mostly predict very similar values.
<p>Huard et al. (2010) Bayesian estimation of intensity–duration frequency curves and of the return period associated to a given rainfall event</p>	<p>Quebec</p>	<ul style="list-style-type: none"> –Recorded data at 6 stations 	<ul style="list-style-type: none"> –GEV distribution is considered. –Used Bayesian inference analysis to study uncertainties and compared result with 3 classical estimators [maximum likelihood method (ML), the method of moments (MOM) and the probability weighted moment method (PWM)]. 	<ul style="list-style-type: none"> –Return period estimates are very sensitive to hypotheses about the given event (Event ever observed or no). –The use of classical estimators in IDF curve development lead to huge uncertainty, particularly for large return period. –Incorporation of parameter uncertainty in the computation of IDF curve and in the estimation of the return period by using Bayesian analysis is suggested. –Bayesian analysis has the advantage that hypotheses are clearly stated.

<p>Adamowski et al. (2010)</p> <p>Influence of Trend on Short Duration Design Storms</p>	<p>Ontario, Canada</p>	<p>–Recorded data at 15 stations</p>	<p>–Linear regression & non-parametric Mann-Kendall tests used to detect trends.</p> <p>–EV1 distribution with moment estimators used to develop IDF.</p>	<p>–Different parts of Ontario show different significant trends and tendencies in extremes of precipitation.</p> <p>–Dominant increasing trend in annual extreme precipitation for all durations.</p> <p>–The presence of trend in rainfall increases the frequency of occurrences of extreme event, and for a given duration, design storms might occur more frequently with return periods increase.</p>
<p>Elsebaie I. H. (2012)</p> <p>Developing rainfall intensity-duration-frequency relationship for two regions in Saudi Arabia</p>	<p>Najran and Hafr Albatin region (Saudi Arabia)</p>	<p>–Recorded precipitation for different time interval</p>	<p>–Used Gumbel and LP3 distributions to calculate rainfall intensity at different durations and return periods.</p> <p>–Used chi-square quantity as goodness of fit test.</p> <p>–Applied logarithm conversion/non-linear regression to derive IDF equations.</p> <p>–IDF formula parameter goodness of fit is based on R^2</p>	<p>–Results from the two methods showed good consistency.</p> <p>–Small difference between IDF curves obtained by Gumbel & LP3 methods</p> <p>–Gumbel distribution gives slight higher results</p>

<p>Solaiman and Simonovic (2011)</p> <p>Development of Probability Based Intensity-Duration-Frequency Curves under Climate Change</p>	<p>City of London, Ontario</p>	<ul style="list-style-type: none"> -29 scenario from AOGCMs (1960-1990) and (2071-2100) -Hourly rainfall data for several stations extracted from DAI Network. 	<ul style="list-style-type: none"> -Regression and cross correlation analysis for station selection -Modified historic datasets with change fields before using them as input to K-NN based weather generator to produce longer sequence of rainfall -Non-parametric K-nearest neighbor approach used for disaggregation (downscaling based disaggregation) -Weather generator integrating principal component analysis (in order to reduce multi-dimensionality and collinearity associated with the large number of input variable) used for the downscaling. -Additional bias correction is applied to the downscaled output using a computed correction factor. 	<ul style="list-style-type: none"> -Rainfall patterns will change in the future -Increase in intensity of future rainfall with a varying degree (scenario indicates approximately 20 to 40% changes in different duration rainfalls for all return periods). -Recommended the use of the multi-model approach, rather than a single scenario. -Generation of future IDF information based on single site is limited. -Use of the wettest and the driest scenario may be useful to capture the upper and lower bound scenario of the future climate change. -Probability based intensity-duration-frequency curve is encouraged in order to apply the updated IDF information with higher level of confidence. -A kernel based plug-in estimation approach is able to incorporate the uncertainties arising from different
---	--------------------------------	--	--	--

			<ul style="list-style-type: none"> -EV1 adopted (to comply with EC procedure) to develop IDF and frequency analysis is performed to the annual maximum rainfall -The IDF relationship is developed by fitting the IDF data to a continuous function and used least square method to estimate the equation parameters. -Durations 1- 2- 6- 12- and 24-h considered -Climate change taken into account with (1960-1990) as baseline and (2070-2100) for the projection. -Non-parametric kernel estimation applied to quantify the uncertainty arising from different AOGCM scenarios 	<p>AOGCM models and provide a more acceptable change in future rainfall extremes.</p> <p>-Scenarios indicated large uncertainty associated with the global climate models.</p>
De Michele et al. (2011) Analytical derivation of rain intensity-	Reno basin, Italy	-Recorded data at 22 stations	-Derived IDAF curves statistically from statistic properties of event maxima of rainfall intensity and Lognormal distributed with a	-The method for the calculation of IDAF curves based on the analysis of event maxima exhibits better performances

<p>duration–area–frequency (IDAF) relationships from event maxima</p>			<p>Poissonian chronology of rain events</p> <ul style="list-style-type: none"> –K-S goodness-of-fit test used –IDAF curves obtained from the event maxima analysis are compared to those calculated via the annual maxima analysis. 	<p>than those based on the annual maxima.</p>
<p>CHENG et al. (2011) A Synoptic Weather Typing Approach to Project Future Daily Rainfall and Extremes at Local Scale in Ontario Canada</p>	<p>Grand, Humber, Rideau, and Upper Thames river basin, in Ontario</p>	<ul style="list-style-type: none"> –3 GCMs (CGCM2, GFDL, ECHAM5) and 2 scenario A2 & B2 –Historical observation from NCEP (1958-2002) for the warm season (April–November) –Observed daily rainfall at stations 	<ul style="list-style-type: none"> –Used automated synoptic weather typing, cumulative logit and nonlinear regression methods to develop within-weather-type daily rainfall simulation models that are used to project possible change in frequency of daily rainfall events –Regression-based downscaling used to downscale GCMs simulations –Time slices considered were (1961–2000), (2046–65), (2081–2100) –Future projections based only on daily rainfall 	<ul style="list-style-type: none"> –Combination of synoptic weather typing, cumulative logit and nonlinear regression analyses, and regression-based downscaling can be useful to project changes in frequency of future daily rainfall events. –Results found that the frequency of future daily rainfall events could increase late this century due to the changing climate projected by GCM scenarios. –the return values of annual maximum 3-day accumulated rainfall totals are projected to increase by 20%–50%, 30%–55%, and 25%–60% for the

				<p>periods 2001–50, 2026–75, and 2051–2100, respectively.</p> <p>–Inter model uncertainties found to be similar to the inter-scenario uncertainties</p>
<p>Peck A. et al. (2012)</p> <p>Rainfall Intensity Duration Frequency curves under Climate Change : City of London, Ontario, Canada</p>	<p>City of London, Ontario</p>	<p>–1 GCM (CCSRINES) simulation for (1961-1990) and (2040-2069)</p> <p>–2 climate change scenario (upper & lower bounds).</p> <p>–Recorded data at London Airport station (1961-2002) for 9 different durations</p>	<p>–Non-parametric K-Nearest Neighbor weather generator (WG) used to downscale 1 GCM (CCSRINES) data and create long time series weather data.</p> <p>–Two future climate change scenario were considered (upper & lower bounds).</p> <p>–For the upper bound scenario, the observed data is modified by monthly climate change factors (from CCSRINES B21) before using them as input into the WG</p> <p>–Gumbel Extreme Value Type I (EV1) was adopted for the quantiles calculation.</p> <p>–IDF curves developed by fitting the IDF data to a 3 parameters</p>	<p>–Rainfall magnitude will increase under climate change for all duration and return periods.</p> <p>–For 100-year short duration events, the climate change low bound and upper bound scenario maximum values are respectively up to 35% and 42% higher than EC maximum values.</p> <p>–Current IDF curves are not sufficient to represent future rainfall patterns.</p> <p>–Small difference observed (~4.5% on average) between upper and lower bound climate change scenarios.</p> <p>–The increase in rainfall intensity & magnitude may have major implications on the design, operation and maintenance of municipality water management infrastructures.</p>

			<p>continuous function recommended by the Ontario Drainage Management Manual and estimated the parameters using least squares method.</p> <ul style="list-style-type: none"> -Compared updated IDF for climate change with the existing curves posted by EC. -Durations 5, 10, 15, 30 minutes and 1, 2, 6, 12 and 24 h considered -Climate change taken into account with (1961-1990) as baseline and (2040-2069) for the projection 	<ul style="list-style-type: none"> -Current IDF should be changed in the range of about +20% in order to account for climate change.
<p>Burn and Taleghani (2012)</p> <p>Estimates of changes in design rainfall values for Canada</p>	Canada	<ul style="list-style-type: none"> -51 rainfall gauging stations across Canada with at least 35 years of record length for each. 	<ul style="list-style-type: none"> -Analyzed trend and change in rainfall data for 9 durations (5 min to 24h) by using respectively a modified Mann-Kendall rank-based test and bootstrap resampling method. 	<ul style="list-style-type: none"> -More significant increasing trend observed in rainfall. -Number of significant trend differs with rainfall duration (more for shorter duration) -Some evidences of spatial grouping of trend location, but not consistent.

			<ul style="list-style-type: none"> -Performed sensitivity analysis for the choice of distribution function & length of most recent years. -Used Walker's test to evaluate the field of significance. -Assessed the suitability of different distributions (GEV, GLO, GNO, EV1, LP3) to fit the data based on PPCC using L-moments method. -Used the best fitting distribution to develop IDF curves. -Climate change projection for the future not considered in this study. 	<ul style="list-style-type: none"> -PT3 best fitting distribution (higher number of occurrence) and Gumbel the worst. -Traditional trend analysis (e.g. Mann-Kendall test) may not be a sufficient criterion in detecting climate change impacts on design quantiles, particularly when the interest is in longer return period events (bootstrap resampling technique is preferred). -When comparing the most recent 20 years to the entire record, there is predominated decreasing trend in the return period for longer rainfall duration (>1h) and predominated increasing for shorter rainfall duration. -Overall more increasing than decreasing trends in the quantiles are observed. -The use of IDF curves that are not recent could result in an inappropriate design of key water infrastructures. -Climate change impact on rainfall magnitude should be carried out on a
--	--	--	---	---

				local basis, as results can differ even for stations in close proximity.
AMEC (2012) Development of Projected IDF Curves for Welland, Ontario	Welland, Canada	<ul style="list-style-type: none"> -16 GCMs (B1, A1B, A2) -Historical IDF curves (EC) along with the record of the intensity of annual extreme event (1964-2000) -Recorded climate data (1964-2011) at Port Colborne station 	<ul style="list-style-type: none"> -Gumbel distribution was fit to the historical annual precipitation maxima. -Applied delta method to calculate projected values of precipitation. -Used delta method again to adjust the historical IDF curves. -Developed projected precipitation intensity values using delta method (adjusted the projected change to the historical IDF curve from EC) -Projected IDF curves based on 2020s and 2050s future time periods. -Durations considered ranged from 5mn to 24h -Used a large ensemble of projections for uncertainty analysis. 	<ul style="list-style-type: none"> -Delta method reduces the bias inherent in climate simulations. -There is some model-to-model disagreement over the magnitude of projected precipitation. -All GCMs used are projecting an increase in temperature. -Existing IDF curves were conservative relative to the current estimates and even relative to the projected values for many duration/return interval combinations.

<p>Liew et al. (2012)</p> <p>Development of intensity-duration-frequency curves: incorporating climate change projection</p>	<p>Jakarta, Indonesia</p>	<ul style="list-style-type: none"> -ECHAM5 (SRES-A2) -Existing IDF curves 	<ul style="list-style-type: none"> -A regional climate model, the Weather Research and Forecasting (WRF) used for downscaling. -Bilinear interpolation based on moving averaging window used to extract rainfall intensity for different duration from the WRF simulations. -GEV distribution selected -Applied delta method to generate projected IDF curves. -Duration considered were 6- 12- 18 and 24-h -Three time slices (2011- 2040), (2041- 2070) and (2071-2100) considered for projections with 1961-1990 as base line. 	<ul style="list-style-type: none"> -WRF is an effective tool for dynamical downscaling. -Increase of about 20% in rainfall extremes by 2070.
<p>Karahan H. (2012)</p> <p>Determining Rainfall-Intensity Duration-</p>	<p>Izmir, Turkey</p>	<ul style="list-style-type: none"> -Observed data (1938-2005) 	<ul style="list-style-type: none"> -Used 8 different IDF relationship formulas -Applied PSO method (using Linear Fitness Scaling to control 	<ul style="list-style-type: none"> -PSO method shows better performance than GA when number of parameters increases.

<p>Frequency Relationship Using Particle Swarm Optimization (PSO)</p>			<p>objective function) to determine formulas parameters</p> <ul style="list-style-type: none"> -MSE used as objective function in optimization -Compared results with genetic algorithm (GA) optimization method. 	<ul style="list-style-type: none"> -PSO is an effective tool for obtaining good IDF relationship. -Length of data set and formulation influence model performance.
<p>Sunyer and Madsen (2012)</p> <p>A Comparison of different regional climate models and statistical downscaling methods for extreme rainfall estimation under climate change.</p>	<p>Copenhagen , Denmark</p>	<ul style="list-style-type: none"> -Four (04) RCMs driven by 2 GCMs (SRES-A1B) -Recorded daily precipitation at 1 station (1979-2007) 	<ul style="list-style-type: none"> -Used the RCM simulations to calculate change factors for all statistics needed in downscaling methods. -Used change factors as input in 5 different downscaling methods (Markov chain WG, semi-empirical WG, NSRP WG, change in mean, change in mean & variance) to generate time series for the future -Analyzed projections for main statistics and extreme event statistics. -The time slice (2071-2100) is considered for the future 	<ul style="list-style-type: none"> -RCM projections need further downscaling in order to be used in climate change impact studies. -Commonly change in mean downscaling method is not suitable to analyze change in extreme events. -Weather generators (WG) downscaling method are recommended when extreme event are main focus or when number of dry/wet days is expected to significantly change in the future. -Significant part of the uncertainty in climate change impact studies is related to RCM model chosen.

			<p>projection with (1979-2007) as base line</p>	<ul style="list-style-type: none"> -All four RCMs have a tendency to overestimate mean and standard deviation but underestimate skewness. -Change factors derived from the different RCMs do not, in general, agree on whether one statistic will increase or decrease -There are large uncertainties on the statistics for the future obtained after statistical downscaling, particularly during the summer months, but a tendency of an increase of the mean precipitation and standard deviation during the winter and spring months and a decrease of the mean precipitation in summer and autumn is observed
--	--	--	---	---

<p>Cheng et al. (2012)</p> <p>Possible impacts of climate change on extreme weather events at local scale in south central Canada</p>	<p>South-central Canada</p>	<ul style="list-style-type: none"> -Four GCMs (CGCM1, CGCM2, GFDL, ECHAM5) simulation and Scenarios A2 & B2 -Historical climate data from EC and from NCEP ranging from (1953-2002) 	<ul style="list-style-type: none"> -Synoptic weather typing and regression methods to analyze climatic change impacts on extreme weather events: -Used various statistical methods for preliminarily data analysis and for downscaling -Principal components and discriminant function analysis used for future synoptic weather type projection and future projections -Comparing future and historical identified extreme-event-related weather type frequencies -Three time windows (1961-2000), (2046-2065), (2081-2100) considered for the GCMs simulation 	<ul style="list-style-type: none"> -Regression-based downscaling methods performed very well in deriving future hourly station-scale climate information for all weather variables -A combination of synoptic weather typing, extreme weather event simulation modeling, and regression-based downscaling can be useful in projecting changes in the frequency and intensity of future extreme weather events and their impacts at a local scale or station scale. -Modeled results from these projects indicated that the frequency and intensity of future daily extreme weather events have the potential to significantly increase late this century
<p>Das et al. (2013)</p> <p>Distribution choice for the assessment of</p>	<p>Upper Thames River Basin (3842 km²),</p>	<ul style="list-style-type: none"> -Hourly rainfall data from DAI network (1965-2003) 	<ul style="list-style-type: none"> -Investigated goodness of fit of GEV, EV1 & LP3 distribution under climate change and address the uncertainty involved 	<ul style="list-style-type: none"> -GEV distribution is the best fit to the synthetic data and EV1 distribution should not be used.

<p>design rainfall for the city of London (Ontario, Canada) under climate change</p>	<p>London, Ontario</p>	<ul style="list-style-type: none"> -Daily rainfall data from EC Weather Office (1965-2003) -Climate data from 7 AOGCMs under different scenario (1961-1990) & (2071-2100). 	<p>in extreme value modeling and estimation of IDF curve for the future:</p> <ul style="list-style-type: none"> -Calculate precipitation change factors for future climate and used them to modify historic datasets. -Modified historic datasets used as input into the KnnCAD weather generator to produce synthetic daily data. -Synthetic daily data are disaggregated into hourly data by means of disaggregation algorithm. -Adjusted distribution functions to maximum annual rainfall series produced from the disaggregated datasets. -Used L-moment ratio diagram, AD, Chi-square & K-S goodness of fit tests to select the best distribution to be used to develop IDF curves. 	<ul style="list-style-type: none"> -Based on historic datasets, EV1 and GEV distribution produce similar IDF curves, but when taking into account future climate data there is a significant difference. -The use of different AOGCMs and different scenario provides for effective uncertainty analysis. -To account for climate change in the future, current IDF curves established from the recorded historic data should be increase by 30%.
--	------------------------	--	--	--

			<ul style="list-style-type: none"> -Discussed the results with those of EC and those obtained from historic perturbed data. -Storm durations of 1, 2, 6, 12, and 24 hours considered -IDF curves relationship not developed in this study 	
<p>Kuo et al. (2013)</p> <p>The climate change impact on future IDF curves in central Alberta</p>	<p>Edmonton, Canada</p>	<ul style="list-style-type: none"> -MM5 driven by CGCM3 & ECHAM5 under SRES-A2. -Recorded data at 13 rain gauges (1984-2010). 	<ul style="list-style-type: none"> -Run MM5 with CGCM3 & ECHAM5 data. (run for May-August for 1971-2000 and for 2041-2100 under SRES A2) -Applied quantile-based bias correction to simulated precipitation. -Applied regional frequency analysis to estimate precipitation extremes at ungauged sites. -Fitted GEV distribution to data. -Used probability weighted moment to calculate distribution parameters. -IDF curved derived on the basis of grid cell in order to compare a 	<ul style="list-style-type: none"> -More intense heavy rainfall expected in future climate -Change is greater in the 2080s than in the 2050s -Relatively increases are noticeably higher for the shorter duration (<6h) rainfall. -In the 2050s, changes are expected to be higher for shorter return periods (<10 years). -Current IDF curve is smaller than the projected upper bound.

			<p>large area of IDF curves. (Individual grid quantiles were obtained from the regional frequency analysis at the grid box scale and then bias correction was applied)</p> <p>–Storm duration range from 15-, 30-min, 1-, 2-, 6-, 12- to 24-hr</p>	
<p>Mirhosseini et al. (2013a)</p> <p>The impact of climate change on rainfall Intensity–Duration Frequency (IDF) curves in Alabama</p>	<p>State of Alabama, USA</p>	<p>–Six (06) NARCAP-RCMs</p> <p>–Recorded precipitation at different stations from NOAA</p>	<p>–Dynamically downscaled 6 GCMs</p> <p>–Quantile-based mapping method used for bias correction</p> <p>–Used stochastic method for data disaggregation</p> <p>–GEV distribution selected to estimate precipitation depth for the different return periods</p> <p>–Applied moment method to estimate GEV parameters and K-S test to evaluate the performance of fit.</p> <p>–IDF curves under the future climate scenarios were compared</p>	<p>–Disparity in the projections and future rainfall intensity decreases or increases depending on the return period</p> <p>–Decreasing rainfall intensity is expected in the future for short durations of rainfall (<4h)</p> <p>–Projections are not consistent with respect to larger events (A large uncertainty on the projected rainfall intensity makes it difficult to obtain any strong conclusion about the expected changes on future rainfall intensity)</p>

			<p>with the IDF curves under the current climate</p> <ul style="list-style-type: none"> -The time slice (2038-2070) is considered for the future projections with (1968-2000) as base line -Storm durations considered (15, 30, and 45 min, 1, 2, 3, 6, 12, 24, and 48 h) 	
<p>Mirhosseini et al. (2013b)</p> <p>Developing Rainfall Intensity-Duration-Frequency (IDF) Curves for Alabama under Future Climate Scenarios using Artificial Neural Network (ANN).</p>	<p>Alabama, USA</p>	<ul style="list-style-type: none"> -Recorded data at 34 stations from NOAA -Five NARCAP-RCMs 	<ul style="list-style-type: none"> -Dynamically downscaled 5 GCMs -Quantile-based mapping used for bias correction -ANN used for disaggregation and performance compared with stochastic method. -Akaike Information criterion (AIC) and NMSE used to select the neuron input datasets. -NSE & correlation coef. used for the ANN performance evaluation. -GEV distribution used to create IDF curves. 	<ul style="list-style-type: none"> -ANN model performed very well for data desegregation and provide better estimation of Max rainfall depths. -Stochastic method tends to under-predict rainfall intensities. -The five different climate models did not provide identical projections. -Decreasing rainfall intensity by 33% to 74% is expected in the future for short durations of rainfall (<2h). -Large uncertainty in the projected rainfall intensities of longer duration events.

			<ul style="list-style-type: none"> -Applied method of moments for GEV parameter estimation with K-S test as goodness of fit test. -The time slice (2038-2070) is considered for the future projections with (1968-2000) as base line 	
<p>Hailegeorgis et al. (2013)</p> <p>Regional frequency analysis of extreme precipitation with consideration of uncertainties to update IDF curves for the city of Trondheim.</p>	<p>City of Trondheim, Norway</p>	<ul style="list-style-type: none"> -Recorded precipitation at 4 stations. 	<ul style="list-style-type: none"> -Used L-moment method for regional frequency analysis. -Mann-Kendall & parametric linear regression tests used for trend and stationarity checking. -Discordancy and homogeneity tested based on H-statistics. -GEV, GLO, P3, GPAR distributions considered. -Z-statistic & L-moment ratio diagrams used for distribution function selection. -Non-parametric balanced bootstrap resampling method used to quantify uncertainty. 	<ul style="list-style-type: none"> -Different types of distributions fit to extreme precipitation events of different durations. -Thorough selection of distributions is indispensable rather than fitting a single distribution for the whole durations. -Uncertainty in quantile estimation needs to be estimated and incorporated. -Large differences between calculated and existing IDF curve.

<p>Hassanzadeh E. et al. (2013)</p> <p>Quantile-based Downscaling of Precipitation using Genetic Programming (GP): Application to IDF Curves in the City of Saskatoon</p>	<p>City of Saskatoon, Canada</p>	<ul style="list-style-type: none"> -GCM3-T47 (A1B, A2, B1) -Historical IDF curve data (1926-1986) -EC-IDF data 	<ul style="list-style-type: none"> -GP technique used to explore equations to map daily AMP quantiles at the GCM scale to the corresponding daily and sub-daily local estimates. -Both duration-variant and duration-invariant quantile-quantile relationships were explored. -Ideal-point-Error (IPE) based on 4 performance criteria used to evaluate the overall performance of the mapping equations. -Mann-Kendall test used for trend checking. -Autocorrelation in local sub-daily AMP time series removed. -GEV distribution selected with maximum likelihood and K-S test for parameter estimation and goodness of fit evaluation respectively. -Future IDF curves at the local scale estimated using the future 	<ul style="list-style-type: none"> -GP can extract mathematical equations to describe the mappings between AMP quantiles at the GCM and local scales. -The duration-variant mapping equations provided more accurate reconstruction of the IDF curves for the baseline period. -Change in future IDF curves depend on scenario, storm duration and return period considered. -Clear increase in quantile for short duration storm (<6h) expected in the future.
---	----------------------------------	---	--	--

			<p>estimates from global climate models assuming that the extracted quantile-quantile relationships remain unchanged with time</p> <ul style="list-style-type: none"> -Compared IDF curves obtained from fitting the GEV distribution to the historical data to the IDF curves approximated using the quantile-quantile equations. -Baseline period considered is 1961-1990 and the future projections period is 2010 to 2100. 	
<p>Zhu J. (2013)</p> <p>Impact of Climate Change on Extreme Rainfall across the United States</p>	USA	<ul style="list-style-type: none"> -HRM3 simulation driven by HadCM3 (SRES-A2). -NCEP reanalysis data 	<ul style="list-style-type: none"> -Compute adjustment factor (AF) according to historic match between climate model result and reanalysis data. -GEV & Gumbel distributions used -Used AF to adjust precipitation intensity for a given duration and return period of future climate model results to make projection 	<ul style="list-style-type: none"> -Dependence of AF values on return period and storm duration. -Rainfall intensities for future conditions consistently higher than historical conditions. -Impacts of climate change on severe storm characteristics would be highly local in nature and investigations should be carried out at the local level.

			<p>of potential future intensity for the same duration and return period.</p> <ul style="list-style-type: none"> –Baseline period considered is 1971-2000 and the future time period is 2041 to 2070 –Bootstrap resampling used for estimate uncertainty. 	<ul style="list-style-type: none"> –Much stronger influence of climate change on rainfall intensities for short-duration.
<p>Mailhot et al. (2013)</p> <p>Regional estimates of intense rainfall based on the Peak-Over-Threshold (POT) approach</p>	<p>Southern Québec, Canada</p>	<ul style="list-style-type: none"> –Maximum rainfall depth at 109 stations for durations ranging from 5-mn to 12-h(years range from 10 to 51 years) 	<ul style="list-style-type: none"> –Developed a regional version of the POT approach –Threshold values were determined by specifying a mean number of six threshold excesses –Applied a declustering technique to eliminate possible temporal correlation in POT series. –GPD used and parameters estimated through joint likelihood function –Intra-annual variability was taken into consideration through a Fourier representation of the GPD parameters. 	<ul style="list-style-type: none"> –Intra-annual variability of the Generalized Pareto Distribution (GPD) parameters needs to be taken into consideration –Models with spatial covariates widely outperformed those without spatial covariates –Threshold selection is a major issue when applying the POT approach and a mean threshold excess rate (MTER) value of 6 per year have seemed to be a reasonable value.

			<ul style="list-style-type: none"> -Introduced spatial covariates to describe the spatial dependency of parameters -Investigated sensitivity of results to threshold values and selected models -Models were selected based on the corrected Akaike criterion -Durations considered are 5-, 10-, 15-, 30-min and 1-, 2-, 6- and 12-h 	
<p>Rodriguez R. et al. (2014)</p> <p>Influence of climate change on IDF curves for the metropolitan area of Barcelona (Spain)</p>	Barcelona , Spain	<ul style="list-style-type: none"> -Five GCMs (EGMAM, CNCM3, ECHAM5, BCM2, CGCM2) -B1, B2, A1B, A2 scenarios -ERA-40 Reanalysis data -Recorded data at 6 stations (1951-1999) 	<ul style="list-style-type: none"> -Applied statistical downscaling method to generate daily rainfall from CGMs output. -Applied 2 temporal downscaling methods (Invariance of climate change factor & Scaling invariance) to obtain sub-daily rainfall data from simulated daily data. -Used empirical exponential function to calculate quantiles. Parameters estimated by the least-squares method 	<ul style="list-style-type: none"> -Clear tendency toward increased extreme daily rainfall. -Average climate change factor has resulted higher as longer the return period is in almost all the scenarios and periods considered. -Considerable variation depending on the GCM and the station that it referred to (implying a strong dependence of downscaling method with initial condition). -Climate change factors obtained for hourly rainfall are in most of the case

			<ul style="list-style-type: none"> -Used climate change factor for comparison and trend analysis. -Control period considered is 1951-1999 and the future time period is 2000 to 2099 	slightly higher than those calculated for daily rainfall.
<p>Asikoglu and Benzeden (2014)</p> <p>Simple generalization approach for intensity–duration–frequency relationships</p>	Aegean region, Turkey	<ul style="list-style-type: none"> -Recorded precipitation at 20 stations 	<ul style="list-style-type: none"> -LN2 and Gumbel distributions adopted -Applied Kolmogorov–Smirnov and Anderson Darling goodness of fit tests. -Used moments estimators -Used simple generalization procedure (SGP) and robust estimation procedure (REP) based on Kruskal-Wallis test statistic to establish IDF relationship. -Used RMSE for the 2 procedure performance comparison. 	<ul style="list-style-type: none"> -Simple generalization procedure (SGP) method avoids undulation or intersection of IDF curves. -SGP gives slightly better estimate of rainfall intensities than REP and maintains temporal trend in the mean.

REFERENCES

Adamowski J., K. Adamowski, J. Bougadis, 2010. Influence of Trend on Short Duration Design Storms. *Water Resource Manage* (2010) 24:401–413. DOI 10.1007/s11269-009-9452-z.

AMEC, 2012. Development of Projected Intensity-Duration-Frequency Curves for Welland, Ontario, Canada. Report prepared by AMEC Environment & Infrastructure for the, February 2012 for the CITY OF WELLAND, STORMWATER AND WASTEWATER INFRASTRUCTURE. Available at: <http://www.welland.ca/Eng/pdfs/AppC-WellandReportFinal.pdf>

Asikoglu O. L. and E. Benzedden, 2014. Simple generalization approach for intensity–duration–frequency relationships. *Hydrol. Process.* 28, 1114–1123 (2014). DOI: 10.1002/hyp.9634.

Ben-Zvi A., 2009. Rainfall intensity–duration–frequency relationships derived from large partial duration series. *Journal of Hydrology* 367 (2009) 104–114.

Bougadis J. and K. Adamowski, 2006. Scaling model of a rainfall intensity-duration-frequency relationship. *Hydrol. Process.* 20, 3747–3757 (2006). DOI: 10.1002/hyp.6386.

Burn D. H. and A. Taleghani, 2012. Estimates of changes in design rainfall values for Canada. *Hydrol. Process.* 27, 1590–1599 (2013). DOI: 10.1002/hyp.9238.

Cheng C. S., LI G., and LI Q. 2011. A Synoptic Weather Typing Approach to Project Future Daily Rainfall and Extremes at Local Scale in Ontario Canada. *JOURNAL OF CLIMATE*. Volume 24. DOI: 10.1175/2011JCLI3764.1

Cheng C. S., H. Auld & Q. Li, and G. Li, 2012. Possible impacts of climate change on extreme weather events at local scale in south central Canada. *Climatic Change* (2012) 112:963–979. DOI 10.1007/s10584-011-0252-0

Coulibaly P. and X. Shi, 2005. Identification of the Effect of Climate Change on Future Design Standards of Drainage Infrastructure in Ontario. Report Available at: http://www.cspi.ca/sites/default/files/download/Final_MTO_Report_June2005rv.pdf

Das S., N. Millington, and S.P. Simonovic 2013. Distribution choice for the assessment of design rainfall for the city of London (Ontario, Canada) under climate change. *Can. J. Civ. Eng.* 40: 121–129 (2013) dx.doi.org/10.1139/cjce-2011-0548

Elsebaie I. H., 2012. Developing rainfall intensity–duration–frequency relationship for two regions in Saudi Arabia. *Journal of King Saud University – Engineering Sciences* (2012) 24, 131–140

De Michele C., E. Zenoni, S. Pecora, R. Rosso, 2011. Analytical derivation of rain intensity–duration–area–frequency relationships from event maxima. *Journal of Hydrology* 399 (2011) 385–393.

Hailegeorgis T. T., S. T. Thorolfsson, K. Alfredsen, 2013. Regional frequency analysis of extreme precipitation with consideration of uncertainties to update IDF curves for the city of Trondheim. *Journal of Hydrology* 498 (2013) 305–318

Hassanzadeh E., A. Nazemi , A. Elshorbagy, 2013. Quantile-based Downscaling of Precipitation using Genetic Programming: Application to IDF Curves in the City of Saskatoon. *Journal of Hydrologic Engineering*. doi:10.1061/(ASCE)HE.1943-5584.0000854.

Hershfield, D.M., “ Rainfall Frequency Atlas of the United States for Durations from 30 Minutes to 24 Hours and Return Periods from 1 to 100 Years”, U.S. Weather Bureau, Washington, D.C., Technical Paper 40, 1961.

Huff, F.A., and Angel, J.R., 1989. Frequency Distribution and Hydraulic Climatic Characteristics of Heavy Rainstorms in Illinois, Bulletin 70, Illinois State Water Survey, Champaign, Illinois, U.S.A, 1989.

Huard D., A. Mailhot, S. Duchesne, 2010. Bayesian estimation of intensity–duration–frequency curves and of the return period associated to a given rainfall event. *Stoch Environ Res Risk Assess* (2010) 24:337–347. DOI 10.1007/s00477-009-0323-1

Karahan H., 2012. Determining Rainfall-Intensity-Duration-Frequency Relationship Using Particle Swarm Optimization. *KSCE Journal of Civil Engineering* (2012) 16(4):667-675. DOI 10.1007/s12205-012-1076-9.

Kuo C.C., N. Jahan, M. S. Gizaw, T. Y. Gan 1, and S. Chan, 2013. The climate change impact on future IDF curves in central Alberta. *EIC Climate Change Technology Conference* 2013.

CCTC 2013 Paper Number 1569716685. Available at:
<http://www.cctc2013.ca/Papers/CCTC2013%20MOD4-2%20Kuo.pdf>

Lee S. H. And S. J. Maeng, 2003. Frequency analysis of extreme rainfall using l-moment. *Irrig. and Drain.* 52: 219–230 (2003). DOI: 10.1002/ird.090.

Liew S. C, S. V Raghavan, S-Y. Liong, R. Sanders, 2012. Development of intensity-duration-frequency curves: incorporating climate change projection. 10th International Conference on Hydro-informatics HIC 2012, Hamburg, GERMANY.

Madsen H., K. Arnbjerg-Nielsen, P. S. Mikkelsen, 2009. Update of regional intensity–duration–frequency curves in Denmark:Tendency towards increased storm intensities. *Atmospheric Research* 92 (2009) 343–349.

Mailhot A., S. Duchesne, D. Caya, G. Talbot, 2007. Assessment of future change in intensity–duration– frequency (IDF) curves for Southern Quebec using the Canadian Regional Climate Model (CRCM). *Journal of Hydrology* (2007) 347, 197– 210

Mailhot, A., Lachance-Cloutier, S., Talbot, G., Favre, (2013). Regional estimates of intense rainfall based on the Peak-Over-Threshold (POT) approach - *Journal of Hydrology*, 476 (7): 188–199.

Millington S. D., N., and S.P. Simonovic, 2013. Distribution choice for the assessment of design rainfall for the city of London (Ontario, Canada) under climate change. *Can. J. Civ. Eng.* 40: 121–129 (2013) [dx.doi.org/10.1139/cjce-2011-0548](https://doi.org/10.1139/cjce-2011-0548).

Mirhosseini G., P. Srivastava, X. Fang, 2013b. Developing Rainfall Intensity-Duration-Frequency (IDF) Curves for Alabama under Future Climate Scenarios using Artificial Neural Network (ANN). *Journal of Hydrologic Engineering*. doi: 10.1061/(ASCE)HE.1943-5584.0000962.

Mirhosseini G., P. Srivastava, L. Stefanova, 2013a. The impact of climate change on rainfall Intensity–Duration–Frequency (IDF) curves in Alabama. *Reg Environ Change* (2013) 13 (Suppl 1). DOI 10.1007/s10113-012-0375-5.

Nguyen V-T-V, N. Desramaut¹ and T-D. Nguyen, 2008. Estimation of Design Storms in Consideration of Climate Variability and Change. 11th International Conference on Urban Drainage, Edinburgh, Scotland, UK, 2008.

Palynchuk B. and Y. Guo, 2008. Threshold analysis of rainstorm depth and duration statistics at Toronto, Canada. *Journal of Hydrology* (2008) 348, 535– 545.

Peck A., P. Prodanovic, and S. P. Simonovic, 2012. Rainfall Intensity Duration Frequency Curves Under Climate Change: City of London, Ontario, Canada. *Canadian Water Resources Journal*. Vol. 37(3): 177_189 (2012). doi: 10.4296/cwrj2011-935.

Rodriguez R., X. Navarro, M. C. Casas, J. Ribalaygua, B. Russo, L. Pougetd and A. Redano, 2014. Influence of climate change on IDF curves for the metropolitan area of Barcelona (Spain). *Int. J. Climatol.* 34: 643–654 (2014). DOI: 10.1002/joc.3712.

Solaiman T. A. and S. P. Simonovic, 2011. Development of Probability Based Intensity-Duration-Frequency Curves under Climate Change. Report document. Department of Civil and Environmental Engineering. The University of Western Ontario London, Ontario, Canada. ISSN: (print) 1913-3200; (online) 1913-3219; ISBN: (print) 978-0-7714-2893-7; (online) 978-0-7714-2900-2. Available at: <http://ir.lib.uwo.ca/wrrr/34/>

Sunyer M.A., H. Madsen, P.H. Ang, 2012. A comparison of different regional climate models and statistical downscaling methods for extreme rainfall estimation under climate change. *Atmospheric Research* 103 (2012) 119–128.

Svensson C., R. T. Clarke, D. A. Jones, 2007. An experimental comparison of methods for estimating rainfall intensity-duration-frequency relations from fragmentary records. *Journal of Hydrology* (2007) 341, 79– 89.

Palynchuk B. and Y. Guo, 2008. Threshold analysis of rainstorm depth and duration statistics at Toronto, Canada. *Journal of Hydrology* (2008) 348, 535– 545.

Zhu J., 2013. Impact of Climate Change on Extreme Rainfall across the United States. *J. Hydrol. Eng.* 2013.18:1301-

8. APPENDIX 2: TREND ANALYSIS RESULTS

(I: Increasing; D: Decreasing; N.S: Not significant; S: Significant)

Station Name	Duration	Linear Trend	Trend Significance	p-value
Ann Arbor	15 minute	I	N.S.	$p = 0.38$
	30 minute	I	N.S.	$p = 0.30$
	1 hour	I	S	$p = 0.018$
	2 hour	I	N.S.	$p = 0.09$
	3 hour	I	N.S.	$p = 0.22$
	6 hour	I	N.S.	$p = 0.50$
	12 hour	I	N.S.	$p = 0.22$
	24 hour	I	N.S.	$p = 0.22$
Barrie	15 minute	I	N.S.	$p = 0.59$
	30 minute	I	N.S.	$p = 0.30$
	1 hour	I	N.S.	$p = 0.32$
	2 hour	I	N.S.	$p = 0.07$

	3 hour	I	N.S.	$p = 0.28$
	6 hour	I	N.S.	$p = 0.08$
	12 hour	I	S	$p = 0.04$
	24 hour	I	N.S.	$p = 0.23$
Chatham	15 minute	I	N.S.	$p = 0.71$
	30 minute	I	N.S.	$p = 0.74$
	1 hour	I	N.S.	$p = 0.39$
	2 hour	D	N.S.	$p = 0.73$
	3 hour	D	N.S.	$p = 0.38$
	6 hour	D	N.S.	$p = 0.46$
	12 hour	D	N.S.	$p = 0.64$
	24 hour	D	N.S.	$p = 0.38$
Fergus	15 minute	I	N.S.	$p = 0.37$
	30 minute	I	N.S.	$p = 0.46$
	1 hour	I	N.S.	$p = 0.24$
	2 hour	I	N.S.	$p = 0.46$
	3 hour	D	N.S.	$p = 0.22$

	6 hour	I	N.S.	$p = 0.63$
	12 hour	D	N.S.	$p = 0.81$
	24 hour	D	N.S.	$p = 0.22$
Hamilton Airport	15 minute	I	N.S.	$p = 0.84$
	30 minute	D	N.S.	$p = 0.69$
	1 hour	D	N.S.	$p = 0.26$
	2 hour	D	N.S.	$p = 0.51$
	3 hour	D	N.S.	$p = 0.65$
	6 hour	D	N.S.	$p = 0.50$
	12 hour	D	N.S.	$p = 0.35$
	24 hour	D	N.S.	$p = 0.65$
Harrow	15 minute	I	N.S.	$p = 0.46$
	30 minute	D	N.S.	$p = 0.76$
	1 hour	I	N.S.	$p = 0.79$
	2 hour	I	N.S.	$p = 0.87$
	3 hour	I	N.S.	$p = 0.69$
	6 hour	I	N.S.	$p = 0.53$

	12 hour	I	N.S.	$p = 0.96$
	24 hour	I	N.S.	$p = 0.69$
Howell	15 minute	D	N.S.	$p = 0.30$
	30 minute	D	N.S.	$p = 0.78$
	1 hour	I	N.S.	$p = 0.99$
	2 hour	D	N.S.	$p = 0.45$
	3 hour	D	N.S.	$p = 0.12$
	6 hour	D	N.S.	$p = 0.09$
	12 hour	D	N.S.	$p = 0.12$
	24 hour	D	N.S.	$p = 0.12$
Kingston	15 minute	I	N.S.	$p = 0.28$
	30 minute	I	N.S.	$p = 0.44$
	1 hour	I	N.S.	$p = 0.59$
	2 hour	I	N.S.	$p = 0.85$
	3 hour	D	N.S.	$p = 0.51$
	6 hour	I	N.S.	$p = 0.99$
	12 hour	I	N.S.	$p = 0.55$

	24 hour	D	N.S.	$p = 0.51$
London Airport	15 minute	D	N.S.	$p = 0.98$
	30 minute	D	N.S.	$p = 0.72$
	1 hour	D	N.S.	$p = 0.96$
	2 hour	I	N.S.	$p = 0.91$
	3 hour	D	N.S.	$p = 0.29$
	6 hour	D	N.S.	$p = 0.45$
	12 hour	I	N.S.	$p = 0.79$
	24 hour	D	N.S.	$p = 0.18$
Marion	15 minute	D	N.S.	$p = 0.66$
	30 minute	I	N.S.	$p = 0.96$
	1 hour	I	N.S.	$p = 0.39$
	2 hour	I	N.S.	$p = 0.80$
	3 hour	D	N.S.	$p = 0.66$
	6 hour	D	N.S.	$p = 0.78$
	12 hour	D	N.S.	$p = 0.82$
	24 hour	D	N.S.	$p = 0.66$

Oshawa	15 minute	I	N.S.	$p = 0.98$
	30 minute	I	N.S.	$p = 0.83$
	1 hour	I	N.S.	$p = 0.78$
	2 hour	I	N.S.	$p = 0.61$
	3 hour	I	S	$p = 0.008$
	6 hour	I	S	$p = 0.008$
	12 hour	D	N.S.	$p = 0.54$
	24 hour	I	S	$p = 0.008$
Toronto	15 minute	I	N.S.	$p = 0.65$
	30 minute	I	N.S.	$p = 0.63$
	1 hour	D	N.S.	$p = 0.56$
	2 hour	D	N.S.	$p = 0.49$
	3 hour	D	S	$p = 0.009$
	6 hour	D	N.S.	$p = 0.58$
	12 hour	D	N.S.	$p = 0.38$
	24 hour	D	S	$p = 0.009$
Toronto Airport	15 minute	D	N.S.	$p = 0.12$

	30 minute	D	N.S.	$p = 0.10$
	1 hour	D	N.S.	$p = 0.11$
	2 hour	D	S	$p = 0.031$
	3 hour	D	N.S.	$p = 0.45$
	6 hour	D	N.S.	$p = 0.11$
	12 hour	D	N.S.	$p = 0.08$
	24 hour	D	N.S.	$p = 0.45$
Trenton	15 minute	D	N.S.	$p = 0.28$
	30 minute	I	N.S.	$p = 0.92$
	1 hour	I	N.S.	$p = 0.25$
	2 hour	I	N.S.	$p = 0.10$
	3 hour	I	N.S.	$p = 0.07$
	6 hour	I	N.S.	$p = 0.12$
	12 hour	I	N.S.	$p = 0.07$
	24 hour	I	N.S.	$p = 0.07$
Windsor Airport	15 minute	D	S	$p = 0.021$
	30 minute	D	S	$p = 0.026$

1 hour	D	S	$p = 0.008$
2 hour	D	N.S.	$p = 0.06$
3 hour	D	N.S.	$p = 0.38$
6 hour	D	N.S.	$p = 0.15$
12 hour	D	N.S.	$p = 0.10$
24 hour	D	N.S.	$p = 0.38$

9. APPENDIX 3: DISTRIBUTIONS AND SELECTION CRITERIA

Distributions investigated

Based on the literature review results (Appendix 1), all the distributions commonly used in Canada for extreme rainfall frequency analysis are selected. In addition, distributions commonly used in Eastern United States are also evaluated. Table A1 provides a list of the distributions evaluated for different rainfall durations.

Table A3. List of distributions evaluated

Abbreviation used	<i>Distribution</i>
GEV	<i>Generalized Extreme Value</i>
N	Normal
LN	<i>Log Normal</i>
Gam	Gamma
EV1	<i>Gumbel Extreme value type 1</i>
LP3	<i>Log-Pearson type 3</i>
Wbl	<i>Weibull</i>

Distribution evaluation criteria

Given that there is no universal single criterion for selecting a distribution, a multi-criteria approach is used to identify the best performing distributions. Table A2 hereafter presents briefly the criteria used to identify the best distributions.

Table A4. Distribution evaluation criteria

	Criteria	Description
1	AIC	AIC stands for Akaike Information Criterion. Founded on the information theory, the AIC is among the most widely used criteria in model selection (Kuipper and Hoijtink, 2011). It is a relative estimate of the information lost when a given model is used to represent the process that generates the data, and therefore allows to rank multiple competing models used in function approximation or curve fitting (Symonds and Moussalli, 2010). Among a set of candidate models fitted to a dataset, the preferred model is the one with the smallest AIC value. AIC penalizes the distributions with the higher number of parameters, it is a parsimony criterion in favor of Occam's Razor.
2	PPCC1	PPCC1 is the linear correlation coefficient between the quantiles of the distribution function and the quantiles of the input sample. The quantiles of the input sample are computed using Matlab function " <i>quantiles</i> ". The parameters of the distribution function are estimated using the <i>maximum likelihood method</i> . The higher the PPCC1 value, the better the correlation is. However, the higher correlation coefficient does not necessary means that the distribution candidate is a good fit. Both the quantiles of the input sample and the quantiles of the distribution function should also be similar, resulting in a good spray of points around the line $y=x$ in the quantile-quantile plot graph (QQ plot Fit). Therefore the PPCC1 values should be used jointly with the QQ plots.

3	QQ plot Fit	<p>Visual appreciation of the fitting quality (G=good, F=fairly good, and P=poor) based on the observation of the quantile-quantile plot graph. The quantile-quantile plot is a simple and practical goodness of fit method that can be used for selecting suitable statistical distributions (Opere et al. 2006). A good fit of the distribution to the data will result in most points been closely aligned on the $y=x$ line. The quantile-quantile plot also facilitates the evaluation of the behaviour of the distribution tail.</p>
4	Blom & Gring	<p>Visual appreciation of the fitting quality (G=good, F=fairly good, and P=poor) based on Blom and Gringorten experimental frequency function graphs. Empirical quantiles are estimated using Blom or Gringorten formula and those quantiles are plotted against the quantiles of the theoretical probability distribution function. Hence a good fit of the distribution to the data will result in most points been closely aligned. Here the parameters of the distribution function are estimated using L-moment method instead of the Maximum Likelihood method in the aforementioned case of “QQ plot fit”. The Blom and Gringorten experimental frequency function graphs are reliable visual tools for selecting a distribution (Anctil et al. 2005), and should be used along with the related linear correlation coefficients (PPCC2).</p>
5	PPCC2	<p>PPCC2 is the linear correlation coefficient related to the Blom and Gringorten (Blom & Gring) experimental frequency function graphs. Characteristics are similar to PPCC1 above.</p>
6	LmDiag	<p>Another useful visual appreciation tool is the L-moments diagram. This diagram consists of presenting in the same graph the L-moments coefficient of kurtosis (L-CK) of each distribution as a function of its L-moment coefficient of skewness (L-CV). For 3-parameter distribution the representation of the L-CK as a function of L-CV will result in a curve while for 2-parameter distribution it will be a point. In the same graph the point corresponding to L-CK as a function of L-CV for the observed data is considered the reference point. The best distribution is the one which curve or point is the closest to the reference point (“point of the observed data”). Distributions are sorted from 1(best), 2(second best), 3(third).....n(worst). This method of selecting the best fit distribution based on the diagram of L-moments has been largely used in the literature since its introduction by Hoskin and Wallis (1995). This method can also be</p>

		used for regional homogeneity analysis by plotting in the same graph the points representing the L-CK of the observed data as a function of L-CV for all the stations.
7	hist Fit	Visual appreciation of the distributions fitting (G =good, F =fairly good, and P =poor) based on the observation of the histogram. Matlab distribution fitting tool “ <i>dfittool</i> ” is used to match the theoretical density probability function to the histogram of the input sample (historical hyetograph).
8	H-ks	H-ks is the statistical test decision for the null hypothesis that the data come from the specified distribution, against the alternative that it does not come from such a distribution, using the one-sample Kolmogorov-Smirnov goodness of fit test . Under this test, the goodness of fit is evaluated by calculating the maximum deviation between the theoretical distribution function and the empirical distribution and then to compare this deviation to critical tabulated values that depend on both the sample size and the significance level (Haan 2002, Opere et al., 2006). The Matlab function “ <i>kstest</i> ” is used to perform this test with significance level set at 0.05. H-ks = 1 if the test rejects the null hypothesis at the 5% significance level, or 0 otherwise (null hypothesis accepted).
9	Pval-ks	Pval-ks is the P-value of the Kolmogorov-Smirnov goodness of fit test , returned as a scalar value in the range [0 1]. It is the probability of observing the test statistic as extreme as or more extreme than the observed value under the null hypothesis. Small value of Pval-ks (less than 0.05) casts doubt on the validity of the hypothesis that the data come from the specified distribution.
10	H-chiq	H-chiq is the statistical test decision for the null hypothesis that the data come from the specified distribution, against the alternative that it does not come from such a distribution, using the chi-square goodness of fit test . Under this test, the discrepancy between the observed and the expected number of observations in k defined histogram classes is evaluated and then compared to a critical value provided in tables at selected significance level (Haan 2002, Anctil et al. 2005). The test usually requires a long data series in order to be effective since one should have at least 5 observations in each histogram classes. The Matlab function “ <i>chi2gof</i> ” is used to perform this test at significance level set at 0.05. H-chiq = 1 if the test rejects the null hypothesis at the 5% significance level, or 0 otherwise.

11	Pval-chiq	<p>Pval-chiq is the P-value of the Chi square goodness of fit test. Idem to Pval-ks above. When the data series is not long enough and that the condition of having at least 5 observations in each histogram class is not met, Pval-chiq evaluation is considered not effective and will result in NaN values that we can see in the case of some of the stations.</p>
----	-----------	---

References

Ancil F., J. Rousselle, Lauzon, N. (2005). Hydrologie: Cheminements de l'eau. Editions Presse Internationale Polytechnique, 317 p.

Haan, C.T. (2002). Statistical Methods in Hydrology. Iowa State Press, Ames, Iowa

Hosking, J.R.M., Wallis, J.R., (1995). A comparison of unbiased and plotting-position estimators of L-moments. Water Resources Research 31 (8), 2019–2025.

Kuipper R. M., Hoijtink, H., Silvapulle, M.J. (2011). An Akaike-type information criterion for model selection under inequality constraints. Biometrika, 98 (2): 495–501.

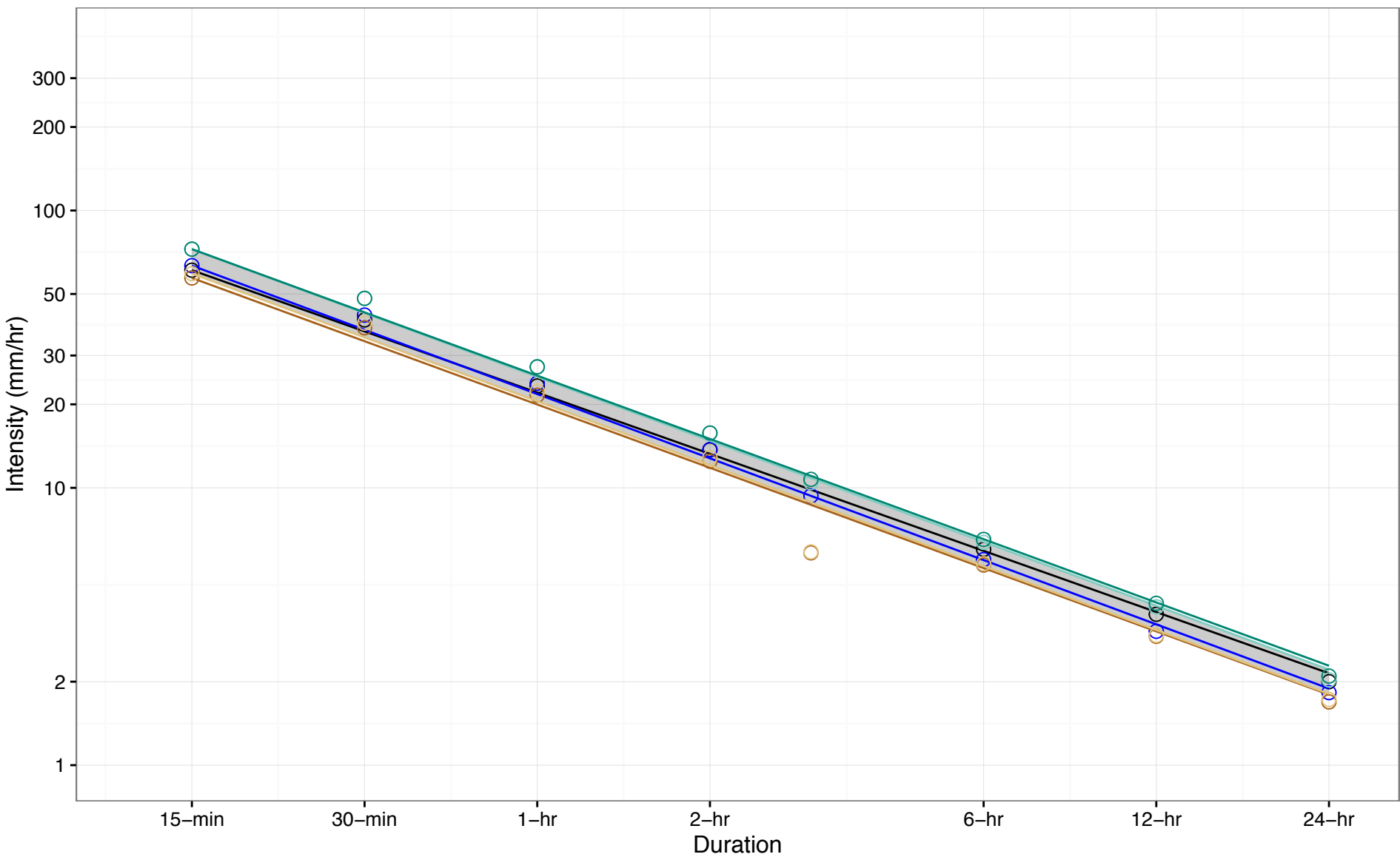
Opere A. O., S. Mkhandi, P. Willems, (2006). At site flood frequency analysis for the Nile Equatorial basins. Physics and Chemistry of the Earth, 31: 919–927.

Symonds, M.R.E., Moussalli, A. (2010). A brief guide to model selection, multimodel inference and model averaging in behavioural ecology using Akaike's information criterion. Behav. Ecol. Sociobiol., 65: 13–21.

A Comparison of Future IDF Curves for Southern Ontario

Addendum – Appendix A: IDF Curve
Overlay Plots

Figure A-1: IDF Curve Comparison for Pearson Airport, 2030s 2-year Return Period Event (10th–90th Percentile)



10th to 90th Percentile Range

(a) Hist. Gumbel: $R=22.05T^{-0.733}$

(b) Hist. GEV: $R=21.78T^{-0.769}$

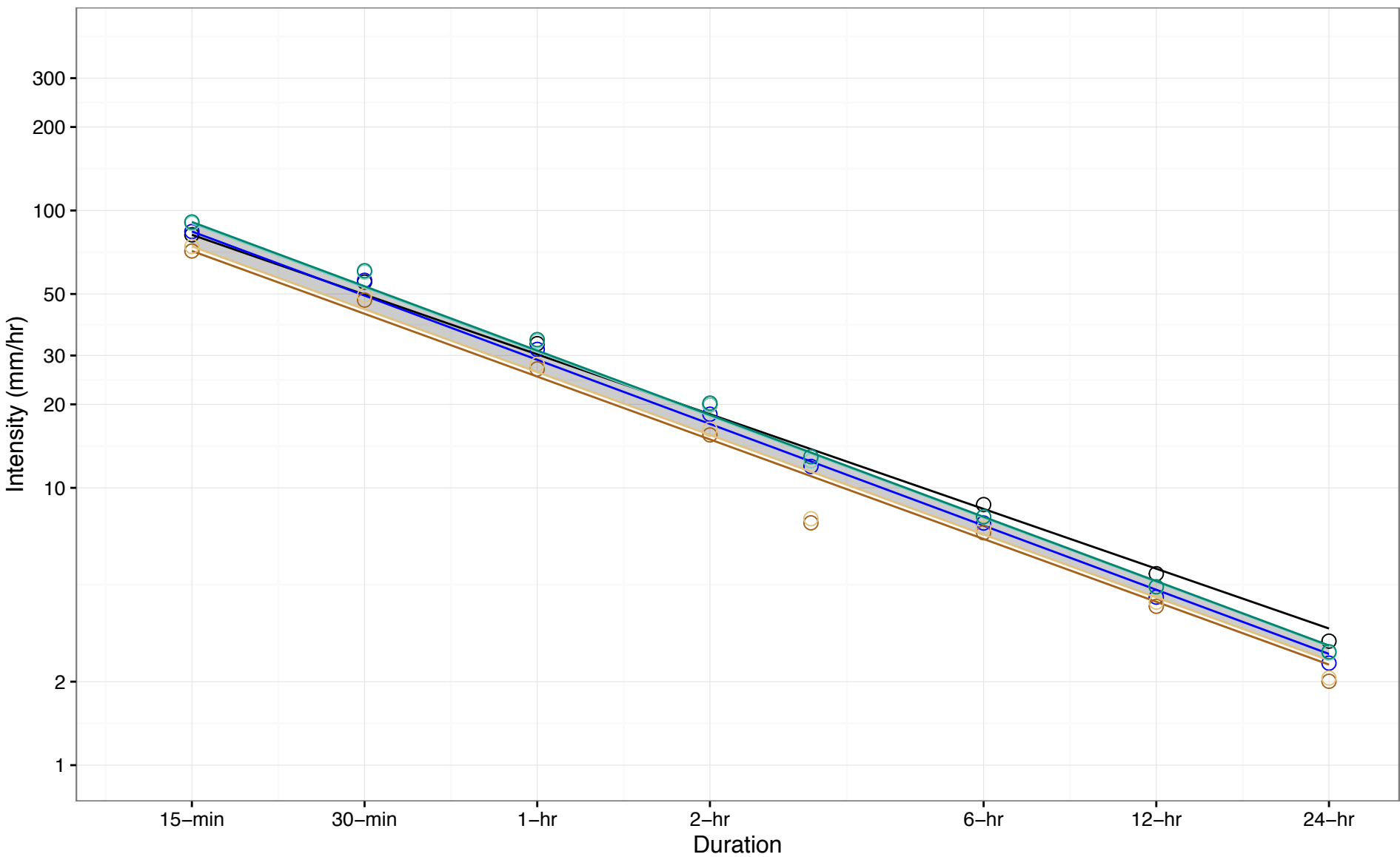
(c) Fut. Ensemble Min.: $R=19.97T^{-0.758}$

(d) Fut. Ensemble 10th Percentile: $R=20.52T^{-0.764}$

(e) Fut. Ensemble 90th Percentile: $R=25.12T^{-0.765}$

(f) Fut. Ensemble Max.: $R=25.38T^{-0.758}$

Figure A-2: IDF Curve Comparison for Pearson Airport, 2030s 5-year Return Period Event (10th-90th Percentile)



⊖ (a) Hist. Gumbel: $R=30.29T^{-0.716}$

⊖ (b) Hist. GEV: $R=28.96T^{-0.768}$

■ 10th to 90th Percentile Range

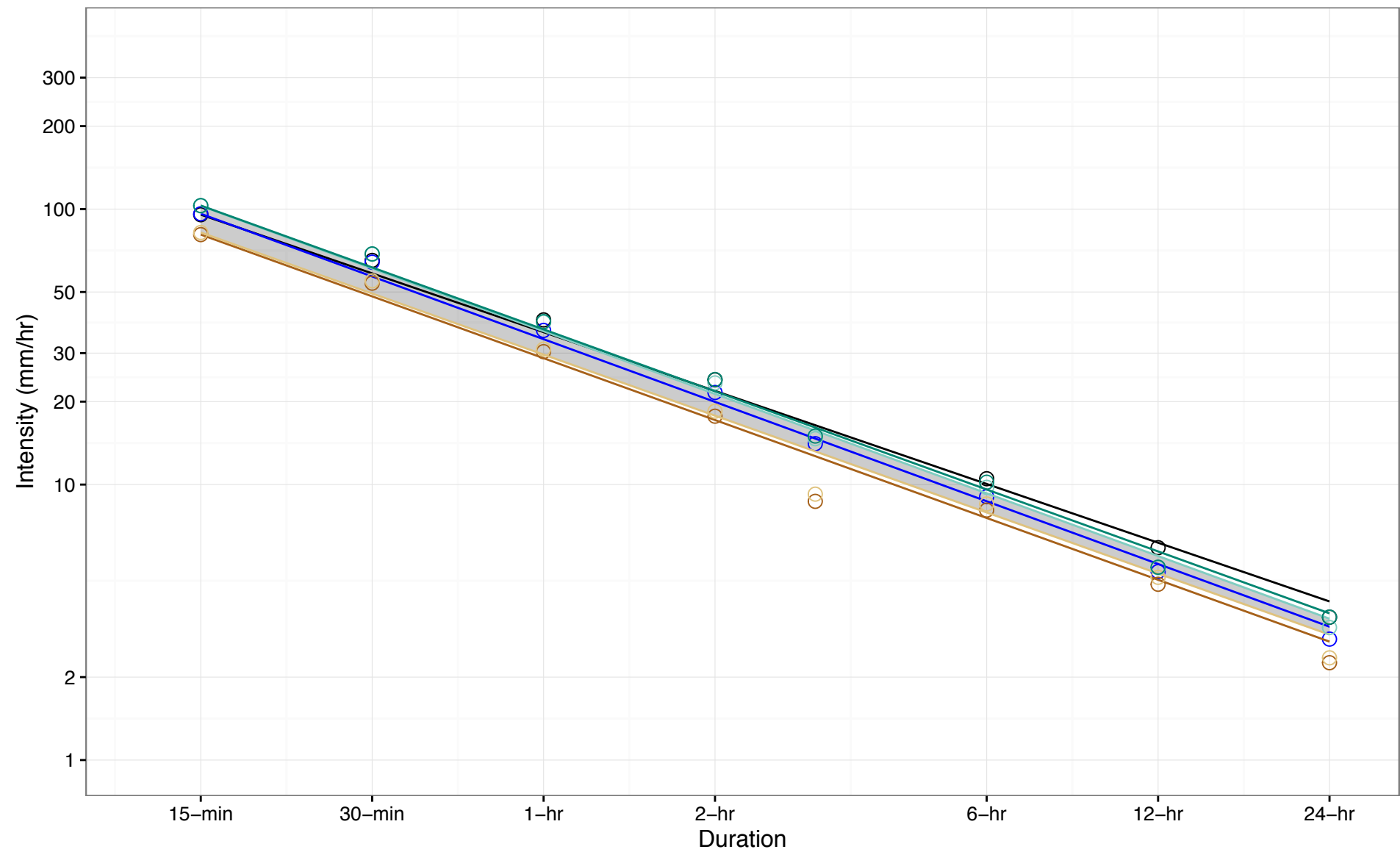
⊖ (c) Fut. Ensemble Min.: $R=25.18T^{-0.752}$

⊖ (d) Fut. Ensemble 10th Percentile: $R=26.14T^{-0.753}$

⊖ (e) Fut. Ensemble 90th Percentile: $R=30.96T^{-0.769}$

⊖ (f) Fut. Ensemble Max.: $R=31.26T^{-0.77}$

Figure A-3: IDF Curve Comparison for Pearson Airport, 2030s 10-year Return Period Event (10th-90th Percentile)



⊖ (a) Hist. Gumbel: $R=35.76T^{-0.708}$

⊖ (b) Hist. GEV: $R=33.71T^{-0.756}$

■ 10th to 90th Percentile Range

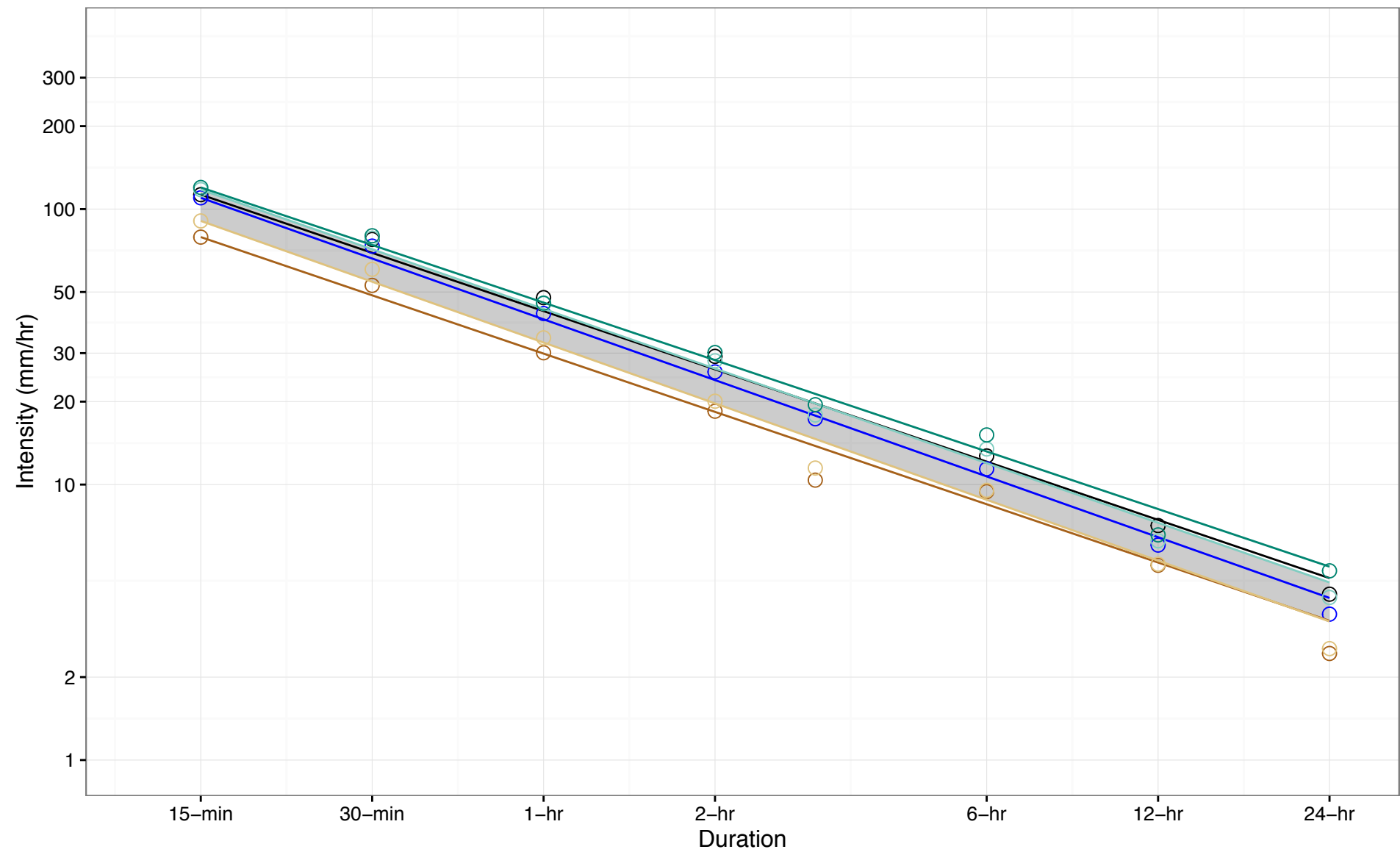
⊖ (c) Fut. Ensemble Min.: $R=28.76T^{-0.745}$

⊖ (d) Fut. Ensemble 10th Percentile: $R=29.63T^{-0.736}$

⊖ (e) Fut. Ensemble 90th Percentile: $R=36.03T^{-0.756}$

⊖ (f) Fut. Ensemble Max.: $R=36.58T^{-0.747}$

Figure A-4: IDF Curve Comparison for Pearson Airport, 2030s 25-year Return Period Event (10th–90th Percentile)



10th to 90th Percentile Range

(a) Hist. Gumbel: $R=42.63T^{-0.702}$

(b) Hist. GEV: $R=39.8T^{-0.733}$

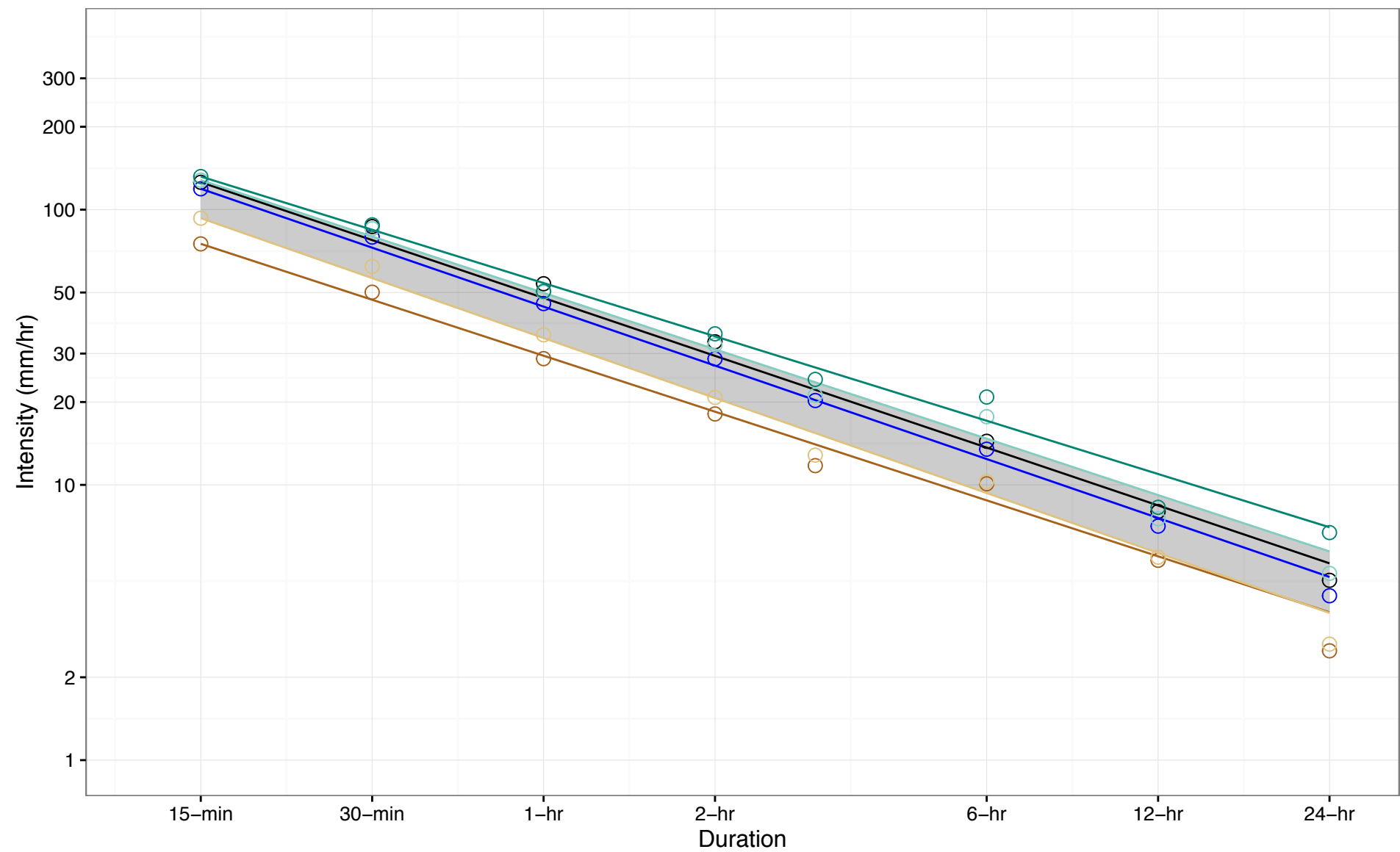
(c) Fut. Ensemble Min.: $R=29.88T^{-0.703}$

(d) Fut. Ensemble 10th Percentile: $R=32.77T^{-0.734}$

(e) Fut. Ensemble 90th Percentile: $R=43.41T^{-0.719}$

(f) Fut. Ensemble Max.: $R=45.77T^{-0.694}$

Figure A-5: IDF Curve Comparison for Pearson Airport, 2030s 50-year Return Period Event (10th-90th Percentile)



10th to 90th Percentile Range

⊖ (a) Hist. Gumbel: $R=47.76T^{-0.698}$

⊖ (b) Hist. GEV: $R=44.42T^{-0.711}$

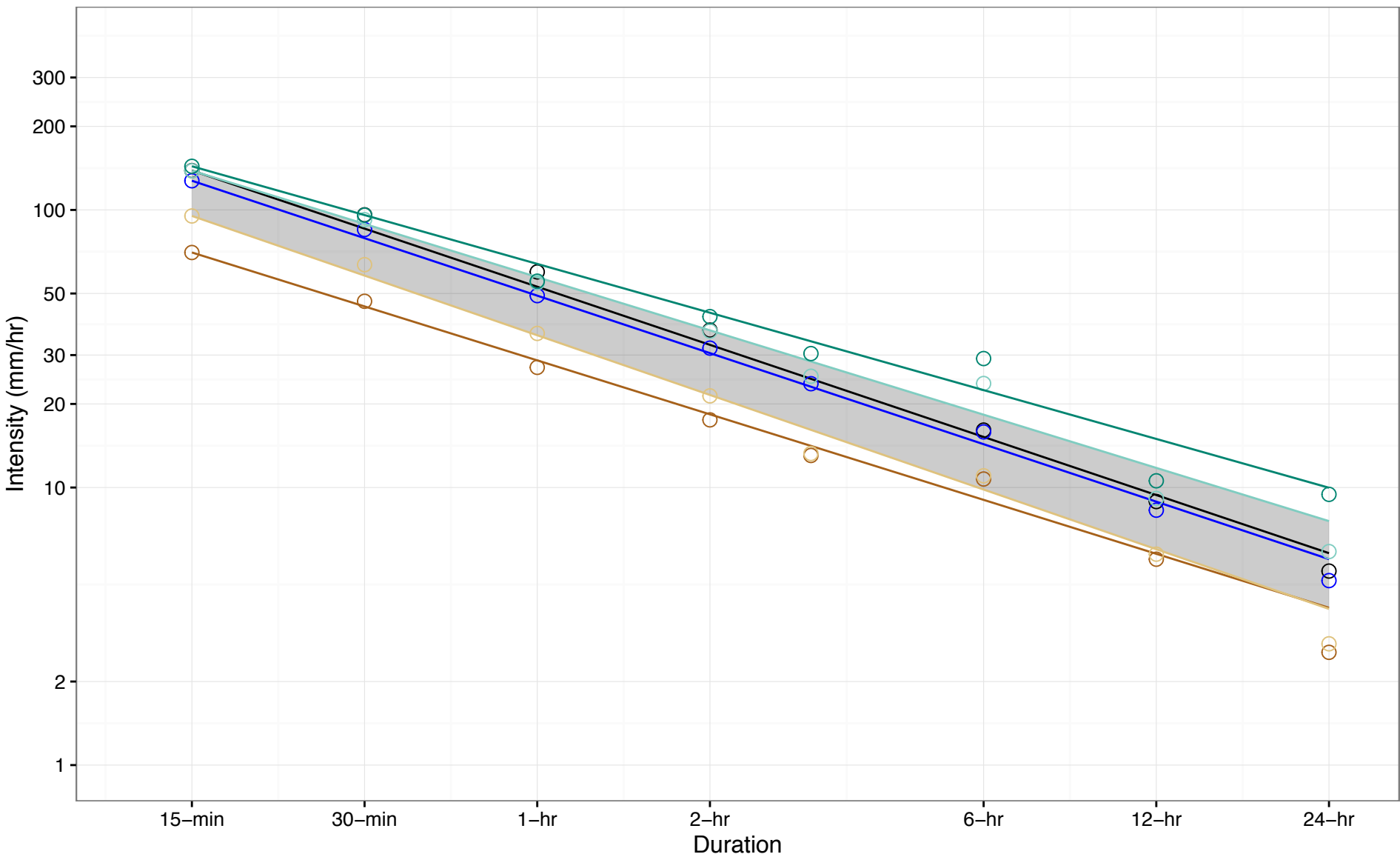
⊖ (c) Fut. Ensemble Min.: $R=29.46T^{-0.675}$

⊖ (d) Fut. Ensemble 10th Percentile: $R=34.15T^{-0.724}$

⊖ (e) Fut. Ensemble 90th Percentile: $R=49.83T^{-0.681}$

⊖ (f) Fut. Ensemble Max.: $R=54.11T^{-0.643}$

Figure A-6: IDF Curve Comparison for Pearson Airport, 2030s 100-year Return Period Event (10th–90th Percentile)



⊖ (a) Hist. Gumbel: $R=52.89T^{-0.695}$

⊖ (b) Hist. GEV: $R=49.11T^{-0.688}$

■ 10th to 90th Percentile Range

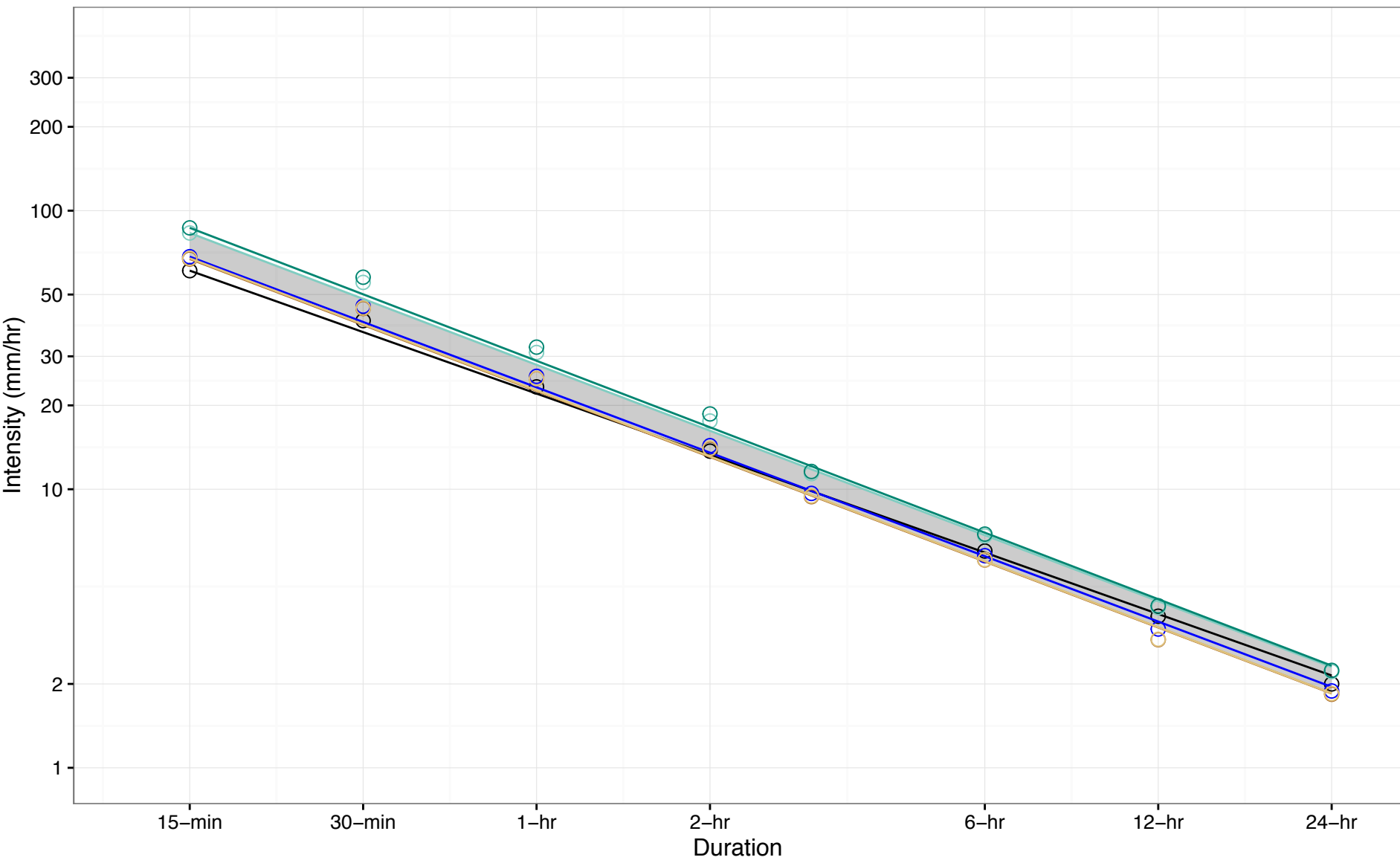
⊖ (c) Fut. Ensemble Min.: $R=28.71T^{-0.646}$

⊖ (d) Fut. Ensemble 10th Percentile: $R=35.35T^{-0.714}$

⊖ (e) Fut. Ensemble 90th Percentile: $R=57.27T^{-0.637}$

⊖ (f) Fut. Ensemble Max.: $R=63.91T^{-0.584}$

Figure A-7: IDF Curve Comparison for Pearson Airport, 2050s 2-year Return Period Event (10th–90th Percentile)



■ 10th to 90th Percentile Range

⊖ (a) Hist. Gumbel: $R=22.05T^{-0.733}$

⊖ (b) Hist. GEV: $R=23.22T^{-0.779}$

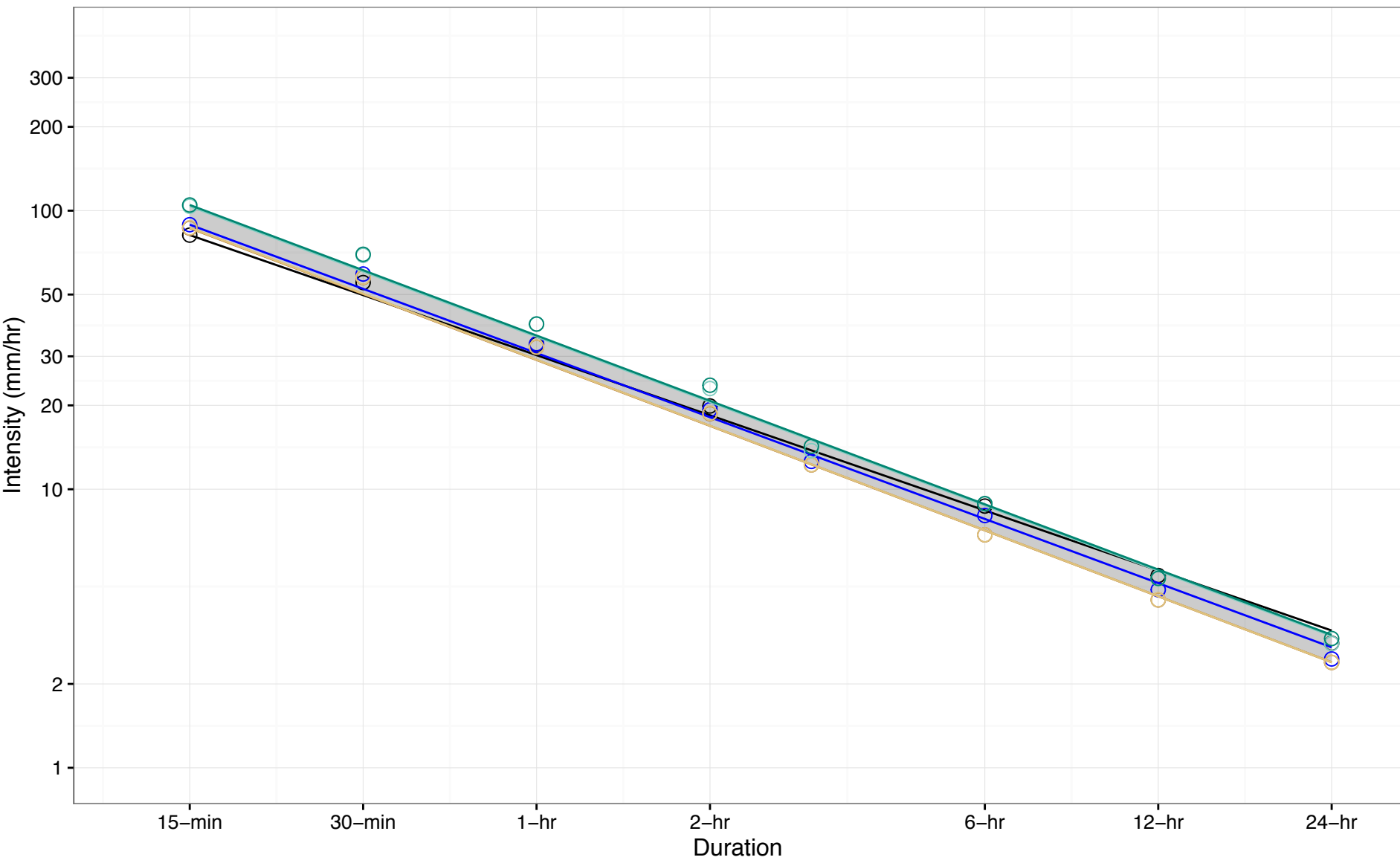
⊖ (c) Fut. Ensemble Min.: $R=22.53T^{-0.787}$

⊖ (d) Fut. Ensemble 10th Percentile: $R=22.64T^{-0.788}$

⊖ (e) Fut. Ensemble 90th Percentile: $R=27.97T^{-0.786}$

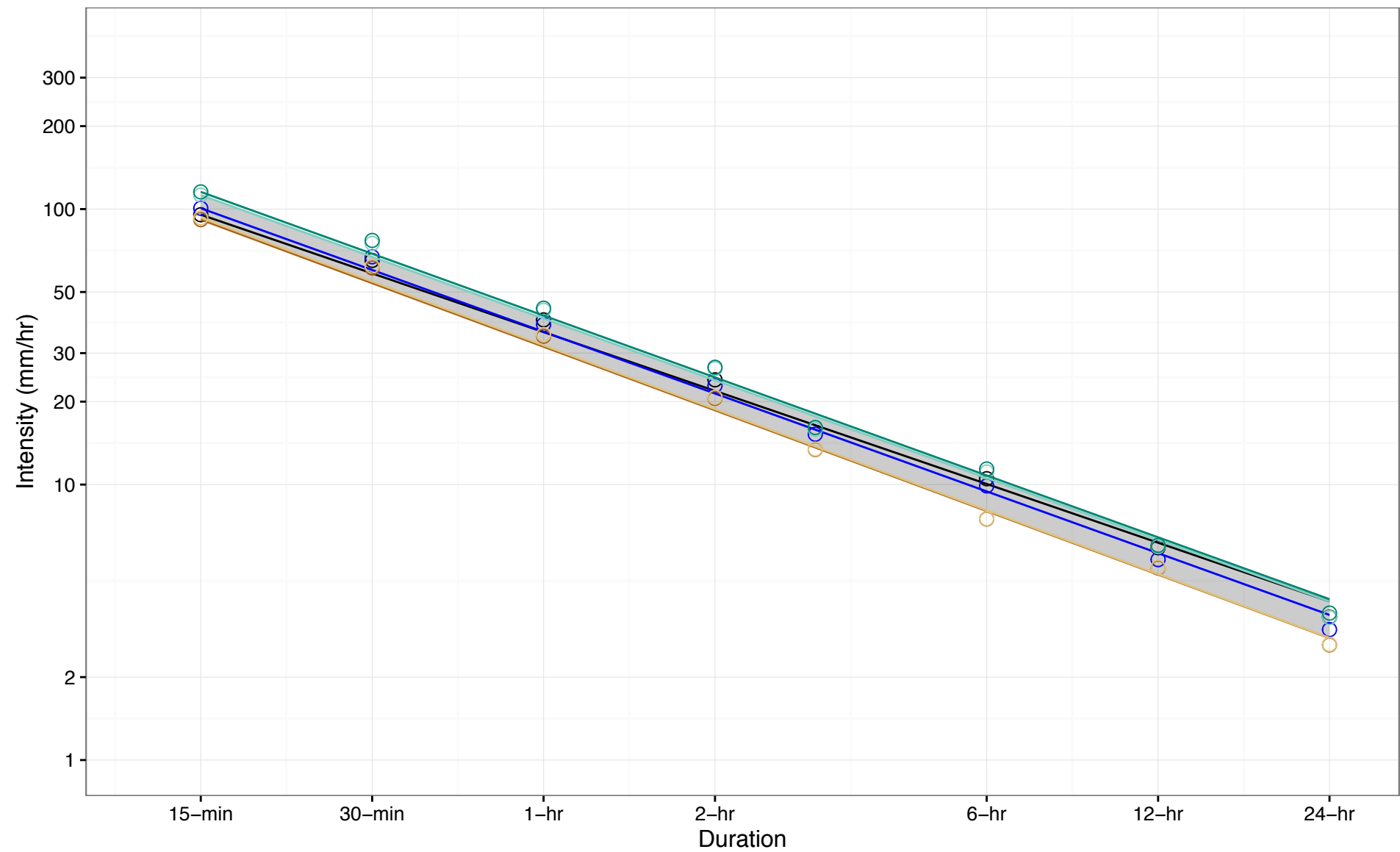
⊖ (f) Fut. Ensemble Max.: $R=28.91T^{-0.793}$

Figure A-8: IDF Curve Comparison for Pearson Airport, 2050s 5-year Return Period Event (10th-90th Percentile)



-

Figure A-9: IDF Curve Comparison for Pearson Airport, 2050s 10-year Return Period Event (10th-90th Percentile)



10th to 90th Percentile Range

(a) Hist. Gumbel: $R=35.76T^{-0.708}$

(b) Hist. GEV: $R=35.87T^{-0.745}$

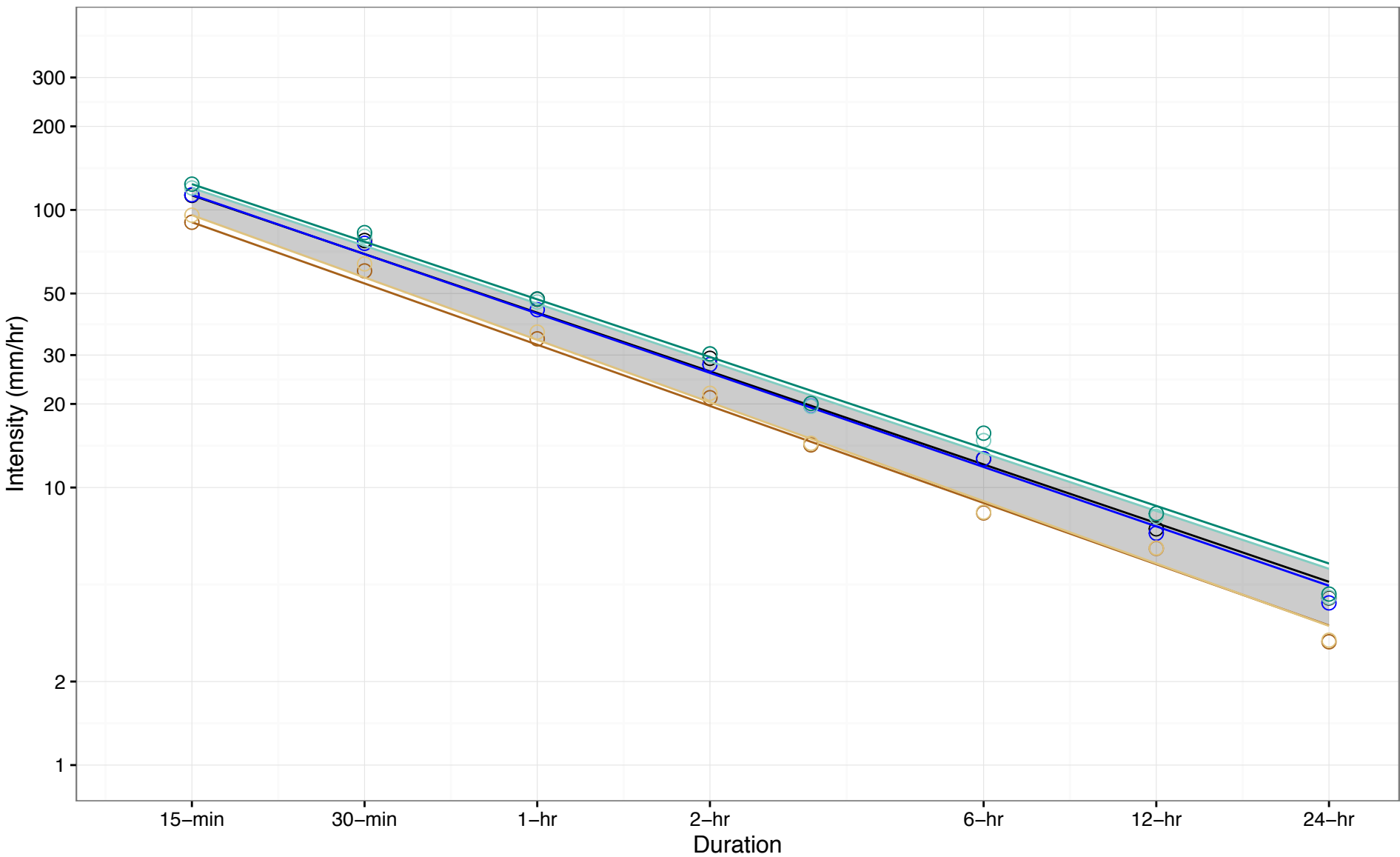
(c) Fut. Ensemble Min.: $R=31.65T^{-0.766}$

(d) Fut. Ensemble 10th Percentile: $R=32.02T^{-0.769}$

(e) Fut. Ensemble 90th Percentile: $R=40.07T^{-0.744}$

(f) Fut. Ensemble Max.: $R=41.06T^{-0.746}$

Figure A-10: IDF Curve Comparison for Pearson Airport, 2050s 25-year Return Period Event (10th-90th Percentile)



10th to 90th Percentile Range

(a) Hist. Gumbel: $R=42.63T^{-0.702}$

(b) Hist. GEV: $R=42.35T^{-0.711}$

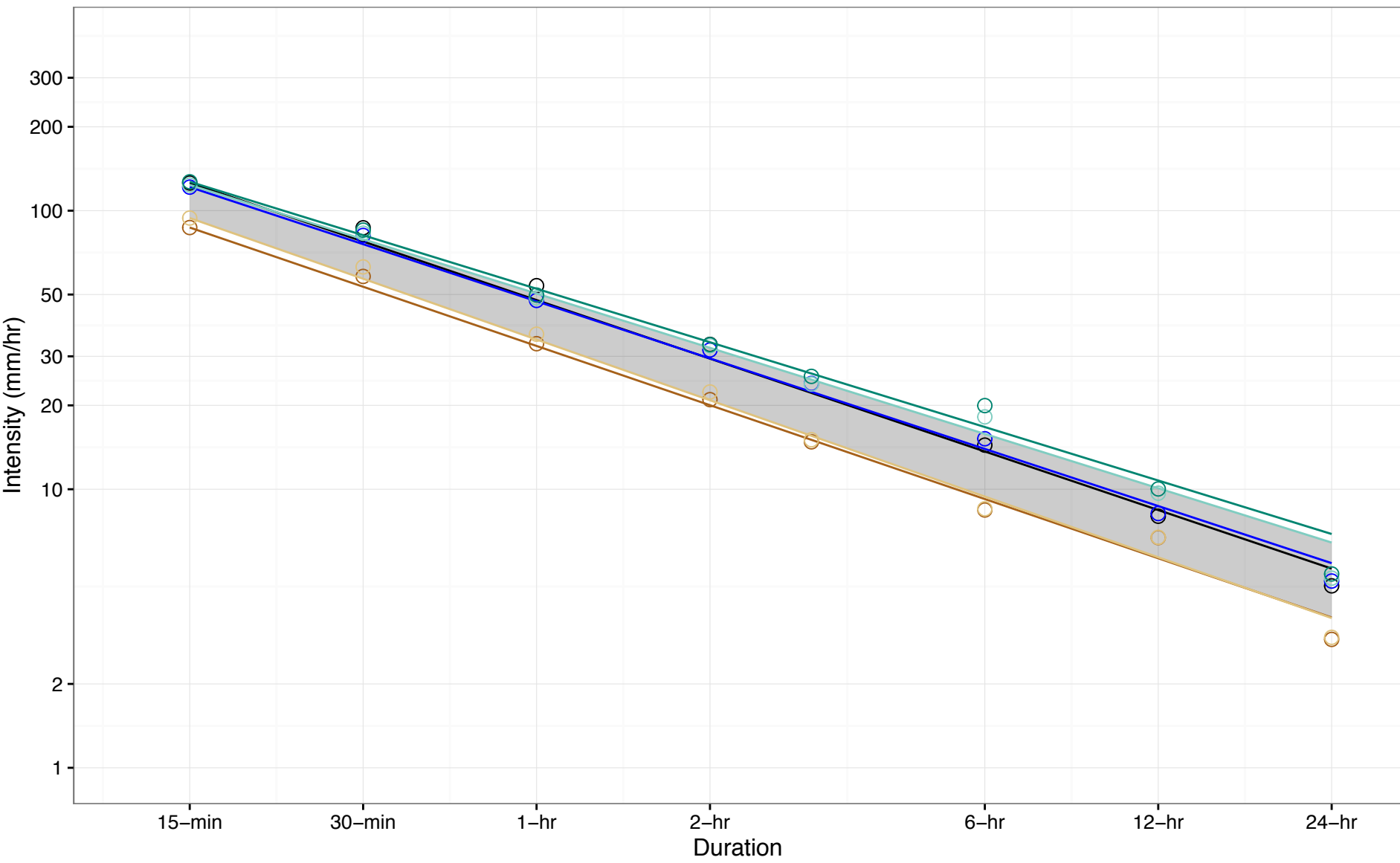
(c) Fut. Ensemble Min.: $R=32.69T^{-0.733}$

(d) Fut. Ensemble 10th Percentile: $R=34.03T^{-0.746}$

(e) Fut. Ensemble 90th Percentile: $R=45.98T^{-0.692}$

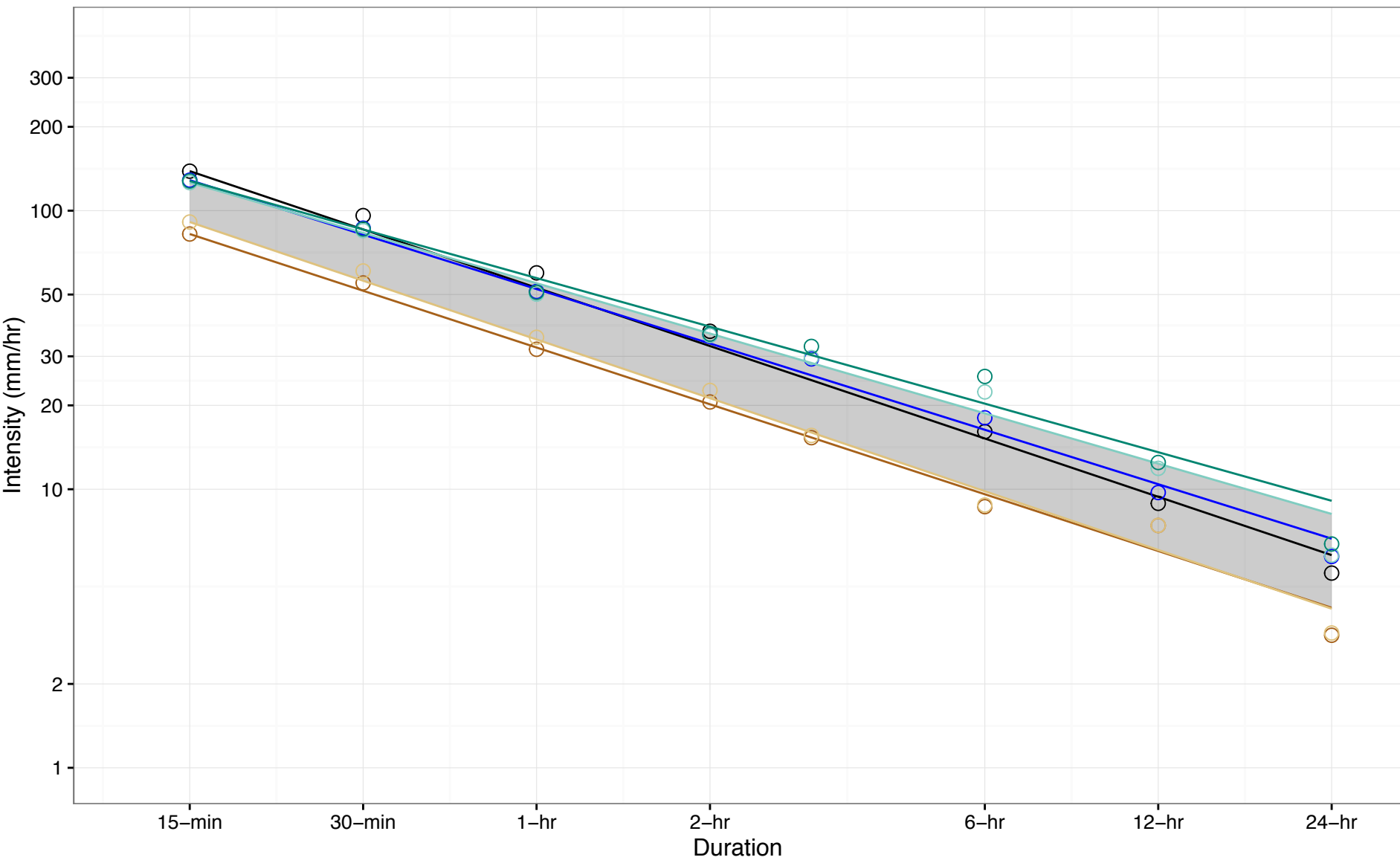
(f) Fut. Ensemble Max.: $R=47.63T^{-0.69}$

Figure A-11: IDF Curve Comparison for Pearson Airport, 2050s 50-year Return Period Event (10th–90th Percentile)



- 10th to 90th Percentile Range
- ⊖ (a) Hist. Gumbel: $R=47.76T^{-0.698}$
- ⊕ (b) Hist. GEV: $R=47.28T^{-0.681}$
- ⊖ (c) Fut. Ensemble Min.: $R=32.68T^{-0.706}$
- ⊕ (d) Fut. Ensemble 10th Percentile: $R=34.47T^{-0.725}$
- ⊖ (e) Fut. Ensemble 90th Percentile: $R=50.42T^{-0.648}$
- ⊕ (f) Fut. Ensemble Max.: $R=52.45T^{-0.638}$

Figure A-12: IDF Curve Comparison for Pearson Airport, 2050s 100-year Return Period Event (10th-90th Percentile)

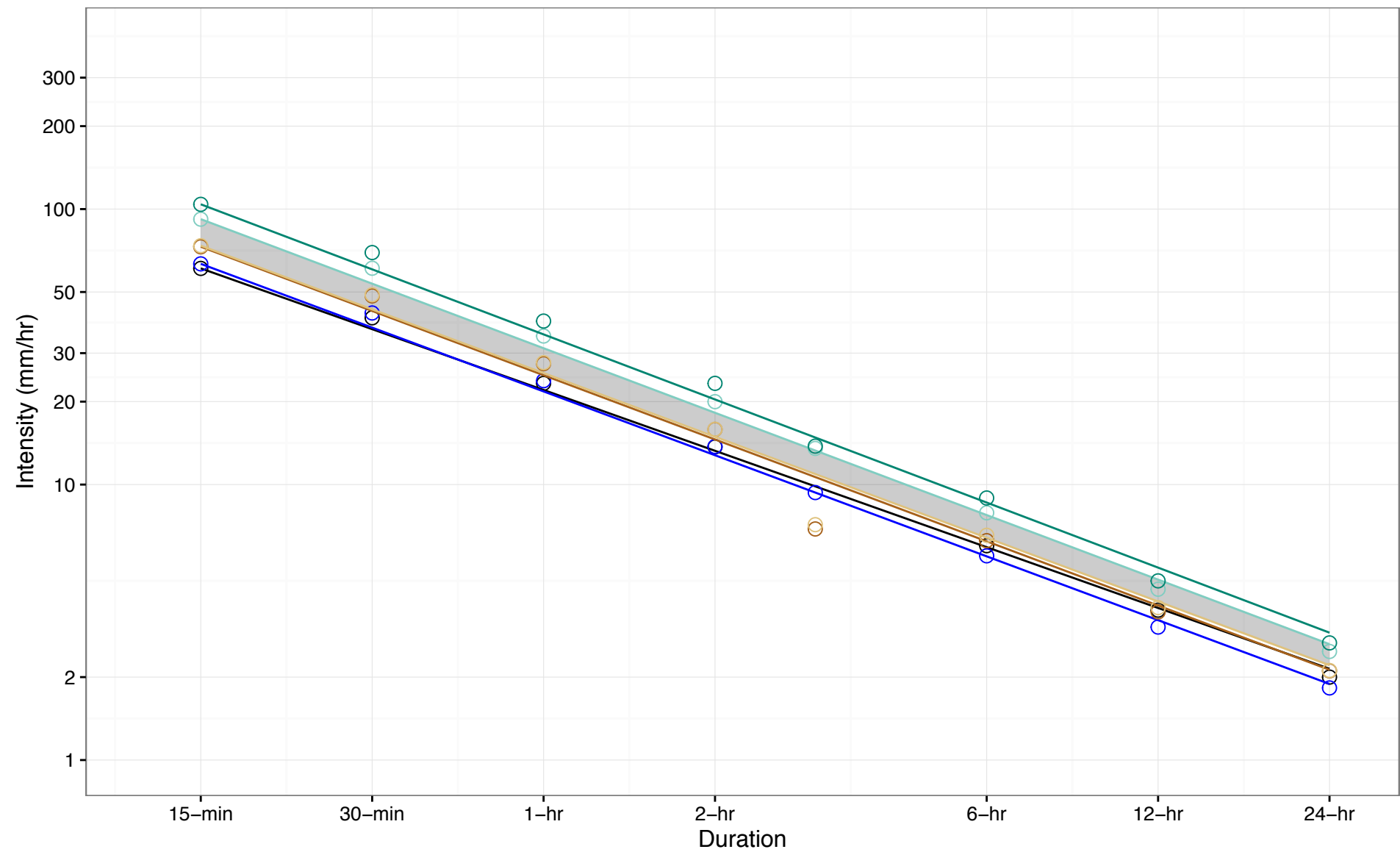


(a) Hist. Gumbel: $R=52.89T^{-0.695}$
 (b) Hist. GEV: $R=52.32T^{-0.649}$
 10th to 90th Percentile Range

(c) Fut. Ensemble Min.: $R=32.27T^{-0.677}$
 (d) Fut. Ensemble 10th Percentile: $R=34.49T^{-0.7}$

(e) Fut. Ensemble 90th Percentile: $R=54.9T^{-0.6}$
 (f) Fut. Ensemble Max.: $R=57.29T^{-0.579}$

Figure A-13: IDF Curve Comparison for Pearson Airport, 2090s 2-year Return Period Event (10th-90th Percentile)



10th to 90th Percentile Range

(a) Hist. Gumbel: $R=22.05T^{-0.733}$

(b) Hist. GEV: $R=21.78T^{-0.769}$

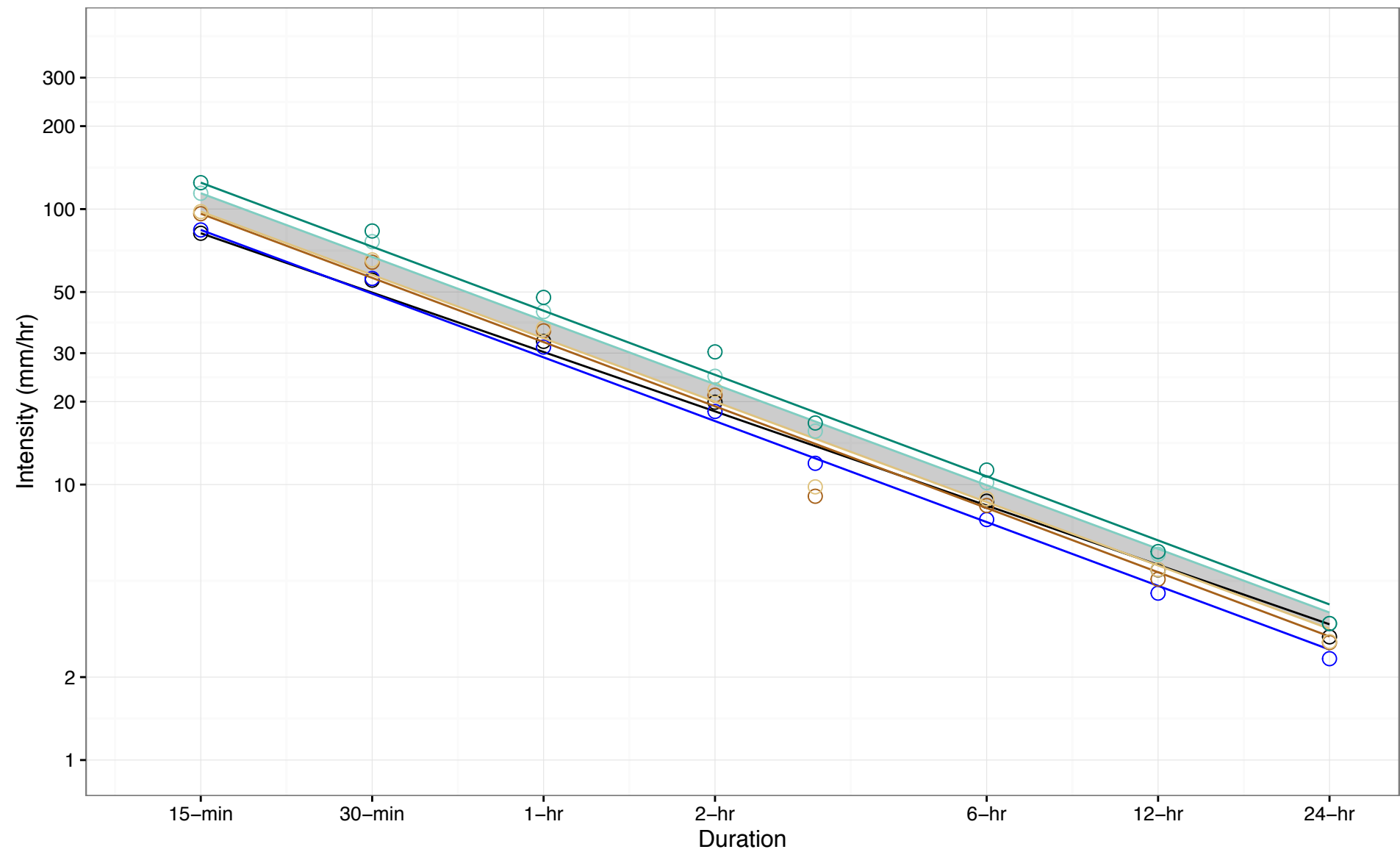
(c) Fut. Ensemble Min.: $R=24.94T^{-0.775}$

(d) Fut. Ensemble 10th Percentile: $R=25.39T^{-0.768}$

(e) Fut. Ensemble 90th Percentile: $R=31.25T^{-0.778}$

(f) Fut. Ensemble Max.: $R=35.08T^{-0.784}$

Figure A-14: IDF Curve Comparison for Pearson Airport, 2090s 5-year Return Period Event (10th-90th Percentile)



⊖ (a) Hist. Gumbel: $R=30.29T^{-0.716}$

⊖ (b) Hist. GEV: $R=28.96T^{-0.768}$

■ 10th to 90th Percentile Range

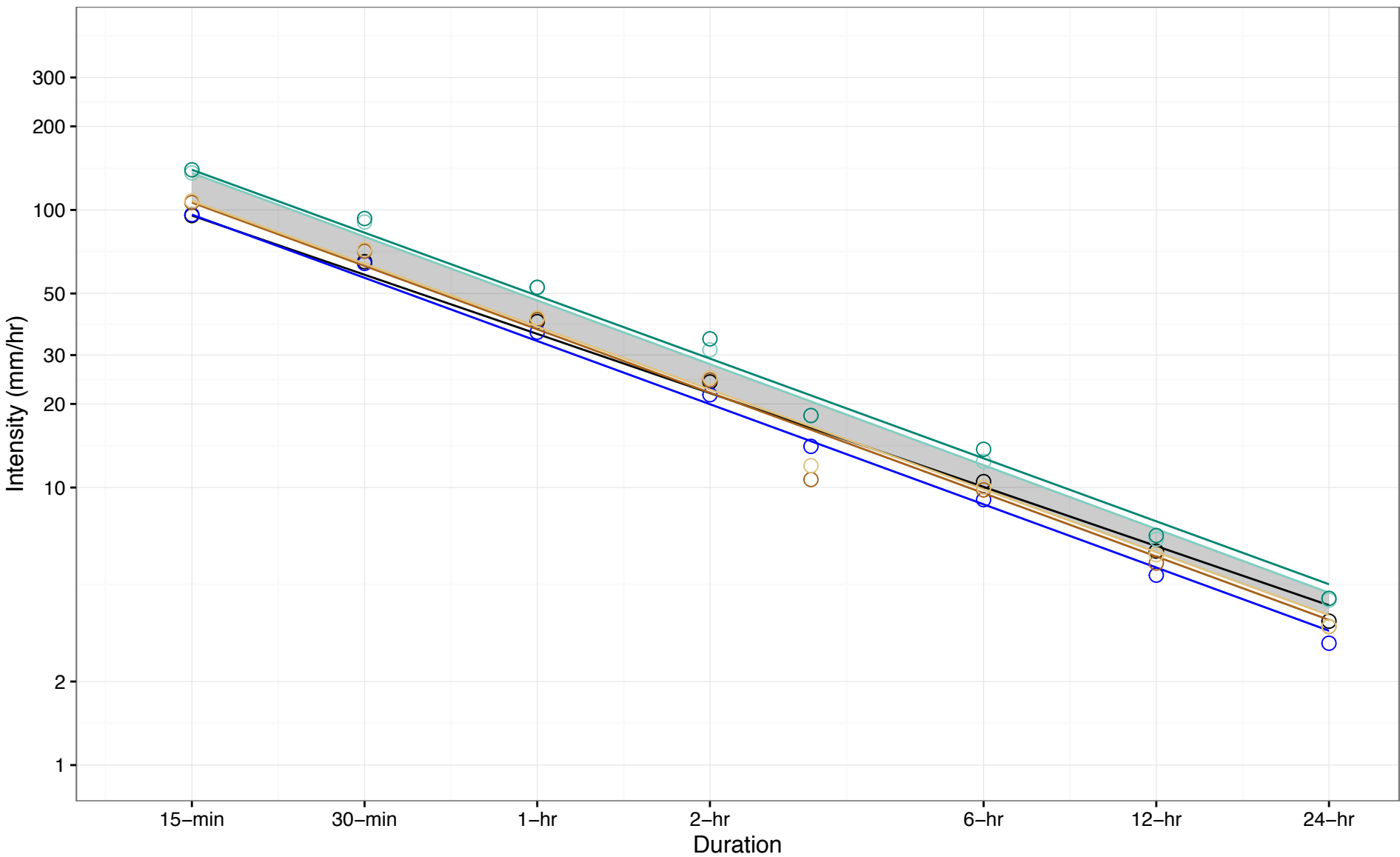
⊖ (c) Fut. Ensemble Min.: $R=32.91T^{-0.774}$

⊖ (d) Fut. Ensemble 10th Percentile: $R=33.96T^{-0.764}$

⊖ (e) Fut. Ensemble 90th Percentile: $R=39.38T^{-0.768}$

⊖ (f) Fut. Ensemble Max.: $R=42.76T^{-0.772}$

Figure A-15: IDF Curve Comparison for Pearson Airport, 2090s 10-year Return Period Event (10th-90th Percentile)



⊖ (a) Hist. Gumbel: $R=35.76T^{-0.708}$

⊖ (b) Hist. GEV: $R=33.71T^{-0.756}$

■ 10th to 90th Percentile Range

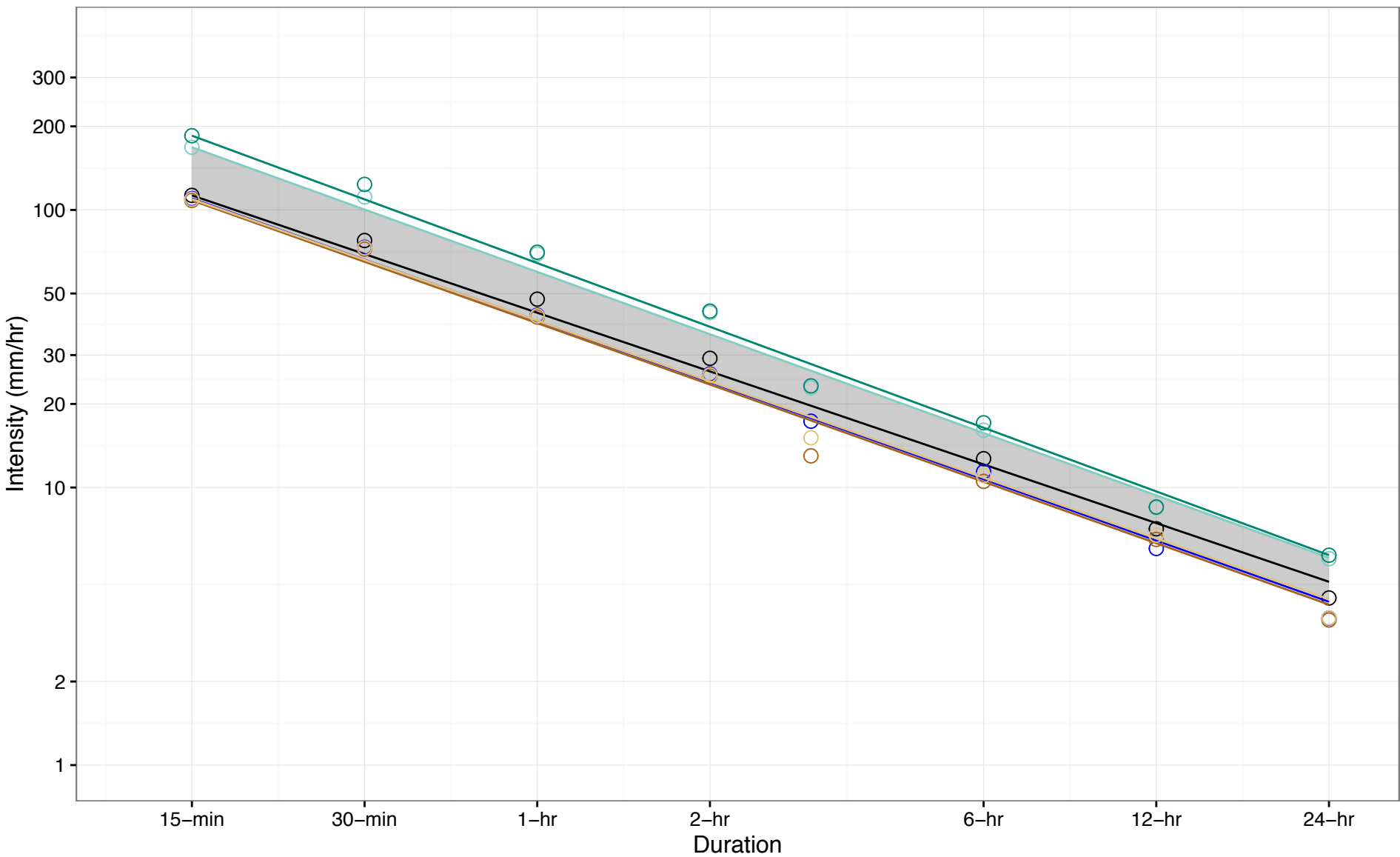
⊖ (c) Fut. Ensemble Min.: $R=37.15T^{-0.759}$

⊖ (d) Fut. Ensemble 10th Percentile: $R=37.97T^{-0.753}$

⊖ (e) Fut. Ensemble 90th Percentile: $R=47.21T^{-0.763}$

⊖ (f) Fut. Ensemble Max.: $R=49.11T^{-0.753}$

Figure A-16: IDF Curve Comparison for Pearson Airport, 2090s 25-year Return Period Event (10th–90th Percentile)



10th to 90th Percentile Range

(a) Hist. Gumbel: $R=42.63T^{-0.702}$

(b) Hist. GEV: $R=39.8T^{-0.733}$

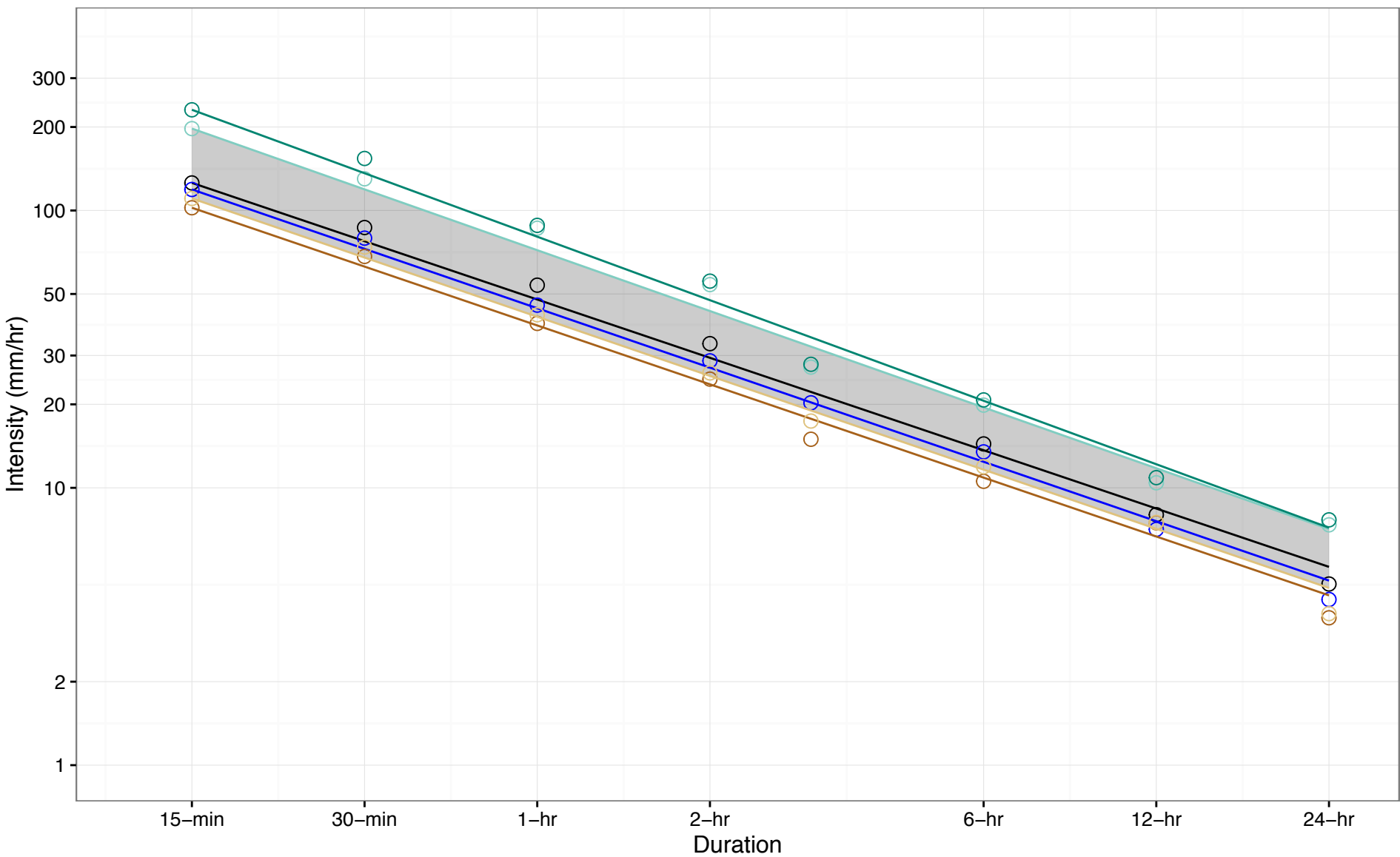
(c) Fut. Ensemble Min.: $R=39.1T^{-0.735}$

(d) Fut. Ensemble 10th Percentile: $R=39.91T^{-0.727}$

(e) Fut. Ensemble 90th Percentile: $R=59.82T^{-0.746}$

(f) Fut. Ensemble Max.: $R=64.35T^{-0.762}$

Figure A-17: IDF Curve Comparison for Pearson Airport, 2090s 50-year Return Period Event (10th–90th Percentile)



⊖ (a) Hist. Gumbel: $R=47.76T^{-0.698}$

⊖ (b) Hist. GEV: $R=44.42T^{-0.711}$

■ 10th to 90th Percentile Range

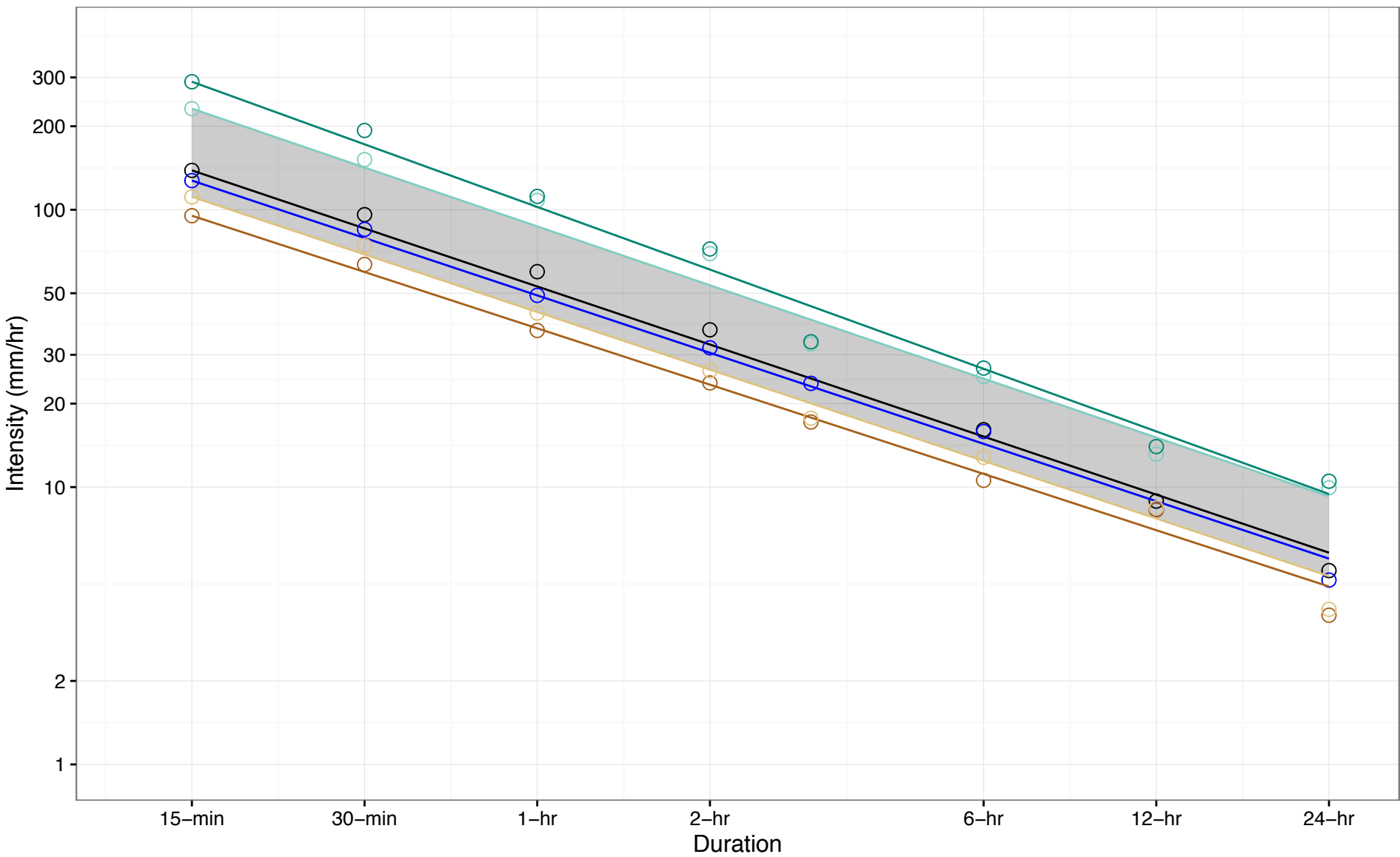
⊖ (c) Fut. Ensemble Min.: $R=38.5T^{-0.705}$

⊖ (d) Fut. Ensemble 10th Percentile: $R=41.4T^{-0.709}$

⊖ (e) Fut. Ensemble 90th Percentile: $R=71.92T^{-0.729}$

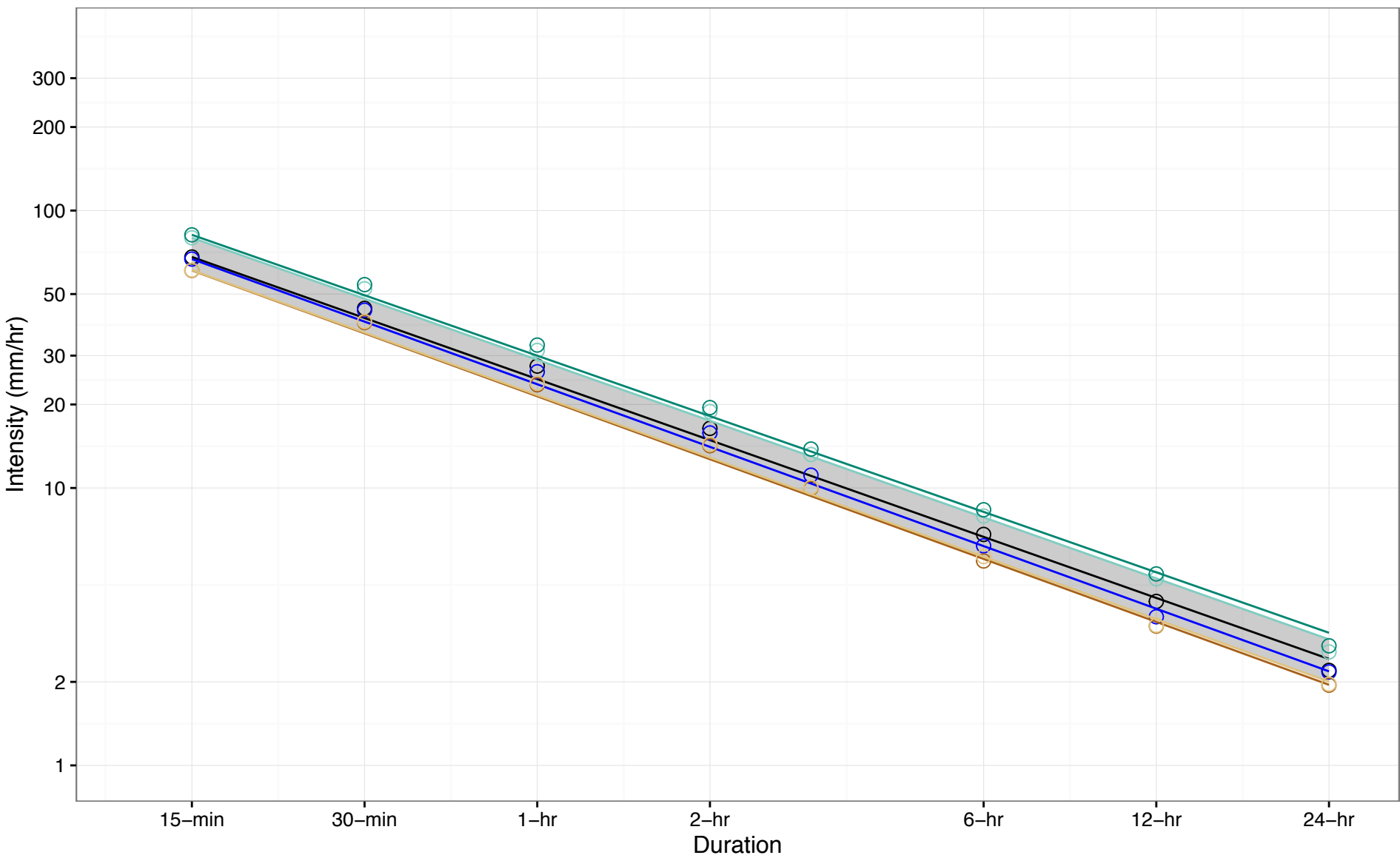
⊖ (f) Fut. Ensemble Max.: $R=80.44T^{-0.76}$

Figure A-18: IDF Curve Comparison for Pearson Airport, 2090s 100-year Return Period Event (10th-90th Percentile)



-
- 10th to 90th Percentile Range
 (a) Hist. Gumbel: $R=52.89T^{-0.695}$
 (b) Hist. GEV: $R=49.11T^{-0.688}$
- (c) Fut. Ensemble Min.: $R=37.36T^{-0.675}$
 (d) Fut. Ensemble 10th Percentile: $R=42.78T^{-0.69}$
- (e) Fut. Ensemble 90th Percentile: $R=87.1T^{-0.705}$
 (f) Fut. Ensemble Max.: $R=102.36T^{-0.75}$

Figure A-19: IDF Curve Comparison for Windsor Airport, 2030s 2-year Return Period Event (10th-90th Percentile)



10th to 90th Percentile Range

(a) Hist. Gumbel: $R=24.69T^{-0.731}$

(b) Hist. GEV: $R=23.65T^{-0.75}$

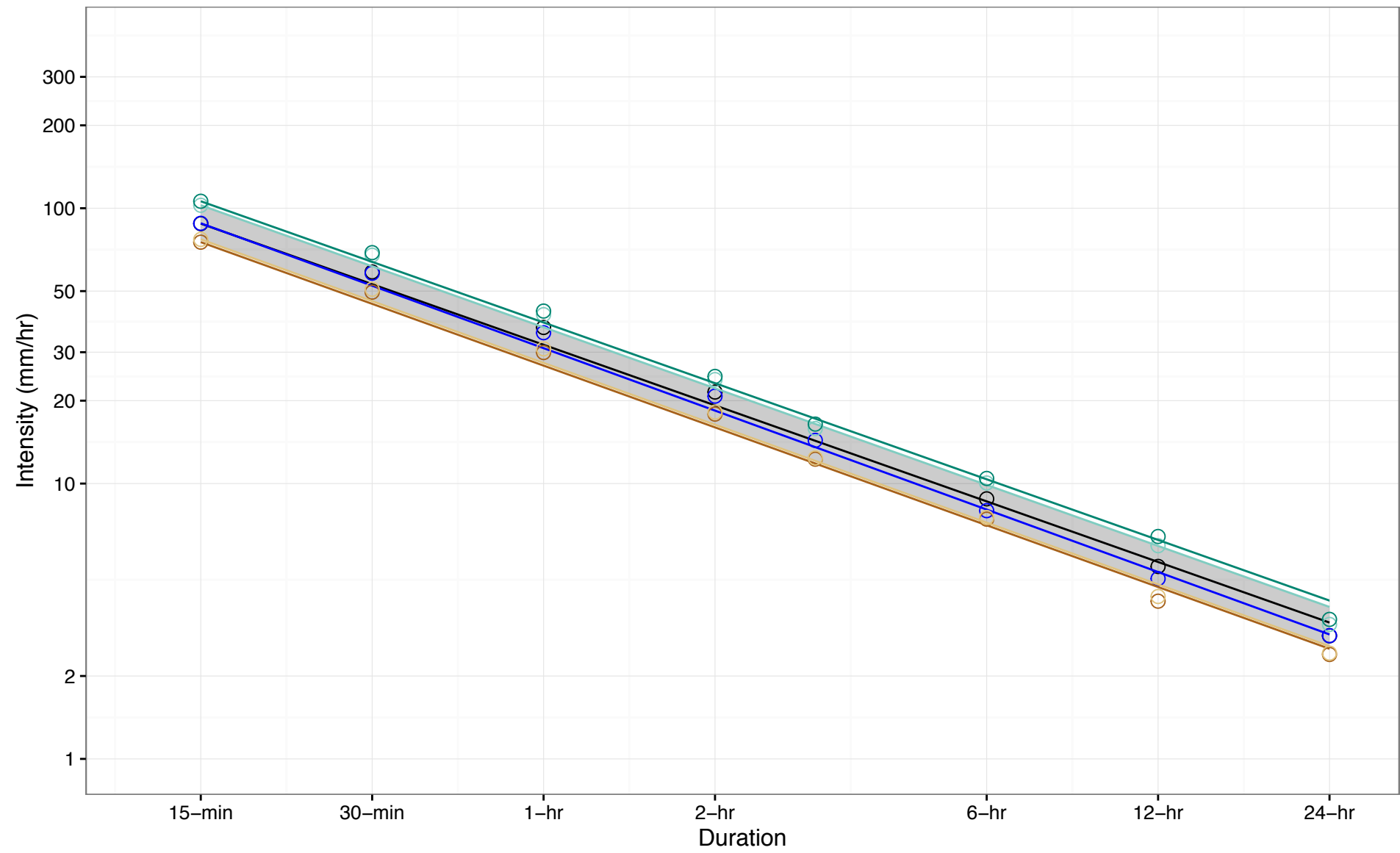
(c) Fut. Ensemble Min.: $R=21.41T^{-0.754}$

(d) Fut. Ensemble 10th Percentile: $R=21.61T^{-0.748}$

(e) Fut. Ensemble 90th Percentile: $R=29T^{-0.73}$

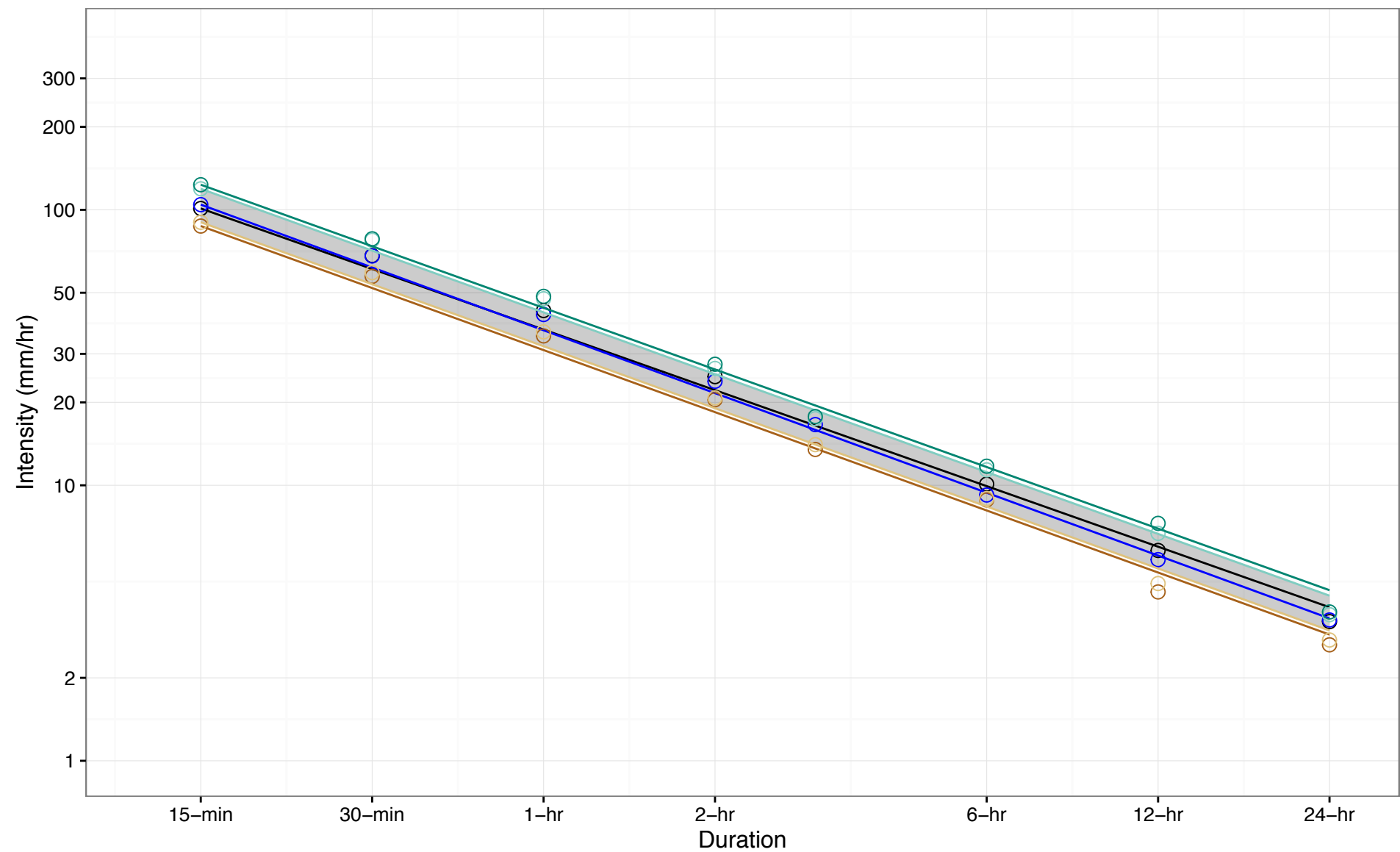
(f) Fut. Ensemble Max.: $R=29.98T^{-0.724}$

Figure A-20: IDF Curve Comparison for Windsor Airport, 2030s 5-year Return Period Event (10th-90th Percentile)



- 10th to 90th Percentile Range
- ⊖ (a) Hist. Gumbel: $R=31.92T^{-0.731}$
- ⊖ (b) Hist. GEV: $R=31.03T^{-0.753}$
- ⊖ (c) Fut. Ensemble Min.: $R=26.81T^{-0.745}$
- ⊖ (d) Fut. Ensemble 10th Percentile: $R=27.42T^{-0.745}$
- ⊖ (e) Fut. Ensemble 90th Percentile: $R=36.96T^{-0.736}$
- ⊖ (f) Fut. Ensemble Max.: $R=38.45T^{-0.732}$

Figure A-21: IDF Curve Comparison for Windsor Airport, 2030s 10-year Return Period Event (10th–90th Percentile)



⊖ (a) Hist. Gumbel: $R=36.75T^{-0.73}$

⊖ (b) Hist. GEV: $R=36.53T^{-0.758}$

■ 10th to 90th Percentile Range

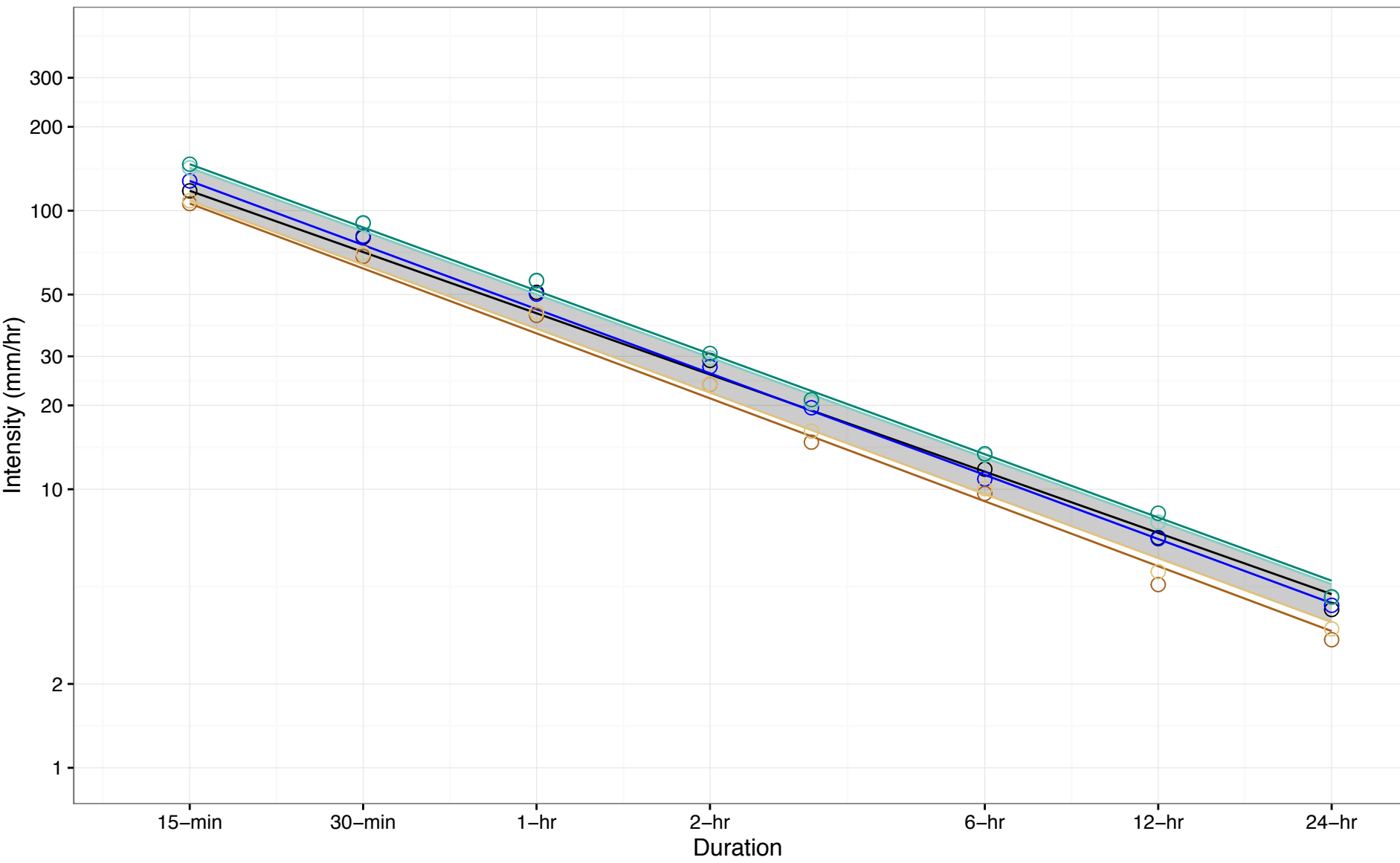
⊖ (c) Fut. Ensemble Min.: $R=30.96T^{-0.748}$

⊖ (d) Fut. Ensemble 10th Percentile: $R=31.97T^{-0.748}$

⊖ (e) Fut. Ensemble 90th Percentile: $R=42.43T^{-0.745}$

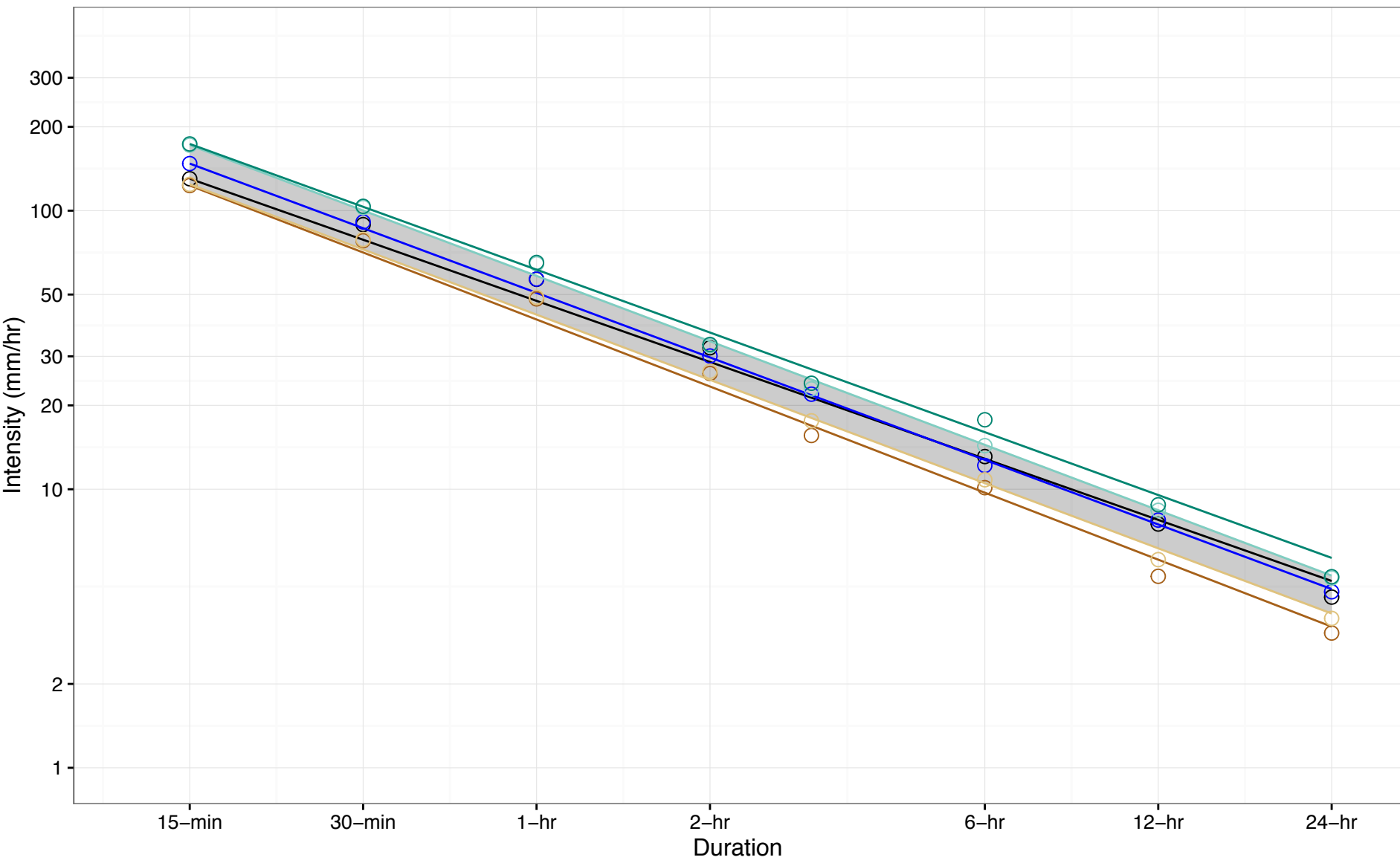
⊖ (f) Fut. Ensemble Max.: $R=44.07T^{-0.743}$

Figure A-22: IDF Curve Comparison for Windsor Airport, 2030s 25-year Return Period Event (10th-90th Percentile)



- ⊖ (a) Hist. Gumbel: $R=42.81T^{-0.731}$
 - ⊖ (b) Hist. GEV: $R=44.3T^{-0.765}$
 - ⊖ (c) Fut. Ensemble Min.: $R=36.26T^{-0.774}$
 - ⊖ (d) Fut. Ensemble 10th Percentile: $R=37.69T^{-0.763}$
 - ⊖ (e) Fut. Ensemble 90th Percentile: $R=50.11T^{-0.754}$
 - ⊖ (f) Fut. Ensemble Max.: $R=51.61T^{-0.754}$
- 10th to 90th Percentile Range

Figure A-23: IDF Curve Comparison for Windsor Airport, 2030s 50-year Return Period Event (10th-90th Percentile)



10th to 90th Percentile Range

(a) Hist. Gumbel: $R=47.45T^{-0.729}$

(b) Hist. GEV: $R=50.72T^{-0.771}$

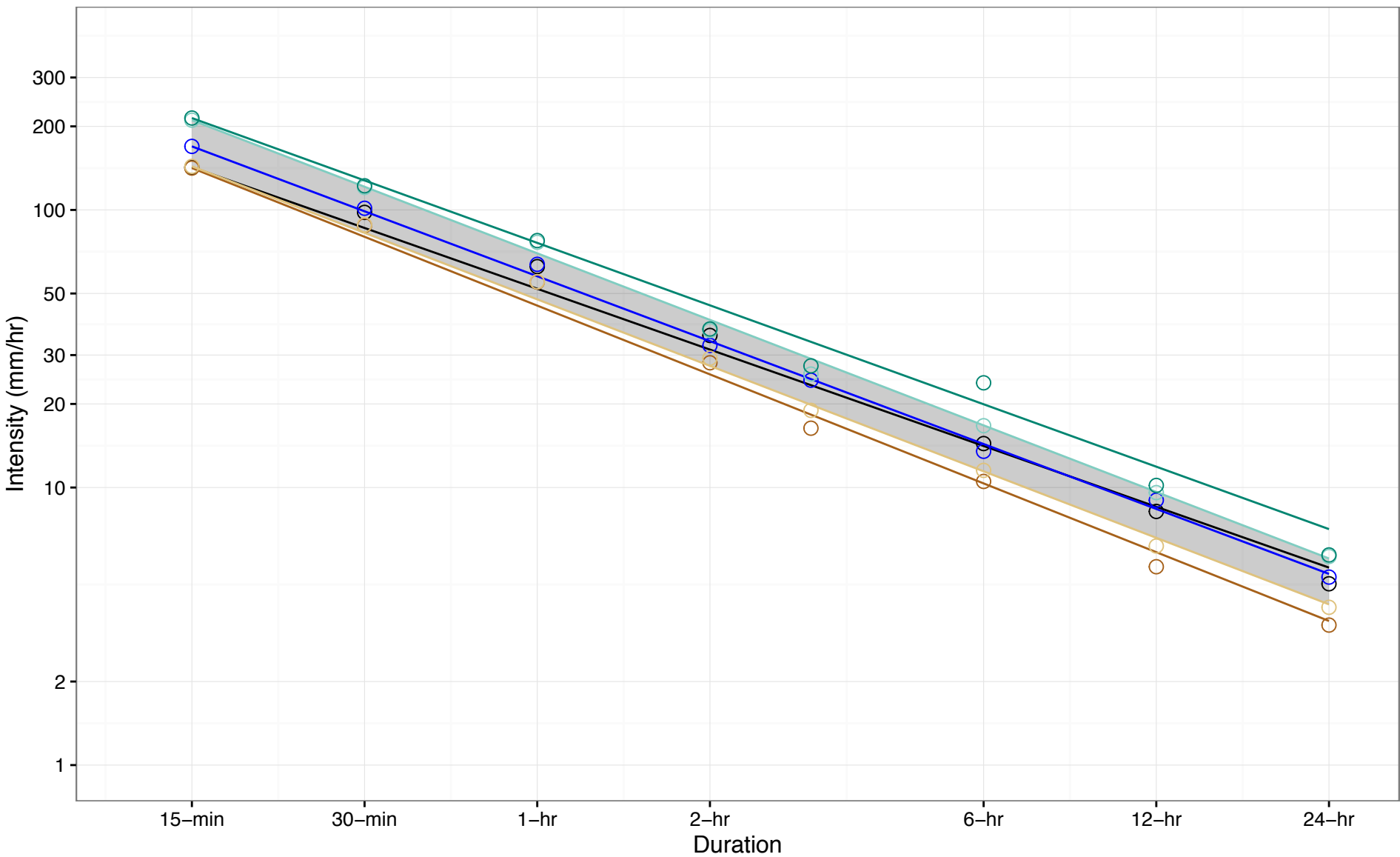
(c) Fut. Ensemble Min.: $R=40.68T^{-0.799}$

(d) Fut. Ensemble 10th Percentile: $R=42.33T^{-0.777}$

(e) Fut. Ensemble 90th Percentile: $R=58.34T^{-0.78}$

(f) Fut. Ensemble Max.: $R=61.41T^{-0.75}$

Figure A-24: IDF Curve Comparison for Windsor Airport, 2030s 100-year Return Period Event (10th–90th Percentile)



⊖ (a) Hist. Gumbel: $R=51.99T^{-0.728}$

⊖ (b) Hist. GEV: $R=57.7T^{-0.777}$

■ 10th to 90th Percentile Range

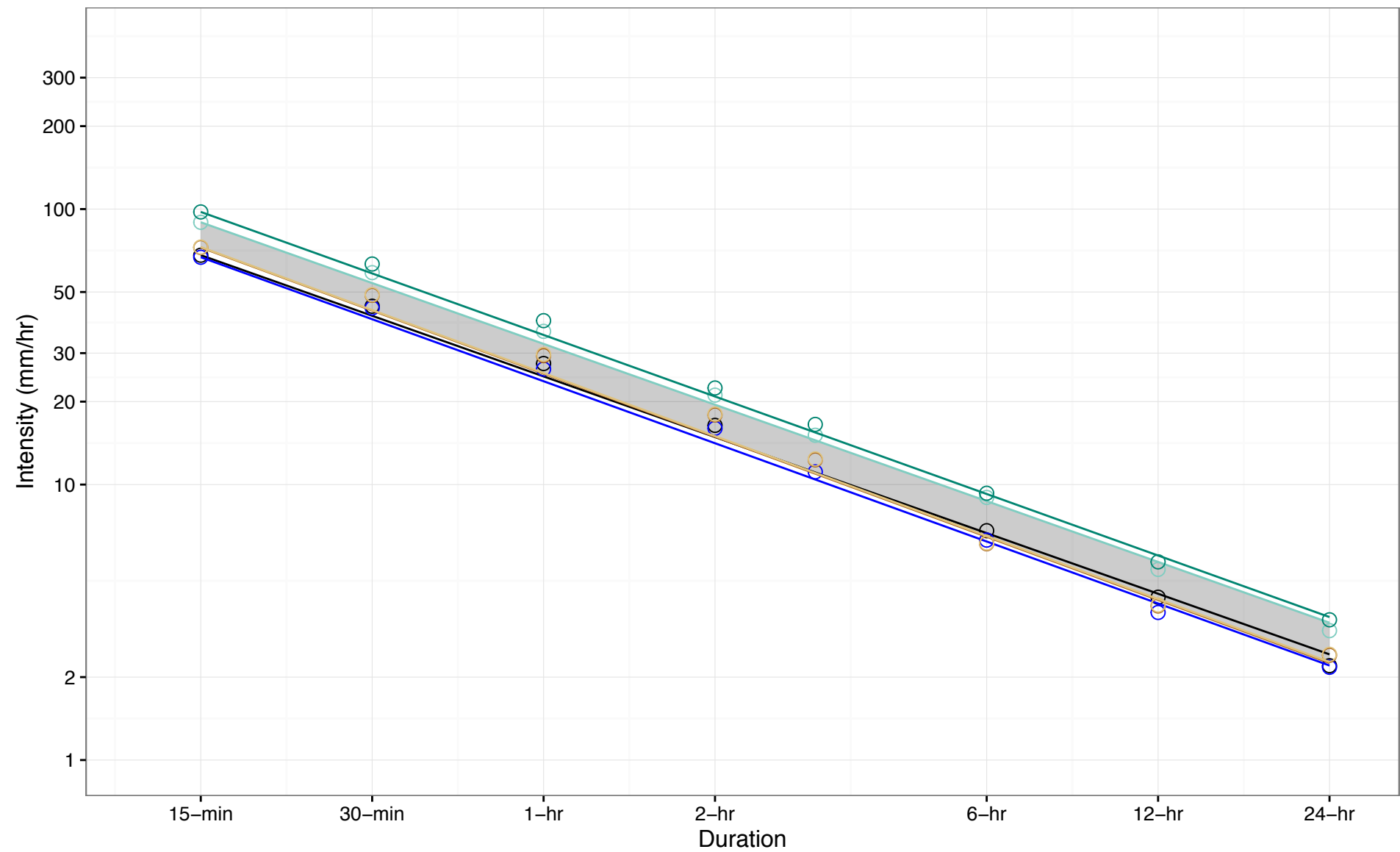
⊖ (c) Fut. Ensemble Min.: $R=45.22T^{-0.823}$

⊖ (d) Fut. Ensemble 10th Percentile: $R=47.62T^{-0.796}$

⊖ (e) Fut. Ensemble 90th Percentile: $R=69.78T^{-0.797}$

⊖ (f) Fut. Ensemble Max.: $R=76.08T^{-0.747}$

Figure A-25: IDF Curve Comparison for Windsor Airport, 2050s 2-year Return Period Event (10th-90th Percentile)



⊖ (a) Hist. Gumbel: $R=24.69T^{-0.731}$

⊖ (b) Hist. GEV: $R=23.72T^{-0.748}$

■ 10th to 90th Percentile Range

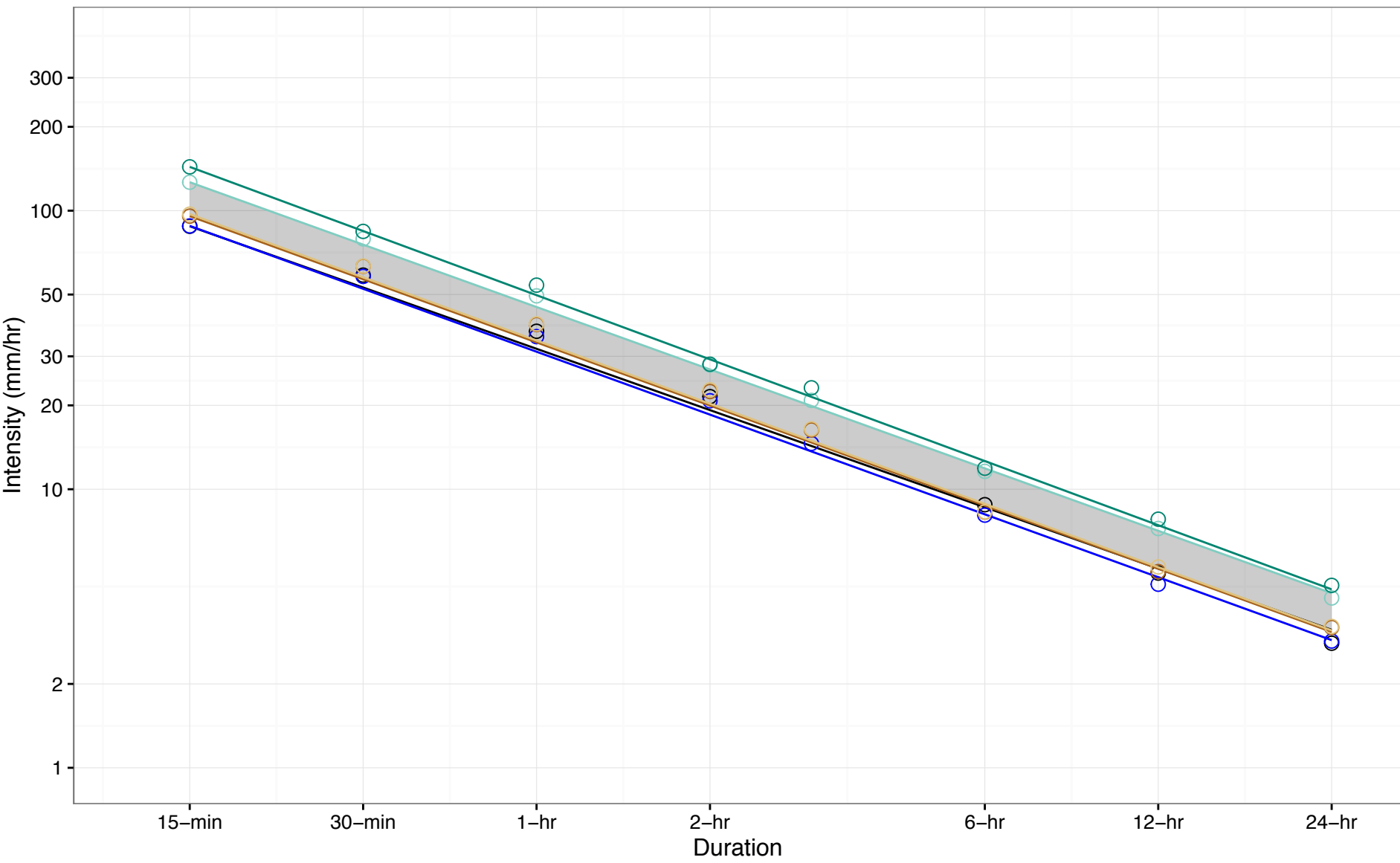
⊖ (c) Fut. Ensemble Min.: $R=25.27T^{-0.761}$

⊖ (d) Fut. Ensemble 10th Percentile: $R=25.39T^{-0.76}$

⊖ (e) Fut. Ensemble 90th Percentile: $R=32.41T^{-0.733}$

⊖ (f) Fut. Ensemble Max.: $R=34.92T^{-0.742}$

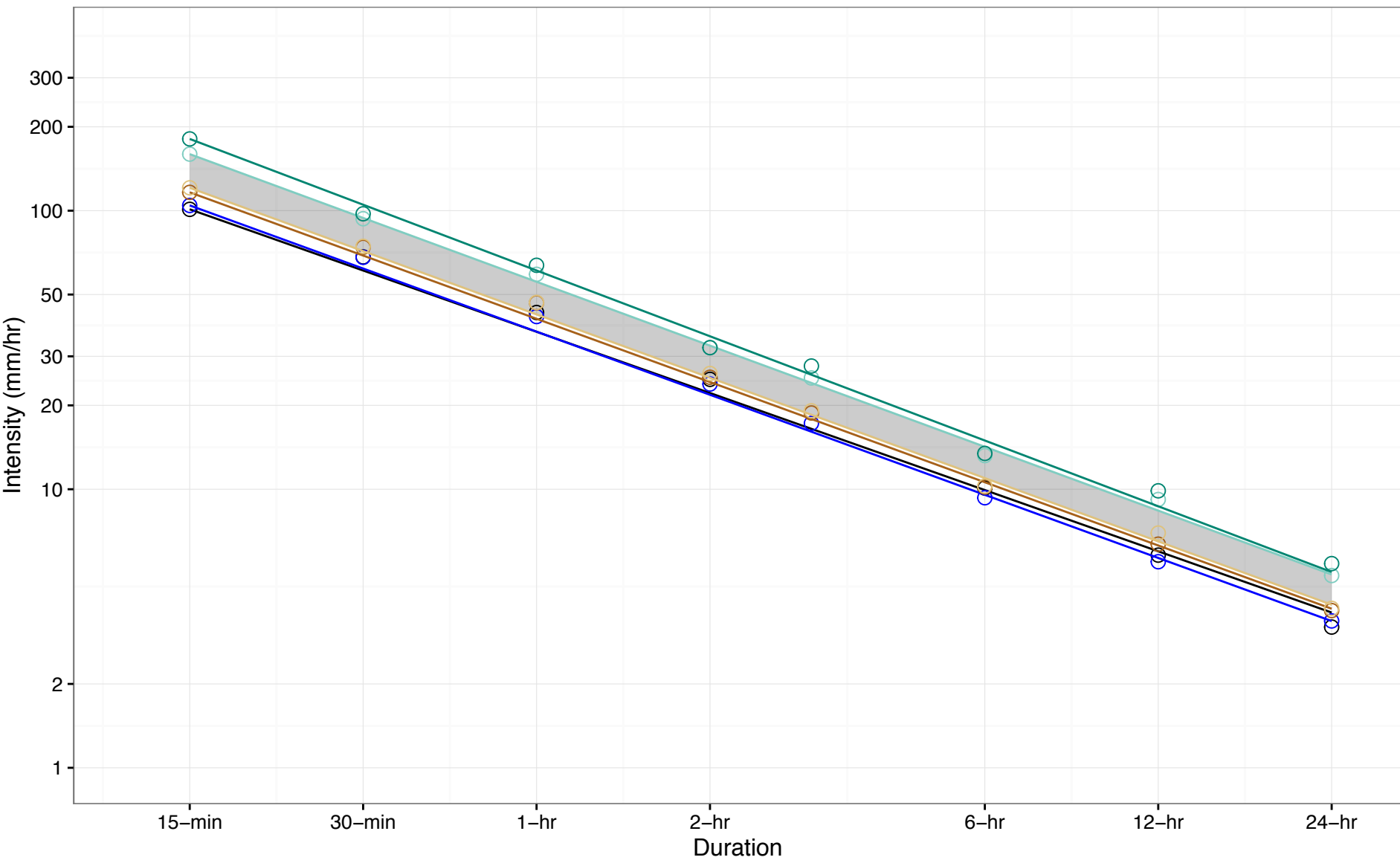
Figure A-26: IDF Curve Comparison for Windsor Airport, 2050s 5-year Return Period Event (10th-90th Percentile)



-

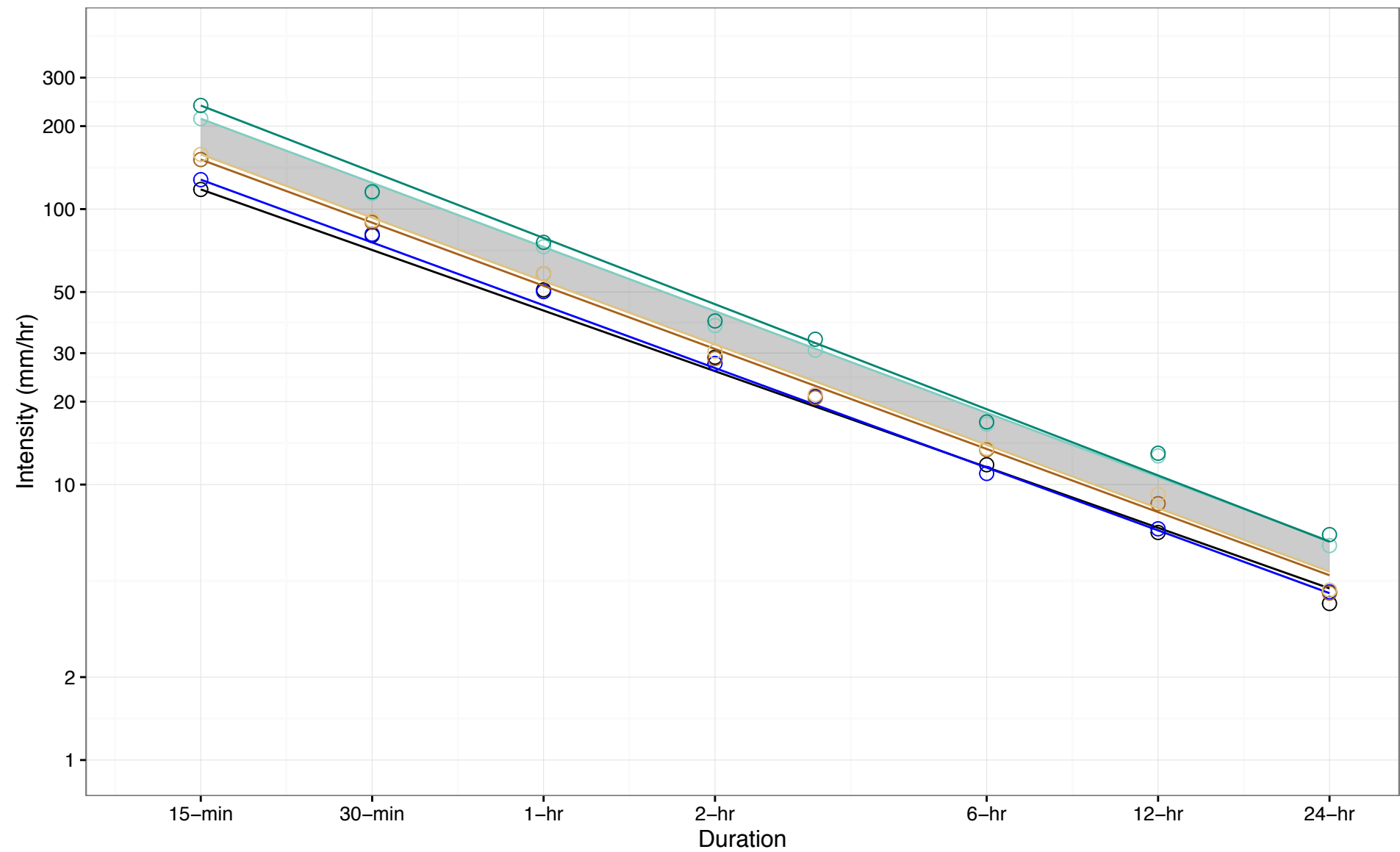
10th to 90th Percentile Range

Figure A-27: IDF Curve Comparison for Windsor Airport, 2050s 10-year Return Period Event (10th-90th Percentile)



- ⊖ (a) Hist. Gumbel: $R=36.75T^{-0.73}$
- ⊖ (b) Hist. GEV: $R=36.79T^{-0.753}$
- ⊖ (c) Fut. Ensemble Min.: $R=40.91T^{-0.754}$
- ⊖ (d) Fut. Ensemble 10th Percentile: $R=42.42T^{-0.755}$
- ⊖ (e) Fut. Ensemble 90th Percentile: $R=55.55T^{-0.761}$
- ⊖ (f) Fut. Ensemble Max.: $R=60.99T^{-0.784}$
- 10th to 90th Percentile Range

Figure A-28: IDF Curve Comparison for Windsor Airport, 2050s 25-year Return Period Event (10th-90th Percentile)



10th to 90th Percentile Range

(a) Hist. Gumbel: $R=42.81T^{-0.731}$

(b) Hist. GEV: $R=44.76T^{-0.757}$

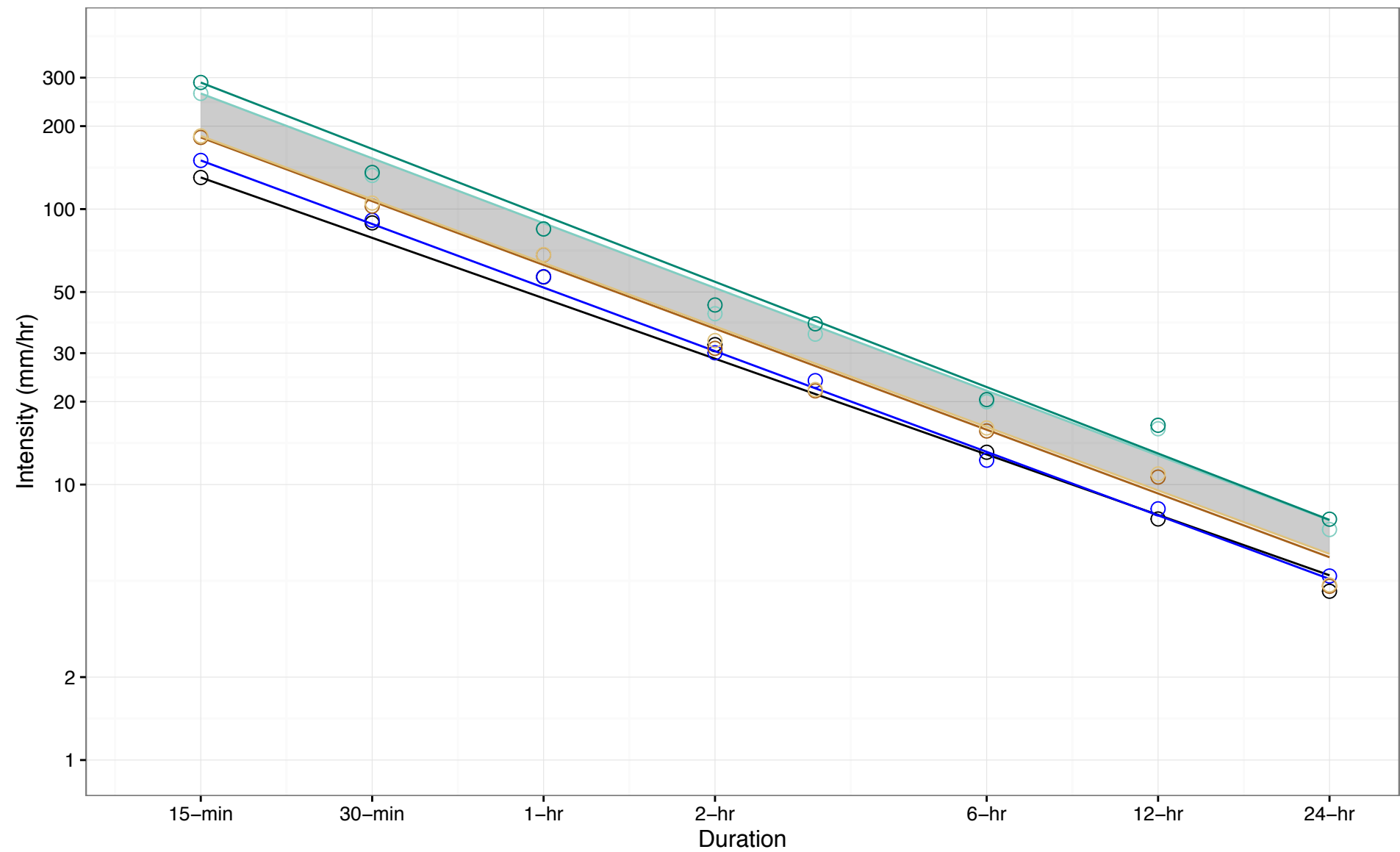
(c) Fut. Ensemble Min.: $R=52.66T^{-0.761}$

(d) Fut. Ensemble 10th Percentile: $R=54.76T^{-0.764}$

(e) Fut. Ensemble 90th Percentile: $R=72.85T^{-0.773}$

(f) Fut. Ensemble Max.: $R=78.54T^{-0.799}$

Figure A-29: IDF Curve Comparison for Windsor Airport, 2050s 50-year Return Period Event (10th-90th Percentile)



⊖ (a) Hist. Gumbel: $R=47.45T^{-0.729}$

⊖ (b) Hist. GEV: $R=51.9T^{-0.766}$

■ 10th to 90th Percentile Range

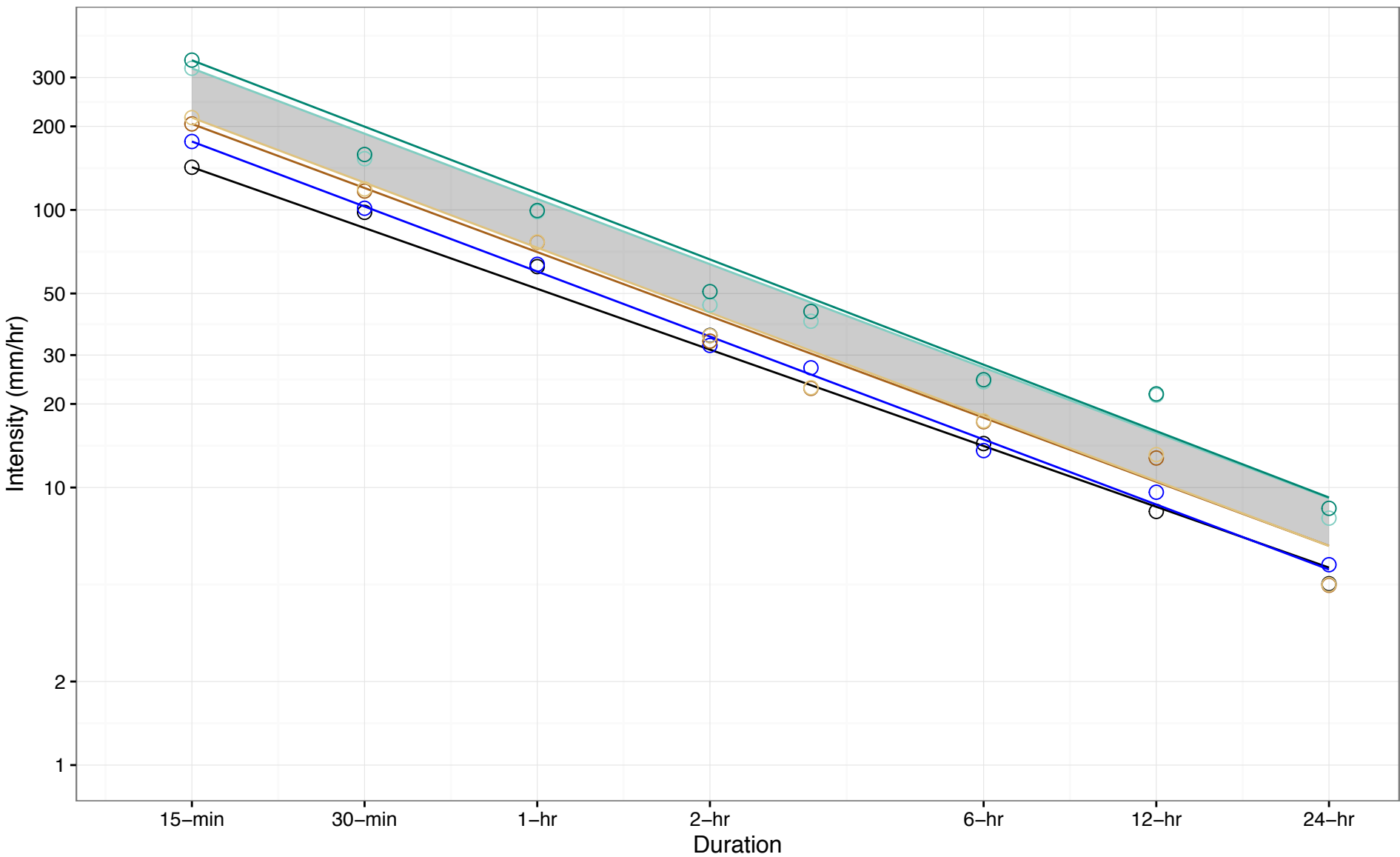
⊖ (c) Fut. Ensemble Min.: $R=62.69T^{-0.769}$

⊖ (d) Fut. Ensemble 10th Percentile: $R=63.78T^{-0.765}$

⊖ (e) Fut. Ensemble 90th Percentile: $R=88.94T^{-0.782}$

⊖ (f) Fut. Ensemble Max.: $R=94.88T^{-0.801}$

Figure A-30: IDF Curve Comparison for Windsor Airport, 2050s 100-year Return Period Event (10th–90th Percentile)



⊖ (a) Hist. Gumbel: $R=51.99T^{-0.728}$

⊖ (b) Hist. GEV: $R=60.01T^{-0.778}$

■ 10th to 90th Percentile Range

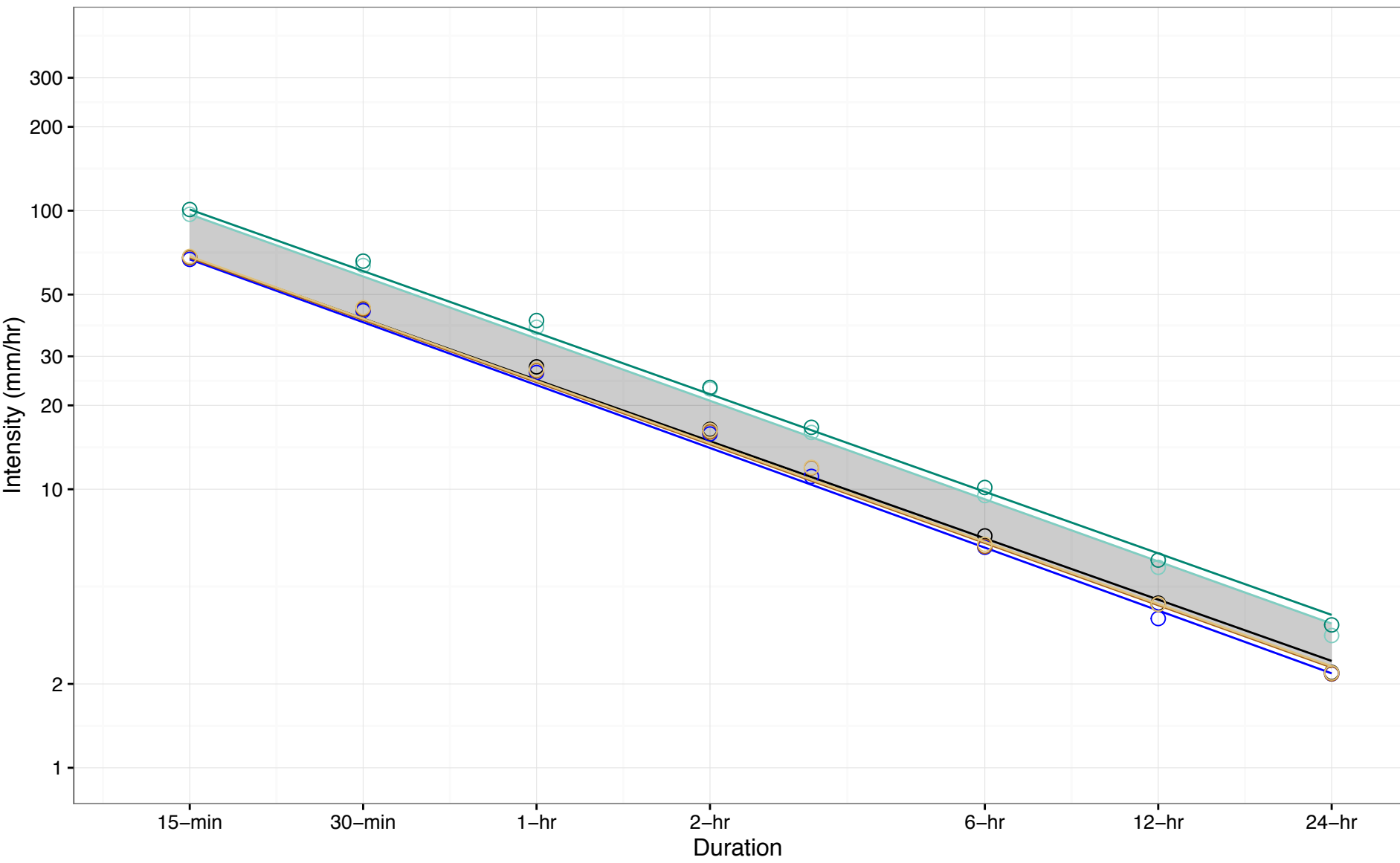
⊖ (c) Fut. Ensemble Min.: $R=70.5T^{-0.767}$

⊖ (d) Fut. Ensemble 10th Percentile: $R=73.1T^{-0.778}$

⊖ (e) Fut. Ensemble 90th Percentile: $R=109.58T^{-0.781}$

⊖ (f) Fut. Ensemble Max.: $R=115.04T^{-0.795}$

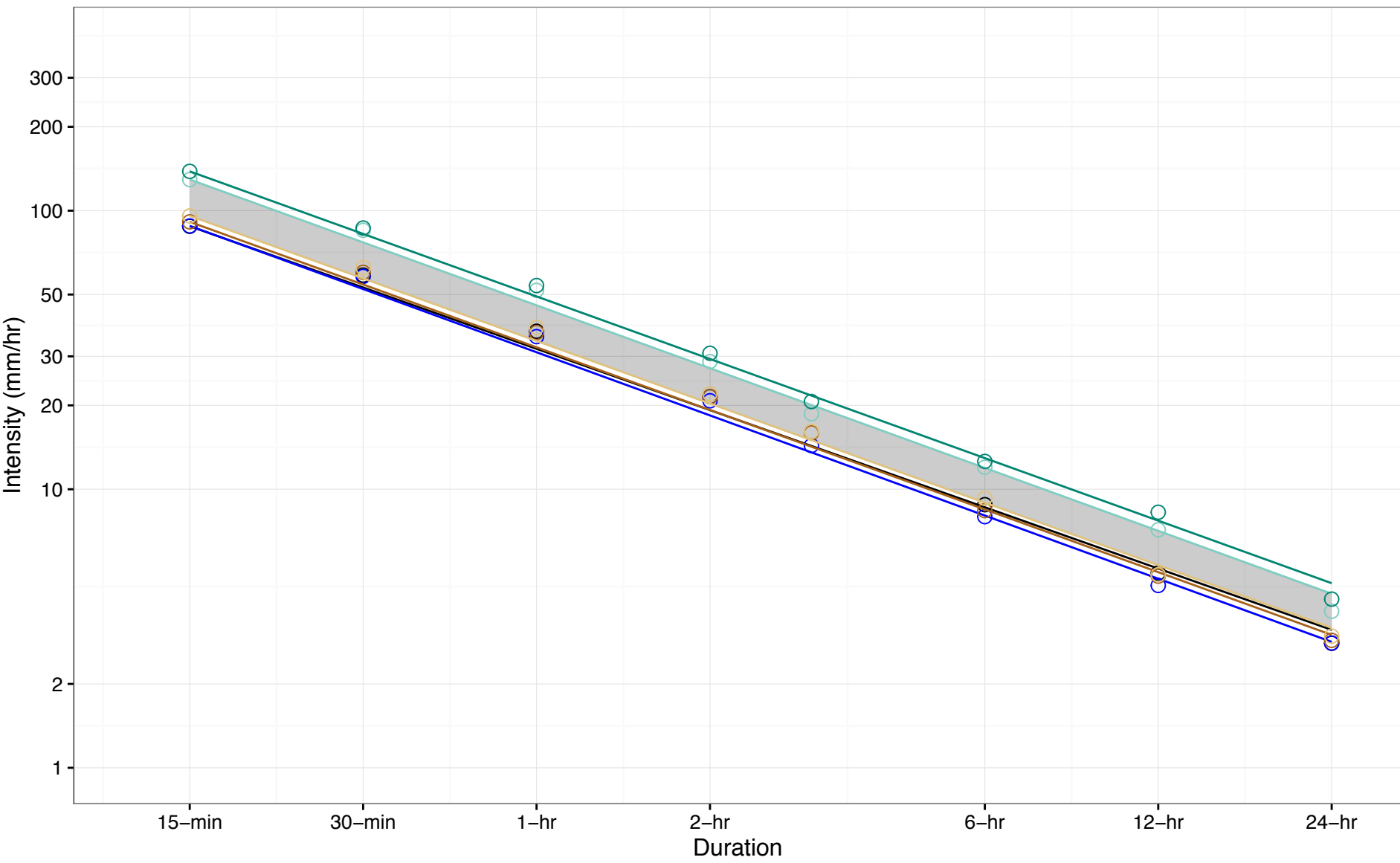
Figure A-31: IDF Curve Comparison for Windsor Airport, 2090s 2-year Return Period Event (10th-90th Percentile)



- (a) Hist. Gumbel: $R=24.69T^{-0.731}$
- (b) Hist. GEV: $R=23.65T^{-0.75}$
- (c) Fut. Ensemble Min.: $R=24.23T^{-0.742}$
- (d) Fut. Ensemble 10th Percentile: $R=24.49T^{-0.742}$
- (e) Fut. Ensemble 90th Percentile: $R=34.74T^{-0.741}$
- (f) Fut. Ensemble Max.: $R=36.5T^{-0.734}$

10th to 90th Percentile Range

Figure A-32: IDF Curve Comparison for Windsor Airport, 2090s 5-year Return Period Event (10th-90th Percentile)

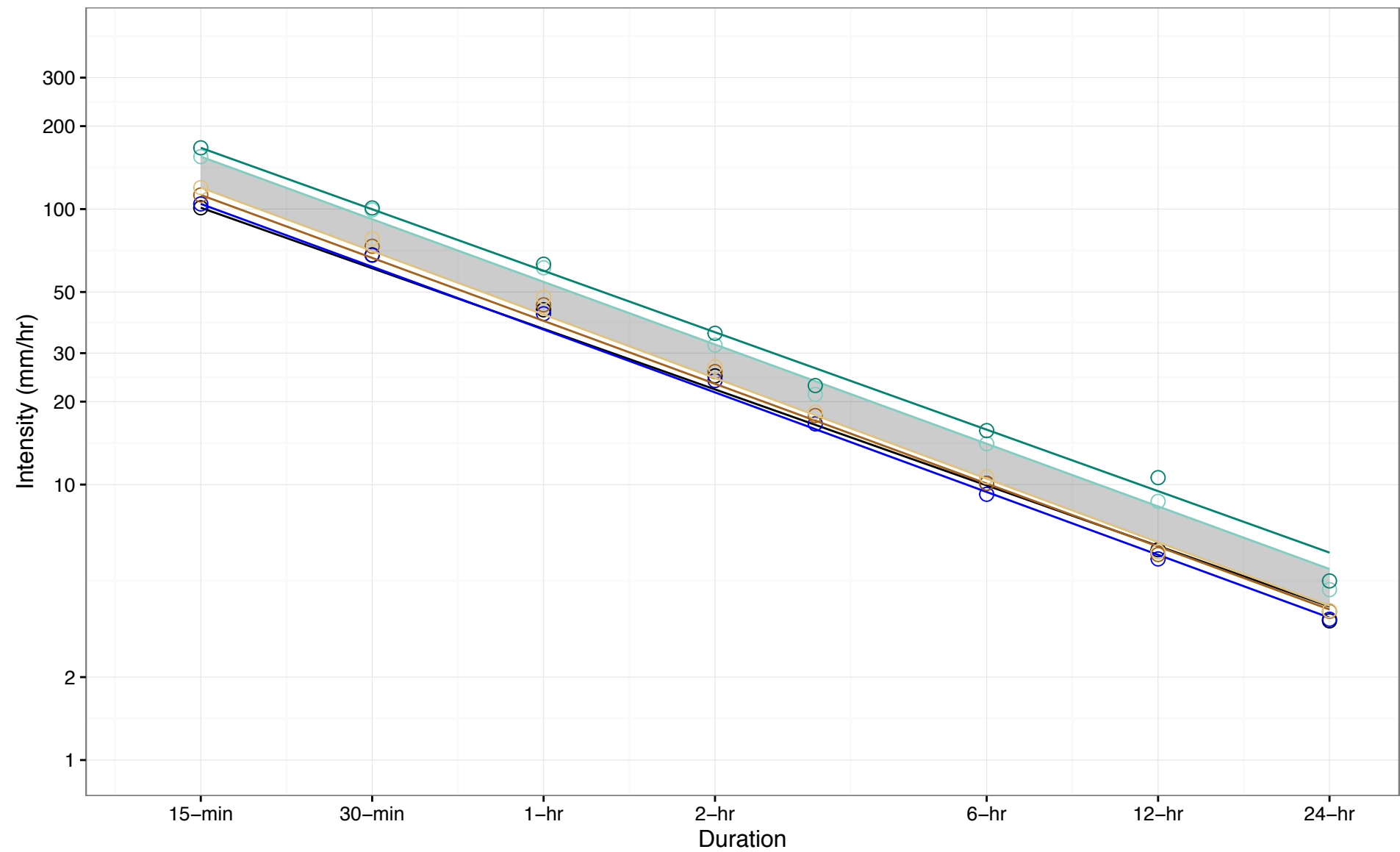


(a) Hist. Gumbel: $R=31.92T^{-0.731}$
 (b) Hist. GEV: $R=31.03T^{-0.753}$
 10th to 90th Percentile Range

(c) Fut. Ensemble Min.: $R=32.33T^{-0.748}$
 (d) Fut. Ensemble 10th Percentile: $R=34.06T^{-0.746}$

(e) Fut. Ensemble 90th Percentile: $R=45.74T^{-0.75}$
 (f) Fut. Ensemble Max.: $R=49.22T^{-0.746}$

Figure A-33: IDF Curve Comparison for Windsor Airport, 2090s 10-year Return Period Event (10th-90th Percentile)



⊖ (a) Hist. Gumbel: $R=36.75T^{-0.73}$

⊖ (b) Hist. GEV: $R=36.53T^{-0.758}$

■ 10th to 90th Percentile Range

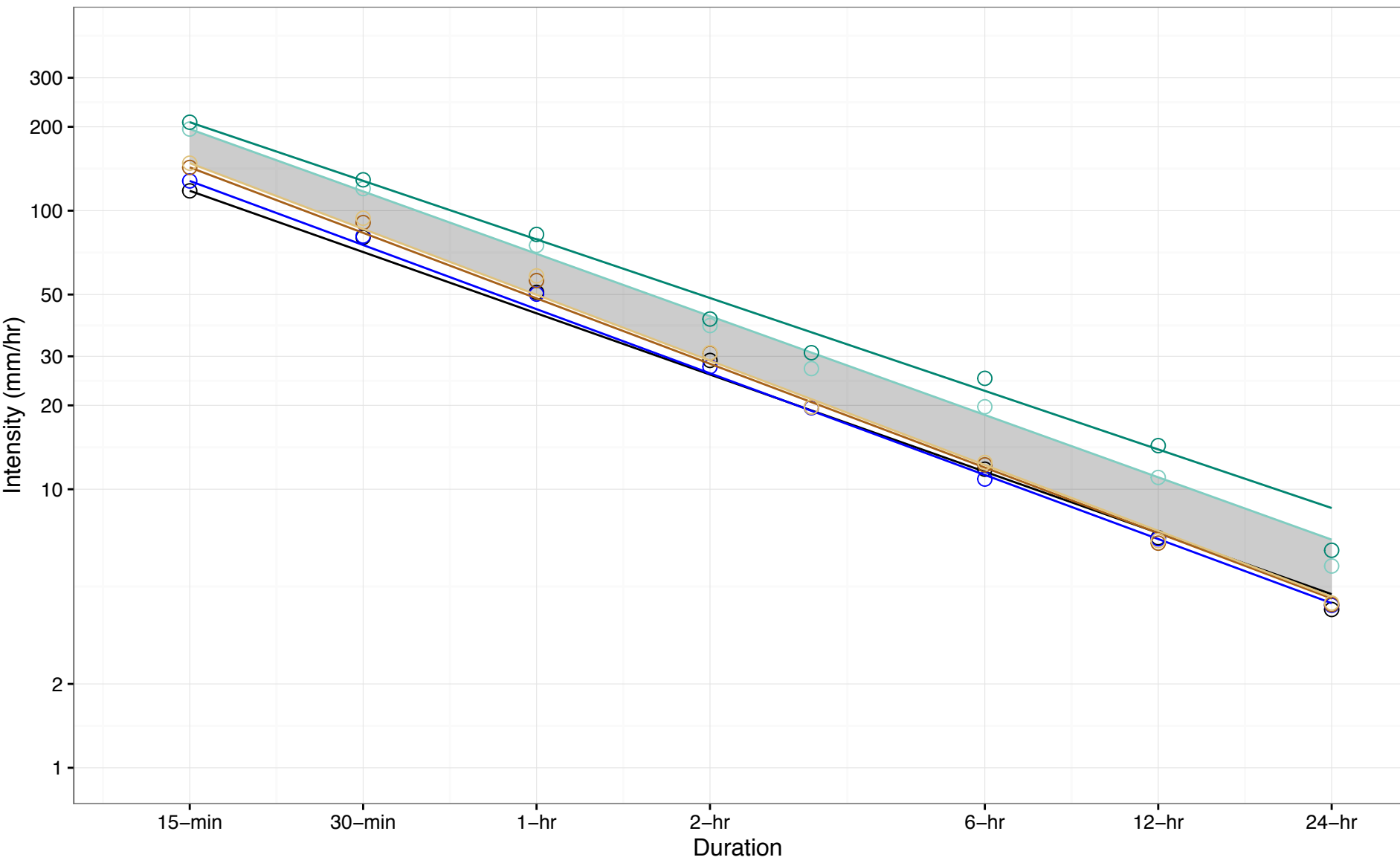
⊖ (c) Fut. Ensemble Min.: $R=39.29T^{-0.759}$

⊖ (d) Fut. Ensemble 10th Percentile: $R=41.42T^{-0.766}$

⊖ (e) Fut. Ensemble 90th Percentile: $R=54.43T^{-0.755}$

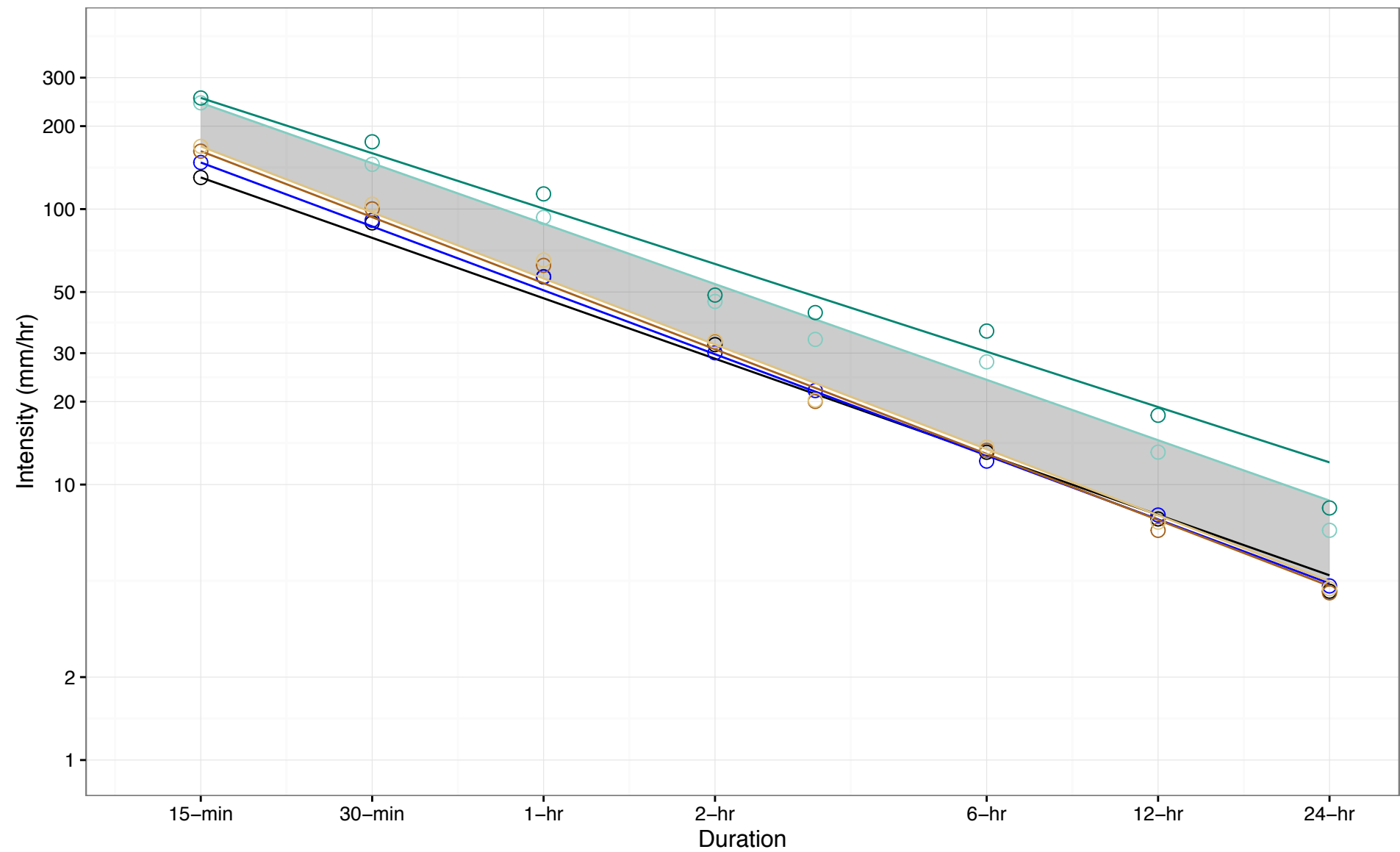
⊖ (f) Fut. Ensemble Max.: $R=59.72T^{-0.741}$

Figure A-34: IDF Curve Comparison for Windsor Airport, 2090s 25-year Return Period Event (10th-90th Percentile)



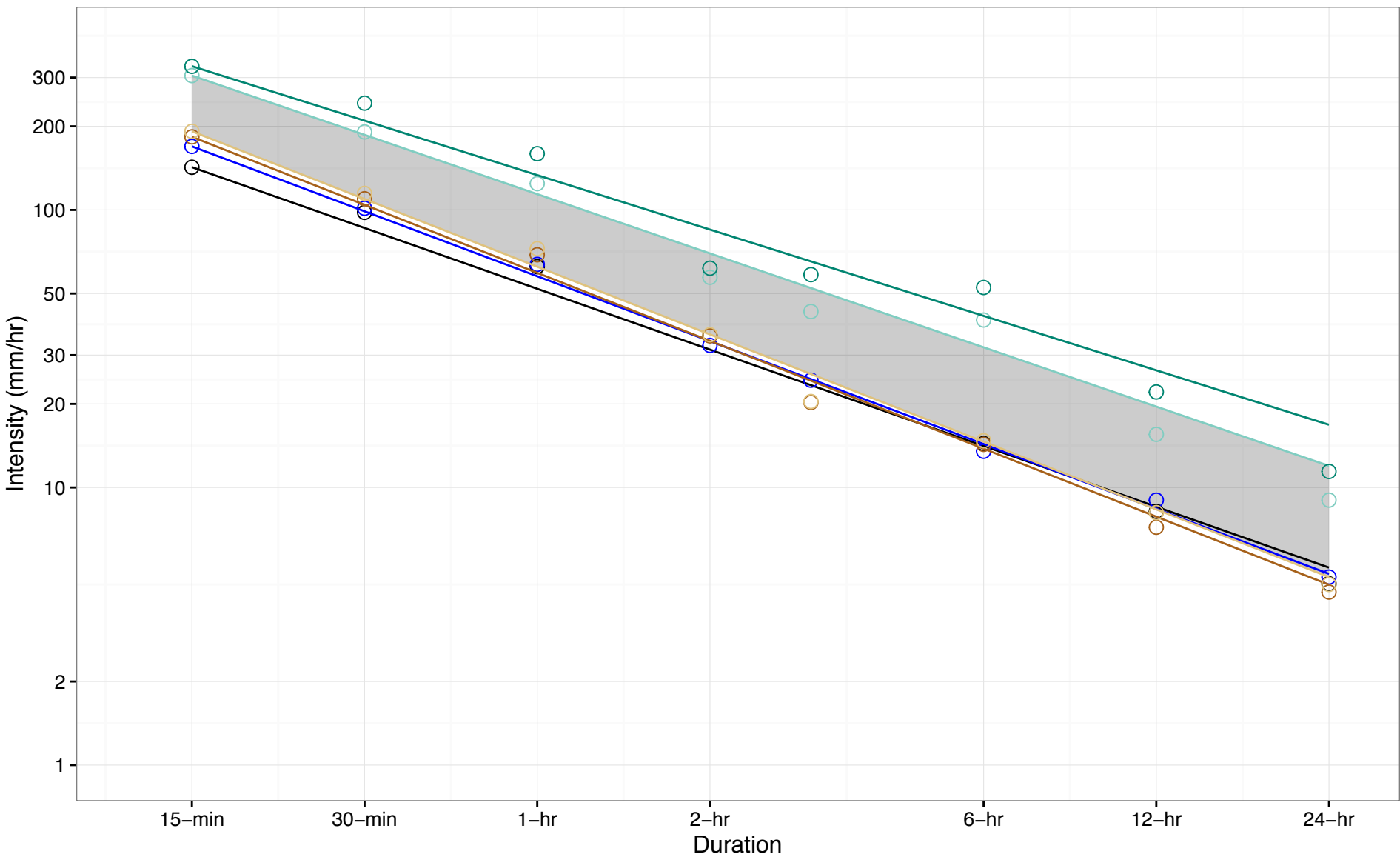
- 10th to 90th Percentile Range
- ⊖ (a) Hist. Gumbel: $R=42.81T^{-0.731}$
- ⊖ (b) Hist. GEV: $R=44.3T^{-0.765}$
- ⊖ (c) Fut. Ensemble Min.: $R=48.46T^{-0.781}$
- ⊖ (d) Fut. Ensemble 10th Percentile: $R=49.88T^{-0.785}$
- ⊖ (e) Fut. Ensemble 90th Percentile: $R=70.04T^{-0.744}$
- ⊖ (f) Fut. Ensemble Max.: $R=78.86T^{-0.699}$

Figure A-35: IDF Curve Comparison for Windsor Airport, 2010s 50-year Return Period Event (10th-90th Percentile)



- 10th to 90th Percentile Range
- ⊖ (a) Hist. Gumbel: $R=47.45T^{-0.729}$
- ⊖ (b) Hist. GEV: $R=50.72T^{-0.771}$
- ⊖ (c) Fut. Ensemble Min.: $R=53.81T^{-0.796}$
- ⊖ (d) Fut. Ensemble 10th Percentile: $R=55.99T^{-0.796}$
- ⊖ (e) Fut. Ensemble 90th Percentile: $R=88.56T^{-0.728}$
- ⊖ (f) Fut. Ensemble Max.: $R=100.41T^{-0.667}$

Figure A-36: IDF Curve Comparison for Windsor Airport, 2090s 100-year Return Period Event (10th–90th Percentile)



⊖ (a) Hist. Gumbel: $R=51.99T^{-0.728}$

⊖ (b) Hist. GEV: $R=57.7T^{-0.777}$

■ 10th to 90th Percentile Range

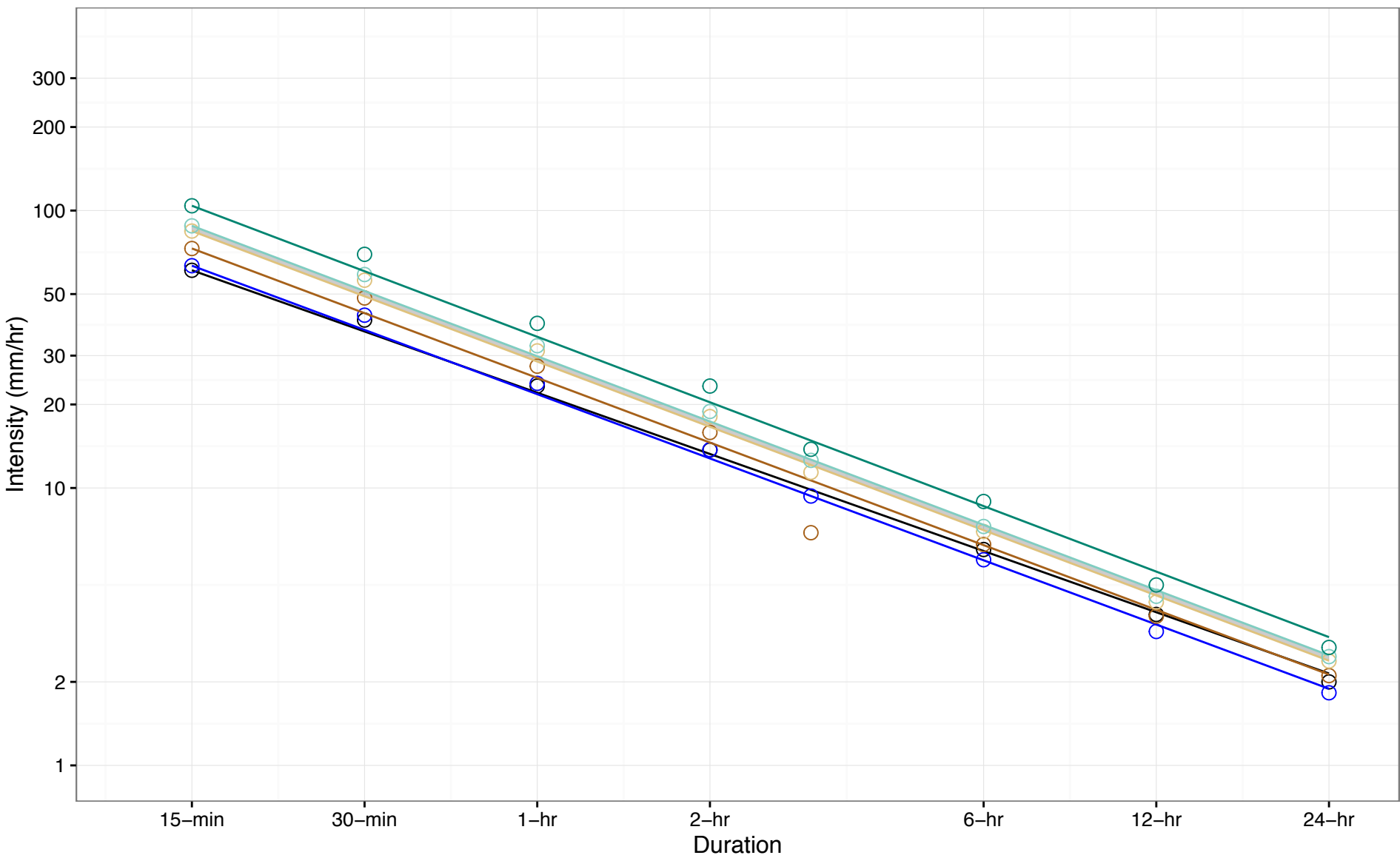
⊖ (c) Fut. Ensemble Min.: $R=59.33T^{-0.814}$

⊖ (d) Fut. Ensemble 10th Percentile: $R=62.44T^{-0.81}$

⊖ (e) Fut. Ensemble 90th Percentile: $R=114.02T^{-0.709}$

⊖ (f) Fut. Ensemble Max.: $R=133.51T^{-0.652}$

Figure A-37: IDF Curve Comparison for Pearson Airport, 2090s 2-year Return Period Event (50th-75th Percentile)



⊖ (a) Hist. Gumbel: $R=22.05T^{-0.733}$

⊖ (b) Hist. GEV: $R=21.78T^{-0.769}$

■ 50th to 75th Percentile Range

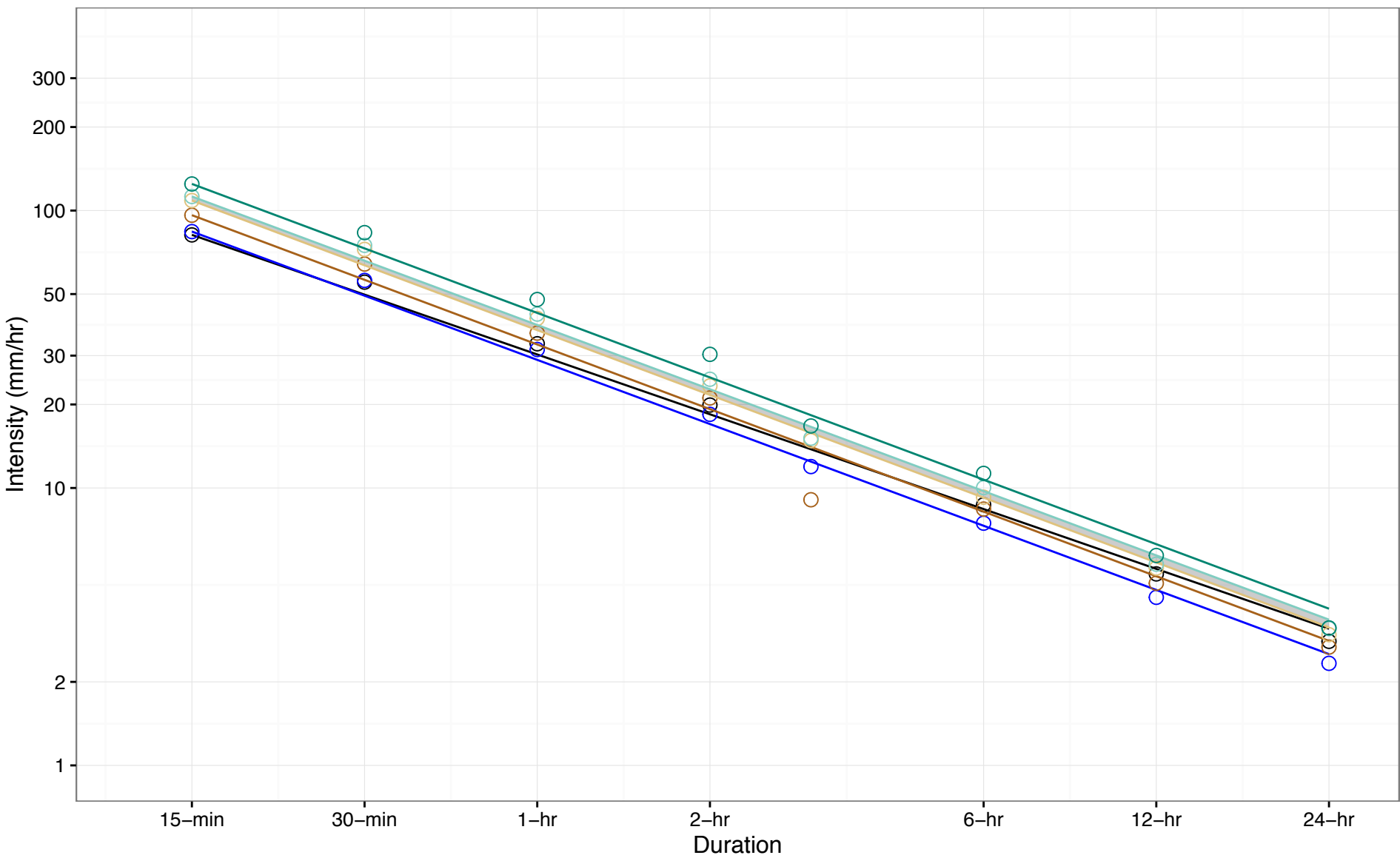
⊖ (c) Fut. Ensemble Min.: $R=24.94T^{-0.775}$

⊖ (d) Fut. Ensemble 50th Percentile: $R=28.56T^{-0.781}$

⊖ (e) Fut. Ensemble 75th Percentile: $R=29.84T^{-0.781}$

⊖ (f) Fut. Ensemble Max.: $R=35.08T^{-0.784}$

Figure A-38: IDF Curve Comparison for Pearson Airport, 2090s 5-year Return Period Event (50th-75th Percentile)



⊖ (a) Hist. Gumbel: $R=30.29T^{-0.716}$

⊖ (b) Hist. GEV: $R=28.96T^{-0.768}$

■ 50th to 75th Percentile Range

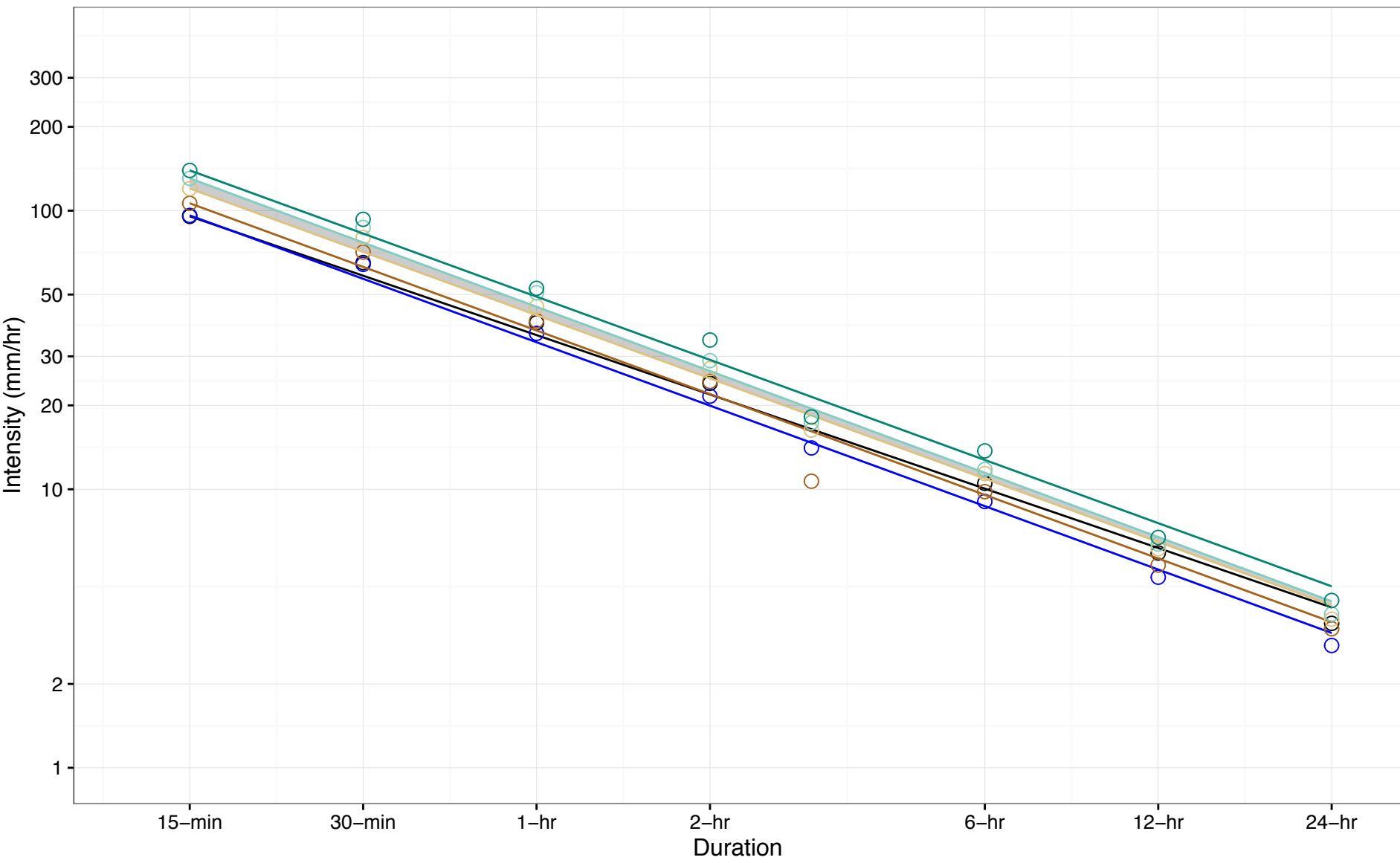
⊖ (c) Fut. Ensemble Min.: $R=32.91T^{-0.774}$

⊖ (d) Fut. Ensemble 50th Percentile: $R=37.07T^{-0.776}$

⊖ (e) Fut. Ensemble 75th Percentile: $R=38.68T^{-0.77}$

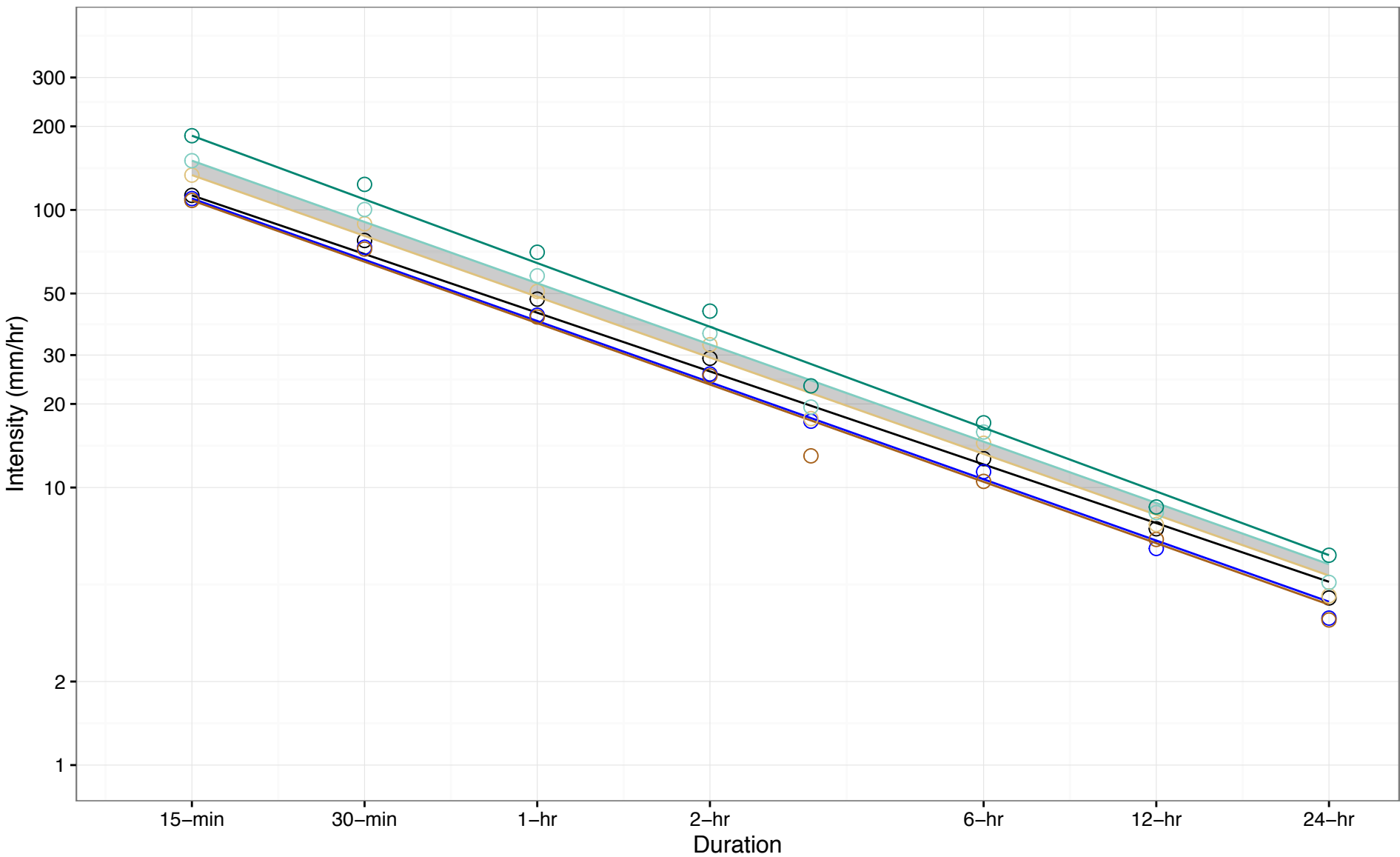
⊖ (f) Fut. Ensemble Max.: $R=42.76T^{-0.772}$

Figure A-39: IDF Curve Comparison for Pearson Airport, 2090s 10-year Return Period Event (50th-75th Percentile)



-
- (a) Hist. Gumbel: $R=35.76T^{-0.708}$
 (b) Hist. GEV: $R=33.71T^{-0.756}$
 50th to 75th Percentile Range
- (c) Fut. Ensemble Min.: $R=37.15T^{-0.759}$
 (d) Fut. Ensemble 50th Percentile: $R=42.18T^{-0.754}$
- (e) Fut. Ensemble 75th Percentile: $R=45.18T^{-0.766}$
 (f) Fut. Ensemble Max.: $R=49.11T^{-0.753}$

Figure A-40: IDF Curve Comparison for Pearson Airport, 2090s 25-year Return Period Event (50th–75th Percentile)



⊖ (a) Hist. Gumbel: $R=42.63T^{-0.702}$

⊖ (b) Hist. GEV: $R=39.8T^{-0.733}$

■ 50th to 75th Percentile Range

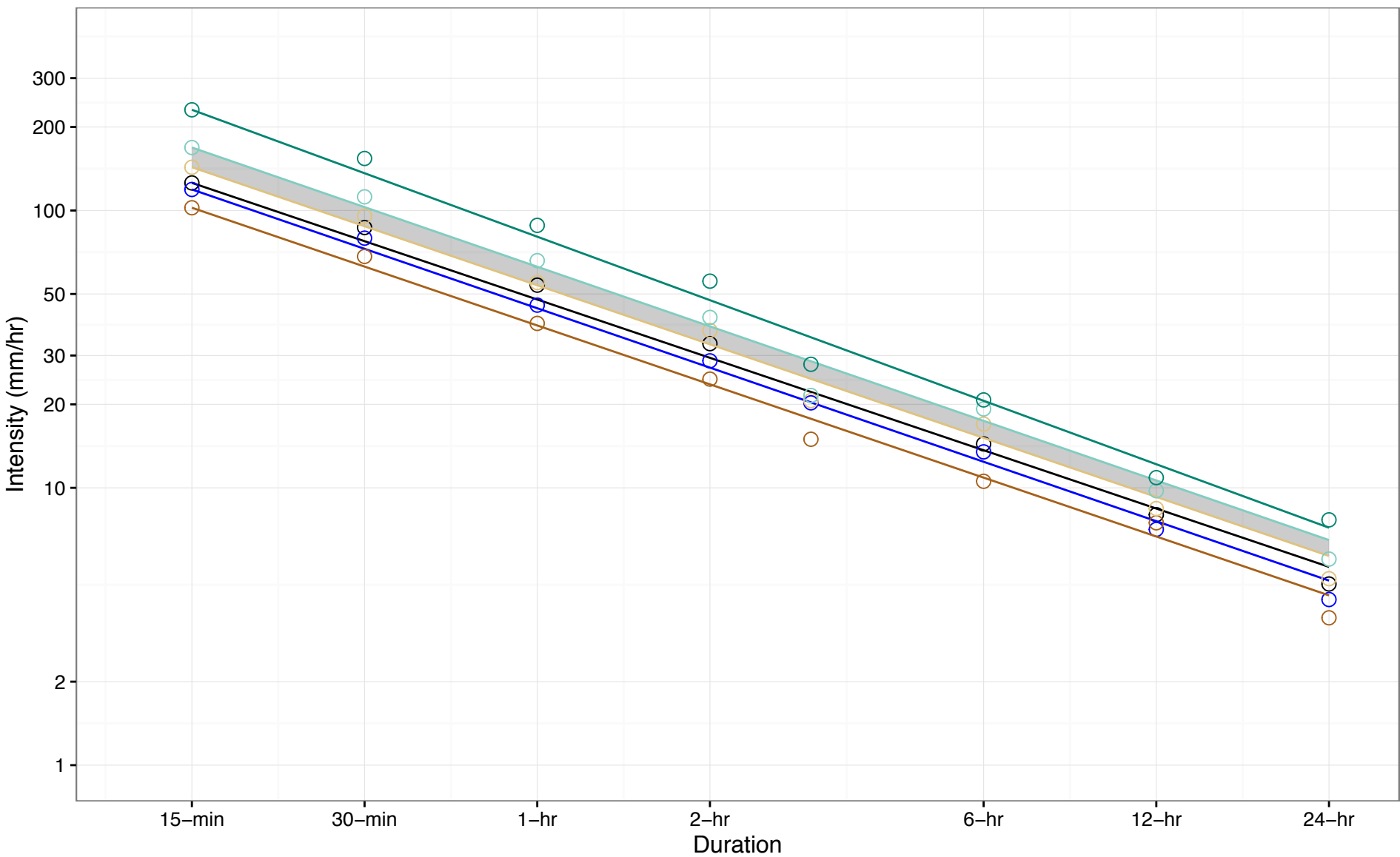
⊖ (c) Fut. Ensemble Min.: $R=39.1T^{-0.735}$

⊖ (d) Fut. Ensemble 50th Percentile: $R=48.68T^{-0.728}$

⊖ (e) Fut. Ensemble 75th Percentile: $R=54.45T^{-0.734}$

⊖ (f) Fut. Ensemble Max.: $R=64.35T^{-0.762}$

Figure A-41: IDF Curve Comparison for Pearson Airport, 2090s 50-year Return Period Event (50th–75th Percentile)



⊖ (a) Hist. Gumbel: $R=47.76T^{-0.698}$

⊖ (b) Hist. GEV: $R=44.42T^{-0.711}$

■ 50th to 75th Percentile Range

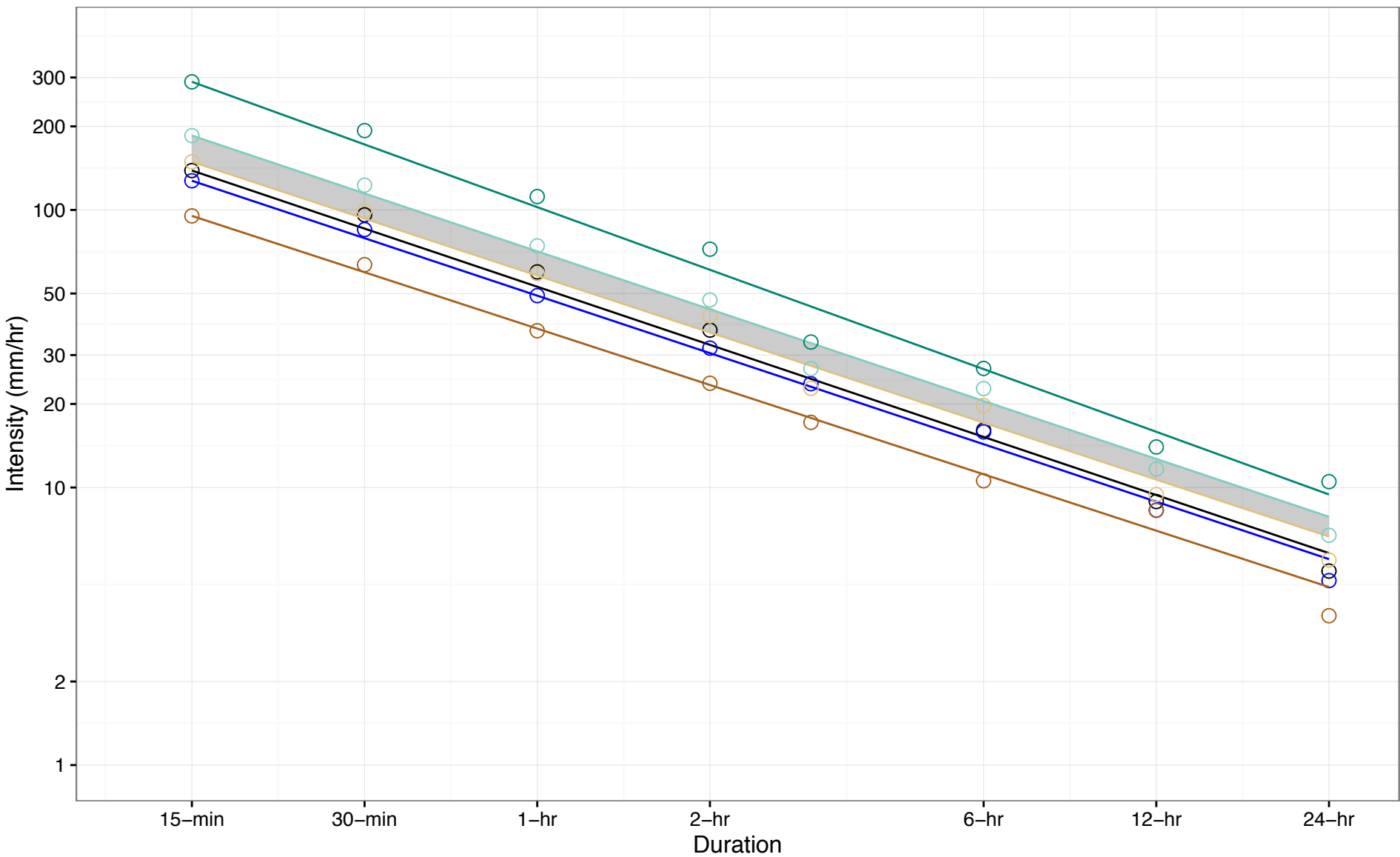
⊖ (c) Fut. Ensemble Min.: $R=38.5T^{-0.705}$

⊖ (d) Fut. Ensemble 50th Percentile: $R=53.74T^{-0.707}$

⊖ (e) Fut. Ensemble 75th Percentile: $R=62.7T^{-0.714}$

⊖ (f) Fut. Ensemble Max.: $R=80.44T^{-0.76}$

Figure A-42: IDF Curve Comparison for Pearson Airport, 2090s 100-year Return Period Event (50th-75th Percentile)



⊖ (a) Hist. Gumbel: $R=52.89T^{-0.695}$

⊖ (b) Hist. GEV: $R=49.11T^{-0.688}$

■ 50th to 75th Percentile Range

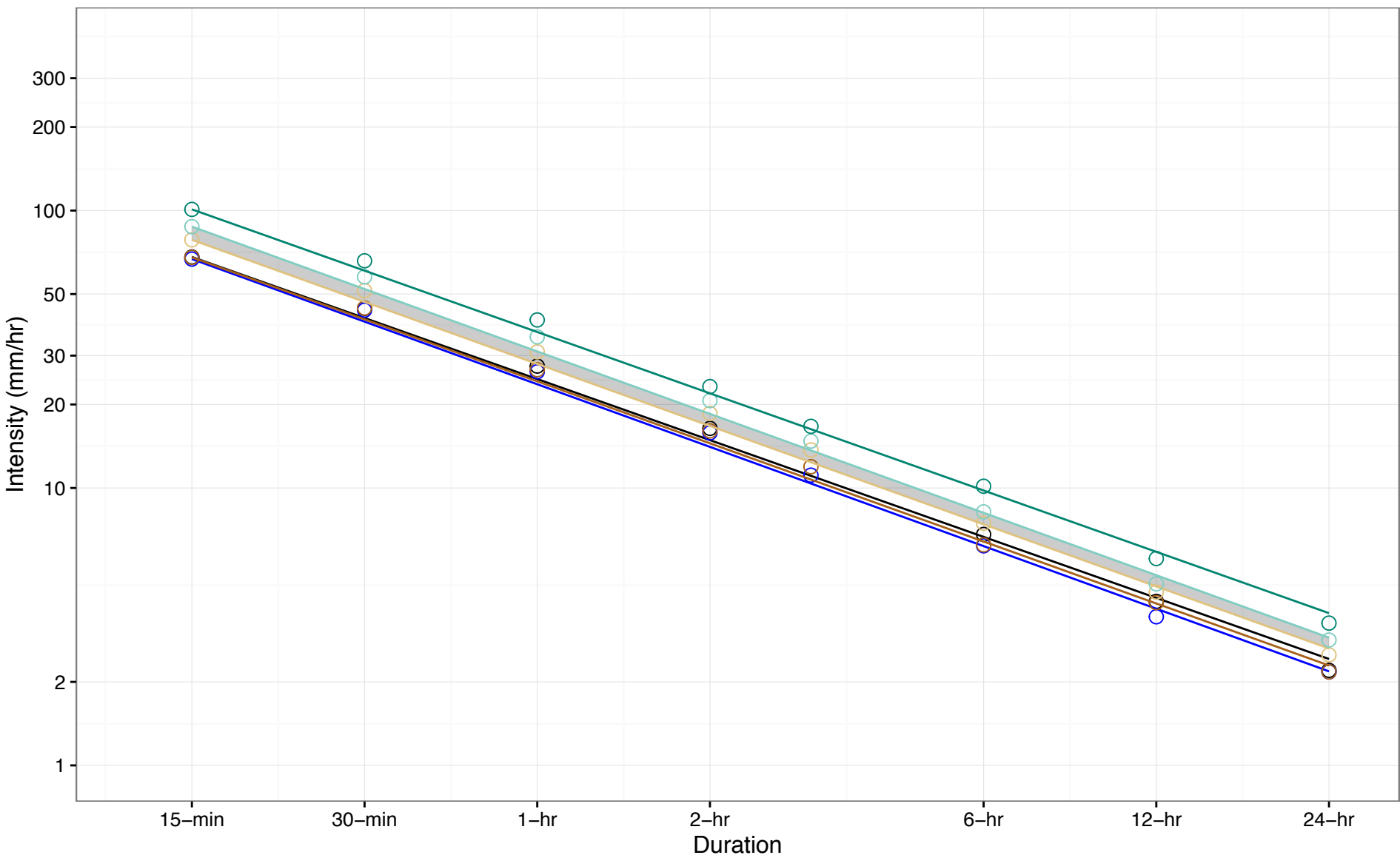
⊖ (c) Fut. Ensemble Min.: $R=37.36T^{-0.675}$

⊖ (d) Fut. Ensemble 50th Percentile: $R=58.01T^{-0.681}$

⊖ (e) Fut. Ensemble 75th Percentile: $R=70.93T^{-0.693}$

⊖ (f) Fut. Ensemble Max.: $R=102.36T^{-0.75}$

Figure A-43: IDF Curve Comparison for Windsor Airport, 2090s 2-year Return Period Event (50th-75th Percentile)



⊖ (a) Hist. Gumbel: $R=24.69T^{-0.731}$

⊖ (b) Hist. GEV: $R=23.65T^{-0.75}$

■ 50th to 75th Percentile Range

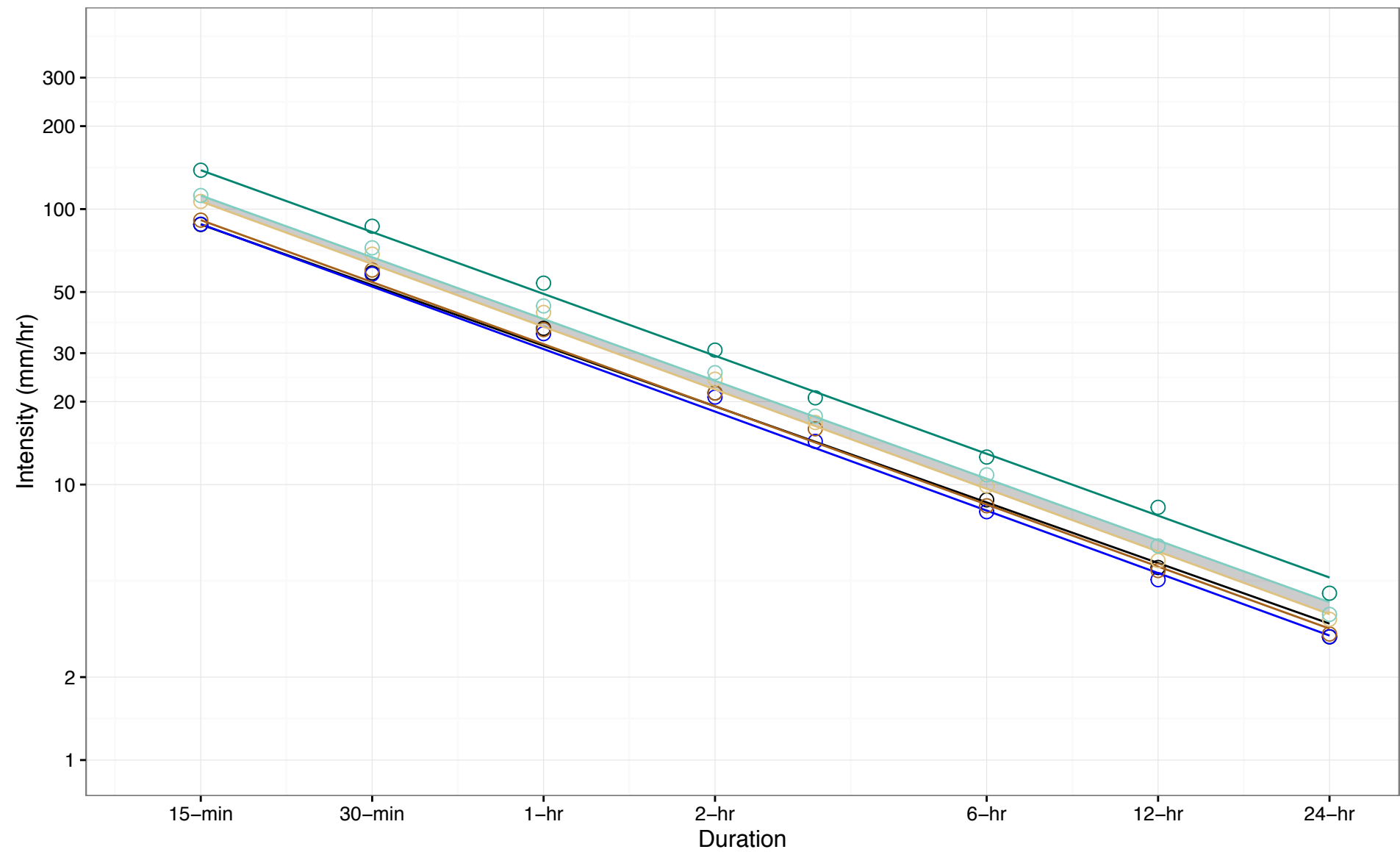
⊖ (c) Fut. Ensemble Min.: $R=24.23T^{-0.742}$

⊖ (d) Fut. Ensemble 50th Percentile: $R=28T^{-0.743}$

⊖ (e) Fut. Ensemble 75th Percentile: $R=31.05T^{-0.747}$

⊖ (f) Fut. Ensemble Max.: $R=36.5T^{-0.734}$

Figure A-44: IDF Curve Comparison for Windsor Airport, 2090s 5-year Return Period Event (50th-75th Percentile)



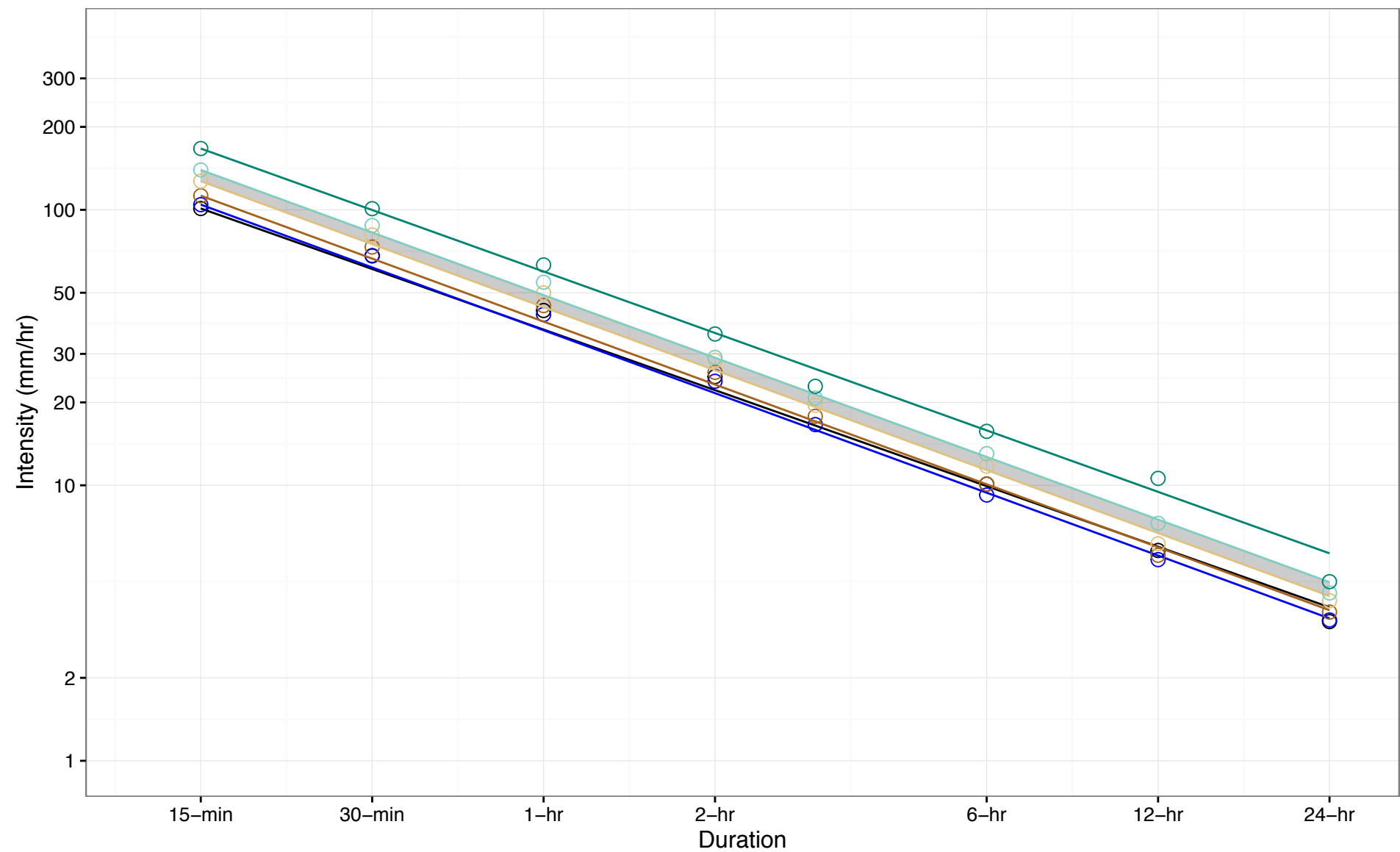
50th to 75th Percentile Range

⊖ (a) Hist. Gumbel: $R=31.92T^{-0.731}$
⊖ (b) Hist. GEV: $R=31.03T^{-0.753}$

⊖ (c) Fut. Ensemble Min.: $R=32.33T^{-0.748}$
⊖ (d) Fut. Ensemble 50th Percentile: $R=37.39T^{-0.756}$

⊖ (e) Fut. Ensemble 75th Percentile: $R=39.9T^{-0.745}$
⊖ (f) Fut. Ensemble Max.: $R=49.22T^{-0.746}$

Figure A-45: IDF Curve Comparison for Windsor Airport, 2090s 10-year Return Period Event (50th-75th Percentile)



⊖ (a) Hist. Gumbel: $R=36.75T^{-0.73}$

⊖ (b) Hist. GEV: $R=36.53T^{-0.758}$

■ 50th to 75th Percentile Range

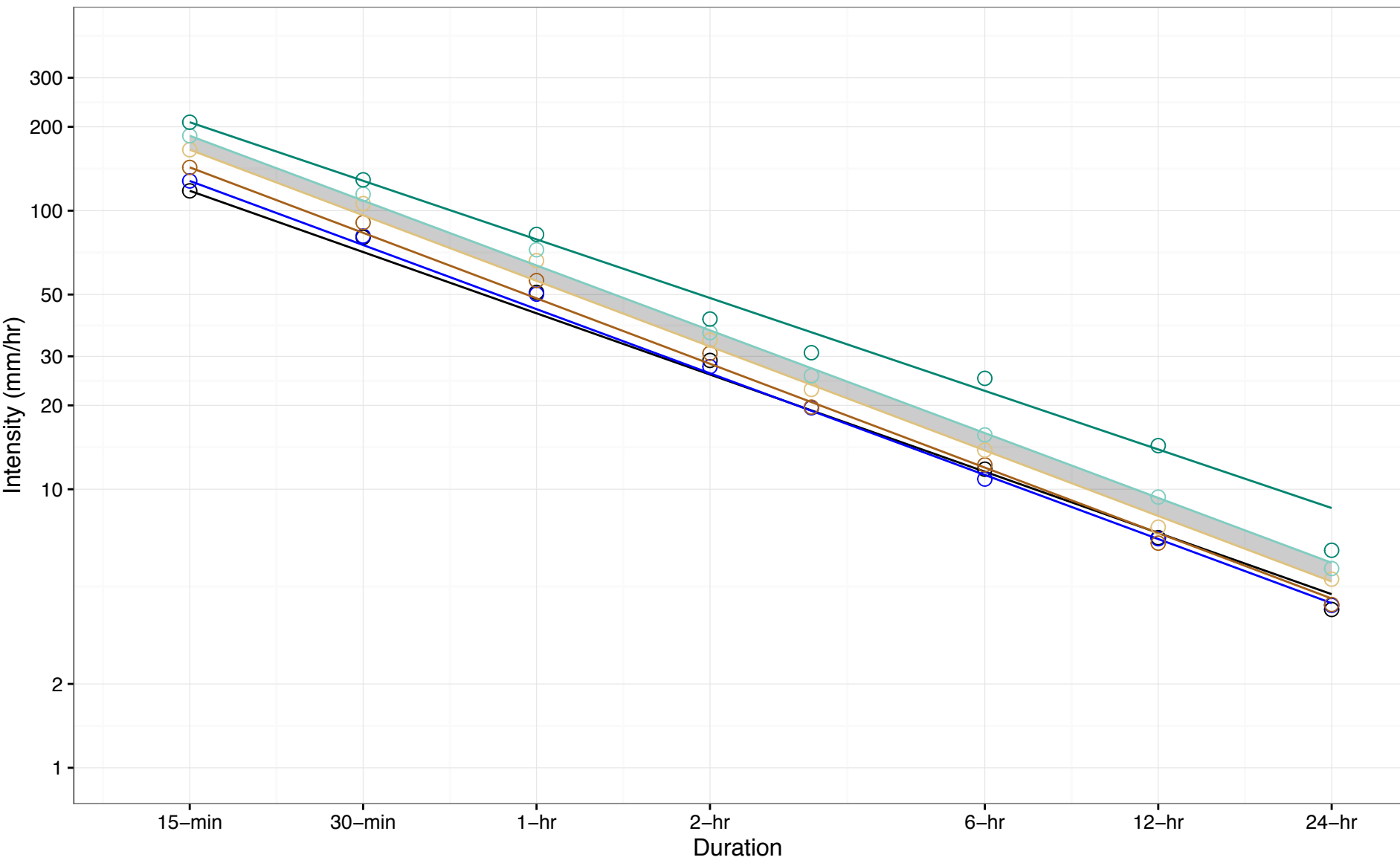
⊖ (c) Fut. Ensemble Min.: $R=39.29T^{-0.759}$

⊖ (d) Fut. Ensemble 50th Percentile: $R=44.32T^{-0.76}$

⊖ (e) Fut. Ensemble 75th Percentile: $R=49.02T^{-0.755}$

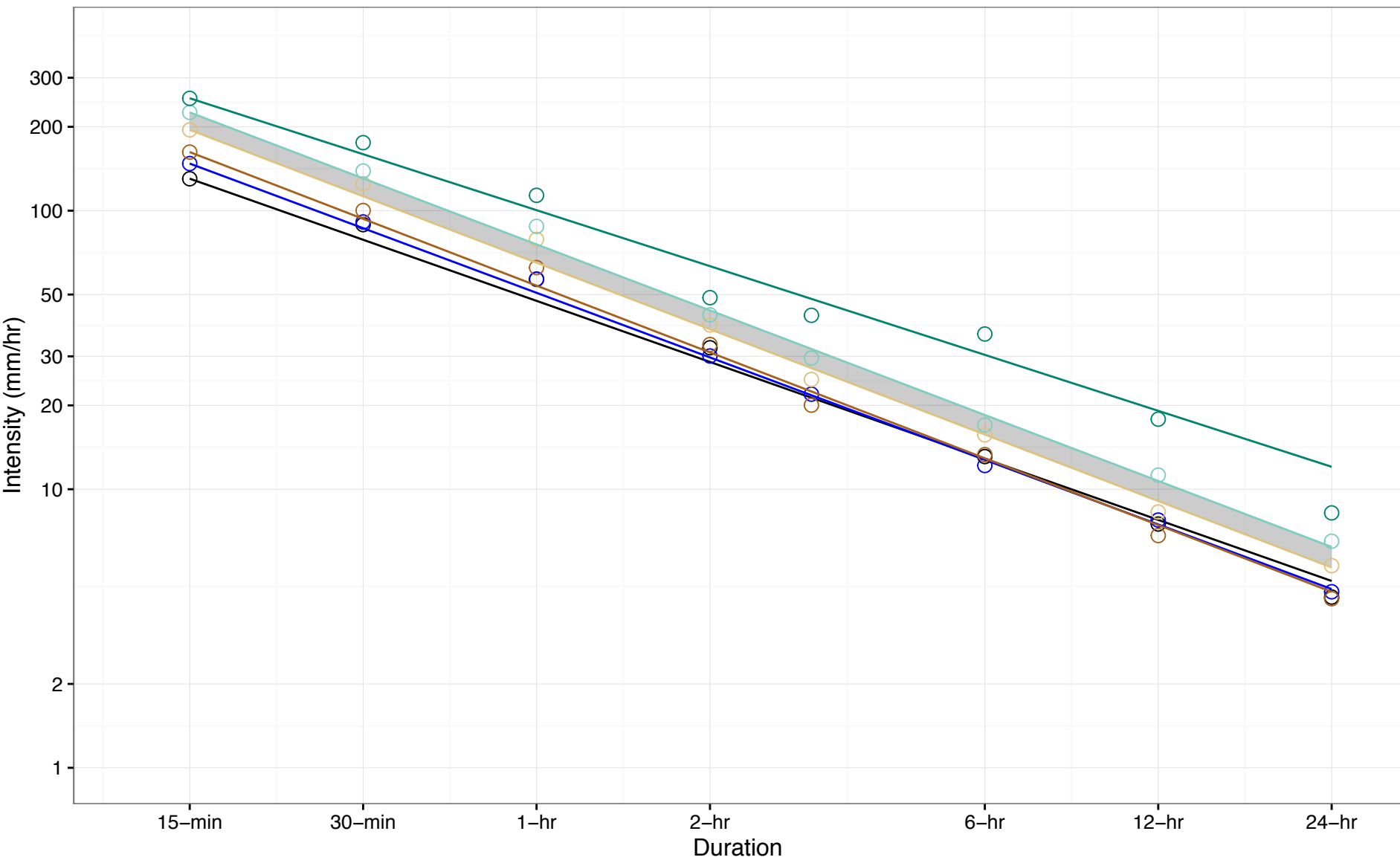
⊖ (f) Fut. Ensemble Max.: $R=59.72T^{-0.741}$

Figure A-46: IDF Curve Comparison for Windsor Airport, 2090s 25-year Return Period Event (50th-75th Percentile)



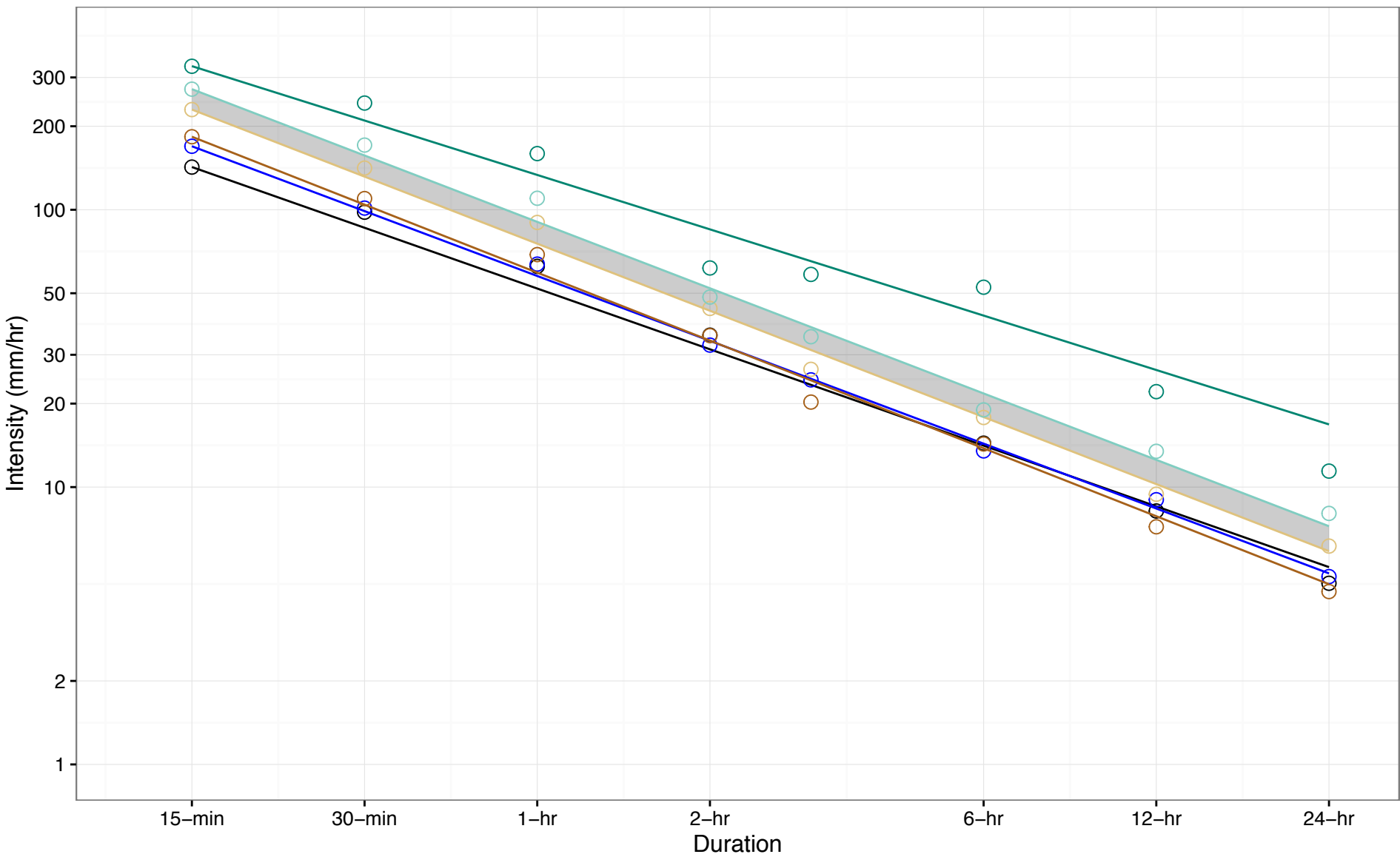
- -
- (a) Hist. Gumbel: $R=42.81T^{-0.731}$
 (b) Hist. GEV: $R=44.3T^{-0.765}$
 50th to 75th Percentile Range
- (c) Fut. Ensemble Min.: $R=48.46T^{-0.781}$
 (d) Fut. Ensemble 50th Percentile: $R=55.98T^{-0.782}$
- (e) Fut. Ensemble 75th Percentile: $R=63.59T^{-0.773}$
 (f) Fut. Ensemble Max.: $R=78.86T^{-0.699}$

Figure A-47: IDF Curve Comparison for Windsor Airport, 2090s 50-year Return Period Event (50th-75th Percentile)



- ⊖ (a) Hist. Gumbel: $R=47.45T^{-0.729}$
 - ⊖ (b) Hist. GEV: $R=50.72T^{-0.771}$
 - ⊖ (c) Fut. Ensemble Min.: $R=53.81T^{-0.796}$
 - ⊖ (d) Fut. Ensemble 50th Percentile: $R=65.03T^{-0.793}$
 - ⊖ (e) Fut. Ensemble 75th Percentile: $R=75.68T^{-0.787}$
 - ⊖ (f) Fut. Ensemble Max.: $R=100.41T^{-0.667}$
- 50th to 75th Percentile Range

Figure A-48: IDF Curve Comparison for Windsor Airport, 2090s 100-year Return Period Event (50th-75th Percentile)



50th to 75th Percentile Range

⊖ (a) Hist. Gumbel: $R=51.99T^{-0.728}$
⊖ (b) Hist. GEV: $R=57.7T^{-0.777}$

⊖ (c) Fut. Ensemble Min.: $R=59.33T^{-0.814}$
⊖ (d) Fut. Ensemble 50th Percentile: $R=75.45T^{-0.803}$

⊖ (e) Fut. Ensemble 75th Percentile: $R=90.42T^{-0.795}$
⊖ (f) Fut. Ensemble Max.: $R=133.51T^{-0.652}$

A Comparison of IDF Curves for Southern

Addendum – Appendix B: IDF Statistics and Curve
Parameters

CONTENTS

1. Pearson Airport 2030s 2-year event	3
2. Pearson Airport 2030s 5-year event	5
3. Pearson Airport 2030s 10-year event	7
4. Pearson Airport 2030s 25-year event	9
5. Pearson Airport 2030s 50-year event	11
6. Pearson Airport 2030s 100-year event	13
7. Pearson Airport 2050s 2-year event	15
8. Pearson Airport 2050s 5-year event	17
9. Pearson Airport 2050s 10-year event	19
10. Pearson Airport 2050s 25-year event	21
11. Pearson Airport 2050s 50-year event	23
12. Pearson Airport 2050s 100-year event	25
13. Pearson Airport 2090s 2-year event	27
14. Pearson Airport 2090s 5-year event	29
15. Pearson Airport 2090s 10-year event	31
16. Pearson Airport 2090s 25-year event	33
17. Pearson Airport 2090s 50-year event	35
18. Pearson Airport 2090s 100-year event	37
19. Windsor Airport 2030s 2-year event	39
20. Windsor Airport 2030s 5-year event	41
21. Windsor Airport 2030s 10-year event	43

22.	Windsor Airport 2030s 25-year event	45
23.	Windsor Airport 2030s 50-year event	47
24.	Windsor Airport 2030s 100-year event	49
25.	Windsor Airport 2050s 2-year event	51
26.	Windsor Airport 2050s 5-year event	53
27.	Windsor Airport 2050s 10-year event	55
28.	Windsor Airport 2050s 25-year event	57
29.	Windsor Airport 2050s 50-year event	59
30.	Windsor Airport 2050s 100-year event	61
31.	Windsor Airport 2090s 2-year event	63
32.	Windsor Airport 2090s 5-year event	65
33.	Windsor Airport 2090s 10-year event	67
34.	Windsor Airport 2090s 25-year event	69
35.	Windsor Airport 2090s 50-year event	71
36.	Windsor Airport 2090s 100-year event	73

1. PEARSON AIRPORT 2030S 2-YEAR EVENT

Duration	OBS_GUM	OBS_GEV	MIN	MAX	P10	P50	P75	P90	BMS
0.25	60.9	63.26	57.1	72.548	59.1915	66.968	69.63625	72.4594	12
0.5	40.3	41.959	37.768	48.23	39.2608	44.448	46.318	48.1054	12
1	23.3	23.823	21.577	27.321	22.2911	25.203	26.0755	27.22	12
3	NA	9.353	5.829	10.727	5.8735	9.8085	10.17275	10.442	12
2	13.7	13.742	12.471	15.76	12.8585	14.5385	14.96275	15.736	12
6	6	5.513	5.269	6.515	5.3253	5.5465	5.83575	6.3573	12
12	3.5	3.039	2.915	3.832	2.9368	3.251	3.3435	3.7209	12
24	2	1.827	1.691	2.095	1.7237	1.9135	1.97375	2.0294	12

Model info for (a) Hist. Gumbel: $R=22.05T^{-0.733}$

	Estimate	Std. Error	t value	Pr(> t)
A	22.046	2.75E-01	80.05	5.76E-09
B	0.7332	8.97E-03	81.78	5.18E-09

Model info for (b) Hist. GEV: $R=21.78T^{-0.769}$

	Estimate	Std. Error	t value	Pr(> t)
A	21.783	3.58E-01	60.78	1.33E-09
B	0.7694	1.18E-02	65.04	8.88E-10

Model info for (c) Fut. EnsembleMin.: $R=19.97T^{-0.758}$

	Estimate	Std. Error	t value	Pr(> t)
A	19.974	3.43E-01	58.22	1.73E-09
B	0.7580	1.23E-02	61.41	1.25E-09

Model info for (d) Fut. Ensemble10thPercentile: $R=20.52T^{-0.764}$

	Estimate	Std. Error	t value	Pr(> t)
A	20.525	3.73E-01	55.07	2.41E-09
B	0.7643	1.31E-02	58.56	1.67E-09

Model info for (e) Fut. Ensemble90thPercentile: $R=25.12T^{-0.765}$

	Estimate	Std. Error	t value	Pr(> t)
A	25.117	3.92E-01	63.99	9.79E-10
B	0.7646	1.12E-02	68.07	6.76E-10

Model info for (f) Fut. EnsembleMax.: $R=25.38T^{-0.758}$

	Estimate	Std. Error	t value	Pr(> t)
A	25.381	3.75E-01	67.60	7.05E-10
B	0.7579	1.06E-02	71.30	5.12E-10

2. PEARSON AIRPORT 2030S 5-YEAR EVENT

Duration	OBS_GUM	OBS_GEV	MIN	MAX	P10	P50	P75	P90	BMS
0.25	81.7	83.978	71.436	90.895	74.1773	84.875	88.63775	89.8709	12
0.5	55.2	55.997	47.51	60.656	49.4616	56.591	59.104	59.9728	12
1	33.1	31.558	26.841	34.23	27.8755	31.897	33.31	33.7987	12
3	NA	11.944	7.478	12.946	7.7377	11.7465	12.291	12.5145	12
2	19.9	18.426	15.513	20.204	16.2756	18.622	19.4495	19.8776	12
6	8.7	7.467	6.886	7.871	7.1598	7.583	7.7355	7.8357	12
12	4.9	4.035	3.739	4.4	3.8693	4.213	4.2495	4.3767	12
24	2.8	2.333	2.007	2.563	2.0607	2.3585	2.4685	2.539	12

Model info for (a) Hist. Gumbel: $R=30.29T^{-0.716}$

	Estimate	Std. Error	t value	Pr(> t)
A	30.286	4.77E-01	63.46	1.84E-08
B	0.7162	1.13E-02	63.38	1.85E-08

Model info for (b) Hist. GEV: $R=28.96T^{-0.768}$

	Estimate	Std. Error	t value	Pr(> t)
A	28.956	5.08E-01	56.96	1.97E-09
B	0.7684	1.26E-02	60.89	1.32E-09

Model info for (c) Fut. EnsembleMin.: $R=25.18T^{-0.752}$

	Estimate	Std. Error	t value	Pr(> t)
A	25.184	4.69E-01	53.68	2.81E-09
B	0.7524	1.34E-02	56.21	2.13E-09

Model info for (d) Fut. Ensemble10thPercentile: $R=26.14T^{-0.753}$

	Estimate	Std. Error	t value	Pr(> t)
A	26.137	5.03E-01	51.98	3.40E-09
B	0.7528	1.38E-02	54.46	2.57E-09

Model info for (e) Fut. Ensemble90thPercentile: $R=30.96T^{-0.769}$

	Estimate	Std. Error	t value	Pr(> t)
A	30.956	5.31E-01	58.27	1.72E-09
B	0.7692	1.23E-02	62.34	1.15E-09

Model info for (f) Fut. EnsembleMax.: $R=31.26T^{-0.77}$

	Estimate	Std. Error	t value	Pr(> t)
A	31.256	5.43E-01	57.55	1.85E-09
B	0.7704	1.25E-02	61.66	1.22E-09

3. PEARSON AIRPORT 2030S 10-YEAR EVENT

Duration	OBS_GUM	OBS_GEV	MIN	MAX	P10	P50	P75	P90	BMS
0.25	95.4	96.121	80.781	102.977	82.2086	96.672	101.28525	102.7176	12
0.5	65.1	64.171	53.831	68.748	54.8831	64.532	67.622	68.5589	12
1	39.6	36.266	30.366	39.053	31.0168	36.458	38.356	38.8423	12
3	NA	14.069	8.691	15.002	9.2308	12.903	14.319	14.6688	12
2	24	21.585	17.708	24.058	18.4604	21.6545	23.09025	23.385	12
6	10.5	9.037	8.077	10.199	8.5019	9.2045	9.6695	9.7715	12
12	5.9	4.833	4.346	5.013	4.6057	4.832	4.9165	4.99	12
24	3.3	2.748	2.256	3.302	2.3498	2.752	2.9575	3.0277	12

Model info for (a) Hist. Gumbel: $R=35.76T^{-0.708}$

	Estimate	Std. Error	t value	Pr(> t)
A	35.755	6.21E-01	57.61	2.98E-08
B	0.7083	1.24E-02	56.93	3.16E-08

Model info for (b) Hist. GEV: $R=33.71T^{-0.756}$

	Estimate	Std. Error	t value	Pr(> t)
A	33.710	5.72E-01	58.93	1.60E-09
B	0.7562	1.22E-02	62.02	1.18E-09

Model info for (c) Fut. EnsembleMin.: $R=28.76T^{-0.745}$

	Estimate	Std. Error	t value	Pr(> t)
A	28.755	5.59E-01	51.44	3.62E-09
B	0.7454	1.40E-02	53.39	2.90E-09

Model info for (d) Fut. Ensemble10thPercentile: $R=29.63T^{-0.736}$

	Estimate	Std. Error	t value	Pr(> t)
A	29.631	5.73E-01	51.70	3.51E-09
B	0.7364	1.39E-02	53.04	3.02E-09

Model info for (e) Fut. Ensemble90thPercentile: $R=36.03T^{-0.756}$

	Estimate	Std. Error	t value	Pr(> t)
A	36.028	6.53E-01	55.17	2.38E-09
B	0.7561	1.30E-02	58.06	1.75E-09

Model info for (f) Fut. EnsembleMax.: $R=36.58T^{-0.747}$

	Estimate	Std. Error	t value	Pr(> t)
A	36.584	6.83E-01	53.59	2.83E-09
B	0.7469	1.34E-02	55.72	2.24E-09

4. PEARSON AIRPORT 2030S 25-YEAR EVENT

Duration	OBS_GUM	OBS_GEV	MIN	MAX	P10	P50	P75	P90	BMS
0.25	112.8	109.876	79.117	119.803	90.5547	110.3445	115.986	117.609	12
0.5	77.6	73.377	52.836	80.007	60.4327	73.6905	77.4485	78.4169	12
1	47.7	41.779	30.084	45.554	34.0814	41.9045	44.35475	45.4199	12
3	NA	17.331	10.377	19.491	11.4802	14.623	16.865	17.8817	12
2	29.2	25.642	18.464	30.151	20.0706	25.589	27.75625	28.1335	12
6	12.7	11.401	9.428	15.14	9.5281	12.252	13.07675	13.4666	12
12	7.1	6.031	5.094	6.566	5.1394	5.79	6.21175	6.2509	12
24	4	3.385	2.437	4.862	2.5377	3.3495	3.71225	3.8921	12

Model info for (a) Hist. Gumbel: $R=42.63T^{-0.702}$

	Estimate	Std. Error	t value	Pr(> t)
A	42.630	7.78E-01	54.79	3.83E-08
B	0.7023	1.31E-02	53.71	4.23E-08

Model info for (b) Hist. GEV: $R=39.8T^{-0.733}$

	Estimate	Std. Error	t value	Pr(> t)
A	39.800	6.51E-01	61.16	1.28E-09
B	0.7329	1.17E-02	62.44	1.13E-09

Model info for (c) Fut. EnsembleMin.: $R=29.88T^{-0.703}$

	Estimate	Std. Error	t value	Pr(> t)
A	29.880	6.41E-01	46.61	6.53E-09
B	0.7027	1.54E-02	45.72	7.34E-09

Model info for (d) Fut. Ensemble10thPercentile: $R=32.77T^{-0.734}$

	Estimate	Std. Error	t value	Pr(> t)
A	32.771	6.41E-01	51.14	3.75E-09
B	0.7335	1.40E-02	52.26	3.29E-09

Model info for (e) Fut. Ensemble90thPercentile: $R=43.41T^{-0.719}$

	Estimate	Std. Error	t value	Pr(> t)
A	43.408	9.63E-01	45.06	8.00E-09
B	0.7193	1.59E-02	45.19	7.86E-09

Model info for (f) Fut. EnsembleMax.: $R=45.77T^{-0.694}$

	Estimate	Std. Error	t value	Pr(> t)
A	45.767	1.14E+00	40.25	1.57E-08
B	0.6945	1.78E-02	39.03	1.89E-08

5. PEARSON AIRPORT 2030S 50-YEAR EVENT

Duration	OBS_GUM	OBS_GEV	MIN	MAX	P10	P50	P75	P90	BMS
0.25	125.7	119.047	75.087	131.887	93.0861	119.5095	127.30225	127.9543	12
0.5	86.8	79.481	50.131	88.053	62.1309	79.799	84.95075	85.2788	12
1	53.8	45.578	28.748	50.494	35.0812	45.668	48.859	50.1025	12
3	NA	20.252	11.747	24.166	12.8242	17.5155	18.869	21.1451	12
2	33.1	28.7	18.102	35.383	20.7767	28.546	31.21925	32.2172	12
6	14.4	13.478	10.091	20.852	10.2833	15.2365	16.435	17.6938	12
12	8	7.082	5.321	8.289	5.4622	6.646	7.3255	7.5343	12
24	4.5	3.956	2.495	6.709	2.6385	3.875	4.403	4.7693	12

Model info for (a) Hist. Gumbel: $R=47.76T^{-0.698}$

	Estimate	Std. Error	t value	Pr(> t)
A	47.761	9.08E-01	52.58	4.70E-08
B	0.6985	1.36E-02	51.28	5.33E-08

Model info for (b) Hist. GEV: $R=44.42T^{-0.711}$

	Estimate	Std. Error	t value	Pr(> t)
A	44.418	7.39E-01	60.09	1.43E-09
B	0.7115	1.19E-02	59.63	1.49E-09

Model info for (c) Fut. EnsembleMin.: $R=29.46T^{-0.675}$

	Estimate	Std. Error	t value	Pr(> t)
A	29.459	7.27E-01	40.54	1.51E-08
B	0.6753	1.76E-02	38.29	2.12E-08

Model info for (d) Fut. Ensemble10thPercentile: $R=34.15T^{-0.724}$

	Estimate	Std. Error	t value	Pr(> t)
A	34.154	7.09E-01	48.14	5.39E-09
B	0.7236	1.49E-02	48.55	5.12E-09

Model info for (e) Fut. Ensemble90thPercentile: $R=49.83T^{-0.681}$

	Estimate	Std. Error	t value	Pr(> t)
A	49.833	1.48E+00	33.59	4.64E-08
B	0.6806	2.13E-02	31.95	6.25E-08

Model info for (f) Fut. EnsembleMax.: $R=54.11T^{-0.643}$

	Estimate	Std. Error	t value	Pr(> t)
A	54.115	1.77E+00	30.66	8.00E-08
B	0.6429	2.33E-02	27.65	1.48E-07

6. PEARSON AIRPORT 2030S 100-YEAR EVENT

Duration	OBS_GUM	OBS_GEV	MIN	MAX	P10	P50	P75	P90	BMS
0.25	138.6	127.364	70.24	143.593	95.1162	128.125	137.645	138.3842	12
0.5	96	84.99	46.871	95.819	63.4852	85.517	91.58275	92.2345	12
1	59.8	49.12	27.089	55.379	35.9051	49.2905	53.4575	54.6659	12
3	NA	23.656	13.046	30.372	13.259	20.9435	21.211	25.1686	12
2	36.9	31.778	17.525	41.265	21.3852	31.584	34.82125	36.5803	12
6	16.1	15.861	10.729	29.145	11.019	19.0065	20.762	23.6999	12
12	8.9	8.286	5.516	10.572	5.7515	7.586	8.62775	9.1292	12
24	5	4.62	2.548	9.447	2.7347	4.4895	5.2305	5.8782	12

Model info for (a) Hist. Gumbel: $R=52.89T^{-0.695}$

	Estimate	Std. Error	t value	Pr(> t)
A	52.886	1.04E+00	51.08	5.44E-08
B	0.6954	1.40E-02	49.60	6.29E-08

Model info for (b) Hist. GEV: $R=49.11T^{-0.688}$

	Estimate	Std. Error	t value	Pr(> t)
A	49.112	8.74E-01	56.18	2.14E-09
B	0.6877	1.27E-02	53.98	2.72E-09

Model info for (c) Fut. EnsembleMin.: $R=28.71T^{-0.646}$

	Estimate	Std. Error	t value	Pr(> t)
A	28.708	8.32E-01	34.49	3.95E-08
B	0.6458	2.07E-02	31.24	7.15E-08

Model info for (d) Fut. Ensemble10thPercentile: $R=35.35T^{-0.714}$

	Estimate	Std. Error	t value	Pr(> t)
A	35.354	7.99E-01	44.23	8.94E-09
B	0.7142	1.62E-02	44.06	9.15E-09

Model info for (e) Fut. Ensemble90thPercentile: $R=57.27T^{-0.637}$

	Estimate	Std. Error	t value	Pr(> t)
A	57.272	2.32E+00	24.67	2.92E-07
B	0.6368	2.89E-02	22.05	5.68E-07

Model info for (f) Fut. EnsembleMax.: $R=63.91T^{-0.584}$

	Estimate	Std. Error	t value	Pr(> t)
A	63.910	2.69E+00	23.77	3.64E-07
B	0.5843	2.98E-02	19.64	1.13E-06

7. PEARSON AIRPORT 2050S 2-YEAR EVENT

Duration	OBS_GUM	OBS_GEV	MIN	MAX	P10	P50	P75	P90	BMS
0.25	60.9	68.348	67.052	86.748	67.4223	75.897	77.6795	83.15	8
0.5	40.3	45.412	44.55	57.687	44.7593	50.407	51.6015	55.2615	8
1	23.3	25.425	24.943	32.367	24.9745	28.539	29.1595	30.9607	8
3	NA	9.66	9.406	11.581	9.4557	10.9025	11.208	11.3787	8
2	13.7	14.337	13.951	18.633	14.0308	16.4935	16.72225	17.5732	8
6	6	5.773	5.572	6.9	5.5804	6.4535	6.7395	6.8013	8
12	3.5	3.149	2.883	3.816	2.8935	3.55	3.7315	3.7579	8
24	2	1.887	1.837	2.237	1.8468	2.114	2.18925	2.2146	8

Model info for (a) Hist. Gumbel: $R=22.05T^{-0.733}$

	Estimate	Std. Error	t value	Pr(> t)
A	22.046	2.75E-01	80.05	5.76E-09
B	0.7332	8.97E-03	81.78	5.18E-09

Model info for (b) Hist. GEV: $R=23.22T^{-0.779}$

	Estimate	Std. Error	t value	Pr(> t)
A	23.218	4.14E-01	56.12	2.15E-09
B	0.7792	1.28E-02	60.79	1.33E-09

Model info for (c) Fut. EnsembleMin.: $R=22.53T^{-0.787}$

	Estimate	Std. Error	t value	Pr(> t)
A	22.535	4.52E-01	49.85	4.37E-09
B	0.7869	1.44E-02	54.53	2.55E-09

Model info for (d) Fut. Ensemble10thPercentile: $R=22.64T^{-0.788}$

	Estimate	Std. Error	t value	Pr(> t)
A	22.635	4.51E-01	50.15	4.22E-09
B	0.7877	1.43E-02	54.91	2.45E-09

Model info for (e) Fut. Ensemble90thPercentile: $R=27.97T^{-0.786}$

	Estimate	Std. Error	t value	Pr(> t)
A	27.973	5.32E-01	52.62	3.16E-09
B	0.7862	1.37E-02	57.50	1.86E-09

Model info for (f) Fut. EnsembleMax.: $R=28.91T^{-0.793}$

	Estimate	Std. Error	t value	Pr(> t)
A	28.912	5.95E-01	48.60	5.09E-09
B	0.7930	1.48E-02	53.56	2.84E-09

8. PEARSON AIRPORT 2050S 5-YEAR EVENT

Duration	OBS_GUM	OBS_GEV	MIN	MAX	P10	P50	P75	P90	EMS
0.25	81.7	89.045	86.554	104.818	86.792	89.266	94.2195	103.7484	8
0.5	55.2	59.234	57.578	69.727	57.7096	59.5475	62.828	69.1355	8
1	33.1	33.288	32.357	39.184	32.3759	33.5595	35.4895	39.1567	8
3	NA	12.588	12.231	14.262	12.2345	12.7125	13.11425	13.7594	8
2	19.9	19.301	18.681	23.621	18.737	19.653	20.6875	22.9903	8
6	8.7	8.047	6.859	8.879	6.8604	8.555	8.7455	8.8559	8
12	4.9	4.357	4.005	4.786	4.0092	4.585	4.641	4.779	8
24	2.8	2.459	2.389	2.911	2.3897	2.483	2.58525	2.7927	8

Model info for (a) Hist. Gumbel: $R=30.29T^{-0.716}$

	Estimate	Std. Error	t value	Pr(> t)
A	30.286	4.77E-01	63.46	1.84E-08
B	0.7162	1.13E-02	63.38	1.85E-08

Model info for (b) Hist. GEV: $R=30.83T^{-0.765}$

	Estimate	Std. Error	t value	Pr(> t)
A	30.829	5.23E-01	58.99	1.59E-09
B	0.7655	1.22E-02	62.82	1.09E-09

Model info for (c) Fut. EnsembleMin.: $R=29.11T^{-0.786}$

	Estimate	Std. Error	t value	Pr(> t)
A	29.114	5.64E-01	51.63	3.54E-09
B	0.7863	1.39E-02	56.43	2.08E-09

Model info for (d) Fut. Ensemble10thPercentile: $R=29.17T^{-0.787}$

	Estimate	Std. Error	t value	Pr(> t)
A	29.169	5.65E-01	51.60	3.55E-09
B	0.7869	1.39E-02	56.44	2.08E-09

Model info for (e) Fut. Ensemble90thPercentile: $R=35.29T^{-0.778}$

	Estimate	Std. Error	t value	Pr(> t)
A	35.287	6.79E-01	51.96	3.41E-09
B	0.7783	1.38E-02	56.23	2.13E-09

Model info for (f) Fut. EnsembleMax.: $R=35.63T^{-0.779}$

	Estimate	Std. Error	t value	Pr(> t)
A	35.634	6.73E-01	52.92	3.06E-09
B	0.7786	1.36E-02	57.29	1.90E-09

9. PEARSON AIRPORT 2050S 10-YEAR EVENT

Duration	OBS_GUM	OBS_GEV	MIN	MAX	P10	P50	P75	P90	EMS
0.25	95.4	100.668	91.542	115.42	92.9861	96.9715	100.958	112.3694	8
0.5	65.1	67.113	61.114	76.947	62.0772	64.6985	67.35025	75.0388	8
1	39.6	38.089	34.538	43.67	35.0357	36.6465	38.346	42.9294	8
3	NA	15.23	13.398	16.113	13.4526	14.417	15.20425	15.8764	8
2	24	22.873	20.556	26.652	20.7471	21.9045	23.23625	26.3531	8
6	10.5	9.89	7.494	11.388	7.5136	9.8855	10.36975	11.1115	8
12	5.9	5.341	4.98	6.012	5.0157	5.204	5.393	5.9546	8
24	3.3	2.975	2.617	3.416	2.6275	2.816	3.00825	3.2907	8

Model info for (a) Hist. Gumbel: $R=35.76T^{-0.708}$

	Estimate	Std. Error	t value	Pr(> t)
A	35.755	6.21E-01	57.61	2.98E-08
B	0.7083	1.24E-02	56.93	3.16E-08

Model info for (b) Hist. GEV: $R=35.87T^{-0.745}$

	Estimate	Std. Error	t value	Pr(> t)
A	35.869	5.71E-01	62.83	1.09E-09
B	0.7447	1.14E-02	65.15	8.79E-10

Model info for (c) Fut. EnsembleMin.: $R=31.65T^{-0.766}$

	Estimate	Std. Error	t value	Pr(> t)
A	31.648	5.92E-01	53.48	2.87E-09
B	0.7665	1.34E-02	57.02	1.95E-09

Model info for (d) Fut. Ensemble10thPercentile: $R=32.02T^{-0.769}$

	Estimate	Std. Error	t value	Pr(> t)
A	32.019	6.17E-01	51.90	3.43E-09
B	0.7694	1.39E-02	55.54	2.29E-09

Model info for (e) Fut. Ensemble90thPercentile: $R=40.07T^{-0.744}$

	Estimate	Std. Error	t value	Pr(> t)
A	40.067	6.84E-01	58.56	1.67E-09
B	0.7442	1.23E-02	60.68	1.35E-09

Model info for (f) Fut. EnsembleMax.: $R=41.06T^{-0.746}$

	Estimate	Std. Error	t value	Pr(> t)
A	41.062	6.95E-01	59.08	1.58E-09
B	0.7459	1.22E-02	61.35	1.26E-09

10. PEARSON AIRPORT 2050S 25-YEAR EVENT

Duration	OBS_GUM	OBS_GEV	MIN	MAX	P10	P50	P75	P90	BMS
0.25	112.8	113.345	90.269	123.839	95.736	105.9015	111.878	119.9687	8
0.5	77.6	75.818	60.284	82.837	63.9345	70.8165	74.8675	80.3359	8
1	47.7	43.729	34.324	47.777	36.2931	40.6285	43.27475	46.5989	8
3	NA	19.66	14.239	20.082	14.4287	17.0855	19.12525	19.606	8
2	29.2	27.74	21.066	30.308	21.8451	25.222	28.01725	30.2317	8
6	12.7	12.693	8.098	15.692	8.1498	11.7515	12.836	14.7596	8
12	7.1	6.843	6.035	8.054	6.0511	6.319	6.991	7.8685	8
24	4	3.84	2.781	4.131	2.8181	3.385	3.934	4.0183	8

Model info for (a) Hist. Gumbel: $R=42.63T^{-0.702}$

	Estimate	Std. Error	t value	Pr(> t)
A	42.630	7.78E-01	54.79	3.83E-08
B	0.7023	1.31E-02	53.71	4.23E-08

Model info for (b) Hist. GEV: $R=42.35T^{-0.711}$

	Estimate	Std. Error	t value	Pr(> t)
A	42.345	6.44E-01	65.76	8.32E-10
B	0.7105	1.09E-02	65.18	8.77E-10

Model info for (c) Fut. EnsembleMin.: $R=32.69T^{-0.733}$

	Estimate	Std. Error	t value	Pr(> t)
A	32.694	6.60E-01	49.52	4.55E-09
B	0.7328	1.45E-02	50.56	4.02E-09

Model info for (d) Fut. Ensemble10thPercentile: $R=34.03T^{-0.746}$

	Estimate	Std. Error	t value	Pr(> t)
A	34.025	7.21E-01	47.21	6.05E-09
B	0.7465	1.52E-02	49.07	4.80E-09

Model info for (e) Fut. Ensemble90thPercentile: $R=45.98T^{-0.692}$

	Estimate	Std. Error	t value	Pr(> t)
A	45.977	9.01E-01	51.03	3.80E-09
B	0.6922	1.40E-02	49.33	4.65E-09

Model info for (f) Fut. EnsembleMax.: $R=47.63T^{-0.69}$

	Estimate	Std. Error	t value	Pr(> t)
A	47.634	1.05E+00	45.55	7.50E-09
B	0.6895	1.57E-02	43.87	9.39E-09

11. PEARSON AIRPORT 2050S 50-YEAR EVENT

Duration	OBS_GUM	OBS_GEV	MIN	MAX	P10	P50	P75	P90	EMS
0.25	125.7	121.488	86.98	126.943	94.0948	111.341	118.78425	123.6894	8
0.5	86.8	81.482	58.071	85.141	62.8219	74.5825	79.6815	82.9941	8
1	53.8	47.626	33.301	49.764	36.0247	43.251	46.61925	48.6384	8
3	NA	23.973	14.797	25.416	15.0518	18.587	22.9285	23.8711	8
2	33.1	31.624	20.969	33.044	22.3424	27.7225	31.772	32.7605	8
6	14.4	15.177	8.424	19.964	8.5059	13.2845	15.0345	18.1881	8
12	8	8.181	6.705	10.025	6.7197	7.414	8.64675	9.6771	8
24	4.5	4.682	2.89	4.964	2.9397	3.9035	4.6335	4.7946	8

Model info for (a) Hist. Gumbel: $R=47.76T^{-0.698}$

	Estimate	Std. Error	t value	Pr(> t)
A	47.761	9.08E-01	52.58	4.70E-08
B	0.6985	1.36E-02	51.28	5.33E-08

Model info for (b) Hist. GEV: $R=47.28T^{-0.681}$

	Estimate	Std. Error	t value	Pr(> t)
A	47.279	7.33E-01	64.53	9.31E-10
B	0.6811	1.11E-02	61.43	1.25E-09

Model info for (c) Fut. EnsembleMin.: $R=32.68T^{-0.706}$

	Estimate	Std. Error	t value	Pr(> t)
A	32.685	7.43E-01	43.98	9.25E-09
B	0.7062	1.63E-02	43.34	1.01E-08

Model info for (d) Fut. Ensemble10thPercentile: $R=34.47T^{-0.725}$

	Estimate	Std. Error	t value	Pr(> t)
A	34.474	8.00E-01	43.11	1.04E-08
B	0.7245	1.66E-02	43.53	9.83E-09

Model info for (e) Fut. Ensemble90thPercentile: $R=50.42T^{-0.648}$

	Estimate	Std. Error	t value	Pr(> t)
A	50.416	1.19E+00	42.20	1.18E-08
B	0.6477	1.69E-02	38.32	2.11E-08

Model info for (f) Fut. EnsembleMax.: $R=52.45T^{-0.638}$

	Estimate	Std. Error	t value	Pr(> t)
A	52.452	1.50E+00	35.03	3.60E-08
B	0.6379	2.03E-02	31.37	6.98E-08

12. PEARSON AIRPORT 2050S 100-YEAR EVENT

Duration	OBS_GUM	OBS_GEV	MIN	MAX	P10	P50	P75	P90	BMS
0.25	138.6	128.644	82.45	127.793	91.0418	115.9165	124.79675	126.0962	8
0.5	96	86.515	55.019	85.942	60.752	77.7815	83.91525	84.7674	8
1	59.8	51.269	31.798	50.93	35.1118	45.6135	49.707	50.1726	8
3	NA	29.376	15.314	32.559	15.6003	20.0955	27.38525	29.6855	8
2	36.9	35.727	20.572	36.062	22.6328	30.258	35.05725	35.6616	8
6	16.1	18.047	8.658	25.4	8.7749	14.9465	17.571	22.3536	8
12	8.9	9.731	7.41	12.473	7.4128	8.709	10.6815	11.8836	8
24	5	5.737	2.991	6.359	3.047	4.405	5.41375	5.7976	8

Model info for (a) Hist. Gumbel: $R=52.89T^{-0.695}$

	Estimate	Std. Error	t value	Pr(> t)
A	52.886	1.04E+00	51.08	5.44E-08
B	0.6954	1.40E-02	49.60	6.29E-08

Model info for (b) Hist. GEV: $R=52.32T^{-0.649}$

	Estimate	Std. Error	t value	Pr(> t)
A	52.321	8.64E-01	60.55	1.36E-09
B	0.6493	1.18E-02	55.11	2.40E-09

Model info for (c) Fut. EnsembleMin.: $R=32.27T^{-0.677}$

	Estimate	Std. Error	t value	Pr(> t)
A	32.265	8.66E-01	37.27	2.49E-08
B	0.6769	1.92E-02	35.27	3.46E-08

Model info for (d) Fut. Ensemble10thPercentile: $R=34.49T^{-0.7}$

	Estimate	Std. Error	t value	Pr(> t)
A	34.491	9.13E-01	37.76	2.30E-08
B	0.7003	1.90E-02	36.91	2.64E-08

Model info for (e) Fut. Ensemble90thPercentile: $R=54.9T^{-0.6}$

	Estimate	Std. Error	t value	Pr(> t)
A	54.903	1.58E+00	34.84	3.72E-08
B	0.6002	2.03E-02	29.50	1.01E-07

Model info for (f) Fut. EnsembleMax.: $R=57.29T^{-0.579}$

	Estimate	Std. Error	t value	Pr(> t)
A	57.286	2.00E+00	28.69	1.19E-07
B	0.5793	2.46E-02	23.52	3.87E-07

13. PEARSON AIRPORT 2090S 2-YEAR EVENT

Duration	OBS_GUM	OBS_GEV	MIN	MAX	P10	P50	P75	P90	BMS
0.25	60.9	63.26	72.97	104.028	73.6188	84.344	88.085	91.8923	12
0.5	40.3	41.959	48.4	69.527	48.8534	56.0945	58.807	60.9868	12
1	23.3	23.823	27.48	39.209	27.706	31.2065	32.56175	34.6016	12
3	NA	9.353	6.899	13.788	7.1504	11.3865	12.5755	13.531	12
2	13.7	13.742	15.852	23.303	15.8707	18.091	18.869	19.9937	12
6	6	5.513	6.257	8.938	6.5444	6.9655	7.26425	7.8974	12
12	3.5	3.039	3.45	4.471	3.5756	3.88	4.0695	4.1697	12
24	2	1.827	2.107	2.662	2.1134	2.377	2.46675	2.4783	12

Model info for (a) Hist. Gumbel: $R=22.05T^{-0.733}$

	Estimate	Std. Error	t value	Pr(> t)
A	22.046	2.75E-01	80.05	5.76E-09
B	0.7332	8.97E-03	81.78	5.18E-09

Model info for (b) Hist. GEV: $R=21.78T^{-0.769}$

	Estimate	Std. Error	t value	Pr(> t)
A	21.783	3.58E-01	60.78	1.33E-09
B	0.7694	1.18E-02	65.04	8.88E-10

Model info for (c) Fut. EnsembleMin.: $R=24.94T^{-0.775}$

	Estimate	Std. Error	t value	Pr(> t)
A	24.940	4.92E-01	50.74	3.93E-09
B	0.7747	1.42E-02	54.66	2.52E-09

Model info for (d) Fut. Ensemble10thPercentile: $R=25.39T^{-0.768}$

	Estimate	Std. Error	t value	Pr(> t)
A	25.388	4.80E-01	52.94	3.05E-09
B	0.7683	1.36E-02	56.57	2.05E-09

Model info for (e) Fut. Ensemble90thPercentile: $R=31.25T^{-0.778}$

	Estimate	Std. Error	t value	Pr(> t)
A	31.255	5.90E-01	52.95	3.05E-09
B	0.7783	1.36E-02	57.30	1.90E-09

Model info for (f) Fut. EnsembleMax.: $R=35.08T^*-0.784$

	Estimate	Std. Error	t value	Pr(> t)
A	35.083	7.88E-01	44.52	8.60E-09
B	0.7845	1.62E-02	48.55	5.12E-09

14. PEARSON AIRPORT 2090S 5-YEAR EVENT

Duration	OBS_GUM	OBS_GEV	MIN	MAX	P10	P50	P75	P90	BMS
0.25	81.7	83.978	96.203	124.688	97.9114	108.6535	112.35625	114.1324	12
0.5	55.2	55.997	64.149	83.27	65.3772	72.451	74.92025	76.166	12
1	33.1	31.558	36.153	47.798	36.9634	40.8315	42.34725	42.4389	12
3	NA	11.944	9.069	16.728	9.8106	14.8245	15.111	15.6267	12
2	19.9	18.426	21.108	30.317	22.0957	23.3415	24.6525	24.7248	12
6	8.7	7.467	8.392	11.288	8.8808	9.2645	10.02975	10.1616	12
12	4.9	4.035	4.535	5.71	4.9057	5.143	5.31025	5.5825	12
24	2.8	2.333	2.67	3.13	2.6905	2.9595	3.11275	3.127	12

Model info for (a) Hist. Gumbel: $R=30.29T^{-0.716}$

	Estimate	Std. Error	t value	Pr(> t)
A	30.286	4.77E-01	63.46	1.84E-08
B	0.7162	1.13E-02	63.38	1.85E-08

Model info for (b) Hist. GEV: $R=28.96T^{-0.768}$

	Estimate	Std. Error	t value	Pr(> t)
A	28.956	5.08E-01	56.96	1.97E-09
B	0.7684	1.26E-02	60.89	1.32E-09

Model info for (c) Fut. EnsembleMin.: $R=32.91T^{-0.774}$

	Estimate	Std. Error	t value	Pr(> t)
A	32.906	6.78E-01	48.56	5.11E-09
B	0.7742	1.48E-02	52.29	3.28E-09

Model info for (d) Fut. Ensemble10thPercentile: $R=33.96T^{-0.764}$

	Estimate	Std. Error	t value	Pr(> t)
A	33.959	6.66E-01	50.98	3.82E-09
B	0.7642	1.41E-02	54.20	2.65E-09

Model info for (e) Fut. Ensemble90thPercentile: $R=39.38T^{-0.768}$

	Estimate	Std. Error	t value	Pr(> t)
A	39.383	6.79E-01	58.02	1.76E-09
B	0.7679	1.24E-02	61.98	1.19E-09

Model info for (f) Fut. EnsembleMax.: $R=42.76T^{-0.772}$

	Estimate	Std. Error	t value	Pr(> t)
A	42.757	9.79E-01	43.68	9.64E-09
B	0.7725	1.65E-02	46.92	6.28E-09

15. PEARSON AIRPORT 2090S 10-YEAR EVENT

Duration	OBS_GUM	OBS_GEV	MIN	MAX	P10	P50	P75	P90	BMS
0.25	95.4	96.121	106.278	139.475	107.7853	119.9855	130.59425	135.8939	12
0.5	65.1	64.171	70.993	93.115	71.9816	80.103	87.06475	90.4696	12
1	39.6	36.266	40.26	52.634	40.8861	45.2695	50.741	52.5269	12
3	NA	14.069	10.685	18.174	11.9838	16.2985	17.332	18.1573	12
2	24	21.585	24.385	34.322	24.8809	27.099	28.94225	31.3169	12
6	10.5	9.037	9.801	13.729	10.0302	11.382	11.776	12.4174	12
12	5.9	4.833	5.342	6.714	5.7295	6.116	6.35325	6.5112	12
24	3.3	2.748	3.156	3.987	3.1574	3.4155	3.5625	3.9315	12

Model info for (a) Hist. Gumbel: $R=35.76T^{-0.708}$

	Estimate	Std. Error	t value	Pr(> t)
A	35.755	6.21E-01	57.61	2.98E-08
B	0.7083	1.24E-02	56.93	3.16E-08

Model info for (b) Hist. GEV: $R=33.71T^{-0.756}$

	Estimate	Std. Error	t value	Pr(> t)
A	33.710	5.72E-01	58.93	1.60E-09
B	0.7562	1.22E-02	62.02	1.18E-09

Model info for (c) Fut. EnsembleMin.: $R=37.15T^{-0.759}$

	Estimate	Std. Error	t value	Pr(> t)
A	37.151	6.99E-01	53.14	2.98E-09
B	0.7585	1.35E-02	56.09	2.16E-09

Model info for (d) Fut. Ensemble10thPercentile: $R=37.97T^{-0.753}$

	Estimate	Std. Error	t value	Pr(> t)
A	37.970	6.52E-01	58.23	1.72E-09
B	0.7529	1.23E-02	61.02	1.30E-09

Model info for (e) Fut. Ensemble90thPercentile: $R=47.21T^{-0.763}$

	Estimate	Std. Error	t value	Pr(> t)
A	47.214	8.76E-01	53.90	2.74E-09
B	0.7630	1.33E-02	57.21	1.92E-09

Model info for (f) Fut. EnsembleMax.: $R=49.11T^{-0.753}$

	Estimate	Std. Error	t value	Pr(> t)
A	49.113	1.05E+00	46.92	6.28E-09
B	0.7533	1.53E-02	49.19	4.73E-09

16. PEARSON AIRPORT 2090S 25-YEAR EVENT

Duration	OBS_GUM	OBS_GEV	MIN	MAX	P10	P50	P75	P90	BMS
0.25	112.8	109.876	108.202	185.078	109.3135	133.471	150.4405	168.2068	12
0.5	77.6	73.377	72.26	123.599	73.0064	89.1345	100.35225	111.3765	12
1	47.7	41.779	41.143	70.409	41.54	50.855	57.90625	69.4051	12
3	NA	17.331	13.003	23.235	15.1071	17.707	19.487	22.8503	12
2	29.2	25.642	25.25	43.192	25.4642	32.68	35.917	42.6583	12
6	12.7	11.401	10.521	17.105	11.0299	14.4385	15.844	16.0873	12
12	7.1	6.031	6.501	8.509	6.7322	7.3535	8.12175	8.445	12
24	4	3.385	3.333	5.702	3.3911	4.0725	4.55175	5.5413	12

Model info for (a) Hist. Gumbel: $R=42.63T^{-0.702}$

	Estimate	Std. Error	t value	Pr(> t)
A	42.630	7.78E-01	54.79	3.83E-08
B	0.7023	1.31E-02	53.71	4.23E-08

Model info for (b) Hist. GEV: $R=39.8T^{-0.733}$

	Estimate	Std. Error	t value	Pr(> t)
A	39.800	6.51E-01	61.16	1.28E-09
B	0.7329	1.17E-02	62.44	1.13E-09

Model info for (c) Fut. EnsembleMin.: $R=39.1T^{-0.735}$

	Estimate	Std. Error	t value	Pr(> t)
A	39.096	6.02E-01	64.98	8.93E-10
B	0.7346	1.10E-02	66.50	7.78E-10

Model info for (d) Fut. Ensemble10thPercentile: $R=39.91T^{-0.727}$

	Estimate	Std. Error	t value	Pr(> t)
A	39.912	5.76E-01	69.30	6.07E-10
B	0.7271	1.04E-02	70.22	5.61E-10

Model info for (e) Fut. Ensemble90thPercentile: $R=59.82T^{-0.746}$

	Estimate	Std. Error	t value	Pr(> t)
A	59.820	1.14E+00	52.54	3.19E-09
B	0.7461	1.37E-02	54.58	2.54E-09

Model info for (f) Fut. EnsembleMax.: $R=64.35T^{-0.762}$

	Estimate	Std. Error	t value	Pr(> t)
A	64.354	1.30E+00	49.46	4.58E-09
B	0.7624	1.45E-02	52.46	3.22E-09

17. PEARSON AIRPORT 2090S 50-YEAR EVENT

Duration	OBS_GUM	OBS_GEV	MIN	MAX	P10	P50	P75	P90	BMS
0.25	125.7	119.047	102.288	230.68	110.5183	143.1725	168.6385	197.3539	12
0.5	86.8	79.481	68.292	154.011	73.8	95.423	112.02925	130.0738	12
1	53.8	45.578	39.162	88.381	42.066	54.96	65.945	86.3261	12
3	NA	20.252	14.968	27.887	17.407	20.633	21.5225	27.2399	12
2	33.1	28.7	24.66	55.613	25.95	36.9255	41.16725	54.047	12
6	14.4	13.478	10.557	20.749	11.9137	16.969	19.24425	19.8705	12
12	8	7.082	7.479	10.883	7.5036	8.4165	9.76375	10.4269	12
24	4.5	3.956	3.399	7.665	3.5179	4.703	5.53425	7.3557	12

Model info for (a) Hist. Gumbel: $R=47.76T^{-0.698}$

	Estimate	Std. Error	t value	Pr(> t)
A	47.761	9.08E-01	52.58	4.70E-08
B	0.6985	1.36E-02	51.28	5.33E-08

Model info for (b) Hist. GEV: $R=44.42T^{-0.711}$

	Estimate	Std. Error	t value	Pr(> t)
A	44.418	7.39E-01	60.09	1.43E-09
B	0.7115	1.19E-02	59.63	1.49E-09

Model info for (c) Fut. EnsembleMin.: $R=38.5T^{-0.705}$

	Estimate	Std. Error	t value	Pr(> t)
A	38.498	6.71E-01	57.38	1.88E-09
B	0.7051	1.25E-02	56.45	2.08E-09

Model info for (d) Fut. Ensemble10thPercentile: $R=41.4T^{-0.709}$

	Estimate	Std. Error	t value	Pr(> t)
A	41.397	6.33E-01	65.40	8.60E-10
B	0.7086	1.10E-02	64.65	9.21E-10

Model info for (e) Fut. Ensemble90thPercentile: $R=71.92T^{-0.729}$

	Estimate	Std. Error	t value	Pr(> t)
A	71.919	1.46E+00	49.21	4.72E-09
B	0.7285	1.46E-02	49.96	4.31E-09

Model info for (f) Fut. EnsembleMax.: $R=80.44T^{-0.76}$

	Estimate	Std. Error	t value	Pr(> t)
A	80.445	1.60E+00	50.39	4.10E-09
B	0.7602	1.43E-02	53.31	2.93E-09

18. PEARSON AIRPORT 2090S 100-YEAR EVENT

Duration	OBS_GUM	OBS_GEV	MIN	MAX	P10	P50	P75	P90	BMS
0.25	138.6	127.364	95.156	289.39	111.2707	149.066	185.25125	231.4334	12
0.5	96	84.99	63.497	193.109	74.2936	99.238	122.81275	151.6399	12
1	59.8	49.12	36.698	111.714	42.4043	58.9805	74.24075	108.0647	12
3	NA	23.656	17.166	33.419	17.7092	22.767	26.83175	32.8193	12
2	36.9	31.778	23.742	72.204	26.2905	41.549	47.3885	69.4514	12
6	16.1	15.861	10.574	26.857	12.7921	19.7445	22.7245	25.0534	12
12	8.9	8.286	8.273	13.999	8.4127	9.434	11.65775	13.1447	12
24	5	4.62	3.452	10.498	3.6232	5.4785	6.72575	9.9362	12

Model info for (a) Hist. Gumbel: $R=52.89T^{-0.695}$

	Estimate	Std. Error	t value	Pr(> t)
A	52.886	1.04E+00	51.08	5.44E-08
B	0.6954	1.40E-02	49.60	6.29E-08

Model info for (b) Hist. GEV: $R=49.11T^{-0.688}$

	Estimate	Std. Error	t value	Pr(> t)
A	49.112	8.74E-01	56.18	2.14E-09
B	0.6877	1.27E-02	53.98	2.72E-09

Model info for (c) Fut. EnsembleMin.: $R=37.36T^{-0.675}$

	Estimate	Std. Error	t value	Pr(> t)
A	37.362	8.25E-01	45.27	7.78E-09
B	0.6745	1.58E-02	42.70	1.10E-08

Model info for (d) Fut. Ensemble10thPercentile: $R=42.78T^{-0.69}$

	Estimate	Std. Error	t value	Pr(> t)
A	42.775	7.87E-01	54.34	2.61E-09
B	0.6898	1.32E-02	52.36	3.26E-09

Model info for (e) Fut. Ensemble90thPercentile: $R=87.1T^{-0.705}$

	Estimate	Std. Error	t value	Pr(> t)
A	87.096	1.93E+00	45.06	8.00E-09
B	0.7053	1.59E-02	44.35	8.80E-09

Model info for (f) Fut. EnsembleMax.: R=102.36T^{-0.75}

	Estimate	Std. Error	t value	Pr(> t)
A	102.355	2.11E+00	48.55	5.12E-09
B	0.7500	1.48E-02	50.69	3.96E-09

19. WINDSOR AIRPORT 2030S 2-YEAR EVENT

Duration	OBS_GUM	OBS_GEV	MIN	MAX	P10	P50	P75	P90	BMS
0.25	68	66.848	60.821	81.735	60.9707	65.716	68.68025	79.7774	12
0.5	44.4	43.748	39.467	54.073	39.8191	43.1025	44.9945	52.2287	12
1	27.5	26.233	23.547	32.745	23.8644	25.8255	26.99075	31.3229	12
3	NA	11.121	9.966	13.812	10.0497	11.1835	12.028	13.2031	12
2	16.4	15.791	14.2	19.489	14.3616	15.615	16.25425	18.8572	12
6	6.8	6.188	5.456	8.346	5.6576	6.501	6.876	7.9221	12
12	3.9	3.434	3.178	4.9	3.1958	3.5155	3.7845	4.7031	12
24	2.2	2.172	1.946	2.698	1.9625	2.1085	2.1985	2.5645	12

Model info for (a) Hist. Gumbel: $R=24.69T^{-0.731}$

	Estimate	Std. Error	t value	Pr(> t)
A	24.693	3.48E-01	71.03	1.05E-08
B	0.7310	1.01E-02	72.35	9.55E-09

Model info for (b) Hist. GEV: $R=23.65T^{-0.75}$

	Estimate	Std. Error	t value	Pr(> t)
A	23.652	3.39E-01	69.84	5.80E-10
B	0.7498	1.03E-02	72.89	4.49E-10

Model info for (c) Fut. EnsembleMin.: $R=21.41T^{-0.754}$

	Estimate	Std. Error	t value	Pr(> t)
A	21.406	2.77E-01	77.29	3.16E-10
B	0.7535	9.30E-03	81.06	2.37E-10

Model info for (d) Fut. Ensemble10thPercentile: $R=21.61T^{-0.748}$

	Estimate	Std. Error	t value	Pr(> t)
A	21.611	2.89E-01	74.66	3.89E-10
B	0.7484	9.62E-03	77.79	3.04E-10

Model info for (e) Fut. Ensemble90thPercentile: $R=29T^{-0.73}$

	Estimate	Std. Error	t value	Pr(> t)
A	28.997	3.37E-01	86.15	1.65E-10
B	0.7303	8.33E-03	87.66	1.48E-10

Model info for (f) Fut. EnsembleMax.: $R=29.98T^{-0.724}$

	Estimate	Std. Error	t value	Pr(> t)
A	29.984	3.72E-01	80.55	2.47E-10
B	0.7237	8.91E-03	81.25	2.34E-10

20. WINDSOR AIRPORT 2030S 5-YEAR EVENT

Duration	OBS_GUM	OBS_GEV	MIN	MAX	P10	P50	P75	P90	BMS
0.25	87.9	88.129	75.294	105.986	77.0385	86.3575	88.819	102.4942	12
0.5	58.7	58.08	49.576	68.981	50.7733	56.881	58.48175	67.5263	12
1	36.9	35.31	29.911	42.312	30.8485	34.5805	35.56375	41.0566	12
3	NA	14.351	12.264	16.441	12.3895	14.121	14.92575	15.8439	12
2	21.5	20.773	17.876	24.499	18.1737	20.316	20.89675	23.8576	12
6	8.8	7.972	7.424	10.438	7.5301	8.16	8.6535	10.047	12
12	5	4.515	3.74	6.423	3.8889	4.5595	4.77025	5.9464	12
24	2.8	2.803	2.395	3.211	2.4201	2.7155	2.7905	3.0785	12

Model info for (a) Hist. Gumbel: $R=31.92T^{-0.731}$

	Estimate	Std. Error	t value	Pr(> t)
A	31.923	5.73E-01	55.68	3.53E-08
B	0.7310	1.29E-02	56.72	3.22E-08

Model info for (b) Hist. GEV: $R=31.03T^{-0.753}$

	Estimate	Std. Error	t value	Pr(> t)
A	31.028	4.93E-01	62.99	1.08E-09
B	0.7533	1.14E-02	66.04	8.10E-10

Model info for (c) Fut. EnsembleMin.: $R=26.81T^{-0.745}$

	Estimate	Std. Error	t value	Pr(> t)
A	26.815	4.72E-01	56.77	2.01E-09
B	0.7451	1.27E-02	58.90	1.61E-09

Model info for (d) Fut. Ensemble10thPercentile: $R=27.42T^{-0.745}$

	Estimate	Std. Error	t value	Pr(> t)
A	27.422	4.67E-01	58.78	1.63E-09
B	0.7455	1.22E-02	61.00	1.30E-09

Model info for (e) Fut. Ensemble90thPercentile: $R=36.96T^{-0.736}$

	Estimate	Std. Error	t value	Pr(> t)
A	36.962	5.34E-01	69.26	6.09E-10
B	0.7360	1.04E-02	71.01	5.25E-10

Model info for (f) Fut. EnsembleMax.: $R=38.45T^{-0.732}$

	Estimate	Std. Error	t value	Pr(> t)
A	38.449	5.16E-01	74.50	3.94E-10
B	0.7317	9.63E-03	75.95	3.51E-10

21. WINDSOR AIRPORT 2030S 10-YEAR EVENT

Duration	OBS_GUM	OBS_GEV	MIN	MAX	P10	P50	P75	P90	BMS
0.25	101.1	104.403	87.305	123.326	90.0976	102.607	107.723	119.1614	12
0.5	68.2	67.996	57.329	78.464	59.1374	66.7745	69.57125	77.5433	12
1	43.1	41.682	34.852	48.502	36.0651	40.933	42.73725	47.5449	12
3	NA	16.609	13.495	17.761	14.0476	16.06	17.37375	17.4417	12
2	24.8	23.856	20.44	27.501	20.76	23.428	24.18825	26.5536	12
6	10.1	9.22	8.845	11.73	8.9496	9.4125	9.97625	11.3771	12
12	5.8	5.371	4.101	7.275	4.3997	5.368	5.59575	6.6921	12
24	3.2	3.244	2.636	3.469	2.7442	3.1585	3.28875	3.3915	12

Model info for (a) Hist. Gumbel: $R=36.75T^{-0.73}$

	Estimate	Std. Error	t value	Pr(> t)
A	36.753	7.12E-01	51.64	5.15E-08
B	0.7303	1.39E-02	52.56	4.72E-08

Model info for (b) Hist. GEV: $R=36.53T^{-0.758}$

	Estimate	Std. Error	t value	Pr(> t)
A	36.534	5.41E-01	67.47	7.13E-10
B	0.7577	1.07E-02	71.14	5.19E-10

Model info for (c) Fut. EnsembleMin.: $R=30.96T^{-0.748}$

	Estimate	Std. Error	t value	Pr(> t)
A	30.960	6.76E-01	45.80	7.26E-09
B	0.7482	1.57E-02	47.71	5.69E-09

Model info for (d) Fut. Ensemble10thPercentile: $R=31.97T^{-0.748}$

	Estimate	Std. Error	t value	Pr(> t)
A	31.973	6.06E-01	52.73	3.12E-09
B	0.7477	1.36E-02	54.89	2.46E-09

Model info for (e) Fut. Ensemble90thPercentile: $R=42.43T^{-0.745}$

	Estimate	Std. Error	t value	Pr(> t)
A	42.434	6.27E-01	67.65	7.02E-10
B	0.7451	1.06E-02	70.18	5.63E-10

Model info for (f) Fut. EnsembleMax.: $R=44.07T^{-0.743}$

	Estimate	Std. Error	t value	Pr(> t)
A	44.068	6.11E-01	72.14	4.77E-10
B	0.7426	9.95E-03	74.59	3.91E-10

22. WINDSOR AIRPORT 2030S 25-YEAR EVENT

Duration	OBS_GUM	OBS_GEV	MIN	MAX	P10	P50	P75	P90	BMS
0.25	117.8	127.843	106.04	146.817	108.5414	127.5805	140.747	142.5017	12
0.5	80.2	81.032	68.527	90.428	70.2405	80.3015	87.38725	89.7802	12
1	50.9	50.172	42.07	56.162	43.1727	49.724	54.395	55.8431	12
3	NA	19.607	14.756	20.96	16.141	18.4915	19.008	20.448	12
2	29	27.523	23.836	30.714	23.9026	27.207	28.99925	29.6039	12
6	11.8	10.878	9.654	13.407	10.0499	11.2385	12.18075	13.2519	12
12	6.7	6.644	4.547	8.201	5.0586	6.7295	6.98975	7.61	12
24	3.7	3.83	2.882	4.11	3.152	3.6675	3.94	4.0837	12

Model info for (a) Hist. Gumbel: $R=42.81T^{-0.731}$

	Estimate	Std. Error	t value	Pr(> t)
A	42.812	9.02E-01	47.46	7.84E-08
B	0.7306	1.51E-02	48.31	7.18E-08

Model info for (b) Hist. GEV: $R=44.3T^{-0.765}$

	Estimate	Std. Error	t value	Pr(> t)
A	44.303	5.57E-01	79.47	2.67E-10
B	0.7647	9.05E-03	84.54	1.84E-10

Model info for (c) Fut. EnsembleMin.: $R=36.26T^{-0.774}$

	Estimate	Std. Error	t value	Pr(> t)
A	36.261	7.92E-01	45.76	7.29E-09
B	0.7744	1.57E-02	49.29	4.68E-09

Model info for (d) Fut. Ensemble10thPercentile: $R=37.69T^{-0.763}$

	Estimate	Std. Error	t value	Pr(> t)
A	37.692	6.74E-01	55.94	2.19E-09
B	0.7633	1.28E-02	59.40	1.53E-09

Model info for (e) Fut. Ensemble90thPercentile: $R=50.11T^{-0.754}$

	Estimate	Std. Error	t value	Pr(> t)
A	50.110	5.86E-01	85.45	1.73E-10
B	0.7541	8.41E-03	89.69	1.29E-10

Model info for (f) Fut. EnsembleMax.: $R=51.61T^{-0.754}$

	Estimate	Std. Error	t value	Pr(> t)
A	51.606	5.37E-01	96.14	8.53E-11
B	0.7544	7.47E-03	100.94	6.37E-11

23. WINDSOR AIRPORT 2030S 50-YEAR EVENT

Duration	OBS_GUM	OBS_GEV	MIN	MAX	P10	P50	P75	P90	BMS
0.25	130.2	147.579	123.069	173.598	124.3123	149.732	161.703	171.8817	12
0.5	89.1	91.083	77.979	103.662	78.8366	91.3575	98.48125	102.6235	12
1	56.7	56.803	48.229	65.168	48.8891	57.0165	61.7375	64.4714	12
3	NA	21.94	15.597	24.012	17.6009	19.959	20.5255	22.924	12
2	32.2	30.086	26.033	33.079	26.5059	29.8035	32.28025	32.7613	12
6	13.1	12.168	10.129	17.756	10.8121	12.4545	14.11375	14.3359	12
12	7.5	7.749	4.869	8.793	5.5888	7.88	8.2745	8.3987	12
24	4.1	4.285	3.046	4.852	3.4379	3.9655	4.5315	4.7976	12

Model info for (a) Hist. Gumbel: $R=47.45T^{-0.729}$

	Estimate	Std. Error	t value	Pr(> t)
A	47.450	1.02E+00	46.39	8.79E-08
B	0.7286	1.55E-02	47.10	8.15E-08

Model info for (b) Hist. GEV: $R=50.72T^{-0.771}$

	Estimate	Std. Error	t value	Pr(> t)
A	50.718	5.79E-01	87.52	1.50E-10
B	0.7706	8.21E-03	93.81	9.89E-11

Model info for (c) Fut. EnsembleMin.: $R=40.68T^{-0.799}$

	Estimate	Std. Error	t value	Pr(> t)
A	40.677	8.87E-01	45.88	7.18E-09
B	0.7989	1.57E-02	50.94	3.84E-09

Model info for (d) Fut. Ensemble10thPercentile: $R=42.33T^{-0.777}$

	Estimate	Std. Error	t value	Pr(> t)
A	42.335	7.00E-01	60.47	1.38E-09
B	0.7773	1.19E-02	65.36	8.63E-10

Model info for (e) Fut. Ensemble90thPercentile: $R=58.34T^{-0.78}$

	Estimate	Std. Error	t value	Pr(> t)
A	58.338	4.62E-01	126.22	1.67E-11
B	0.7796	5.70E-03	136.81	1.03E-11

Model info for (f) Fut. EnsembleMax.: $R=61.41T^{-0.75}$

	Estimate	Std. Error	t value	Pr(> t)
A	61.410	1.05E+00	58.43	1.69E-09
B	0.7497	1.23E-02	60.98	1.31E-09

24. WINDSOR AIRPORT 2030S 100-YEAR EVENT

Duration	OBS_GUM	OBS_GEV	MIN	MAX	P10	P50	P75	P90	BMS
0.25	142.5	169.398	141.518	214.311	143.5199	172.714	185.42775	210.5205	12
0.5	98	101.393	87.794	122.147	88.3648	101.1435	110.85675	120.5205	12
1	62.5	63.679	54.971	77.567	55.12	63.8285	69.6225	76.47	12
3	NA	24.352	16.355	27.434	18.9581	21.315	22.69825	25.6273	12
2	35.3	32.506	28.146	37.24	29.2239	31.611	35.54075	36.7649	12
6	14.4	13.504	10.516	23.833	11.5271	13.7055	15.298	16.696	12
12	8.2	9.003	5.183	10.174	6.1548	9.0645	9.35675	9.5846	12
24	4.5	4.756	3.194	5.716	3.7023	4.355	5.19125	5.642	12

Model info for (a) Hist. Gumbel: $R=51.99T^{-0.728}$

	Estimate	Std. Error	t value	Pr(> t)
A	51.992	1.16E+00	44.96	1.03E-07
B	0.7278	1.60E-02	45.60	9.58E-08

Model info for (b) Hist. GEV: $R=57.7T^{-0.777}$

	Estimate	Std. Error	t value	Pr(> t)
A	57.702	6.87E-01	83.93	1.93E-10
B	0.7769	8.57E-03	90.68	1.21E-10

Model info for (c) Fut. EnsembleMin.: $R=45.22T^{-0.823}$

	Estimate	Std. Error	t value	Pr(> t)
A	45.224	1.02E+00	44.29	8.87E-09
B	0.8232	1.63E-02	50.63	3.98E-09

Model info for (d) Fut. Ensemble10thPercentile: $R=47.62T^{-0.796}$

	Estimate	Std. Error	t value	Pr(> t)
A	47.619	7.05E-01	67.57	7.07E-10
B	0.7960	1.07E-02	74.74	3.86E-10

Model info for (e) Fut. Ensemble90thPercentile: $R=69.78T^{-0.797}$

	Estimate	Std. Error	t value	Pr(> t)
A	69.777	5.66E-01	123.38	1.91E-11
B	0.7966	5.83E-03	136.58	1.04E-11

Model info for (f) Fut. EnsembleMax.: $R=76.08T^{-0.747}$

	Estimate	Std. Error	t value	Pr(> t)
A	76.079	2.20E+00	34.52	3.94E-08
B	0.7471	2.08E-02	35.90	3.11E-08

25. WINDSOR AIRPORT 2050S 2-YEAR EVENT

Duration	OBS_GUM	OBS_GEV	MIN	MAX	P10	P50	P75	P90	BMS
0.25	68	66.848	72.518	97.633	72.7623	83.8715	85.21675	89.5375	8
0.5	44.4	43.748	48.652	63.182	48.9145	55.715	56.13325	58.7881	8
1	27.5	26.26	29.386	39.352	29.6842	33.5395	34.02325	35.9899	8
3	NA	11.121	12.297	16.532	12.3873	13.9765	14.2815	15.1005	8
2	16.4	16.001	17.905	22.414	18.0275	20.1255	20.45675	21.119	8
6	6.8	6.286	6.098	9.3	6.1288	7.858	8.54675	8.9801	8
12	3.9	3.434	3.626	5.241	3.6512	4.5065	4.7575	4.9204	8
24	2.2	2.172	2.402	3.229	2.4195	2.7295	2.7895	2.9497	8

Model info for (a) Hist. Gumbel: $R=24.69T^{-0.731}$

	Estimate	Std. Error	t value	Pr(> t)
A	24.693	3.48E-01	71.03	1.05E-08
B	0.7310	1.01E-02	72.35	9.55E-09

Model info for (b) Hist. GEV: $R=23.72T^{-0.748}$

	Estimate	Std. Error	t value	Pr(> t)
A	23.720	3.44E-01	68.87	6.31E-10
B	0.7477	1.04E-02	71.69	4.96E-10

Model info for (c) Fut. EnsembleMin.: $R=25.27T^{-0.761}$

	Estimate	Std. Error	t value	Pr(> t)
A	25.270	5.38E-01	46.95	6.26E-09
B	0.7608	1.53E-02	49.70	4.45E-09

Model info for (d) Fut. Ensemble10thPercentile: $R=25.39T^{-0.76}$

	Estimate	Std. Error	t value	Pr(> t)
A	25.387	5.49E-01	46.22	6.87E-09
B	0.7599	1.55E-02	48.87	4.92E-09

Model info for (e) Fut. Ensemble90thPercentile: $R=32.41T^{-0.733}$

	Estimate	Std. Error	t value	Pr(> t)
A	32.409	4.42E-01	73.29	4.34E-10
B	0.7334	9.79E-03	74.88	3.82E-10

Model info for (f) Fut. EnsembleMax.: $R=34.92T^{-0.742}$

	Estimate	Std. Error	t value	Pr(> t)
A	34.921	4.40E-01	79.37	2.69E-10
B	0.7419	9.05E-03	82.00	2.22E-10

26. WINDSOR AIRPORT 2050S 5-YEAR EVENT

Duration	OBS_GUM	OBS_GEV	MIN	MAX	P10	P50	P75	P90	BMS
0.25	87.9	88.129	95.577	143.638	97.1842	115.517	117.9195	126.5055	8
0.5	58.7	58.08	63.127	84.253	63.2502	75.598	76.37275	79.2046	8
1	36.9	35.31	39.016	54.038	39.2274	46.2805	47.11475	49.4495	8
3	NA	14.599	16.32	23.125	16.4621	17.5255	18.575	20.8409	8
2	21.5	20.773	22.422	28.105	22.7391	26.493	27.24	27.9195	8
6	8.8	8.073	8.275	11.895	8.2967	10.5525	11.2195	11.5933	8
12	5	4.561	5.062	7.806	5.2601	6.317	6.7985	7.2278	8
24	2.8	2.851	3.188	4.517	3.2153	3.4225	3.62775	4.0704	8

Model info for (a) Hist. Gumbel: $R=31.92T^{-0.731}$

	Estimate	Std. Error	t value	Pr(> t)
A	31.923	5.73E-01	55.68	3.53E-08
B	0.7310	1.29E-02	56.72	3.22E-08

Model info for (b) Hist. GEV: $R=31.16T^{-0.75}$

	Estimate	Std. Error	t value	Pr(> t)
A	31.165	4.80E-01	64.93	8.98E-10
B	0.7502	1.11E-02	67.80	6.93E-10

Model info for (c) Fut. EnsembleMin.: $R=33.66T^{-0.753}$

	Estimate	Std. Error	t value	Pr(> t)
A	33.660	5.89E-01	57.16	1.93E-09
B	0.7531	1.26E-02	59.92	1.45E-09

Model info for (d) Fut. Ensemble10thPercentile: $R=34.19T^{-0.754}$

	Estimate	Std. Error	t value	Pr(> t)
A	34.185	5.59E-01	61.12	1.29E-09
B	0.7540	1.18E-02	64.14	9.66E-10

Model info for (e) Fut. Ensemble90thPercentile: $R=45.09T^{-0.744}$

	Estimate	Std. Error	t value	Pr(> t)
A	45.091	3.96E-01	113.95	3.08E-11
B	0.7443	6.30E-03	118.09	2.49E-11

Model info for (f) Fut. EnsembleMax.: $R=49.73T^{-0.765}$

	Estimate	Std. Error	t value	Pr(> t)
A	49.728	5.02E-01	99.09	7.12E-11
B	0.7652	7.25E-03	105.48	4.90E-11

27. WINDSOR AIRPORT 2050S 10-YEAR EVENT

Duration	OBS_GUM	OBS_GEV	MIN	MAX	P10	P50	P75	P90	EMS
0.25	101.1	104.403	116.346	180.977	120.7945	140.5105	144.11675	159.5969	8
0.5	68.2	67.996	73.907	97.464	74.488	89.2055	91.53	93.5496	8
1	43.1	41.682	46.693	63.669	46.8428	55.272	57.0255	59.0868	8
3	NA	17.238	18.773	27.689	19.1251	19.8635	21.60575	25.0871	8
2	24.8	23.856	25.228	32.233	26.0379	30.254	31.37275	32.2141	8
6	10.1	9.32	10.186	13.447	10.2637	12.8575	13.07025	13.2069	8
12	5.8	5.492	6.351	9.871	6.9635	7.6865	8.86125	9.1857	8
24	3.2	3.367	3.667	5.408	3.7356	3.8795	4.22	4.8998	8

Model info for (a) Hist. Gumbel: $R=36.75T^{-0.73}$

	Estimate	Std. Error	t value	Pr(> t)
A	36.753	7.12E-01	51.64	5.15E-08
B	0.7303	1.39E-02	52.56	4.72E-08

Model info for (b) Hist. GEV: $R=36.79T^{-0.753}$

	Estimate	Std. Error	t value	Pr(> t)
A	36.786	5.18E-01	70.97	5.27E-10
B	0.7528	1.01E-02	74.35	3.98E-10

Model info for (c) Fut. EnsembleMin.: $R=40.91T^{-0.754}$

	Estimate	Std. Error	t value	Pr(> t)
A	40.915	5.11E-01	80.07	2.55E-10
B	0.7541	8.97E-03	84.04	1.91E-10

Model info for (d) Fut. Ensemble10thPercentile: $R=42.42T^{-0.755}$

	Estimate	Std. Error	t value	Pr(> t)
A	42.416	5.27E-01	80.42	2.49E-10
B	0.7551	8.94E-03	84.50	1.85E-10

Model info for (e) Fut. Ensemble90thPercentile: $R=55.55T^{-0.761}$

	Estimate	Std. Error	t value	Pr(> t)
A	55.554	6.76E-01	82.22	2.18E-10
B	0.7612	8.74E-03	87.09	1.54E-10

Model info for (f) Fut. EnsembleMax.: $R=60.99T^{-0.784}$

	Estimate	Std. Error	t value	Pr(> t)
A	60.991	1.18E+00	51.85	3.46E-09
B	0.7844	1.39E-02	56.53	2.06E-09

28. WINDSOR AIRPORT 2050S 25-YEAR EVENT

Duration	OBS_GUM	OBS_GEV	MIN	MAX	P10	P50	P75	P90	BMS
0.25	117.8	127.843	151.271	237.772	157.9462	175.1975	187.33125	212.9262	8
0.5	80.2	81.032	89.429	115.58	90.9725	105.4975	113.138	114.026	8
1	50.9	50.172	58.251	75.734	58.2692	66.408	71.6275	72.9949	8
3	NA	20.884	20.675	33.694	21.1811	24.519	26.416	30.7498	8
2	29	27.523	28.698	39.257	30.4466	34.284	35.24725	37.7695	8
6	11.8	10.972	13.373	16.884	13.5221	15.088	15.6135	16.5732	8
12	6.7	6.908	8.525	12.991	9.211	10.5195	12.1425	12.7089	8
24	3.7	4.079	4.038	6.581	4.1367	4.789	5.159	6.0056	8

Model info for (a) Hist. Gumbel: $R=42.81T^{-0.731}$

	Estimate	Std. Error	t value	Pr(> t)
A	42.812	9.02E-01	47.46	7.84E-08
B	0.7306	1.51E-02	48.31	7.18E-08

Model info for (b) Hist. GEV: $R=44.76T^{-0.757}$

	Estimate	Std. Error	t value	Pr(> t)
A	44.761	5.48E-01	81.73	2.26E-10
B	0.7572	8.79E-03	86.12	1.65E-10

Model info for (c) Fut. EnsembleMin.: $R=52.66T^{-0.761}$

	Estimate	Std. Error	t value	Pr(> t)
A	52.660	6.61E-01	79.64	2.64E-10
B	0.7612	9.02E-03	84.36	1.87E-10

Model info for (d) Fut. Ensemble10thPercentile: $R=54.76T^{-0.764}$

	Estimate	Std. Error	t value	Pr(> t)
A	54.764	8.07E-01	67.85	6.89E-10
B	0.7640	1.06E-02	72.12	4.78E-10

Model info for (e) Fut. Ensemble90thPercentile: $R=72.85T^{-0.773}$

	Estimate	Std. Error	t value	Pr(> t)
A	72.847	1.59E+00	45.76	7.30E-09
B	0.7735	1.57E-02	49.22	4.72E-09

Model info for (f) Fut. EnsembleMax.: $R=78.54T^{-0.799}$

	Estimate	Std. Error	t value	Pr(> t)
A	78.538	2.22E+00	35.42	3.38E-08
B	0.7987	2.03E-02	39.31	1.81E-08

29. WINDSOR AIRPORT 2050S 50-YEAR EVENT

Duration	OBS_GUM	OBS_GEV	MIN	MAX	P10	P50	P75	P90	BMS
0.25	130.2	150.152	181.98	288.164	184.283	213.862	228.066	262.9983	8
0.5	89.1	91.083	102.495	135.791	105.1291	117.2255	126.20775	132.4527	8
1	56.7	56.803	68.22	84.684	68.3691	74.37	84.363	84.6315	8
3	NA	23.835	21.883	38.327	22.1238	28.141	31.21875	35.1609	8
2	32.2	30.086	31.218	44.854	33.3208	36.567	38.249	41.6984	8
6	13.1	12.256	15.652	20.344	16.0475	16.6025	17.81125	19.9828	8
12	7.5	8.165	10.645	16.414	10.9299	13.5495	15.47525	15.9422	8
24	4.1	4.655	4.274	7.486	4.3209	5.4965	6.09725	6.8672	8

Model info for (a) Hist. Gumbel: $R=47.45T^{-0.729}$

	Estimate	Std. Error	t value	Pr(> t)
A	47.450	1.02E+00	46.39	8.79E-08
B	0.7286	1.55E-02	47.10	8.15E-08

Model info for (b) Hist. GEV: $R=51.9T^{-0.766}$

	Estimate	Std. Error	t value	Pr(> t)
A	51.899	6.03E-01	86.06	1.66E-10
B	0.7664	8.35E-03	91.75	1.13E-10

Model info for (c) Fut. EnsembleMin.: $R=62.69T^{-0.769}$

	Estimate	Std. Error	t value	Pr(> t)
A	62.687	1.26E+00	49.56	4.52E-09
B	0.7687	1.45E-02	53.00	3.03E-09

Model info for (d) Fut. Ensemble10thPercentile: $R=63.78T^{-0.765}$

	Estimate	Std. Error	t value	Pr(> t)
A	63.776	1.27E+00	50.24	4.17E-09
B	0.7654	1.43E-02	53.50	2.86E-09

Model info for (e) Fut. Ensemble90thPercentile: $R=88.94T^{-0.782}$

	Estimate	Std. Error	t value	Pr(> t)
A	88.939	2.60E+00	34.17	4.18E-08
B	0.7817	2.11E-02	37.14	2.54E-08

Model info for (f) Fut. EnsembleMax.: $R=94.88T^{-0.801}$

	Estimate	Std. Error	t value	Pr(> t)
A	94.881	3.25E+00	29.17	1.07E-07
B	0.8009	2.47E-02	32.46	5.68E-08

30. WINDSOR AIRPORT 2050S 100-YEAR EVENT

Duration	OBS_GUM	OBS_GEV	MIN	MAX	P10	P50	P75	P90	EMS
0.25	142.5	176.418	204.099	346.426	215.0456	257.397	286.71275	323.8391	8
0.5	98	101.393	116.937	158.387	118.9523	128.862	139.1475	152.9529	8
1	62.5	63.679	76.417	99.473	76.6312	84.082	94.5515	98.5385	8
3	NA	26.988	22.758	43.082	22.8826	32.178	36.7605	39.7143	8
2	35.3	32.506	33.675	50.779	35.2017	39.2375	41.2	45.4513	8
6	14.4	13.581	17.258	24.45	17.3707	19.6335	21.40625	24.0356	8
12	8.2	9.617	12.773	21.742	13.1412	16.618	19.529	21.5159	8
24	4.5	5.271	4.445	8.414	4.4695	6.285	7.1795	7.7567	8

Model info for (a) Hist. Gumbel: $R=51.99T^{-0.728}$

	Estimate	Std. Error	t value	Pr(> t)
A	51.992	1.16E+00	44.96	1.03E-07
B	0.7278	1.60E-02	45.60	9.58E-08

Model info for (b) Hist. GEV: $R=60.01T^{-0.778}$

	Estimate	Std. Error	t value	Pr(> t)
A	60.005	8.80E-01	68.15	6.72E-10
B	0.7779	1.06E-02	73.71	4.20E-10

Model info for (c) Fut. EnsembleMin.: $R=70.5T^{-0.767}$

	Estimate	Std. Error	t value	Pr(> t)
A	70.500	1.90E+00	37.17	2.53E-08
B	0.7668	1.93E-02	39.65	1.72E-08

Model info for (d) Fut. Ensemble10thPercentile: $R=73.1T^{-0.778}$

	Estimate	Std. Error	t value	Pr(> t)
A	73.096	2.08E+00	35.18	3.52E-08
B	0.7783	2.04E-02	38.07	2.19E-08

Model info for (e) Fut. Ensemble90thPercentile: $R=109.58T^{-0.781}$

	Estimate	Std. Error	t value	Pr(> t)
A	109.576	4.66E+00	23.49	3.90E-07
B	0.7812	3.06E-02	25.52	2.39E-07

Model info for (f) Fut. EnsembleMax.: $R=115.04T^{-0.795}$

	Estimate	Std. Error	t value	Pr(> t)
A	115.041	4.98E+00	23.11	4.30E-07
B	0.7947	3.11E-02	25.52	2.38E-07

31. WINDSOR AIRPORT 2090S 2-YEAR EVENT

Duration	OBS_GUM	OBS_GEV	MIN	MAX	P10	P50	P75	P90	BMS
0.25	68	66.848	67.77	100.962	68.4804	78.413	87.479	97.016	12
0.5	44.4	43.748	44.5	65.894	44.8724	51.4505	57.6825	63.5379	12
1	27.5	26.233	26.684	40.332	26.9129	30.948	35.05425	38.1522	12
3	NA	11.121	11.932	16.681	11.9791	13.709	14.7515	15.9902	12
2	16.4	15.791	16.062	23.201	16.2876	18.5585	20.65275	22.914	12
6	6.8	6.188	6.234	10.145	6.3433	7.4625	8.20475	9.4892	12
12	3.9	3.434	3.86	5.568	3.8685	4.2125	4.512	5.2437	12
24	2.2	2.172	2.174	3.258	2.1915	2.5015	2.83125	2.9841	12

Model info for (a) Hist. Gumbel: $R=24.69T^{-0.731}$

	Estimate	Std. Error	t value	Pr(> t)
A	24.693	3.48E-01	71.03	1.05E-08
B	0.7310	1.01E-02	72.35	9.55E-09

Model info for (b) Hist. GEV: $R=23.65T^{-0.75}$

	Estimate	Std. Error	t value	Pr(> t)
A	23.652	3.39E-01	69.84	5.80E-10
B	0.7498	1.03E-02	72.89	4.49E-10

Model info for (c) Fut. EnsembleMin.: $R=24.23T^{-0.742}$

	Estimate	Std. Error	t value	Pr(> t)
A	24.234	3.23E-01	75.01	3.78E-10
B	0.7421	9.57E-03	77.51	3.10E-10

Model info for (d) Fut. Ensemble10thPercentile: $R=24.49T^{-0.742}$

	Estimate	Std. Error	t value	Pr(> t)
A	24.486	3.17E-01	77.14	3.19E-10
B	0.7421	9.31E-03	79.72	2.62E-10

Model info for (e) Fut. Ensemble90thPercentile: $R=34.74T^{-0.741}$

	Estimate	Std. Error	t value	Pr(> t)
A	34.737	4.88E-01	71.15	5.19E-10
B	0.7412	1.01E-02	73.44	4.29E-10

Model info for (f) Fut. EnsembleMax.: $R=36.5T^{-0.734}$

	Estimate	Std. Error	t value	Pr(> t)
A	36.497	4.80E-01	76.04	3.48E-10
B	0.7343	9.44E-03	77.78	3.04E-10

32. WINDSOR AIRPORT 2090S 5-YEAR EVENT

Duration	OBS_GUM	OBS_GEV	MIN	MAX	P10	P50	P75	P90	BMS
0.25	87.9	88.129	91.156	138.383	95.7681	106.583	111.99825	129.3324	12
0.5	58.7	58.08	60.076	86.637	62.4046	68.604	72.33925	85.0228	12
1	36.9	35.31	36.523	53.847	38.0996	42.141	44.499	51.7572	12
3	NA	14.351	15.931	20.646	16.1087	16.804	17.7065	18.6584	12
2	21.5	20.773	21.487	30.764	22.0297	24.128	25.481	28.7324	12
6	8.8	7.972	8.376	12.586	9.274	9.884	10.84825	11.995	12
12	5	4.515	4.874	8.267	4.9313	5.3	5.98575	7.1517	12
24	2.8	2.803	2.867	4.032	2.9698	3.2425	3.37725	3.6468	12

Model info for (a) Hist. Gumbel: $R=31.92T^{-0.731}$

	Estimate	Std. Error	t value	Pr(> t)
A	31.923	5.73E-01	55.68	3.53E-08
B	0.7310	1.29E-02	56.72	3.22E-08

Model info for (b) Hist. GEV: $R=31.03T^{-0.753}$

	Estimate	Std. Error	t value	Pr(> t)
A	31.028	4.93E-01	62.99	1.08E-09
B	0.7533	1.14E-02	66.04	8.10E-10

Model info for (c) Fut. EnsembleMin.: $R=32.33T^{-0.748}$

	Estimate	Std. Error	t value	Pr(> t)
A	32.330	4.86E-01	66.55	7.74E-10
B	0.7481	1.08E-02	69.31	6.07E-10

Model info for (d) Fut. Ensemble10thPercentile: $R=34.06T^{-0.746}$

	Estimate	Std. Error	t value	Pr(> t)
A	34.062	5.13E-01	66.38	7.86E-10
B	0.7460	1.08E-02	68.94	6.27E-10

Model info for (e) Fut. Ensemble90thPercentile: $R=45.74T^{-0.75}$

	Estimate	Std. Error	t value	Pr(> t)
A	45.736	7.24E-01	63.21	1.05E-09
B	0.7502	1.14E-02	66.01	8.13E-10

Model info for (f) Fut. EnsembleMax.: $R=49.22T^{-0.746}$

	Estimate	Std. Error	t value	Pr(> t)
A	49.218	6.20E-01	79.39	2.69E-10
B	0.7459	9.05E-03	82.44	2.15E-10

33. WINDSOR AIRPORT 2090S 10-YEAR EVENT

Duration	OBS_GUM	OBS_GEV	MIN	MAX	P10	P50	P75	P90	BMS
0.25	101.1	104.403	112.503	166.863	119.699	127.018	139.5415	155.01	11
0.5	68.2	67.996	73.271	100.955	78.1179	81.047	87.6975	99.3585	12
1	43.1	41.682	44.916	63.082	47.9177	49.929	54.59975	61.2248	12
3	NA	16.609	17.804	22.875	18.3205	19.522	20.723	21.2555	12
2	24.8	23.856	25.707	35.42	26.7912	28.416	29.121	32.0691	12
6	10.1	9.22	10.104	15.698	10.6558	11.7285	13.02625	14.0689	12
12	5.8	5.371	5.572	10.595	5.7003	6.1325	7.27375	8.6905	12
24	3.2	3.244	3.465	4.468	3.4867	3.813	4.06525	4.1557	12

Model info for (a) Hist. Gumbel: $R=36.75T^{-0.73}$

	Estimate	Std. Error	t value	Pr(> t)
A	36.753	7.12E-01	51.64	5.15E-08
B	0.7303	1.39E-02	52.56	4.72E-08

Model info for (b) Hist. GEV: $R=36.53T^{-0.758}$

	Estimate	Std. Error	t value	Pr(> t)
A	36.534	5.41E-01	67.47	7.13E-10
B	0.7577	1.07E-02	71.14	5.19E-10

Model info for (c) Fut. EnsembleMin.: $R=39.29T^{-0.759}$

	Estimate	Std. Error	t value	Pr(> t)
A	39.294	6.14E-01	63.99	9.79E-10
B	0.7591	1.12E-02	67.59	7.06E-10

Model info for (d) Fut. Ensemble10thPercentile: $R=41.42T^{-0.766}$

	Estimate	Std. Error	t value	Pr(> t)
A	41.419	7.20E-01	57.51	1.86E-09
B	0.7659	1.25E-02	61.27	1.27E-09

Model info for (e) Fut. Ensemble90thPercentile: $R=54.43T^{-0.755}$

	Estimate	Std. Error	t value	Pr(> t)
A	54.429	8.31E-01	65.48	8.53E-10
B	0.7552	1.10E-02	68.82	6.33E-10

Model info for (f) Fut. EnsembleMax.: $R=59.72T^*-0.741$

	Estimate	Std. Error	t value	Pr(> t)
A	59.721	9.90E-01	60.33	1.39E-09
B	0.7412	1.19E-02	62.27	1.15E-09

34. WINDSOR AIRPORT 2090S 25-YEAR EVENT

Duration	OBS_GUM	OBS_GEV	MIN	MAX	P10	P50	P75	P90	BMS
0.25	117.8	127.843	142.983	207.699	148.086	165.4655	185.70325	196.3266	12
0.5	80.2	81.032	90.629	129.068	93.9484	106.034	114.62675	120.0269	12
1	50.9	50.172	56.114	82.178	58.3428	66.151	72.3915	75.0216	12
3	NA	19.607	19.714	30.909	19.7253	22.815	25.55275	27.1075	12
2	29	27.523	30.776	40.831	30.9041	34.3115	36.501	38.6892	12
6	11.8	10.878	12.233	25.007	12.4752	13.812	15.66725	19.7717	12
12	6.7	6.644	6.403	14.34	6.5374	7.3095	9.3715	11.0236	12
24	3.7	3.83	3.855	6.037	3.9024	4.7535	5.191	5.3008	12

Model info for (a) Hist. Gumbel: $R=42.81T^{-0.731}$

	Estimate	Std. Error	t value	Pr(> t)
A	42.812	9.02E-01	47.46	7.84E-08
B	0.7306	1.51E-02	48.31	7.18E-08

Model info for (b) Hist. GEV: $R=44.3T^{-0.765}$

	Estimate	Std. Error	t value	Pr(> t)
A	44.303	5.57E-01	79.47	2.67E-10
B	0.7647	9.05E-03	84.54	1.84E-10

Model info for (c) Fut. EnsembleMin.: $R=48.46T^{-0.781}$

	Estimate	Std. Error	t value	Pr(> t)
A	48.456	8.09E-01	59.87	1.46E-09
B	0.7808	1.20E-02	64.99	8.92E-10

Model info for (d) Fut. Ensemble10thPercentile: $R=49.88T^{-0.785}$

	Estimate	Std. Error	t value	Pr(> t)
A	49.885	8.69E-01	57.41	1.88E-09
B	0.7852	1.25E-02	62.66	1.11E-09

Model info for (e) Fut. Ensemble90thPercentile: $R=70.04T^{-0.744}$

	Estimate	Std. Error	t value	Pr(> t)
A	70.042	1.06E+00	66.12	8.05E-10
B	0.7436	1.09E-02	68.46	6.53E-10

Model info for (f) Fut. EnsembleMax.: $R=78.86T^{-0.699}$

	Estimate	Std. Error	t value	Pr(> t)
A	78.864	1.79E+00	44.13	9.07E-09
B	0.6987	1.62E-02	43.04	1.05E-08

35. WINDSOR AIRPORT 2090S 50-YEAR EVENT

Duration	OBS_GUM	OBS_GEV	MIN	MAX	P10	P50	P75	P90	BMS
0.25	130.2	147.579	162.27	253.099	168.8436	195.015	225.2655	243.0523	12
0.5	89.1	91.083	100.151	175.488	104.1469	124.946	138.825	145.3434	12
1	56.7	56.803	62.457	113.535	65.2897	78.885	87.83175	93.3009	12
3	NA	21.94	20.035	42.099	20.2296	24.777	29.571	33.6495	12
2	32.2	30.086	33.081	48.729	33.2731	38.8795	42.26975	46.2053	12
6	13.1	12.168	13.31	36.079	13.6784	15.6715	17.00925	27.8985	12
12	7.5	7.749	6.82	17.845	7.3027	8.2865	11.23975	13.1128	12
24	4.1	4.285	4.045	8.223	4.1873	5.3145	6.507	6.8223	12

Model info for (a) Hist. Gumbel: $R=47.45T^{-0.729}$

	Estimate	Std. Error	t value	Pr(> t)
A	47.450	1.02E+00	46.39	8.79E-08
B	0.7286	1.55E-02	47.10	8.15E-08

Model info for (b) Hist. GEV: $R=50.72T^{-0.771}$

	Estimate	Std. Error	t value	Pr(> t)
A	50.718	5.79E-01	87.52	1.50E-10
B	0.7706	8.21E-03	93.81	9.89E-11

Model info for (c) Fut. EnsembleMin.: $R=53.81T^{-0.796}$

	Estimate	Std. Error	t value	Pr(> t)
A	53.814	8.90E-01	60.43	1.38E-09
B	0.7964	1.19E-02	66.88	7.51E-10

Model info for (d) Fut. Ensemble10thPercentile: $R=55.99T^{-0.796}$

	Estimate	Std. Error	t value	Pr(> t)
A	55.991	8.82E-01	63.50	1.03E-09
B	0.7964	1.13E-02	70.28	5.58E-10

Model info for (e) Fut. Ensemble90thPercentile: $R=88.56T^{-0.728}$

	Estimate	Std. Error	t value	Pr(> t)
A	88.555	2.18E+00	40.55	1.50E-08
B	0.7284	1.77E-02	41.16	1.38E-08

Model info for (f) Fut. EnsembleMax.: $R=100.41T^{-0.667}$

	Estimate	Std. Error	t value	Pr(> t)
A	100.410	3.21E+00	31.33	7.03E-08
B	0.6674	2.28E-02	29.26	1.06E-07

36. WINDSOR AIRPORT 2090S 100-YEAR EVENT

Duration	OBS_GUM	OBS_GEV	MIN	MAX	P10	P50	P75	P90	BMS
0.25	142.5	169.398	183.324	329.133	191.9028	229.7055	272.15275	304.7169	12
0.5	98	101.393	109.728	242.499	114.7103	141.341	171.04975	190.9384	12
1	62.5	63.679	68.914	159.401	72.5052	89.9915	110.007	124.3782	12
3	NA	24.352	20.253	58.47	20.4114	26.579	34.85375	43.0457	12
2	35.3	32.506	35.179	61.663	35.511	44.079	48.437	57.1592	12
6	14.4	13.504	14.303	52.563	14.7382	17.8215	18.98825	40.1219	12
12	8.2	9.003	7.192	22.088	8.1159	9.423	13.45875	15.5394	12
24	4.5	4.756	4.2	11.42	4.4747	6.1275	8.03725	9.0031	12

Model info for (a) Hist. Gumbel: $R=51.99T^{-0.728}$

	Estimate	Std. Error	t value	Pr(> t)
A	51.992	1.16E+00	44.96	1.03E-07
B	0.7278	1.60E-02	45.60	9.58E-08

Model info for (b) Hist. GEV: $R=57.7T^{-0.777}$

	Estimate	Std. Error	t value	Pr(> t)
A	57.702	6.87E-01	83.93	1.93E-10
B	0.7769	8.57E-03	90.68	1.21E-10

Model info for (c) Fut. EnsembleMin.: $R=59.33T^{-0.814}$

	Estimate	Std. Error	t value	Pr(> t)
A	59.331	9.76E-01	60.81	1.33E-09
B	0.8140	1.18E-02	68.75	6.37E-10

Model info for (d) Fut. Ensemble10thPercentile: $R=62.44T^{-0.81}$

	Estimate	Std. Error	t value	Pr(> t)
A	62.438	9.04E-01	69.10	6.18E-10
B	0.8101	1.04E-02	77.76	3.05E-10

Model info for (e) Fut. Ensemble90thPercentile: $R=114.02T^{-0.709}$

	Estimate	Std. Error	t value	Pr(> t)
A	114.020	4.30E+00	26.53	1.89E-07
B	0.7094	2.70E-02	26.25	2.02E-07

Model info for (f) Fut. EnsembleMax.: $R=133.51T^{-0.652}$

	Estimate	Std. Error	t value	Pr(> t)
A	133.508	5.63E+00	23.71	3.70E-07
B	0.6517	3.01E-02	21.65	6.33E-07